1. INTRODUCTION

The Sudbury Structure is located in Canada, Ontario, and consists of three major components (Fig 1.1) the sedimentary Sudbury Basin, the Sudbury Igneous Complex (SIC) which surrounds the Basin and forms and elliptical collar (60 km by 30km); and an outer 80 km zone of mechanically shocked footwall rocks of Archean granitoids to the north and Proterozoic volcanics, sediments to the south.

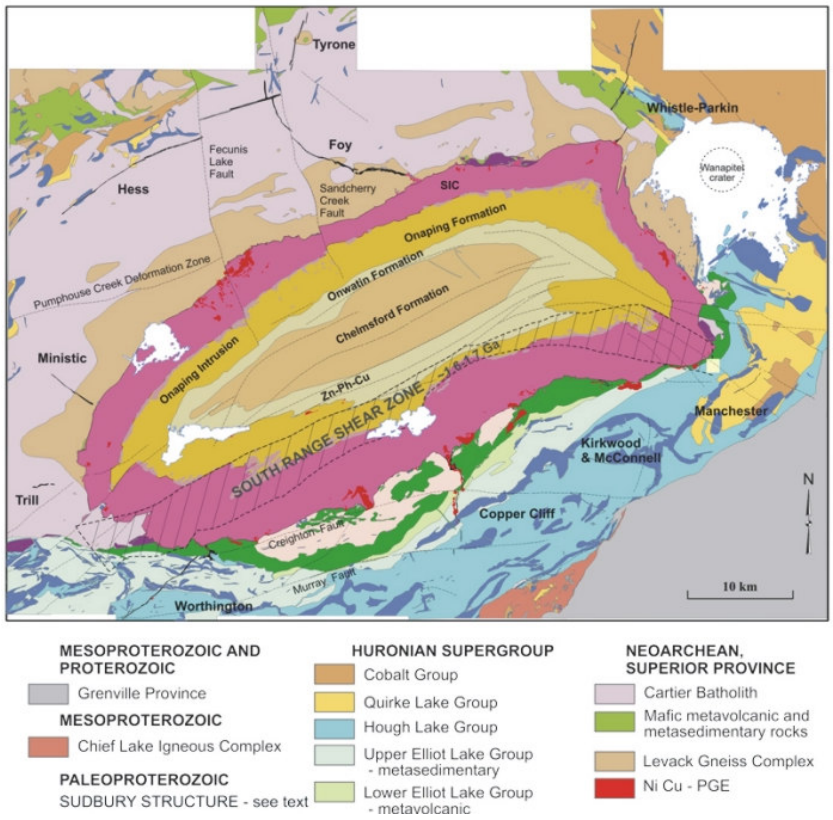

Figure 1.1 Geology of the Sudbury Region and the Sudbury Igneous Complex (SIC).

The Sudbury Structure is an unique geological feature hosting one of the largest concentration of Ni-Cu ore in World; 1500 Mt past and present resource with grades of 1% Ni and 1% Cu and 1 g/t combined Pt and Pd (Farrow and Lightfoot, 2002). The structure has been variously interpreted as the product of explosive volcanism (Muir, 1984), impact cratering (Dietz, 1964) or both impact cratering and magmatism (Dessler et al, 1987; Chai and Eckstrand, 1994). The current interpretation for the origin of the Sudbury Structure is that it represents a tectonized and deeply eroded remnants of 100-200 km diameter peak-ring or multi-ring impact basin (Grieve et al., 1991; Grieve et al.,1995; Deutch and Grieve, 1994). According to this interpretation a 15 km diameter bolide, at speed of 50 km/s impacted the geologically very complex border area of the Archean Superior Province and the Proterozoic Southern Province (Fig 2.1) and excavated a 30 km deep and 100-200 km diameter transient cavity which later became occupied by superheated 1700°C, and 14,000 km^3 crustal melt sheet covered by breccias of the back fall ejectas derived from country rocks

(Deutsch at. al 1995). The shock wave generated during the impact propagated down and outwards from the impact crater and formed deep fractures in concentric and radial patterns occupied by „pseudotachylite" a partially melted highly comminuted rock flour matrix breccia, termed the Sudbury Breccia. Shatter cones, striated conical fracture surfaces typical for meteorite impact sites, also developed in may rock formations. Planar deformation features (PDF; dense parallel planar micro cracks) and other shock metamorphic features are developed in rock forming quartz grains and silicates of many plutonic and metamorphic rocks within the host rocks of Sudbury Structure (Dressler, 1984).

During the cooling and crystallization history of the crustal melt sheet, tectonic-isostatic readjustment of the impact crater caused the impact melt sheet to inject into radial and concentric fractures to form an early (marginal) phase of Quartz Diorite Offset dykes. After this event, density-compositional stratification occurred in the melt sheet and the lower part become saturated in S and sulphide silicate immiscibility occurred (Lightfoot et al, 2001). This first formed sulphide liquid started to deplete the coexisting mafic silicate liquid in Ni, Cu, PGE and much of the sulphide liquid has been removed during a second phase of major injection into radial fractures already occupied by earlier barren quartz diorite. This injection resulted in isolated lenses of inclusion bearing and mineralized central quartz diorite usual size of 300 m long 10 to 40 m wide located either in the center or the at the margin of pre-existing barren inclusion free quartz diorite. Accumulations of sulphides in pipe-like lenses of the late inclusion-bearing quartz diorite form the Offset-type deposits. The remaining sulphide in the density stratified impact melt sheet started to re-equilibrate with silicate liquid partially depleted in Cu, Ni, PGE and the 4 g/cm^3 immiscible sulphide droplets settled out gravitationally trough the 3 g/cm^3 liquid and coalesced at the base of the melt in trap structures. Favorable trap structures existed all around the crater rim in forms of terraces, basal sections of troughs, embayments usually partly covered, filled with breccia, swept out from the crater floor by basal surge during impact or formed by collapses of crater wall and terraces. Immiscible sulphides sank and become trapped into these structures which currently form the contact-type Ni-Cu-PGE ore deposits along the periphery of the SIC. The density stratified meltsheet started to crystallize from the bottom upwards and from the top downwards to form a megascopic layered igneous complex the SIC. The SIC consists of four units which are, from the outside in and bottom to top; Contact Sublayer (xenolithic mafic norite), norite quartz gabbro (transition zone) and Main Mass Granophyre. The Footwall Breccia represents variably brecciated footwall rocks and locally underlies the Contact Sublayer in the Northern part of the SIC. In the South Range, East Range and several zones along the North Range Sudbury Breccia form extensive belts (South Range Breccia Belt, Frood-Stobie Breccia Belt) in approximately concentric arrangement to the SIC. These breccia belts are host to the volumetrically generally smaller concentric quartz diorite offsets.

The Contact Sublayer, the Offset Dykes along with Footwall Breccia are the main host to the Ni-Cu-PGE deposits of the SIC.

Cu-Ni-PGE ores also occur as veins and vein stockworks in footwall rocks (primarily Sudbury Breccia) 100 to 500 meters away from the contact of the SIC. These Cu and PGM-PM enriched ores are interpreted as either hydrothermal deposit units (Farrow, 1994; Watkinson, 1999; Molnár et al., 2001) or as injections of highly fractionated sulphide ore derived from the fractional crystallization of monosulphide solid solution (mms) from a sulphide liquid (Li and Naldrett, 1993; Naldrett et al., 1999). This type of mineralization is well known from the North range and recently become popular for regional exploration (Farrow et al., 2005; Molnár et al, 2001; Hanley et al, 2005; Péntek et al., 2008) around the SIC contact. Although exists, this mineralization type has been rarely studied from the South Range of the SIC and most commonly found to be associated with veins or shear zones in close proximity of primary sulphide mineralization (Molnár et al., 1997, 1999).

The bulk of the deformation of the SIC occurred along the South Range Shear Zone (SRSZ)(Shanks and Schwerdter, 1989). The SRSZ is about 50 km long, 6 km wide and consists of strongly foliated rocks with L-S tectonic fabric developed during a northwest-directed reverse ductile shearing and contraction of the SIC (Shanks and Schwerdter, 1991). The age of this deformation is generally considered to be of Penokean 1.9-1.7 Ma. Fueten and Redmond (1997) first suggested the bulk deformation of the SIC may be have happened synchronous with the ca. 1.45 Ga Chieflakian compressional tectonic-magmatic event based on similarities of orientation, kinematics, and micro-textures of the SRSZ and pre-Grenvillian, Chieflakian shear zones along the GFTZ. Alternatively a Mazatzal-Labradorian age, 1.7-1.6 Ga, ductile deformation of the South-Range SIC was suggested, based on U-P titanite and $^{40}Ar/^{39}Ar$ biotite ages of shear zones from the Thayer Lindsley mine (Bailey et al., 2004).

2. AIMS AND SCOPE OF THE STUDY

The Sudbury Structure is an unique geological feature hosting one of the largest concentration of Ni-Cu ore in world; 1500 Mt past and present resource grades 1% Ni and 1% Cu and 1 g/t combined Pt and Pd. Half of the resource is hosted within quartz diorite offset dykes. Radial and concentric quartz diorite dykes host ore deposits richest in Cu and PGE among the different deposit types of the SIC. Significant sulphide ore deposits (Creigthon, Whistle) are found within funnel-shaped embayment structures along the basal contact of the SIC where quartz diorite dykes originate from and extend for 10 to 30 kilometers into the footwall rocks. These areas therefore are highly potential for Ni-Cu-PGE sulphide ore exploration. In recent times, the exploration potential for low-sulphide Cu-Ni-PGE deposits in footwall rocks along the SIC contact was recognized by many major and junior exploration companies.

One of the aims of this study was to produce a geology and mineralization map of the proximal Worthington Offset which is occupied by the highly tectonized quartz diorite of the Victoria Embayment at the contact of the SIC. Detailed outcrop mapping, at 1:500 m scale, was carried out in order to produce a surface geology map that could serve as a solid geological framework for a number of deposit types located and examined in details in this study. The mapping project was supported by INCO Ltd between 2000 and 2002, therefore the primary focus aimed by INCO was to locate, characterize and carry out reconnaissance surface assay sampling of mineralized areas and describe these occurrences in relation to the local geology. The prospectively of the area based on two past producer mines the Victoria mine and the Vermilion mine as well as a number of mineral occurrences not studied in details. The only operating Crean Hill mine was close to closure in 2000. The Victoria mine is located in a strongly faulted embayment structure, whereas the Vermilion mine is hosted within a Sudbury Breccia Belt extending for many kilometers to the east. This breccia belt is host to two of the largest offset deposits in the Frood-Stobie mines. Only very limited studies and descriptions (mostly company reports, or field reports) exist from the Victoria and Vermilion mines. The Vermilion mine is superior focus of this study from many aspects. The Ni-Cu-PGE deposit of the Vermilion mine appears to be the *locus typicus* of four minerals; sperrylite $PtAs_2$, the most common Pt (and PGE) mineral of the World, michenerite PdBiTe, violarite $FeNi_2S_4$ and arsenohauchecornite ($Ni_{18}Bi_3AsS_{16}$).

The mineralizations mapped on surface have been evaluated to be potential for low-sulphide Cu-Ni-PGE-type mineralization, popular exploration target of recent interests. The most detailed study of Vermilion mineralization was aimed to explain the multistage history of formation of such deposit types and the origin of very complex platinum group mineral assemblage including the four minerals first discovered from this deposit.

The renewed interest in recently (2000) found PGE-enriched deep parts of the Crean Hill mine triggered a mine visit down to the 4040 (1300 m depth) level. Sampling of PGE-enriched sulphide ores of the 4040 level aimed to describe sulphide minerals and to characterize PGE-minerals responsible for the enrichment.

During the early stages of filed mapping, the importance of tectonic elements, a number of narrow northeast-trending shear zones have been recognized. These shear zones are responsible for the segmentation of the once existing Victoria Embayment structure and the Contact Sublayer at the base of the SIC. Field evidences suggested that some of the shear zones have played a major role in re-distribution and re-location of pre-existing magmatic Ni-Cu-PGE sulphides. During this deformation the pre-existing sulphide ores have mostly lost their primary properties and developed geological features not studied specially before.

Exploration activity initiated by FNX Mining Incorporation in 2002 drilled up several tectonized sulphide occurrences located by surface mapping. Exploration drillcores provided an unique source for fresh samples to study this special type of mineralization. Detailed study of the No.2 West Zone was undertaken in order to explain sulphide and PGE mineral composition, formation constraints of deformed sulphides ores, typical for the map area.

Detailed studies of PGE-rich Ni-Cu sulphides of the Vermilion mine and the No.2 West Zone included ore petrography, mineral chemistry, mineral thermobarometry, fluid inclusion petrography and thermometry methods in order to characterize and understand the geological processes responsible for PGE-enrichment and mineralization in these deposits.

Part of this study aimed to characterize the deformation zones at map-, macroscopic- and microscopic scales, deduce the sense of movement and link these structures to known and existing other structural elements of the SIC. Upon recognition of the similarities of deformation features, in the mapping area, to the South Range Shear Zone the possibility arose to age date the deformation. The South Range Shear Zone is a result of whole-scale deformation of the once circular SIC. The age of deformation is still a matter of debate, although few suggestions span between 1850 and 1450 Ma. In this study potassium-bearing syn-tectonic mineral in shear zones were located and sampled for K/Ar and Ar/Ar radiometric geochronology studies.

3. GEOLOGY OF THE SUDBURY REGION AND GEOLOGY, MINERALIZATION OF THE SUDBURY IGNEOUS COMPLEX (SIC)

3. 1. Regional Geology, Geochronology of footwall rocks of the Sudbury Structure

The Sudbury Structure is located near the triple junction of the three main geological terrains of the Canadian Shield; the Superior Province, the Southern Province and the Grenville Province (Fig 3.1). It straddles the main contact between the Early Proterozoic Huronian supracrustal rocks of the Southern Province and Archean plutonic rocks of the Superior Province. The Sudbury Structure lies some 10 km north of the Grenville Front Tectonic Zone (GFTZ) the Northern limit of the Grenville Province.

3.1.1. *Superior Province*

The Superior Province north of the Sudbury Structure comprises several lithostratigrahic components; greenstone belts, metasedimentary belts, felsic plutons, gneiss granulite terrains occurring in alternating E-W trending belts (Subprovinces).

Metavolcanic and associated metasedimentary rocks with felsic intrusives occur in greenstone belts of the Wabigoon, Wawa and Abitibi subprovinces. Zircon U-Pb ages of various rocks of the greenstone belts reveals that post-volcanic tectonism and metamorphism occurred between 2770 Ma

and 2680 Ma (Krogh and Davis; 1971; Percival and Krogh, 1983). Metavolcanic rocks near the Sudbury Structure occur in the Benny and Parking greenstone belts.

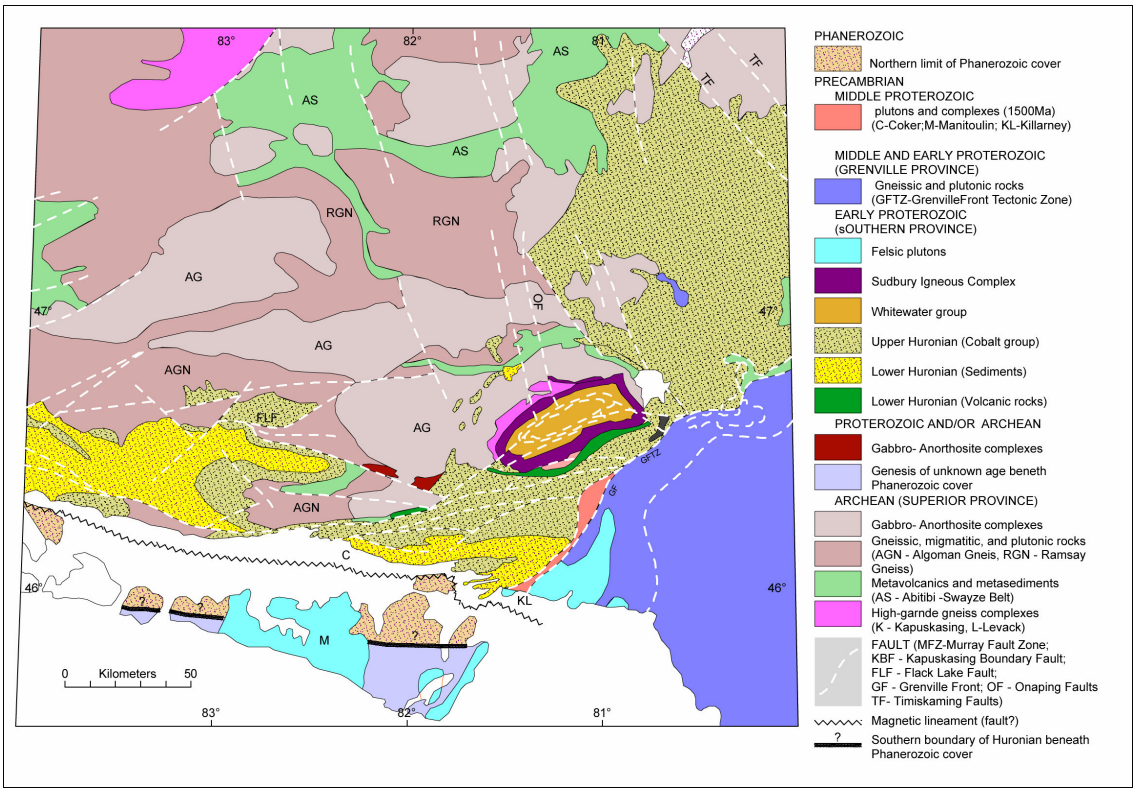

Figure 3.1 Regional Geology of the Canadian Shield around the Sudbury Structure.

The most prominent high-grade gneiss terrain of the Superior Province is the narrow northeast-trending Kapuskasing Zone. The Levack gneiss complex adjoining the SIC is a small but similar high grade gneiss terrain. The Levack gneiss complex (U-Pb: 2711 +/- 7 Ma; Krogh et al., 1984) is comprised of an assortment of felsic, mafic, ultramafic and sedimentary rocks) metamorphosed to granulite facies at depth 21-28 km (750-900 ºC, 6-8.5 kb) at 2647 +6- 2 Ma (U-Pb; Krogh et al., 1984; Wodicka, 1995). The Levack gneiss complex which is inferred to core large paleotopographic dome now occurs as discontinuous fringe around the north margin of he SIC, suggesting it may be the basement of it. The timing of regional amphibolite facies retrograde metamorphism (500-550 ºC, 1.5-3 kb) accompanying uplift to depth 5-11 km is uncertain but may be as late as the Sudbury Event at 1850 Ma (James et al., 1992; Wodicka 1995; Krogh et al., 1984). Contact metamorphic thermal aureole induced by the SIC overlying the Levack Gneiss extends 1.2 km and characterized by three major zones (1) pyroxene hornfels; an assemblage of plagioclase, orthopyroxene, clinopyroxene, (2) amphibole hornfels; amphibole, biotite, quartz and (3) zone of recrystallized stubby desiccate plagioclase (Dressler, 1984). Thermobarometry calculations indicate that thermal overprint occurred at depth 11 km (1.5-3 kb) at temperature 800-1050 ºC (James and Dressler, 1992; Wodicka, 1995.)

Much of the Archean Abitibi Subprovince north of the SIC consist of massive coarse-grained granular to porphyritic felsic plutonic of the Cartier Batholith. The Carter Batholith forms a part of

Neo-Archean Algoma plutonic domain, one of the largest post-tectonic batholitic complexes of the Superior Province (Card, 1979). The Carter Batholith was emplaced at 2642 Ma. (U-Pb on zircon, Meldrum et al., 1997) intruding both the Benny Greenstone belt and the Levack Gneiss Complex.

Approximately 20-25 km north of the SIC isolated remnants of Huronian sediments (see below) form a discontinuous ring that rest unconformable on all rocks of the Archean basement. The occurrences have been interpreted to represent down-faulted cover along a major ring fracture developed as a result of the Sudbury impact (Dressler, 1984; Grieve et al., 1991; Wodicka, 1995).

A large number of northeast trending metamorphosed mafic dykes crosscut all rock types of the Superior province. These dykes are equivalent to the Matachewan dyke swarm and dated at 2452 +/- 2 Ma (U-Pb; Heaman, 1989). Rousell et al., 1997 pointed out that these dykes tend to show radial and locally concentric pattern with respect to the SCI within 10-20 km from its contact. This may indicate that the area occupied by the SIC could have been a local magmatic doming of the Archean crust that may also be responsible for the uplift of deep crustal rock of the Levack Gneiss Complex.

3.1.2. *Southern Province*

The early Proterozoic supracrustal rock sequences of the Southern Province form a discontinuous linear fold belt some 1300 km along the southern margin of the Superior Province. The Southern Province is geographically subdivided into the Marquette Range Supergroup, Animikie Group in the west and the Huronian Supergroup in the East. In the west the Southern Province is transected by the 1100 Ma Midcontinent Rift System, and in the east by the 1000 Ma Grenville Front, the tectonic contact with the Grenville Province (Fig 3.1).

The Huronian Supergroup is a sequence of sedimentary and volcanic rocks up to 12 km thick which thins northward across the Murray Fault Zone to a maximum 5 km. Huronian deposition began at 2450 Ma the age of Copper Cliff Rhyolite in the Sudbury area (Krogh et al. 1984) and was complete by 2200 Ma the age of the Nipissing Intrusive Suite (Corfu and Andrews, 1986). The Huronian Supergroup is composed of four unconformity bounded groups (Roscoe 1969, Robertson et al, 1969) in ascending order: Elliot Lake, Hough Lake, Quirke Lake and Cobalt groups, which overlap northward onto Superior Province Archean Basement. The clastics sediments were derived mainly from the Archean terrain to the north.

The Elliot Lake group at the base of Huronian consists of heterogeneous assemblage of volcanics, turbiditic wacke, arkose and conglomerate including uraniferous quartz pebble conglomerate.

This is succeeded by three sedimentary megacycles, i.e., Hough Lake, Quirke Lake and Cobalt groups, each characterized by an unconformity related lower conglomeratic unit, a middle

siltstone wacke unit, and an upper quartz-rich sandstone unit. The Cobalt Group forms a widespread cover extending far beyond the limit of older Huronian strata.

The Elliot Lake group is the only part of Huronian that contains volcanic formations and it shows lateral changes in faces and thickness of component units throughout the region. The volcanic accumulations, bimodal tholeiitic basalt-rhyolite and mildly alkaline suits, were deposited under subaqueous to subaerial conditions. Layered gabbro-anorthosite intrusions are present at the base of the Elliot Lake group and they constitute part of the Huronian Magmatic Belt (Peck et al., 2002). The distribution and ages of the main elements of the Huronian Magmatic belt are in approximate chronological order (James et al., 2002): basal mafic and felsic volcanic rocks of the Elliot Lake Group at 2450 Ma (Krogh et al., 1984), the north-northeast trending Mattachewan dykes 2452 Ma (Heaman, 1989), and the East Bull Lake Suit (intrusive layered gabbro anortosite sills dykes and plutons; East Bull Lake, Agnew Lake/Shakespeare-Dunlop, River Valley) at 2491-2475 Ma (Krogh et al., 1984; Prevec, 1993). The East Bull Lake Suit intrusives contain economic PGE mineralizations associated with minor disseminated magmatic sulphides (James et al., 2002). Several felsic granitic plutons were also emplaced during the early part of the Huronian. The Murray Pluton (U-Pb, 2477 Ma; Krogh et al., 1984) and the Creighton pluton (U-Pb, 2333 Ma; Frarey et al., 1982) are in contact, more than 20 km in length, with the SIC in the South Range.

A succession of basalt flows and volcanogenic sediments up to 2600 m in thickness (Elsie Mountain Formation) and rhyolite flows (Copper Cliff Formation) up to 2600 m in thickness forms the basal part of the Elliot Lake Group in the Sudbury area. The McKim Formation, a pelite-wacke-quartz arenite unit at the top of the group is 3000 m thick near Sudbury where it thins westward and pinches out near Elliot Lake. In the Elliot Lake area west of Sudbury, the Matinenda Formation, a subarkose with lenses of uraniferous pyritic quartz pebble conglomerate (paleoplacers) were deposited directly on Archean basement and partly on Huronian basalts.

The overlying Hough Lake and Quirke Lake Groups constitute two major sedimentary cycles, each comprising lower conglomeratic unit, middle wacke-siltstone unit, and upper crossbedded sandstone units. Both groups thicken from about 1500 m from the northwest to over 6000 m in the southeast. The upper Huronian the Cobalt Group ha a maximum thickness of 5000 m in the Sudbury area and it consists of a heterogeneous assemblage of conglomerate, siltstone, sandstone, wacke, arkose.

The Huronian Supergroup were deposited under fluviatile, deltaic, and shallow marine conditions in regressive depositional cycles controlled by synsedimentary faulting and differential block faulting of the Archean basement (Card et al., 1984). Each cycle began with normal fault subsidence triggered debris flow resulting in deposition of conglomerate that was followed by wacke and siltstone bouma sequence deposited from turbidity currents in relatively deep waters, in part

deltaic conditions. The upper crossbedded sandstones were deposited after a return to shallow water and emergent conditions. The Gowganda Formation of the Cobalt Group was deposited by glacial processes (Young, 1970).

More than 25% of the areas of the Southern Province in Ontario are covered by gabbroic, tholeiitic dykes and sills of irregular shape intrusive rocks referred to collectively as either Nipissing Gabbro or Nipissing Diabase (Miller, 1911). The Nipissing Gabbro intrusions were emplaced into Archean basement rock and sedimentary rock of the Huronian Supergroup during a major magmatic event spanned a short interval between 2217-2210 Ma (Corfu and Andrews, 1986; Noble and Lightfoot, 1992; Buchan et al, 1998). Stratabound or basal-contact style disseminated, net-textured Ni-Cu-PGE mineralizations are known from many Nipissing gabbro bodies (James et al., 2002).

The Nipissing Gabbro intrusions were emplaced into the Huronian Supergroup after early deformation of the Huronian strata (2450-2300 Ma Blezardian Orogeny) but prior to subsequent deformation and metamorphism during the Penokean (1887-1883 Ma) (Card et al., 1972; Morris, 1997).

Alkali metasomatism, albite, aegirine, riebeckite alteration, is widely distributed in the Southern Province and is spatially associated wit gold m mineralization (Gates, 1991). Schandl et al. (1994) dated this metasomatism from on monazite (U-Pb: 1700 Ma) and noted that it is coeval with a period of granitic plutonism e.g. the Chief Lake Batholith.

Hornblende diabase dykes strike N-W and are associated with faults of the Murray Set (Cochrane, 1991) and they occur along the Creighton Fault from the Creighton mine to the Grenville Front. These dykes are also referred as lamprophyre, quartz diabase or “trap dykes” (Grant and Bite, 1984). On the basis of crosscutting relationship these dykes are younger than quartz diorite but older that olivine diabase dykes.

Olivine Diabase dykes of the Sudbury Dykes are ubiquitous in the Sudbury area and represent the latest intrusive event 1238 Ma. (U:Pb; Krogh et al., 1987).

The Huronian rocks record two major deformation and metamorphic events: an early folding that predated 2210 Ma intrusion of Nipissing Gabbros, and a later post-Nipissing polyphase event that produced folding and thrust faulting of Huronian strata (Card, 1978a,b). Riller et al. (1996) suggested that the early deformation event and amphibolite facies metamorphism were coeval with emplacement of the Creighton and Murray Plutons and this deformation produced south-verging antiforms. Post-Nipissing deformation was associated with greenshist-facies metamorphism of the Matachewan-type mafic dykes, Huronian sediments, Nipissing Gabbro and possible retrograde alteration of the Levack Gneiss. Shortening of the Huronian and deformation of the SIC were accomplished by buckle folding and northwestward thrusting generally thought to be related to the ca. 1900-1800 Penokean orogeny.

3.2. Geology of the Sudbury Igneous Complex SIC

The 1850 Ma old Sudbury Impact Structure straddles the boundary between granitic plutons and gneiss of the Archean Superior Province and Paleoproterozoic Huronian sediments and volcanics of the Southern Province. The Sudbury Structure comprises the sedimentary *Sudbury Basin*, the Sudbury *Igneous Complex (SIC)* and an outer 80 km zone of mechanically shocked footwall rocks.

In a zone up to 80 km around the SIC, the Archean and the Proterozoic Footwall rocks are riddled, with veinlets, dykes and irregular masses of pesudotachylite generally know as *Sudbury Breccia* (Dressler, 1984). Pseudotachylite comprises microscopic to metre-sized fragments and blocks of adjacent wall rock and less commonly exotic material in dark fine-grained to aphanitic matrix. Shock metamorphic features include shatter cones in zones up to 20 km beyond the margin of the SIC and planar deformation features in quartz, feldspar and zircon, and kink bands in biotite up to 8-10 km away from the SIC (Dressler, 1984). Lens or irregularly-shaped breccia bodies, referred to as *Footwall Breccia*, occur within a discontinuous zone up to 150m thick beneath the SIC. The *Footwall breccia* is a heterotypic breccia with angular to subrounded locally derived fragments of diverse size.

The Sudbury Igneous Complex (SIC) is traditionally divided in the geographic North, South and East Ranges. This subdivision reflects geographical differences between the igneous rocks and ore types (Fig 3.2). The main igneous units of the SIC: (1) Dyke-like bodies of quartz diorite termed *Concentric and Radial Offsets* (Thomson 1935; Grant and Bite, 1984). (2) Discontinuous zone of complex inclusion and sulphide-rich rock traditionally termed the *Sublayer* (Pattison, 1979). (3) A norite above the Sublayer in the South Range traditionally termed *Quartz Rich Norite* and the discontinuous zone of orthopyroxene-rich poikilitic melanorite in the North Range traditionally termed *Mafic Norite* above the Sublayer in the North Range (Naldrett and Hewins, 1984). (4) a thick unit of uniform norite termed the *South Range Norite* in the South Range and *Felsic Norite* in the North Range. (5) A unit is called *Transition Zone Quartz Gabbro (TZQG)* between the underlying Norite on overlaying *Granophyre*. All of the units except the Offsets and Sublayer have been grouped into the *Main Mass* of the Sudbury Igneous Complex.

The most basal norites of the Main Mass of the North Range are orthopyroxene-rich poikilitic-textured melanorites with 40-60 modal percent cumulate orthopyroxene, 4-6 modal percent intercumulus augite, 20-40 modal percent intercumulus plagioclase, and 20-25 modal percent intercumulus quartz and feldspar micrographic intergrowths (Naldrett et al, 1970; Hewins, 1971). The overlying felsic norite is marked by a hypidiomorphic granular-textured
norite with <15 modal percent hypersthene, 5-20 modal percent augite; 40-55 modal percent plagioclase, and 20-30 modal percent quartz and micrographic intergrowths (Naldrett et al, 1970); only plagioclase feldspar appears to be a cumulate-textured mineral The overlying TZQG is marked

by the entry of abundant cumulate opaque oxides, apatite and sphene and the disappearance of intercumulus hypersthene; plagioclase retains a cumulate texture (Gasparinni and Naldrett, 1972). The granophyre is marked by the presence of abundant granophyric intergrowths of K-feldspar and quartz with cumulate-textured plagioclase.

The Sublayer occurs discontinuously around the Complex, and traditionally the concentric and radial Offset dykes have been described as variants of the Sublayer (Pattison, 1979). The igneous-textured silicate contact Sublayer below the Main Mass is a fine- to medium-grained norite with low modal quartz content and abundant pyroxenes (Naldrett and Kullerud, 1967; Naldrett et al., 1972; Naldrett et al., 1984) This Sublayer type is gradational into brecciated metamorphic-textured rocks termed *Footwall Breccias* (Pattison, 1979).

Naldrett (1989) noted that the introduction of the *Sublayer* and the *Main Mass* was a complicated process with variable age relationship between these units at different locations. For Example:

(1) Inclusions of Main Mass quartz-rich norite and rocks texturally similar to Main Mass Mafic Norite occur as inclusions in the Sublayer (e.g. close to the base of the Main Mass in the Whistle Embayment (Plate, 3.1)

(2) Dykes of Sublayer norite have been observed in and cutting the Main Mass (e.g. at the Creighton and Little Stobie Mine embayments; e.g. Naldrett et at, 1984; Lightfoot et al., 1993).

(3) Grant and Bite (1984) and Pekeski et al. (1994, 1995) describe field evidence supporting at least two different phases of quartz diorite within the Worthington Offset.

(4) Lightfoot et al., (1997a) showed that inclusions of norite (containing blue quartz, and apparently derived from the Main Mass) occur in the Sublayer-Offset lithologies in the embayment structure north of the old Victoria Mine. Thus, although intrusive contacts and inclusion relationships are recognized, there has never been a complete documented case study which can unequivocally demonstrate the relative sequence of event and the time span covered.

The center of the ring-shaped SIC is called the Sudbury Basin, filled with sediment collectively named the *Whitewater Group* (Fig 3.2). The Whitewater Group comprises four formations; the Onaping Formation, a lower breccia unit at least 1500 m thick; thin 5-50 m Vermilion Formation hosting Zn-Pb-Cu-Ag deposits; the Onwatin Formation, a middle carbonaceous slate some 300 m thick; and the Chelmsford Formation, an upper turbiditic wacke unit 850 m thick.

The Onaping Formation is a thick, unsorted, grossly stratified enigmatic breccia unit composed of fragments of volcanic, sedimentary, and granitic rocks in a variably carbonaceous matrix of devitirified glass shards and mineral fragments. Some stratification is present but the units are thick and lack well-defined bedding except in the upper part. The formation generally fines upward. At the base of the Onaping

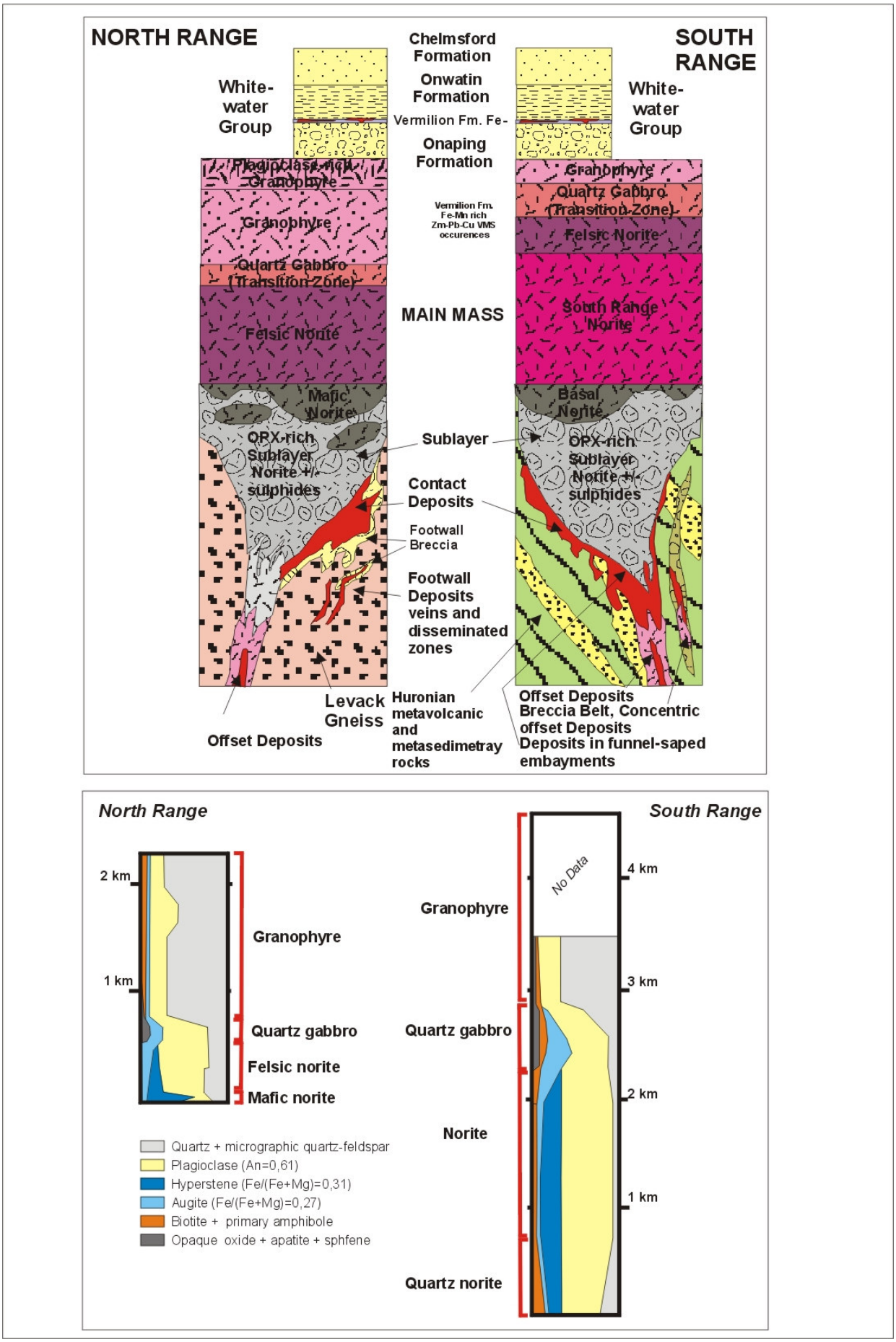

Figure 3.2 Lithostratigraphy, mineralization types and petrology of the SIC.

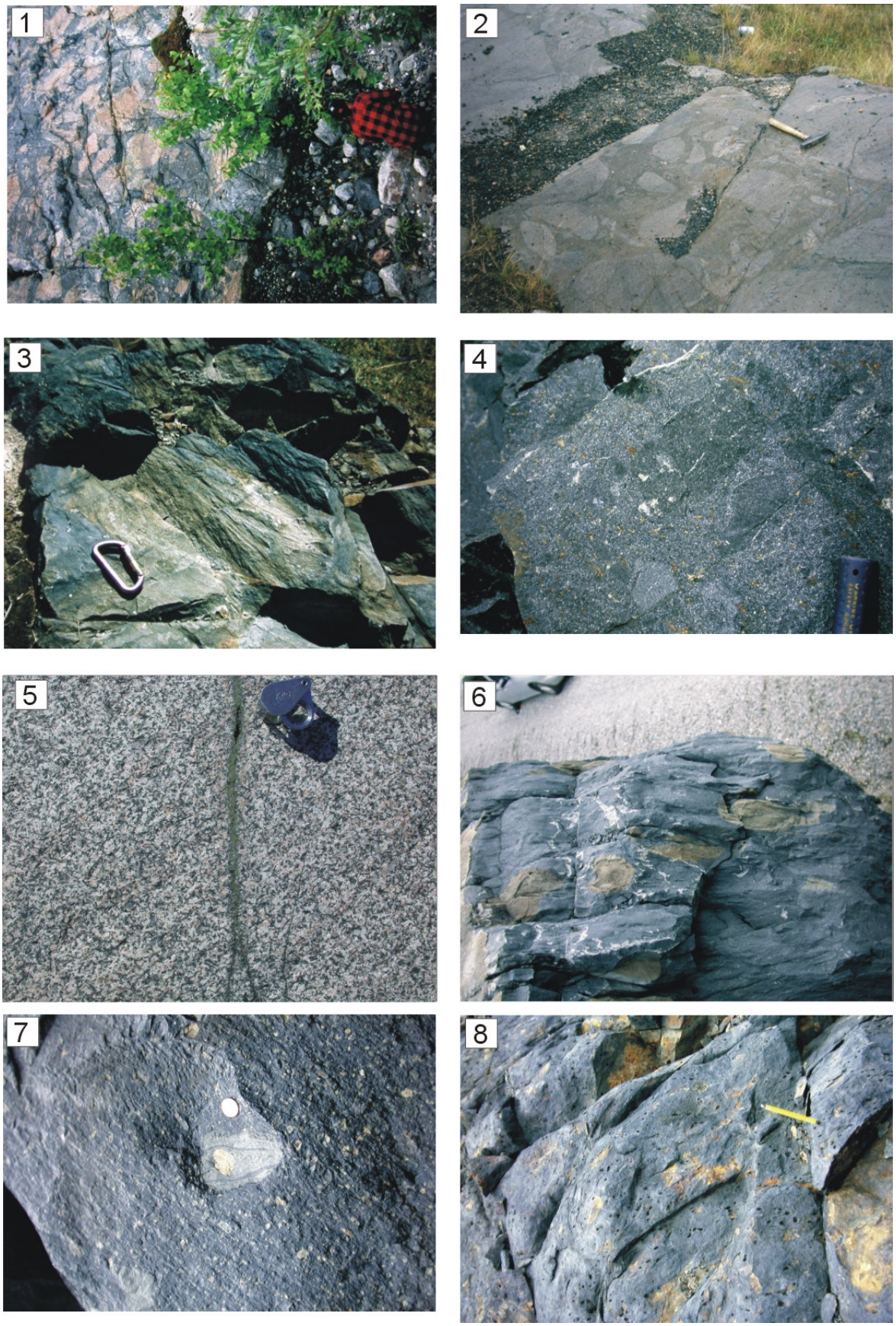

PLATE 3.1. (1) dark-matrix Sudbury Breccia in Levack Gneiss, North Range (2) Sudbury Breccia in McKim metapelite, South Range (3) Shatter Cones in McKim metapelite (4) Mafic Sublayer norite with sulphides hosting inclusions of felsic norite and mafic, ultramafic inclusions, Whistle open pit, North Range (5) Granophyre, with characteristic epidote-actinolite veinlets (6) Chelmsford Formation wacke with carbonate concretions (7) Onaping Formation flow-texture in clast, black carbonaceous matrix, North Range (8) Quartz diorite with blebby sulphides, typical weathered surface outcrop.

there is a discontinuous member containing large blocks of quartzite and granite, some of which show evidence of fusion. The quartzite blocks are similar to some Huronian units, notably the Lorrain Formation, and the granite blocks are similar to Archean granites of the adjacent Superior Province. The lower part of the formation above the basal breccia has lenticular units of hydroclastic breccia composed mainly of juvenile volcanic fragments. The upper part of the formation has laterally continuous stratified units with fewer shards (Gibson et al., 1994). The Errington and Vermilion Cu-Zn-Pb-Ag-Au sulphide deposits occur in Vermilion Formation, a carbonate-chert unit at the top of the Onaping Formation (Ames and Gibbson, 1995). The Onaping Formation has been interpreted as a fallback breccia from meteorite impact (Dietz, 1964) or as a glowing avalanche deposit produced by explosive volcanism (Williams, 1957). Recent studies by Gibson et al. (1994) suggest that hydroclastic volcanism played a major role in the evolution of the Onaping Formation.

The Onwatin Formation has a gradational contact with the Onaping. It is a fine-grained, carbonaceous pyritic slate with a thin local carbonate-rich unit at its base. The abruptly overlying Chelmsford Formation is made up mainly of proximal facies turbiditic wacke (Rousell, 1972) with thick, well-developed bouma cycles. Carbonate concretions are common. Paleocurrent studies show that the Chelmsford depositional currents flowed southwestward parallel to the long axis of the Basin (Cantin and Walker, 1972); this indicates basin was not circular at this early stage in its evolution. The proximal character of the Chelmsford turbidites suggests that the present basin is merely a portion of a formerly extensive depositional regime. The abrupt, possibly disconformable contact between and Onwatin Formation and the sedimentological characteristics of the turbidites suggest that the Chelmsford Formation may represent flysch with northward thrusting during late Penokean orogenic events. This is in general agreement with interpretation of reflection seismic data by Wu et al. (1994) indicating that deposition of the Chelmsford sediments post-dated the major of the Sudbury Structure. The Whitewater Group has been weakly metamorphosed and deformed, especially in the half of the Basin where the rocks are folded into a series of canoe-shaped axial planar cleavage. Along the south side of the Basin, the Whitewater strata dip and face north. The Huronian strata immediately to the south dip and face south. Hence the Whitewater and Huronian strata have a back-to-back relationship across a discontinuity now occupied by the SIC, indicating it is not part of the Huronian.

3.3. Genetic Models of the Main Mass and Ore Deposits of the SIC

Several models exist to explain the origin of the SIC based on geochemical and isotope modeling. One group of models demands wholesale melting of the upper crust in response to a meteorite impact (Faggart et al., 1985; Golightly, 1994; Grieve, 1994). Another model demands 70% contamination of mantle derived magma by upper crust (Naldrett et al., 1986) or permits the addition

of up to 20% mafic magma to a crustal melt (Lightfoot et al., 1997b). A third model considers the marked difference between norite and granophyre, requiring that the granophyre comprises 100 percent impact melt sheet and then noritic rocks comprise mantle derived magmas that were heavily contaminated by lower crustal rocks (Chai and Eckstrand, 1993, 1994)

Early petrography and geochemical studies recognized that the main mass rocks are compositionally very unusual and show evidence of significant crustal contribution, including elevated SiO_2, Rb, and K_2O contents, steep REE profiles and Sr, Nd isotope compositions (Naldrett et al, 1986). The models explained major, trace element, Sr-Nd isotope variation and accommodated the demand for mantle contribution to explain the elevated Ni, Cu, and PGE tenors of magmatic ores. Grieve (1994) modeled that the Main Mass could be generated by in situ melting of the upper crusts. Chai and Eckstrand (1994) that a marked compositional break the TZQG between the Norite and Granophyre could not be readily explained by in situ dedifferentiation of a single magma and they strove to incorporate mantle contribution to the noritic rocks. Mungall et al. (2004) studied the matrix composition of the Onaping Formation (an impact fall-back breccia and concluded that it represents a mixture of the original surficial sedimentary strata, shock-melted lower crust and the impactor itself. Therefore they infer that the hypervelocity impact caused a partial inversion of the compositional layering of the continental crust

The most recent data demonstrate that the norite and granophyre have remarkably similar ratios of incompatible trace elements, although it remains possible up to 20 percent mafic contribution to the crustal melt, there is no major difference in the source characteristics of norites and granophyres (Lightfoot et al, 1997b). Lightfoot et al. (2001) presented new lithochemostatigraphic data on samples collected from several traverses and drill holes across the Main Mass in the North Range (Fig 3.3). Their data indicate systematic major and trace element changes relative to statigraphic position in the SIC (Fig 3.3 A)

The abundances of the Incompatible elements trough the quartz gabbro approach those of the basal granophyre. The sudden decline of trace element abundance levels corresponds to entry of augite. The trace element ratios are consistent throughout the Main Mass expect for Ce/Yb in the quartz gabbro which my have been modified due to the presence of apatite. These features indicate that the norite and granophyre crystallized from the same magma (Lightfoot et al., 2001). The Cu, Ni, and S shows a very strong rapid decline from mafic norite to the top of the felsic norite along with decline of MgO and the wt % S (Fig 3.3B). In the granophyre Cu and S is widely scattered do to hydrothermal alterations. Based on these systemic variations of major, trace, incompatible elements and similar Sr/Nd isotope ratios Ligtfoot et al. (2001) propose that the parental 1700 ºC superheated melt was compositional stratified (Golightly, 1994; Marsh and Zieg, 1999) with composition equivalent to average upper crust. Golightly (1994) proposed hat the Archean footwall granite

gneisses, and Huronian granitiods would have been the principal contributors to the granophyric upper part, whereas the Huronian volcanics and Nipissing Gabbros would have contributed to the noritic lover part of the melt sheet. In this two layer model the norite rock would crystallize from the base upward and the granophyric rocks from the top downward. Lightfoot et al. (2001) showed that the average quartz diorite offset dykes provide a close approximation to the composition of the initial Main Mass melt

The sulphide saturation history of the SIC is closely confined to the early evolution of the impact melt sheet. Lightfoot et al., (2001) showed that main mass rock with higher than 30 ppm Ni have tight linear correlation between Ni and S and Cu and S with constant Cu/Ni ratios. These finding indicate the variation of Ni, Cu, S trough the lower part of the Main Mass is controlled by the abundance of Ni-Cu suplides and sulphides are cogenetic with the underlying Sublayer (Keays and Lightfoot, 1999, 2000).

Variation of whole rock Ni abundance with MgO content of Main Mass with power law arrays for within-plate basalt and picrite (not equilibrated with magmatic sulphides) of West Greenland as well as country rock of the Sudbury structure are shown in Figure 3.3 C (Lightfoot et al., 2001). Main mass rocks with >7 wt % MgO contain nikeliferous magmatic sulphide but rock with lower MgO content plot below the average mantle and crust array lines. The Ni/MgO ratio, the index of sulphide control, falls systemically upward trough the SIC indicative of crystallization of these rocks from a magma which has been stripped of Ni. The Ni and Cu abundances in 100 percent sulphide falls upwards as well from the base of mafic norite to the top felsic norite. This would all indicate (Lightfoot et al., 2001) that the lower part of the melt has equilibrated with magmatic sulphide which settled through the main mass and strongly depleted the melt in Ni and Cu. Consequently the later formed sulphide liquid would have lower Ni and Cu tenor.

The incompatible element concentration in the barren marginal quartz diorite is similar to the felsic norite implying the same parental melt, but the Ni, Cu and PGE contents are markedly higher (i.e quartz diorite with 83 ppm Ni, and norite with 36 ppm Ni). Quartz diorite samples plot over a narrow range of Mg but are displaced to high Ni over MgO values attributed to modal Ni sulphide content. This indicate that the melt gave rise to the quartz diorite has not been stripped of Ni and Cu due to scavenging sulphide liquid prior to its emplacement into the radial fractures as oppose to the felsic norite which has formed from a Ni-Cu-PGE depleted magma. Marginal quartz diorite contains ~83ppm Ni and ~98ppm Cu values which fall within the average upper crust. (Taylor and McLeman, 1985). The main mass magma has been modeled to contain ~210ppm Ni and ~100ppm Cu at initial crystallization of mafic Norite (Lightfoot et al, 2001) and it had ~265ppm Ni and ~172ppm Cu before sulphide segregation. Mass balance calculation for the mineralized sulphide laden central quartz diorite facies and the offset ore deposits indicate a parental magma composition of 310 ppm

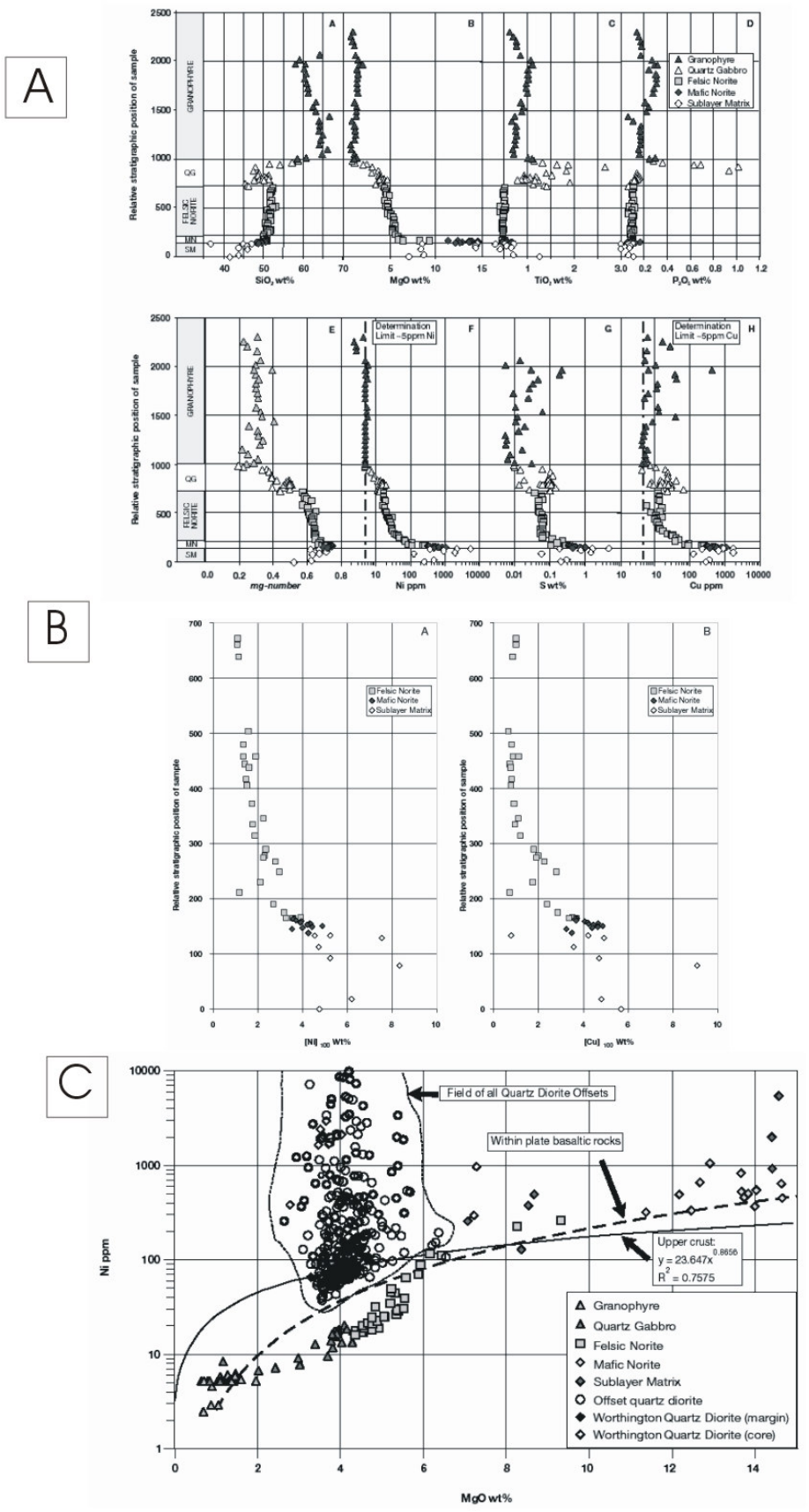

Figure 3.3 Chemostratigaphy of the Main Mass of the SIC (Lightfoot et al, 2001)

Ni and 311 ppm Cu (Naldrett et al 2001, Lightfoot et al, 2001). These values are three times higher that of the marginal facies but (Lightfoot et al, 2001) suggest that segregation into lower mafic and upper felsic melt would account for the difference that happened in between the two major pulses of injection of quartz diorite magma into radial fractures around the SIC. The second pulse of quartz diorite injection would remove the early formed immiscible sulphide liquid having the highest Ni-Cu-PGE tenor and Pd/Ni ratios. The falling Ni/Pd ratios than could explain the sequence of events required to produce the changing Ni and Cu tenors and Cu/Ni ratios of sulphides.

3.4. Genetic Models of Ore Deposits of the Sudbury Igneous Complex

The Ni-Cu-PGE sulphide deposits of the SIC are generally classified into three main groups: (1) Contact Deposits (2) Offset Deposits and (3) Footwall Deposits (mostly Cu-Ni-PGE deposits).

Contact-type Ni-rich deposits are historically the most important ore type in Sudbury and were the first to be mined in the Sudbury camp (Souch et al., 1969). This deposit type located at the base of the SIC within embayment structures, and is hosted in either Sublayer Norite or Footwall Breccia (Souch et al,. 1969; Pattison 1979; Coats and Snajdr, 1984; Davis, 1984; Morrison, 1984; Naldrett, 1984a). Ore deposits of this type comprise inclusion-rich massive to semi-massive sulphides (Plate 3.2/1,2,3). Sulphide assemblage is dominated by pyrrhotite and minor pentlandite, with Cu/Ni ratios of approximately 0.7 and Pt+Pd+Au contents of <1 g/t (Naldrett 1984b, Farrow and Lightfoot 2002). Irvine (1975) suggested that assimilation of SiO_2 rich crustal material by the Sudbury mafic magma could lower the solubility of sulphur and led to sulphide saturation and settling out sulphide liquid gravitationally to from massive orebodies in trap structures at the base of the intrusion/melt sheet. Mineralogy, texture and composition of these ores are easily explained by results of experimental studies of the Cu-Fe-Ni-Cu system (Craig and Kullerud, 1969; Kullerud et al, 1969). Similar studies from the Srathcona mine (Naldret and Kullerud, 1967) indicate that crystallization of monosulphide solid solution (Mss) from immiscible sulphide melt would start about 1125 ºC and pyrrhotite would be joined by magnetite at about 1055 ºC. As temperature decreases, exsolution from Mss occurs with pyrite, below 700 ºC, chalcopyrite below 450 ºC, and pentlandite below 300 ºC. The vertical compositional variation of sulphide ore (increasing Cu toward depth) in many Contact Sublayer deposits has been modelled by fractional crystallisation of sulphide liquid (Naldrett et al., 1997, Naldrett et al., 1999). In this model the residual Cu-rich sulphide liquid escapes from the crystallized Mss and forms Cu, Pt, Pd and Au enriched deeper zones or footwall vein deposits (Fig 3.5). The high Cu content enhances wetting properties of the sulphide liquid facilitating strong mobility (Ebel and Naldrett, 1996). Naldrett et al. (1997) demonstrated that sulphide liquid when succeeded >32 wt. % Cu content will fractionate intermediate solid solution (Iss) as cumulus phase. Naldrett et al. (1999) models the Sudbury Contact Deposit with Rh/Cu versus

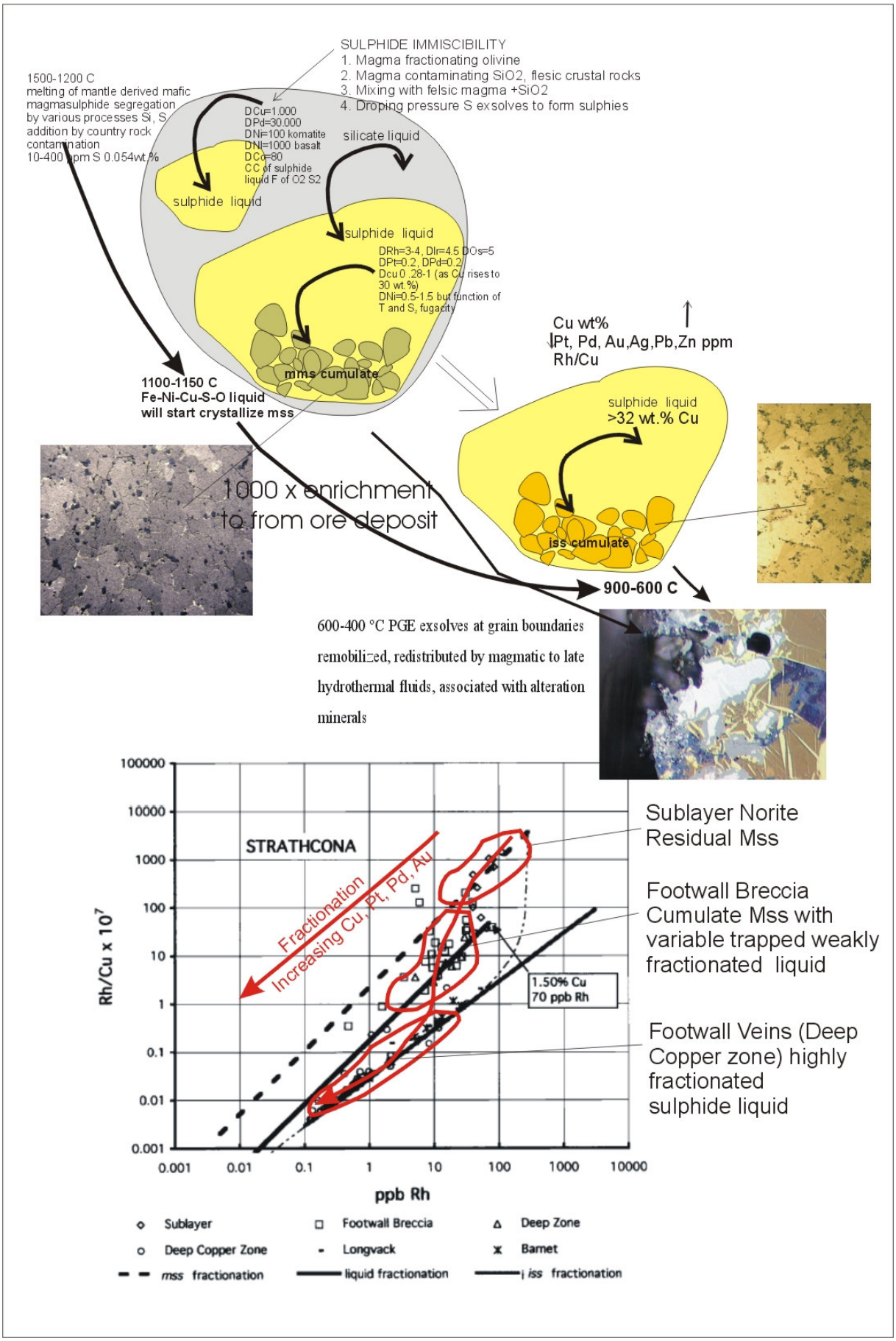

Figure 3.4 Sketch Diagram of magmatic sulphide evolution trend and Rh/Cu vs Rh plot of a contact-type Deposit.

Rh plots, where Rh marks the progress of Mss fractionation whereas variation of the Rh/Cu ratio at constant Rh reflects the proportion of cumulus Mss to Liquid (Fig 3.4).

The most economically productive offset environments to date in Sudbury are radial offsets that extend into the footwall from the base of the SIC, such as the Copper Cliff and Worthington offsets. The deposits are associated with discontinuities along the length of the offsets that may be the result of swells or pinches in the thickness of the dykes due to country rock lithological changes or fault-related displacements (Cochrane, 1984; Mourre, 2000; Farrow and Lightfoot 2002; Lightfoot and Farrow, 2002). The offset deposits are mineralogically similar to contact-type deposits, with dominant pyrrhotite and minor pentlandite and chalcopyrite. The sulphide minerals commonly form 0.5 to 2 cm blebs (Plate 3.2/4,5) or ragged disseminated grains ((Plate 3.2/6) up to 5-50 vol.% and occur in pipe-like vertical bodies within a relatively barren marginal quartz diorite. The offset-hosted sulphides typically have higher base metal tenors than sulphides in contact deposits, higher Cu/Ni ratios (1.5 to 2) and higher PGE contents (Pt+Pd+Au >2.5 g/t) (Farrow and Lightfoot, 2002). The offset deposits are considered to have been formed by second pulse of sulphide-rich quartz diorite (Chapter 3.3) and injected along channels now constitute the pipe-like deposits. Copper-PGE vein systems have been reported in offset-style deposits, typically at the margins to Ni-rich zones in both the Worthington and Copper Cliff offset dykes (Cochrane, 1984; Farrow and Lightfoot, 2002; Lightfoot and Farrow, 2002).

South Range Breccia Belt deposits were classified as a separate deposit type by Farrow and Lightfoot (2002). These deposits, typified by the large Frood Mine system, range from pyrrhotite-rich, Ni-bearing mineralization at higher elevations in the sulphide- mineralized system through to Cu- and PGE-rich mineralization at depth. This type of mineralization is hosted in well-developed zones of Sudbury Breccia that contain pods of barren QD and are developed in Huronian supracrustal rocks.

Footwall-type deposits are characterized by chalcopyrite-rich, PGE-bearing sulphide assemblages, hosted within brecciated rocks in the footwall of the SIC. They are commonly found in the North Range and include McCreedy West, McCreedy East, Coleman, Strathcona, Fraser and Victor mines (Abel et al., 1979; Coats and Snajdr, 1984; Naldrett, 1984; Li et al., 1992; Morrison et al., 1994; Farrow and Watkinson, 1997). Cu/Ni ratios are typically >6, Pt+Pd+Au contents exceed 7 g/t, and the ratio Pt/(Pt+Pd) is between 0.45 and 0.5 in most economic occurrences (Farrow and Lightfoot, 2002). Deposits comprise complex sulphide vein stockworks comprising chalcopyrite, cubanite, with minor pyrrhotite, pentlandite, millerite, bornite and magnetite, and variably developed amphibole, epidote, quartz, chlorite, titanite alteration selvages (Abel et al., 1979; Farrow and Watkinson, 1992; Li et al., 1992; Money, 1993; Jago et al., 1994; Everest, 1999; Kormos, 1999;

Molnár et al., 1997, 1999, 2001). PGM occur as discrete, microscopic (<150 μm in diameter) bismuthides and tellurides that are commonly located at sulphide and silicate grain boundaries. The vein systems are typically oriented sub-parallel to the base of the SIC. These deposit types are classified to (1) sharp-walled vein (2) disseminated low sulphide and (3) hybrid based on basically their massive vein sulphide and disseminated sulphide content (Farrow et al., 2005).

In the last 15 years footwall type deposits have been a major focus of exploration within the Sudbury area. The magmatic sulphide differentiation model cannot explain some features observed in footwall deposits, and the presence of hydrothermal alteration along veins and in the mineral assemblages suggests that hydrothermal processes played a significant role in the ore genesis. One model proposed for origin of footwall ores is that hot, highly saline and acidic hydrothermal fluids driven by the heat of the cooling Sudbury Igneous Complex leached metals from the contact deposits and redeposited them in the brecciated footwall units (Farrow, 1994; Marshall et al., 1999; Molnár et al, 1997, 1999, 2001; Molnár and Watkinson, 2001; Watkinson, 1999; Péntek et al., 2008). Sudbury Breccia has traditionally been considered important in the preparation of the country rock for, and is an important host to, Cu-Ni-PGE mineralization in the footwall (Farrow 1994; Fedorowich et al., 1999; Hanley and Mungall 2003).

These ore deposits are modelled by an evolution form magmatic to hydrothermal conditions (Farrow and Lightfoot, 2002; Molnár et al., 2001, Farrow et al., 2005, Hanley et al., 2005). As the Ni-rich ore bodies evolved down-temperature, intermediate temperature aqueous volatiles circulated in the footwall and offset environments, driven by the heat (Farrow and Watkinson, 1996, 1999; Farrow and Lightfoot, 2002). With continued cooling, the PGE and other metals were variably distributed into the semi-permeable breccias, the Sudbury Breccia. Halogen-bearing aqueous fluids established convection cells driven by the heat of the cooling SIC, thereby contributing to the re-mobilization process (Farrow and Watkinson, 1992, 1997; Li and Naldrett, 1992; Farrow et al., 1994; Jago et al., 1994; Farrow and Lightfoot, 2002; McCormick et al, 2002; Hanley and Mungall, 2003). The fluid flux containing PGE, Cu, Ni, S-species, Au, Te, Bi, C-species, H2O, Cl, and other halogens, Si, Mg, Fe, Ti and LREE became important to the metal transportation process (Farrow, 1994; Farrow et al., 1994; Hanley and Mungall, 2003; Mungall and Brenan, 2003). 'Low-sulphide'-type PGE mineralization was deposited from this fluid as solubility was lost due to decreasing temperature and evolution of the fluid composition through fluid/rock interaction. A final tectonic re-adjustment and the development of dilatational features resulted in the final 'freezing' of the system, possibly as a result of decompression, as the Cu–PGE-rich 'sharp-walled' veins were formed (Farrow et al., 2005).

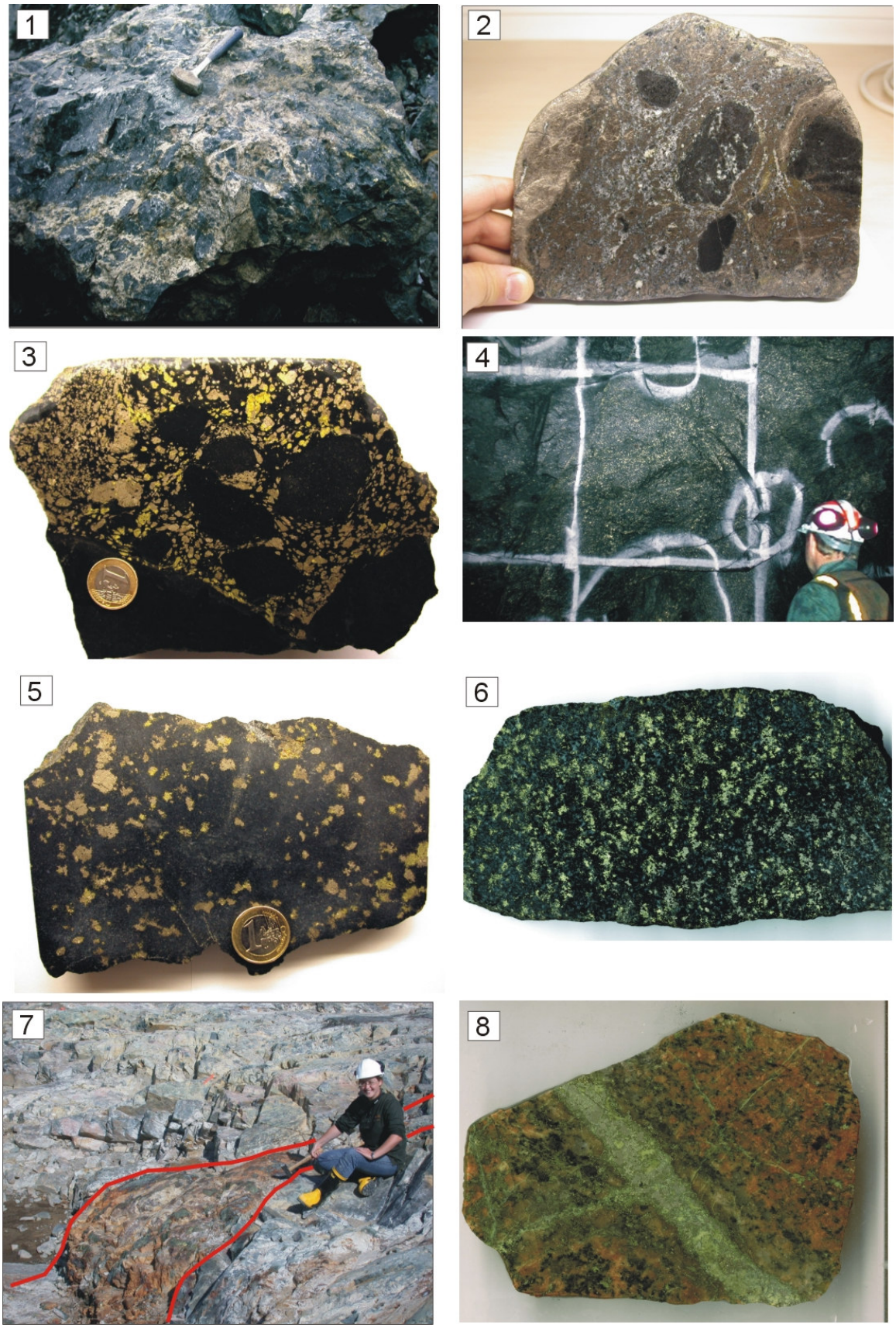

PLATE 3.2. (1) Sulphide matrix breccia of the Contact Sublayer, Whistle open pit, North Range (2) Sulphides in Footwall Breccia of the North Range (3) Semi-massive accumulations of sulphide blebs in inclusions quartz diorite, Copper Cliff South mine (4) High-grade blebby sulphide mineralization in mine exposure, Copper Cliff North mine (5) Blebby sulphide in quartz diorite, Copper Cliff North mine (6) Disseminated sulphide in quartz diorite, Copper Cliff North mine (7) Sharp-walled massive chalcopyrite vein, Podolsky, North Range (8) Quartz-epidote-sulphide-PGE veinlets in the footwall granite of the Whistle Deposit (mined out). The vein is 1 cm in width.

Table 3.1 GSC OPEN FILE 1787: Sudbury Ore mineral list and description (Ames, 2003)

	Mineral	Formula	Description - occurrence
Primary minerals	**pyrrhotite**	Fe1-xSx	massive to disseminated, major part of primary assemblage
	pentlandite	(Fe,Ni,Co)9S8	massive to disseminated, major part of primary assemblage, intergr. .w po, exsolving Ni-py,Ni-po,violarite (s.l.); altering to violarite and other Ni-sulphides
	chalcopyrite	CuFeS2	trace to massive; replacing primary FeNi-sulphides and invading silicates in host rock
	magnetite	Fe3O4	euhedral to rounded crystals in po-pn: minor but essential part of primary assemblage
Other oxides	**ilmenite**	FeTiO3	exsolution lamellae in magnetite and as parallel elongate grains after replacement of mt in po, pn, cpy; discrete grains in gangue
	rutile	TiO2	alteration product of FeTi-oxides
	cassiterite	SnO2	rare
Other copper minerals	bornite	Cu5FeS4	ith Ag in late cpy-bornite veins
	cubanite	CuFe2S3	in Cu-rich veins
	covellite	CuS	alteration of cpy-rich assemblages
	digenite	Cu9S5	rare
	chalcosite	Cu2S	rare
	talnakhite	Cu9(Fe,Ni)8S16	extremely rare
Sn	stannite	Cu2FeSnS4	extremely rare
	mawsonite	Cu6Fe2SnS8	extremely rare
Zn Cd	**sphalerite**	(Zn,Fe,Cd)S	minor but essential mineral in cpy-bearing assemblages
	hawleyite	CdS	extremely rare
Other Fe, Ni sulphides	**pyrite**	FeS2	as euhedral porphyroblasts in po-pn-cpy; Co or Ni-rich, possibly zoned metamorphic
	Ni-pyrite	(Fe,Ni)S2	small euhedral grains (exsolution/alteration) in pn and po
	marcasite	FeS2	alteration product: white granular fine crystals or flamme replace po
	bravoite	(Ni,Fe)S2	small euh. grains (exsolution/alteration) in pn and po
	Ni-po	(Fe,Ni)x-1Sx	small euh. grains (exsolution/alteration) in pn and po
	mackinawite	Fe9S8 (tet.)	rare, could be confused with pyrrhotite
	violarite	(Fe,Ni)3S4	as massive alteration product of pn
	polydymite	NiNi2S4	very rare in altered/metamorphosed assemblages
	millerite	NiS	minor to major mineral in late cpy-rich veins
Ni-arsenides	maucherite	Ni11As8	with nickeline and millerite in cpy-rich veins
	nickeline	NiAs	with maucherite and millerite in cpy-rich veins
	arsenopyrite	FeAsS	rare
	cob-gersd.	(Co,Ni)AsS	quite common in South Range deposits, < common in NR; small white, sharply euhedral crystals in po or cpy, zoned with respect to Co,Ni; occasionally intergrown with sperrylite
	gersdorffite	NiAsS	gersdorffite can occur as anh. to massive grains in contrast to cobaltite
Mo	molybdenite	MoS2	rare; only in South Range deposits -Copper Cliff & Worthington
Pb-minerals	**galena**	Pb(S,Se)	common trace mineral: small blebs in cpy (ass. w. BiTe, sph)
	clausthalite	PbSe	tiny blebs associated with galena, BiTe in cpy
	altaite	PbTe	tiny blebs associated with galena, BiTe in cpy
	wehrlite	*(Bi,Pb)(Te,Sb)*	*mineral name not IMA approved;probably Pb-Sb-bearing tsumoite*
Bi-minerals	native Bi	Bi	rare
	bismuthinite	Bi2S3	rare
	tsumoite	BiTe	most common Bi-mineral: tiny yellowish white anh. grains, in PGM-bearing cpy-veins
	tellurobismuthite	Bi2Te3	rare
	tetradymite	Bi2Te3S	tiny, elongate, white, euh. grains in cpy veins
	pilsenite	Bi4Te3	easily confused with tsumoite
	Bi telluride	BiTe	*unspecified BiTe minerals*
NiBi-sulphides	parkerite	Ni3Bi2S2	rare, w. other Bi-minerals in cpy-rich veins
	hauchecornite	Ni9(Bi,Sb,Te)2S8	rare, chocolate-milk brown anh. grains in cpy; host of wide variety of PGM's
	Te-hauchecornite	(Ni9BiTeS8)	rare, chocolate-milk brown anh. grains in cpy; host of wide variety of PGM's
	As-hauchecornite	Ni9(Bi,As)2S8	rare, chocolate-milk brown anh. grains in cpy; host of wide variety of PGM's
Sb	stibnite	Sb2S3	only in Strathcona
PRECIOUS METAL MINERALS	native Ag	Ag	in bornite-cpy veins w. (AgCuFe)3S2
	Ag-pn	Ag(Fe,Ni)8S8	as pinkish brown "flamme" in cpy, rarely euhedral crystals-Totten
	hessite	Ag2Te	common trace mineral; dirty grey-white associated with BiTe, volynskite, galena in cpy-veins
	empressite	AgTe	rare, only in Strathcona, Victor Deep
	stuetzite	Ag5-xTe3	rare, only at Victor Deep
	dyscrasite	Ag3Sb	extremly rare: only at Strathcona
	acanthite	Ag2S	rare
	naumannite	Ag2Se	rare, only in Barnet and Norman
	matildite	AgBiS2	rare, associated w. hessite, BiTe, gn, etc. in cpy veins
	bohdanowiczite	AgBiSe2	rare, associated w. hessite, BiTe, gn, etc. in cpy veins
	volynskite	AgBiTe2	rare, associated w. hessite, BiTe, gn, etc. in cpy veins
Au	electrum	Au:Ag	rare; small grains in cpy-veins
	native Au	Au:Ag	rare; small grains in cpy-veins
PGE MINERALS	paolovite	Pd2Sn	rare; only in North Range deposits-Victor, Strathcona, McCreedy East
Sn	stannopalladinite	Pd2Sn2	rare; only at Victor Deep & Strathcona
	niggliite	PtSn	rare; only in North Range deposits- Victor deep, Longvack, Strathcona, McCreedy East
Sb	stibiopalladinite	Pd5Sb2	rare; only at Copper Cliff N
	sudburyite	(Pd,Ni)Sb	rare; only at Copper Cliff N and S
	mertieite II	Pd8(Sb,As)3	extremely rare; found in Victor Deep, Creighton
	geversite	PtSb2	extremely rare; only found in Victor Deep
As	**sperrylite**	PtAs2	most common Pt mineral in the S range; small to coarse, euhedral to anhedral commonly associated w. cobaltite/gersdorffite in cpy
	hollingworthite	RhAsS	as submicroscopic inclusions and zones in cobaltite/gersdorffite grains; rare as discrete mineral in amphibole
	irarsite	IrAsS	as submicroscopic inclusions and zones in cobaltite/gersdorffite grains; rare as discrete mineral in amphibole
	ruarsite	RuAsS	as submicroscopic inclusions and zones in cobaltite/gersdorffite grains; rare as discrete mineral in amphibole
Bi	insizwaite	Pt(Bi,Sb)2	rare
	froodite	PdBi2	second most common Pd-mineral after michenerite; can be Au-bearing
	sobolevskite	PdBi	rare
	polarite	Pd(Bi,Pb)	extremely rare; only reported from Copper Cliff N Mine
BiTe	maslovite	(Pt,Pd)(Bi,Te)2	rare
TeBi	moncheite	(Pt,Pd)(Te,Bi)2	rare
TeBi	**michenerite**	PdBiTe	most common PGM; white anhedral blebs in cpy
TeBi	merenskyite	(Pd)(Te,Bi)2	not uncommon
Te	keithconnite	Pd3-xTe	extremely rare
Te	kotulskite	PdTe	rare
	melonite	NiTe2	rare, commonly Pd±Bi or Pt-bearing
ALTERATION MINERALS	hematite	Fe2O3	common alteration mineral
	limonite/goethite	FeOOH	common alteration mineral
	valleriite	4(Fe,Cu)S.3(Mg,Al)(OH)2	rare alteration mineral
	chalcanthite	CuSO4.5H2O	rare alteration mineral
	melanterite	FeSO4.7H2O	rare alteration mineral
	morenosite	NiSO4.7H2O	rare alteration mineral
	annabergite	Ni3(AsO4)2.8H2O	rare alteration mineral
	erythrite	Co3(AsO4)2.8H2O	rare alteration mineral
	akaganeite	betaFe(O,OH,Cl)	rare alteration mineral
	lawrencite	FeCl2	rare alteration mineral
OTHERS	unnamed	Pd(Bi,Sb,Te)	possibly several different minerals with similar formula
	wittichenite	Cu3BiS3	very rare, only in Vermilion
	tetrahedrite	(Cu,Fe)12Sb4S13	very rare, only at Denison Mine
	native copper	Cu	rare, at Copper Cliff, Vermilion
	joseite-B	Bi4Te2S	very rare, only at Frood
	siegeneite	(Ni,Co,Fe)3S4	as euhedral inclusions in po and pn
	stuetzite	Ag5-xTe3	rare, easily confused with hessite
	S-geffroyite	(Ag,Cu,Fe)9(S,Se)8	distinctive blue mineral with native Ag in cpy-bornite veins
	unnamed	(Ag,Cu,Fe)3S2	possibly the same mineral as S-geffroyite with Ag and bornite in cpy-bornite veins
	tellurite	TeO2	only at Norman in intergrowth with AgBi-Tellurides

Table 3.1 Compilation of mineralogy data of ore deposits of the SIC (Ames et al., 2003).

3.5 PGE-minerals of ore deposits of the SIC

The bulk of the PGE in Sudbury ore occur in discrete PGE-minerals rather that in solid solution in sulphides. The only significant Pd carried is pentlandite in Cu-rich Footwall vein deposits with up to 2088 ppb Pd (Li et al., 1992). Sulfarsenides, commonly found in the South Range contain much higher PGE in solid solution that sulphides. Cobaltite-gersdorffite may contain up to 4.5 wt.% Pt, 23.3 wt.% Pd 41.1 wt.% Rh (Cabri and Laflamme, 1984). Discrete PGE-sulfaresines such as hollingworthite (RhAsS), irarsite (IrAsS) and sperrylite often occur as cores of grains within host cobaltite-gerdsdorrfite (Cabri and Laflamme, 1984, Szentpéteri et al., 2002).

The PGM in Sudbury deposit are dominated by tellurides, bismuth-tellurides and in the South Range arsenides. Micheneirte (PdBiTe) is the most common Pd mineral in the Sudbury camp followed by froodite ($PdBi_2$), merenskyite ($PtTe_2$), sudburyite (PdSb), sobolevskite (PdBi), kotulskite (PdTe) in approximate decreasing order of abundance (Farrow and Lightfoot, 2002). Among the Pt minerals sperrylite ($PtAs_2$), completely dominate the South Range and very rare in the North Range. In the North range typical Pt-minerals include moncheite (PtT_2) and rare niggliite (PtSn), insizwaite ($PtBi_2$). More than hundred of sulphide and PGE minerals are described by large number of authors from various deposits of the Sudbury camp. The latest compilation of mineralogy data is presented by Ames et al. (2003: Table 3.1).

4. GEOLOGY OF THE WORTHINGTON, VICTORIA AND VERMILION QUARTZ DIORITE OFFSETS AND THEIR HURONIAN HOST ROCKS

4.1. The Quartz Diorite Offsets Dykes of the SIC

Coleman (1905) first applied the term “offsets” to quartz diorite dyke radiating out form the Main Mass of the SIC. He observed their homogeny and believed that they were related to the SIC. He also noted that quartz diorite offsets show sudden break along strike and dip, without faulting, and these zones are associated with intense brecciation and ore deposits, so he introduced the term “offsets” rather than dykes. Coleman (1913) first applied the term “funnel” for trough-like embayment structures along the SIC/footwall contact which emerge from the SIC. Collins (1934) postulated that offset dykes have formed from escaped magma during final phases of norite differentiation. Burrows and Rickaby (1935) suggested that quartz diorite offset dykes are younger than the Main Mass. Thomson demonstrated that the average chemical composition of quartz diorite is intermediate between the norite and granophyre and it may represent the parental magma composition. Slaught (1951) studied the proximal Copper Cliff Offset and concluded that quartz diorite develops gradationally from basal Main Mass norite confirming the genetic relationship. Morris and Pay (1980) suggested, on the basis of paleomagnetic evidence, that the offset dykes were formed by a series of separate magmatic pulses. Szentpéteri (1999) mapped a central inclusion and

sulphide-bearing and inclusion-free barren phases in quartz diorite of the Copper Cliff Offset (Fig 4.1) Lightfoot et al. (2001) presented a geochemical model (see Chapter 3) for multiple emplacements of marginal barren and central sulphide and inclusion-bearing mineralized quartz diorite facies. A multiple emplacement of the Whistle-Parkin Offset is proposed by Murphy and Spray (2002).

The quartz diorite offset dykes are generally grouped into three major types: (1) Radial Offset Dykes: These begin at embayment of the Footwall contact of the Main Mass and extend for several kilometres into the footwall rocks. (2) Parallel or concentric Offset Dykes: These are continuous to semi-continuous dykes of quartz diorite which strike parallel with the base of Main Mass in zones of massive Sudbury Breccia. (3) Discontinuous Quartz Diorite occurrences. These are small bodies within embayment structures.

The three types of Quartz Diorite Offsets named after the dominant mafic mineral present, are; (1) hyperstene, (2) pyroxene (hypersthene+clinopyroxene) (3) amphibole-biotite quartz diorite. Amphibole-biotite quartz diorite predominantly occurs in the South Range and its composition is generally attributed to regional metamorphic of primary igneous phases (Grant and Bite, 1984). There are eight major quartz diorite offset in the SIC of which the Copper Cliff and Worthington Offset are economically the most important.

4.2. Geology of the Worthington Offset

The Worthington offset dyke is located in Denison and Drury Townships at the southwestern margin of the Sudbury Igneous Complex (Fig 4.2) and extends for approximately 15 km from the main mass of the Sudbury Igneous Complex (Card, 1964, 1968; Ginn, 1965). The offset dyke joins the main mass in an intensely faulted and poorly exposed embayment structure at the Victoria mine. The dyke thins and locally disappears at surface to the south of the Victoria mine before it merges with two irregular sheets of variable- textured, weakly sulphide-mineralized, medium- to coarse-grained quartz diorite in the area north of Ethel Lake (Grant, 1982). Geological mapping presented in this thesis has covered this less constriend proximal segment of the Worthington Offset (see Chapter 6).

South of these sheetlike intrusions, the dyke forms two bodies. The eastern part is not exposed at surface but has been identified in drilling and plunges and broadens at depth toward the southeast (Grant and Bite, 1984). The western part, termed the “Worthington offset dyke,” extends to the southwest for 15 km, with a width of 30 to 100 m and a dip 80 degree to the southeast.

Close to the Sudbury Igneous Complex and to the north of the Creighton fault, the Worthington offset dyke crosscuts Huronian metavolcanic rocks. South of the Creighton fault, the dyke cuts a series of metasedimentary and metavolcanic rocks of the Huronian Supergroup and a series of broadly east-west-trending metagabbro to amphibolite intrusions. These rocks have locally

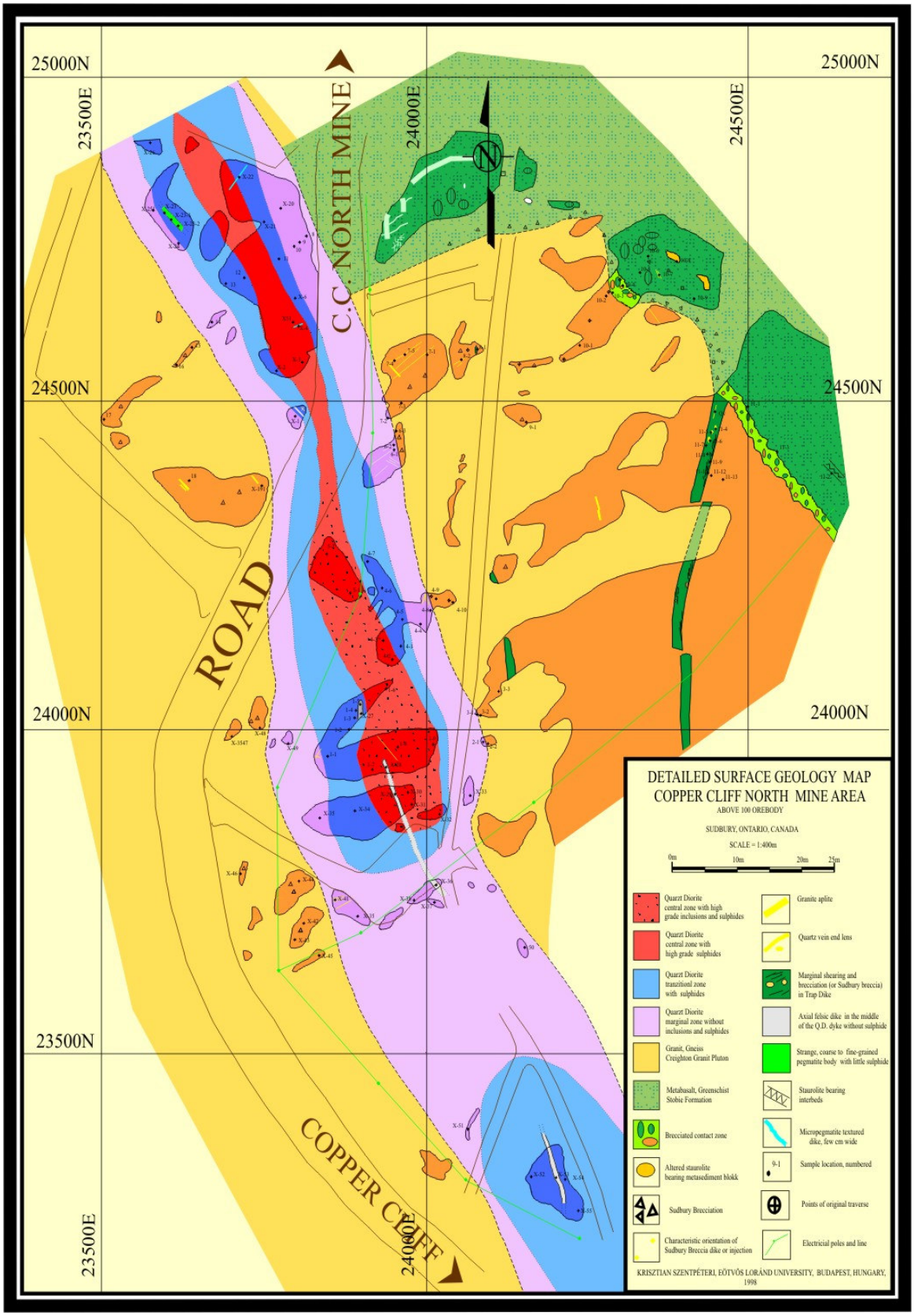

Figure 4.1 Detailed outcrop map of the surface extension of 100 orebody in the Copper Cliff North Offset (Szentpéteri, 1999).

been termed “Sudbury gabbro”; they are grouped with the 2.2 Ga (Corfu and Andrews, 1986; Noble and Lightfoot, 1992) Nipissing gabbro.

Unmineralized quartz diorite of the Worthington offset dyke tends to be in sharp contact with the Huronian metasedimentary rocks but sometimes contains fragments of locally entrained metasedimentary rock along the margin. The margin of the dyke consists of “spherulitic”-textured quartz diorite, a texture of radiating needles of plagioclase and amphibole presumably after primary orthopyroxene, which was most likely produced by primary chilling of the melt against the country rocks and, in places, the matrix and fragments in zones of Sudbury breccia (Grant and Bite, 1984). This quartz diorite grades inward over 1 to 5 m from spherulitic-textured quartz diorite into medium-grained amphibole- biotite quartz diorite, and then over 1 to 5 m into a coarser grained version of the same rock type. These sulphide and inclusion-poor rocks are locally in sharp contact with the inclusion- and sulphide-rich quartz diorite (inclusion-rich quartz diorite), although these contacts can also be gradational over less than 1 m (Lightfoot and Farrow, 2002).

The Sudbury gabbro is composed largely of amphibolite that is texturally similar to many of the amphibolite inclusions within the Worthington offset dyke. In most locations where quartz diorite is in contact with Sudbury gabbro country rocks, the quartz diorite contains 1 to 5 percent sulphide and up to 10 percent inclusions; the chilled quartz diorite and marginal sulphide-free quartz diorite are not developed (Lightfoot and Farrow, 2002). The contacts between Sudbury gabbro and quartz diorite are characterized by a very irregularly textured megabreccia of 0.25- to 10-m-long fragments of amphibolite which are separated by sulphide-bearing inclusion-rich quartz diorite (inclusion-rich quartz diorite) (Fig. 4.3). Locally, the Sudbury gabbro bodies are intruded for 1 to 25 m away from the main offset dyke by stringers of inclusion-rich quartz diorite that carry sulphide. Adjacent to these stockworks, the inclusion- rich quartz diorite that is developed at the center of the offset dyke may contain an anomalously high abundance of amphibolite inclusions which range in diameter from 10 cm to 5 m. There is a continuum from a megabreccia of Sudbury gabbro country rock (5–10% inclusion-rich quartz diorite matrix; 90–95% inclusions) to inclusion-rich quartz diorite (5–10% amphibolite inclusions).

The dominant inclusion types within the Worthington offset dyke are medium-grained amphibolite and metagabbro (Lightfoot and Farrow, 2002). These inclusions tend to be subrounded, they are devoid of sulphides and biotite, and they vary in size from 1 cm to 5 m. The inclusions always occur within the sulphide-rich portions in the dyke core or between the core and one of the margins, where the dyke cuts through Sudbury gabbro. Texturally and mineralogically, the inclusions resemble the Sudbury gabbro country rock. Locally, these groups of inclusions are aligned end-to-end for distances of several meters, but there is no strong preferred orientation of individual inclusions.

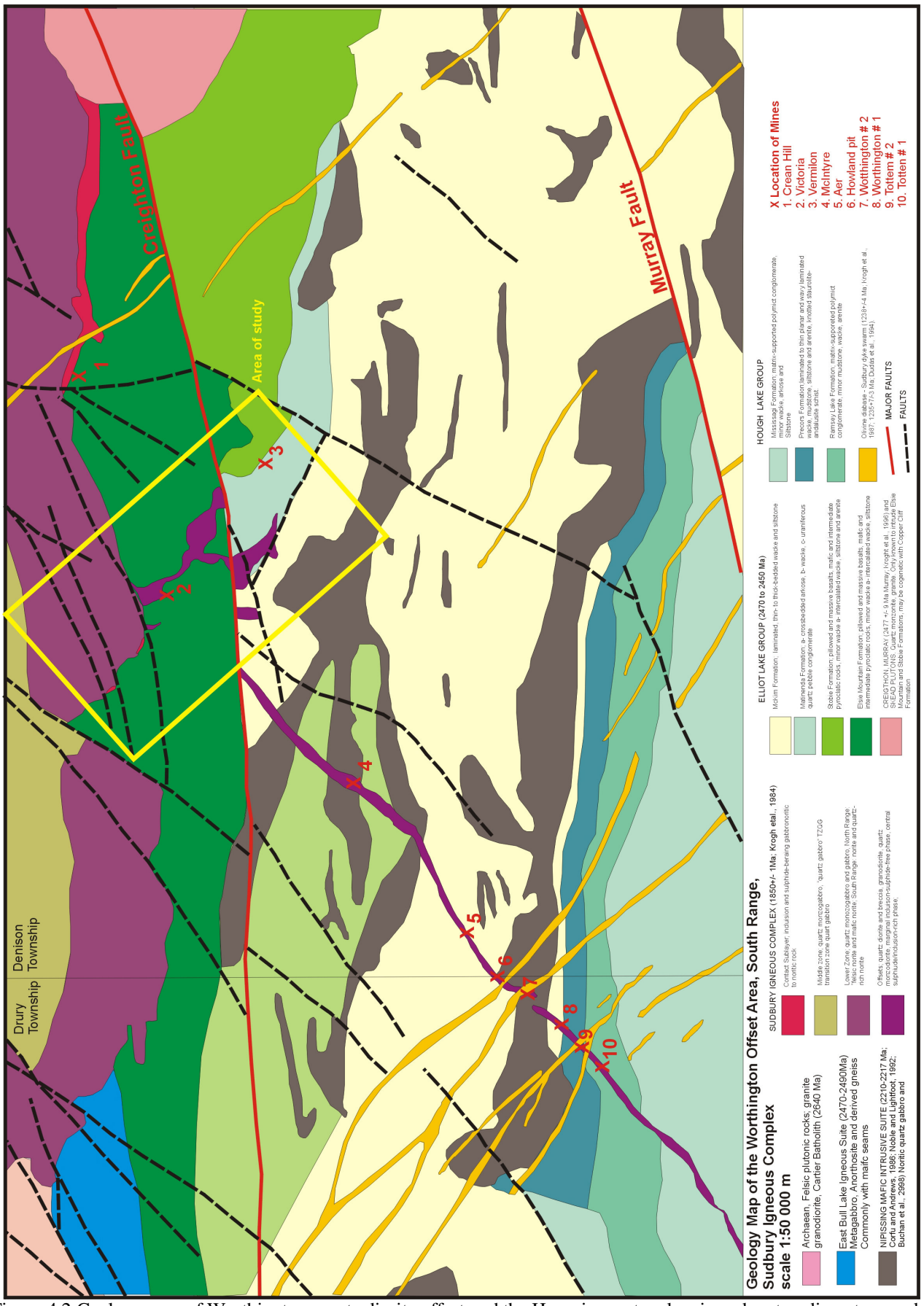

Figure 4.2 Geology map of Worthington quartz diorite offset and the Huronian metavolcanic and metasedimentary rocks in the South Range of the Sudbury Igneous Complex (Card, 1978, Ames, 2003).

Another common inclusion type that occurs in areas of inclusion-rich quartz diorite with abundant amphibolite inclusions is inclusion-poor quartz diorite (Lightfoot and Farrow, 2002). These quartz diorite inclusions range from 25 cm up to 2 m in diameter and occasionally contain small fine-grained amphibolite fragments that are 0.2 to 2 cm in length and have a very strong fabric. The inclusion-rich quartz diorite of the offset dyke contains 1- to 10-mm fragments of fine-grained amphibolite, which may originate from the Huronian metavolcanic country rocks. There is a strong spatial association between inclusions and the location of nickel sulphide mineralization (Lightfoot and Farrow, 2002).

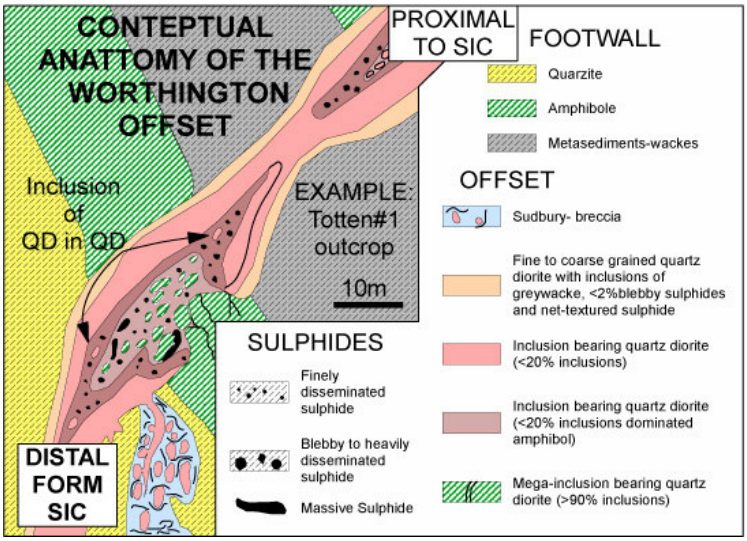

Figure 5.3 Conceptual anatomy of the Worthington Offset (Lightfoot and Farrow, 2002).

4.3. The Vermilion Offset

The Vermilion Offset Dyke consists of several small amphibole quartz diorite pods in a large Sudbury Breccia zone developed at the contact of tholeiitic basalt flows of the Elsie Mountain Formation and feldspar-rich greywacke of Matinenda Formation (Grant and Bite, 1984). The lens-shaped pipe-like quartz diorite bodies occur along 200 m northwest-trending zone, parallel with the eastern limb of the Worthington Offset. The pods are zoned and the centre areas contain local country rock xenoliths, exotic grey gabbro and pyroxenite xenoliths and feldspar rich xenoliths

Precious metals, as well as the copper-nickel sulphides, are within or near the contact of the north-eastern portion of this pod. The quartz diorite pod has a pipe-like shape which plunges steeply to the southwest. A concentration of grey gabbro and rhyolite inclusions occur within the QD pod and it is associated with precious metals. INCO exploration drilling in 1984 confirmed that these inclusions form a vertical train which has the same boundaries as the precious metal distribution. The association between grey gabbro inclusions and precious metal distribution appears to be very strong (Grant and Peredery, 1980). Detailed geology, mineralogy and genetic studies of the Vermilion mine is presented in Chapter 10.

The Vermilion deposit was worked on a small scale intermittently between 1887 and 1918. From 1903 to 1916 over 14000 tons of ore grading 6.611% Ni and 6.89% Cu with 'important amounts' of platinum group minerals were mined (Card, 1968). The ore occurred as small veins and irregular lenses from a few inches to 15 feet (4.57 m) in diameter (the largest being 15 by 38 feet, or 3.57 m by 11.58 m) spatially related to a body of quartz diorite in Sudbury breccia. Mining was on two main levels (50 and 115 feet); the deepest known ore occurs at 150 feet level. Lateral drilling in 1915 from the second level extended 50 feet to the NE and SW and about 100 feet to the NW and SE but found no new ore.

4.4. Huronian Footwall Rocks

4.4.1. *Elsie Mountain Formation*

Mafic dominantly metavolcanic rocks of the of the Elsie Mountain formation (Fig 4.4) are exposed in an NE-SW tending belt along the southern margin of the SIC (Card, 1978a). The formation is intruded by the Gabbro-Anorthosite series the Creighton Granite, Nipissing Diabase intrusives and the quartz diabase, olivine diabase dykes. In the Sudbury area the Elsie Mountain Formation has a thickness of 1000 m and consists of mainly metabasalt with minor intercalated pelitic metasediments and mafic tuffaceous rocks. Mafic flow thickness varies from 30 to 90 m and decrease upward and westward within the formation. The rocks are medium- to coarse-grained to porphyritic with large plagioclase phenocryst of 5 cm. Some flows in the upper part of the formation show pillows, pillow breccias and amygdaloidal tops. Amygdales are composed of quartz, amphibole and chlorite and 1 cm in diameter.

Well bedded pelitic and quartz rich metasediments intercalations are laterally persistent and 9 to 18 m thick. Bedding is about 0.3 m in average and most beds are rich in aluminous minerals such as staurolite, garnet and white micas, those formed during prograde metamorphism prior to formation of the SIC (Card, 1964, 1978a)

The metabasalt of the Elsie Mountain Formation is dark green to black medium- to coarse-grained rock which display coarse gabbroic and fine foliated textures. The metabasalt consists of amphiboles (hornblende, plagioclase (An20 to An 40), quartz, chlorite and accessory biotite, epidote, garnet, apatite, titanite, magnetite, ilmenite, pyrite, pyrrhotite. This assemblage represents a product of metamorphic re-crystallization under amphibolite to greenschist facies metamorphism, that Card et al. (1977) and Card (1978b) considers to be pre-SIC in age. Major oxide and trace element data indicate that the Elsie Mountain Formation metamafic rocks are tholeiitic subalkaline basalts (Card et al., 1977; Grant, 1982). Most of the metasediments intercalations have similar chemical trend to those displayed by the metavolcanics indicating that they were probably derived from the metavolcanics.

4.4.2. *Stobie Formation*

Rocks of the Stobie Formation (Fig 4.4) include mafic metavolcanic flows and intrusions, tuffs, metasediments, overlie the Elsie Mountain Formation conformably or gradationally (Card, 1978a) The contact between the two formations is marked by appearance of sulphide-bearing (> 3 %) pelitic metasediment intercalations. The west the Stobie Formation is intercalated with greywacke and quartz-feldspar sandstone of the McKim and Matinenda formations. The Stobie formation has a 1500 m thickness in Drury Township and

thins rapidly westward. The proportion and thickness (23 to 1.5 m) of flows decreases upward in the formation from about 80% in the lower part and 5 % in the upper part. Rocks of the formation show cyclic repetition, a typical cycle consisting of basalt flow overlain by thin siltstone or greywacke of 0.3 to 3 m thickness, which is in turn overlain by sulphide-free pelite and quartz-feldspar sandstone. The mafic flow tops typically show stirred tops consisting of crude layering and fragmentation of both the basalt and the overlaying sediment. This may suggest extrusion of flow into basins with rapid sedimentation or tops simple represent tuffaceous materials (Card, 1978a).

The Metavolcanic rocks of the Stobie Formation are similar of those of the underlying Elsie Mountain Formation, consisting of massive and foliated fine- to coarse-grained metabasalt. Amygdules are common, and pillows are present.

Sulphide-rich pelitic metasediments of the Stobie Formation contain up to ten percent sulphide minerals, mainly pyrrhotite with lesser amount of pyrite and chalcopyrite (Card, 1978a). Sulphide rich units are in general less than 3 m in thickness but persistent along strike for up to 8 km. Sulphide minerals occur as disseminations, thin stratiform massive sulphide layers and along fracture surfaces. Most sulphide mineral occur in the stirred tops of the mafic flows and their amount increases into the overlaying pelitic metasediments an decreases in the uppermost quartz-feldspar sandstones. Innes (1972) considered these sulphide accumulations as VMS occurrences and suggested that metallic elements were extracted by H_2S-rich hydrothermal solutions, and they were deposited in the overlaying sediments. The volcanic rocks of the Stobie Formation are chemically similar to those of the Elsie Mountain Formation, but slightly richer in alumina.

4.4.3. *Copper Cliff Formation*

Felsic Metavolcanic rocks of the 730 m thick Copper Cliff Formation (Fig 4.4) form a 25 km northwest trending belt along the southern margin of the SIC. They conformably overlay rocks of the Stobie Formation and are conformably overlain by the McKim Formation. The rocks of Copper Cliff Formation represent felsic differentiate of a volcanic cycle which begun with the extrusion of Elsie Mountain basalts (Card, 1968). The major lithologies include; crystal tuffs, flow banded and massive

rhyolite, fragmental units (lithic tuffs). Crystal tuffs are massive non-bedded quartz porphyry. Flow banded rhyolite may represent welded tuff since some of these units can be traced along a 8 km strike length (Burrows and Rickaby, 1934). Fragments units consist of angular fragments of rhyolite in fine rhyolite or dacite matrix. The felsic metavolcanic rocks of the Copper Cliff Formation are composed of fine-grained intergrowths of microperthite, orthoclase, plagioclase, quartz with minor sericite, biotite, chlorite, carbonate, garnet, iron oxides and sulphides. Phenocryst of quartz, plagioclase and microperthite (up to 1 cm) are commonly deformed rotated, reflecting well developed foliation (Card et al., 1977).

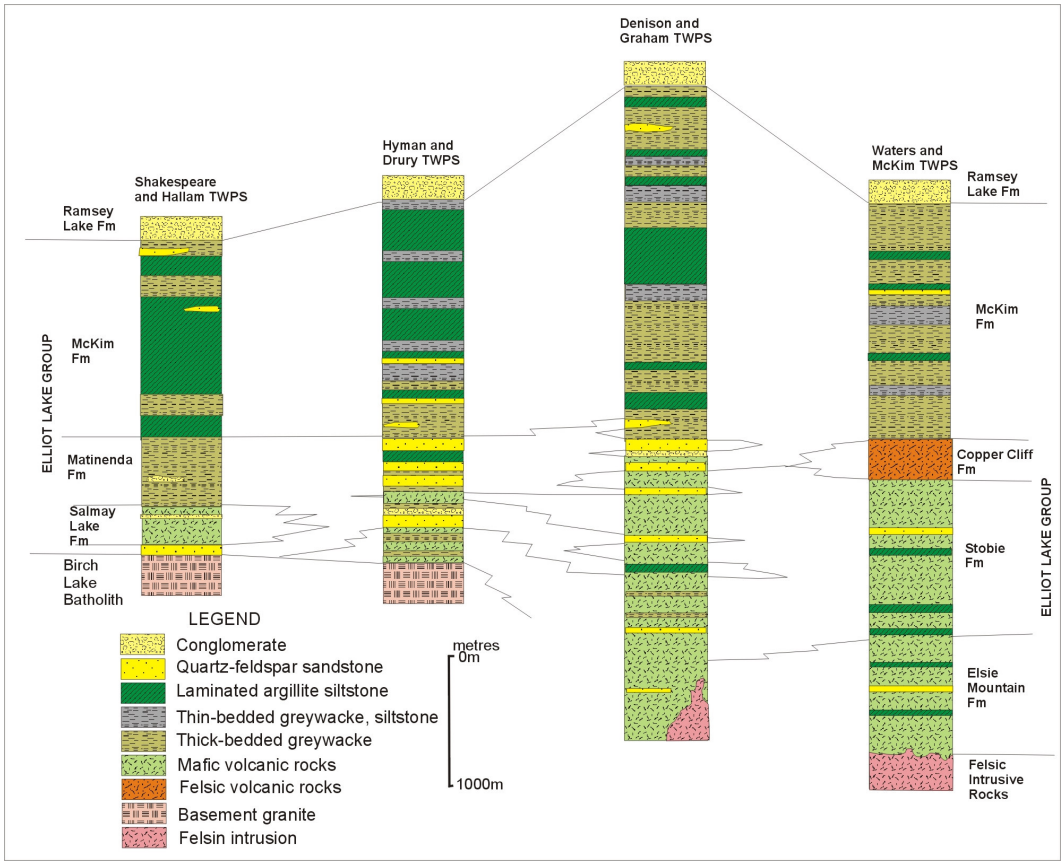

Figure 4.4 Facies variation within the Elliot Lake and Hough Lake Groups, Sudbury Manitoulin Area (Card, 1668)

4.4.4. *Matinenda Formation*

Rocks of the Matinenda Formation (Fig 4.4) include poorly sorted sandstone, metamorphosed pelite and conglomerate in order of abundance. The formation is as thick as 300 meters in the east (Elliot Lake area) and thins out to then east over the mapping area. Here sandstones of the formation are intercalated with thick zones of wacke and metavolcanic rocks of the Stobie Formation (Fig. 4.4). Two main types of sandstone present in the formation; (1) medium- to thinck-bedded, medium- to coarse-grained, poorly- to moderately-sorted white-pink feldspar-rich sandstone and (2) thin-bedded fine- to medium-grained micaceous sandstone that is commonly associated with pelitic rocks.

Sedimentary structures in the Matinenda Formation include, cross-bedding, scour surfaces, cross laminations, parallel lamination, graded bedding.

4.5. Mineral deposits of the Huronian Rocks

The largest and best known deposits (now exhausted) are the paleoplacer uranium deposits of the Elliot Lake area (Agnew Lake, Pronto mines) in pyritic quartz-pebble conglomerate of the Matinenda Formation (Innes and Colvine, 1984). The Huronian volcanic and intercalated sedimentary units contain relatively small volcanogenic (VMS-type) copper deposits (Patter mine) (Innes and Colvine, 1984) or Zn-deposits of massive sphalerite (Ginn, 1965). Nipissing Diabase intrusions are associated with disseminated to semi-massive Ni-Cu-PGE sulphide mineralization at several locations (James et al., 2002). Massive sulphide accumulations are located at the base of intrusions and characterized by economically potential grades of 1.5% to 3% Ni+Cu and >250 ppb PGE (James et al., 2002). The only identified mineral occurrence is the Shakespeare Deposit with inferred resource of 3.6 Mt 0.4 % Cu, 0.34% Ni and 1 g/t PGE. (Falconbridge Ltd, 2002). The Nipissing intrusions are locally also associated with hydrothermal carbonate-quartz veins containing complex Au, Ag, Pb, Zn, Cu, Co, As, Bi, U, Ba mineralization (Cobalt Camp) (Innes and Colvine, 1984). Gold mineralization is locally associated with Nipissing intrusives but generally occur along fault zones or in silicified metasedimentary rock of the Huronian Supergroup (Card, 1978a).

5. METHODOLOGY

5. 1. Field Mapping, Map Construction

An initial field mapping program was carried out by using classical triangulation method with simple field geology tools; Freiberg-type geology compass and hip chain and/or metal measuring tape. A base station was established with referenced GPS lat/long coordinates and all field points were recorded as azimuth of bearing and distance as polygons. Survey stations were set on major outcrop and the shape and dimensions of outcrops were drawn on vellum paper laid on a field board. Several field polygons were linked back to the base station allowing error calculations. The resulting outcrop map was finally copied onto a master sheet where geological interpretation was made.

In the later phases of mapping, a base map was constructed from existing 1980-1981 INCO Company maps (GEOL, L-50-W and GEOL, K-50_W), partly covering the targeted mapping area of the thesis. In this base map, the major assess roads, outlines of lakes, pounds and rivers were shown. Field mapping was carried out at a scale of 1:500 m for most of the mapped areas. At the Vermilion mine and Victora mine sites a more detailed scale 1:200 m and 1:400 respectively was applied. Field mapping polygons were initiated from roads and ended up on roads again for easy identification. The several field sheets of outcrop mapping were compiled onto a main vellum sheet and then scanned

into digital images in raster (jpg) format. The jpg images were imported into Corel Draw software and fitted together to develop a summary outcrop map of the entire area.

Four black and white digital scans of 20 cm by 20 cm aerial photographs, taken in 1980, of the study area were obtained. The scanned aerial images were used to correct some of the positions of the outcrops. In the final state of mapping tree layers; the base map, the aerial image and resultant geology map were all overlain and fit together by the Corel Draw software.

5.2. GIS database

In year 2005, four sheets of scale 1:20 000 m topographic maps were obtained as coloured geotiffs from First Base Solutions Inc, Markham, Ontario. The geotiffs were registered and georeferenced into UTM(NAD83) Zone 17. This coordinate system was used for the GIS compilation of all existing maps and spatial information. Geology map constructed in this thesis, base map used for field mapping, and aerial images were all georeferenced by MapInfo software. The geology map was digitized into MapInfo and finalized into a workspace. Map illustrations of this thesis were printed of this final unified workspace. All GIS referenced spatial information made through this work or compiled/used by this work are located onto a DVD of Appendix 1.

5.3. Field observations, sampling

During field/outcrop mapping general field tools e.g., 10 x hand lens, pen magnet and pen scribe, were used to identify minerals and describe rocks macroscopically. At some important areas cleaning of outcrops were carried out by hand or brush or occasionally using bleach to remove thick caribou moss. A Freiberg-type geology compass was utilized to measure planar and liner data, wit and accuracy of approximately five degrees.

Within the shear zones, several structural measurements were taken to average the final reading which was then added to the map. Outcrop-scale macroscopic kinematic indicators such as drag folds, sheet folds, and sigmoid streaked vein fragments were observed and analysed for interpretation of movement. The shear zones mapped at several outcrops were linked during interpretation of mapping and final map construction (Appendix 1). All samples, sampled for micro-structural geology measurements, were oriented on the outcrop before collection. Oriented sampling required accurate locating and outcrop characteristics where several lines could have been drawn onto the sample surface. These lines included the traces of horizontal and vertical planes in addition to the line of the measured feature such as foliation or lineation as well as pitch if it was observable. Orientation lines were drawn onto rock surface using the libels of the Freiberg-type geology compass.

A total of 296 samples were collected for microscopic petrography, micro-structural geology, fluid inclusion and radiometric geochronology geochemistry and assay studies.

5.4. Sample preparation, Petrography

Standard petrography studies were carried out on 171 polished thin sections and grain mounts. Petrographic and fluid inclusion samples were prepared in the rock laboratory at Carleton University, Ottawa, Canada and thin section laboratory at Eötvös Loránd University, Budapest, Hungary.

Routine petrography work on polished thinsections was carried out on Zeiss Axioskop research-grade transmitted and reflected light polarizing microscope at the Department of Mineralogy, Eötvös Loránd University. Microscope-spectrophotometry measurements for rapid identification of minerals during ore petrography were carried out on same microscope equipped with a Zeiss MPM 400 Microscopy Spectrophotometer. Modal mineral compositions of rocks were estimated by digital image analysis of thinsections scanned in plane- and crossed-polarized lights.

Micro structural kinematic indicators were observed in oriented thinsections cut from oriented samples. A pair of thinections were cut and polished from oriented samples; one is perpendicular to the foliation and parallel with the stretching lineation (or vertical) and the other is perpendicular to the foliation, near horizontal.

Microscopic shear sense indicators were collected during routine petrography. Simple optical method was used for collection of rotation and tiling angles of feldspar porphyroclast in cataclastic protomylonite zones, as well rotation angle measurements of sub grain boundary in deformed quartz porphyroclasts in sheared quartz-rich sediments. Quartz and carbonate C-axis orientation data were collected by 5-axis universal stage from oriented thinsections. Universal stage data was plotted by StereoNett 2.46 freeware software.

5.5. Mineral Chemistry

Sulphide and silicate mineral grains in polished thin sections were examined by scanning electron microscopy (JSM-6400), and analyzed using energy-dispersive spectrometry (SEM-EDS) at Department of Earth Sciences, Carleton University, Ottawa. Quantitative analyses were made on a Camebax MBX electron microanalyzer using wavelength dispersive spectrometry (EPMA-WDS). Operating conditions were 20kv accelerating potential and a beam current of 35 nA. Counting times were 30 s or 40 000 counts, whichever was achieved first. Raw X-ray data were converted to elemental wt. % by the Cameca PAP matrix correction program. A suite of well-characterized natural and synthetic minerals and compounds were used as standards.

Thermobarometry calculations were performed on amphibole-plagioclase, garnet-amphibole, garnet-biotite mineral pairs based on cation exchange reactions according to Blundy and Holland, 1990; Thompson, 1976; Holdaway and Lee, 1977; Perchuk and Lavrentjeva, 1983; Dasgupta et al., 1991; Bhattacharya et al, 1992 as well as Ti and Al substitution in amphibole (Hammarston and Zen,

1986; Thomas and Ernst, 1990; Hollister et al., 1987; Johnson and Rutheford, 1989; Blundy and Holland, 1990, Ernst and Liu, 1998).

Chlorite thermometry calculations were based on their chemical compositions, (Wiewióra and Weiss, 1990) obtained by the microprobe according to Cathelineau, 1988; Kranidiiotis and MacLean, 1987; Jowett, 1991; Zang and Fyfe, 1995.

5.6. Fluid Inclusion Studies

Fluid inclusion microthermometry was carried out on doubly polished thick (70 to 150 μm) sections at the Department of Mineralogy, Eötvös Loránd University on quartz, calcite and clinozoisite from veins with a Chaixmeca type apparatus calibrated using synthetic fluid inclusions and pure chemicals for achieving 0.1°C, and 1.0°C reproducibility during freezing and heating runs, respectively. The apparatus was mounted on a Carl Zeiss Jena, Amplival Pol polarizing microscope. Regular polished thinsections were first investigated by the aid of petrographic microscope. Fluid inclusion petrography helped to establish common fluid populations in the samples. Only those samples were selected for fluid inclusions microthermometry measurements, in which, fluid inclusion petrography study clearly indicated the primary and/or secondary nature of inclusions and the size of inclusions were found good enough for clear observations Fluid inclusion data were evaluated using Excel software and using pre-written macros based on equations of Bodnar (1994), Zhang and Frantz (1987) for calculating salinity and isochors. Raman spectroscopy studies have been performed on one selected sample from the No.2 West Zone and one sample from the Vermilion mine in order to clarify the presence of CO_2 and other compressed gases in the vapour phase in some fluid inclusions. Analysis of three fluid inclusion samples has been performed at University of Vienna with Leica Reinshaw RM-1000 Raman Microscope fitted with red (632.8 nm) laser, calibrated by Si intensity. The other sample has been analysed with a Jobin-Yvon Labram Raman microscope using a 532.06 nm laser at Budapest University of Technology and Economics.

5.7. Geochemistry

Fire Assays of outcrop grab-samples were submitted to INCO Technical Services, laboratory and analyzed with traditional Ni-Fire Assay for base metals and Pt, Pd, Au. Lihtogeochemistry samples were submitted to and analysed for major oxides, trace elements and sulphur isotope in the laboratory of Geological Survey of Canada by combined whole rock XRF, ICP MS (Au+34) and Mass Spectroscopy methods. Detection limits for major elements varied between 0.02% and 0.5 % and 1-5 ppm for trace element depending on the element. Supplementary Pt, Pd, Au analysis have been performed in Activation Laboratories Ltd., Ancaster, Ontario, by ICPMS method. Detection limits were 0.3 ppb for Pd and 2 ppb for Pt and Au.

5. 8. K/Ar Geochronology

K/Ar dating has been performed in the Institute of Nuclear Research of the Hungarian Academy of Sciences (ATOMKI), Debrecen, Hungary.

K concentration has been determined with flame photometry on a pulverized 50 mg split of the samples after digesting it with HF + HNO_3 and dissolving in 50 ml strongly diluted HCl. K concentration has been measured, after a further dilution pending on the K concentration and the addition of 100 ppm Na as buffer and 100 ppm Li as internal standard, by using standard solutions of K.

Interlaboratory standards LP-6 for Ar and HD-B1 for K have been used for calibration, Ar fractionation in the mass spectrometer has been checked by everyday measurement of atmospheric Ar. Accuracy of measurements has been shown by the result of an interlaboratory calibration (Odin et al., 1982).

The standard stable isotope dilution techniques has been used for the determination of radiogenic Ar. A set of samples has been loaded into the Ar extraction line which has been evacuated and baked at about 250 ºC for 2 days. Samples were dropped in turn into a Mo crucible and degassed at about 1400 ºC with high frequency induction heating. The ^{38}Ar spike has been introduced into the extraction line before beginning the degassing of the sample. Ti sponge, SAES getters of St707 type and glass cold fingers cooled with liquid N_2 have been used for cleaning the Ar. Ar has been transported within the system by charcoal fingers cooled with liquid N_2.

The cleaned Ar has been directly introduced into a magnetic sector type noble gas mass spectrometer of 150 mm radius and 90º deflection degree, which was operated in the static mode. The mass spectrometer and the extraction line were designed and built in the ATOMKI. Details of experimental techniques, the parameters of the instruments have been described by Balogh (1985). 4-11 mg minerals have been used for Ar determination.

Error of analytical ages is based on the equation given by Cox and Dalrymple (1967) and cited by Dalrymple and Lanphere (1969) and modified in order to account for the ^{36}Ar content of the ^{38}Ar spike (Balogh, 1985) and considering the nonlinear dependence of age of older rocks on the ^{40}Ar (rad) content. Possible effect of „sampling error” has been disregarded

5. 9. Ar/Ar Geochronology

The samples were crushed, washed in deionized water, dried at room temperature and sieved to obtain the size fractions of (1) 0.25-0.125 mm (2) 0.125-0.080 (3) >0.06. The final separates were analyzed by X-Ray powder diffraction method on Siemens D5000 equipment to monitor the monominerralic composition of each final separates. Results indicate that all separates contained one

mineral phase in between 95 and 100 vol. % (Appendix 13). Mineral separates were washed in acetone, dried, wrapped in aluminum foil and stacked in an irradiation capsule with similar-aged samples and neutron flux monitors (Fish Canyon Tuff sanidine (FCs), 28.02 Ma (Renne et al., 1998).

The samples were irradiated at the McMaster Nuclear Reactor in Hamilton, Ontario, for 90 MWH, with a neutron flux of approximately $6x10^{13}$ neutrons/cm^2/s. Analyses (n=44) of 20 neutron flux monitor positions produced errors of <0.5% in the J value.

The samples were analyzed at the Noble Gas Laboratory, Pacific Centre for Isotopic and Geochemical Research, University of British Columbia, Vancouver, BC, Canada. The mineral separates were step-heated at incrementally higher powers in the defocused beam of a 10W CO_2 laser (New Wave Research MIR10) until fused. The gas evolved from each step was analyzed by a VG5400 mass spectrometer equipped with an ion-counting electron multiplier. All measurements were corrected for total system blank, mass spectrometer sensitivity, mass discrimination, radioactive decay during and subsequent to irradiation, as well as interfering Ar from atmospheric contamination and the irradiation of Ca, Cl and K (Isotope production ratios: $(^{40}Ar/^{39}Ar)_K$=0.0302±0.00006, $(^{37}Ar/^{39}Ar)_{Ca}$=1416.4±0.5, $(^{36}Ar/^{39}Ar)_{Ca}$=0.3952±0.0004, Ca/K=1.83±0.01($^{37}Ar_{Ca}/^{39}Ar_K$)).

5. 10. X-ray powder diffraction analysis

X-ray powder diffraction analyses (XRD) have been performed on SIEMENS D5000 equipment at the Department of Mineralogy, Eötvös Loránd University, Budapest. Acceleration voltage was 40 kV with 40 nA beam current, and 2 sec detection time at 0.05 degree steps. Diffractograms were acquired in electronic format (.raw) and have been evaluated using PowderX and EVA (Brooker) software at the Department of Mineralogy, Eötvös Loránd University, Budapest and at Miskolc Technical University.

6. RESULTS OF FIELD MAPPING: GEOLOGY AND MINERALIZATION OF THE AREA BETWEEN THE VICTORIA AND THE VERMILION MINES

6.1. Introduction

This chapter is based on the interpreted geology map presented in Appendix 1. The description of geology, rock units and mineral occurrences of the mapping area will start from the north and proceeds to the south. First, a cross section across the SIC/footwall amphibolite contact is described northwest of Mond Lake. Than the area with faulted bodies of the Victoria quartz diorite offset was mapped between the Mond Lake and Ethel Lake. Finally, the area south of Ethel Lake, including the Vermilion mine site is described and discussed. Detailed studies of selected deposits characteristic for the map area, tectonic and geochronology study of the shear zones north of Victoria mine are discussed in separate subsequent chapters.

6.2. South Range Norite

6.2.1. *Occurrence*

In the northernmost part of the mapping area, typical South Range norite is exposed. In this area South Range norite is about 1400 m thick and the Transition Zone Quartz Gabbro (TZQG) is relatively thin at about 300 m or partially absent. The granophyre thickens up to a maximum of 5.5 km due to tectonic repetitions in the South Range Shear Zone (SRSZ). The granophyre and transition zone quartz gabbro do not crop out in the mapping area.

6.2.2. *Field Characteristics*

The South Range Norite is a fine- to medium-grained mesocratic equigranular, greenish grey-colored rock in outcrops. Macroscopically, the rock consists of 1 to 4 mm plagioclase, minor quartz, large 1 to 5 mm pyroxene, altered to amphibole and chlorite (Plate 06.2, 5). The mafic mineral content of the rock is about 25-35 vol. %. The South Range Norite is cut by several 1 to 10 m wide northeast-trending shear zones. Several outcrop form steep cliffs and alignment along the shear zones, therefore the deformation zones can be traced easily on aerial photographs. Cataclastic fracturing, grain size reduction, and chlorite alteration occur along the numerous shear zones. South Range Norite occasionally contains 1 to 10 cm thick quartz, quartz-sulphide veins with chlorite, amphibole and carbonate alteration within the vein and along the vein walls (Chapter 7). These veins occur only in close proximity, i.e. within 200 to 300 m distance from the contact with Basal Norite, a quartz-rich norite, Contact Sublayer and metavolcanic footwall rocks. The presence of these veins indicates local and minor hydrothermal re-mobilization of magmatic sulphide ore that occurs in Contact Sublayer to the South. Aplitic felsic dykes are 10 cm to 1 m think and found mostly in South Range Norite. The contact zone of the South Range Norite has been mapped in details along 1600 m length north of the abandoned Victoria mine site (Appendix 1). To the north of the Victoria mine the contact is tectonic and defined by the northeast-trending Victoria Shear Zone. Northwest of the Victoria mine the contact zone is northwest-trending and it is cut by several narrow northeast-trending shear zones parallel- sub-parallel with the main Victoria Shear zone.

6.2.3. *Petrography*

Petrography study of five South Range Norite rock samples indicates an average composition of 65% clouded plagioclase, 10 % pyroxene, 25 %amphibole, chlorite, quartz, epidote, sericite. Plagioclase is subhedral blocky and typically clouded by sub-microscopic inclusions, therefore it is pinkish-brown and semi-transparent (Plate 06.2, 5). Minor quartz is interstitial to plagioclase. Plagioclase is partially recrystallized into fine polygonal aggregate of albite, quartz, platy chlorite

and rare amphibole. Some grains are completely altered to epidote, sericite and chlorite. Augite is coarse-grained, 2 to 4 mm, subhedral, subophitic, moderately pleochroic, colorless to light green. It is completely or partially altered to fibrous actinolite. Augite is schillered contains extremely fine, oriented exsolutions of ilmenite platelets. This schiller texture disappears by the alteration of pyroxene. Two types of amphibole can be distinguished based on optical and morphological properties. Colorless to slightly pleochroic actinolite forms coarse fibrous aggregates, probable pseudomorphs, after pyroxene. Patches of fibrous amphibole appears randomly in large altering pyroxene. Strongly pleochroic, green-bluish green, hornblende forms homogenous rims on fibrous actinolite aggregates, or on pyroxene. Chlorite, carbonate, quartz and rare albite occur together in fine interstitial aggregates or they form micro shear-bands, indicating minor partial re-crystallization of the rock due to non-penetrative deformation between the observed shear zones. Alteration mineral assemblage indicates a greenschist facies metamorphic alteration.

6.3. Felsic Aplitic Dykes

6.3.1. *Occurrence*

Felsic aplitic dykes are ubiquitous in the mapped SIC rocks in the area but only rarely found in footwall units, mostly in Nipissing Gabbro. During mapping, felsic aplitic dykes were found most commonly in South Range Norite.

6.3.2. *Field Characteristics*

Felsic aplitic dykes are light grey to white colored, fine-grained equigranular-textured on outcrops (Plate 6.2, 1, 2), light grey pinkish colored when freshly broken. Some of these dykes show sheared walls along its contact with the enclosing norite. The orientation of these larger dykes seems to be consistent northwest-southeast. Their width varies between 5 cm to 1.5 meter. Thicker individual felsic dykes can be followed along strike for several tens of meters. They intrude all SIC units and are strongly associated with shear zones. Field evidences suggest that felsic dykes were emplaced prior to the shear zones, they are often boudinaged or truncated by the shear zones or faults. Most of the felsic aplitic dykes show a constant macroscopic composition of about 30 vol. % quartz and 70 vol. % feldspar.

6.3.3. *Petrography*

Petrography study of some felsic dykes show that they exhibit hipidiomorphic-xenomorphic equigranular texture of 0.5 to 0.7 mm grains. Aplitic dykes are composed of 60-70 vol. % euhedral blocky albite and polycrystalline granular aggregate of interstitial quartz referring to later re-crystallization of magmatic quartz (Plate 6.1, 3, 4, 5). Strongly strained magmatic quartz contains

abundant fluid inclusions whereas recrystallized quartz is inclusion free (Plate 6.1, 6). Re-crystallization takes place along grain boundaries of quartz and albite. Albite displays a distinct chessboard twinning patterns, a combination of pericline (010) and albite (001) twining visible on the 100 sections under crossed polars (Plate 6.1, 3, 4, 5). Accessory minerals include pyroxene, biotite, and amphibole. Trace minerals; zircon, rutile, titanite are ubiquitous. Zircon is quite frequent and forms large, 10 to 300 μm, strongly zones crystals (Plate 6.1, 7). Alteration minerals; chlorite, epidote (often zoned), carbonate (Plate 6.1, 8).usually occur within microscopic veins or in micro-shear bands.

6.3.4. *Timing of Emplacement*

Microtexture; deformed (bent) albite, partial re-crystallization, zoned mineral grains all suggest that these dykes were emplaced prior to deformation along the shear zones. The modal mineralogy of the dykes refers to trondjemitic composition. These dykes have been rarely studied in the SIC and were observed only in the eastern South Range where they appear to cut across the contact between South Range Norite and footwall amphibolites (Ames 2002, pers. com.). The dykes are considered to represent the minor melts formed due to the thermal contact of the SIC and mostly originated from the Creighton and Murray felsic plutons. Ames et al. (2003) dated these dykes at 1848+/-4 Ma coeval with the SIC. Narrow axial felsic dykes were described from the Copper Cliff quartz diorite Offset (Szentpéteri, 1999) with mostly granitic composition. Those dykes may have formed during late crystallization of the quartz diorite magma.

6.4. Mafic norite

6.4.1. *Occurrence*

This rock type locally occurs in between the South Range Norite and the quartz-rich Basal Norite, observed only north of No.2 West Zone. The rock is quite distinct from the South Range Norite on outcrops and it is distinguished by its darker color and apparently finer-grain size. In fact petrography studies revealed that the distinct macroscopic features are the result of intense chlorite-pyrite hydrothermal alteration of the quartz rich norite which is the basal unit (Basal Norite) of the SIC in the South Range. Although mafic norite is rather an alteration zone it forms a mappable unit about 40 to 60 m wide and 300 m long, traceable along northwest strike in contact with the quartz-rich norite. The physical contacts in the field neither with South Range Norite, nor with the quartz rich norite (Basal Norite) were found, but the striking difference between these rocks may suggest the contact to be sharp.

6.4.2. *Field Characteristics*

When wet, the mafic norite is massive dark greenish-grey to black in color and contains 0.1 to 5 mm, 1 to 5 vol. % euhedral, hexahedral pyrite and 1 to 4 mm occasional quartz with a very distinct blue color (Plate 6.2, 6). When the rock is dry, large 1 to 3 mm biotite flakes and subhedral pyroxene grains can be seen more easily. Quartz-calcite- actinolite (radial fibrous) veins and patches with chalcopyrite occurs along fractures or shear planes in close proximity to the main mylonite zones (Chapter 7).

6.4.3. *Petrography*

Petrography studies of the mafic norite indicate an average mineralogical modal composition of 40-50 % chlorite, 30 % amphibole 5-10 % quartz, and 10 % plagioclase, and sericite, biotite, apatite and pyroxene. Augite forms the coarsest 1 to 5 mm grains in the rock. It is anhedral subhedral, usually with blocky embayment that are now filled by aggregates of chlorite-biotite, or amphibole. This remnant texture refers to original poikilitic-subophitic texture in which the chadacrysts were plagioclase and hypersthene. Augite is schillered, contains very fine parallel trails of inclusions, well preserved in the cores of the crystals. Inclusions are hair-like rodlets of ilmenite and/or magnetite and anhedral phase that was probably orthopyroxene. Augite is progressively altered to amphibole at its edges, removing the characteristic schiller texture and exhibiting more intense pleochroism.

Amphibole usually forms euhedral-subhedral blocky or platy crystals, fibrous aggregates, probably pseudomorphs after hypersthene. Lamellar twins are observed but difficult to see due to the fibrous habit. Pleochroism of amphibole is variable and often colorful; usually pale yellow –green – slight bluish green. The composition of amphibole varies between actinolite and actinolitic hornblende (Table 6.1). Amphibole often alters to fine grained platy aggregates of chlorite-biotite. There seems to be a variation in the amount of these fibrous actinolite aggregates between samples that could represent the original orthopyroxene-clinopyroxene ratio. The biotite content of the rock is about 3-4 %. There are two types of biotite: (1.) Large, 2 to 4 mm, homogenous grains mimicking the sub-ophitic habit of augite. Augite is occasionally mantled by this type of biotite. Biotite contains minute mafic inclusions or anhedral masses of leucoxene-ilmenite. (2.) Smaller platy crystals of biotite form fine aggregates. Biotite-chlorite aggregates appear to be pseudomorphous after amphibole or biotite-1. Rarely some parts of the large biotite grains are recrystallized into fine platy biotite. The composition the coarse biotite is intermediate between phlogopite and syderophyllite (Table 6.2).

Plagioclase is rarely observed. It is difficult to see any grains in the rock but remnant texture suggests that plagioclase was a large blocky cumulus phase in the rock. Plagioclase in this rock type is intensely altered to a chlorite>>sericite>biotite -quartz-albite mass. This alteration gave rise the

appearance of a fine grained mafic rock in the field. Interestingly no epidote grains are observed in this fine alteration mass.

Chlorite occurs as platy crystals mostly in plagioclase but in amphibole and biotite too. The chlorite content of the rock may vary between 20 and 50 %.

Quartz is anhedral, interstitial strained, contains inclusion of sulphide blebs, mainly chalcopyrite along microfractures. Quartz often shows the "flood" texture which refers to optically continuous quartz grain in many separated interstitial pore spaces. Apatite is included in quartz as thick 0.4 mm, almost blocky grains.

Sulphide minerals present in mafic norite is ubiquitous pyrite and traces of pyrrhotite, chalcopyrite. Pyrite occurs as weakly disseminated euhedral solitary grains or groups of grains. Pyrite appears to be enriched along small fracture planes (or shear bands) associated with quartz and amphibole. Small amounts of chalcopyrite and pyrrhotite are associated with pyrite.

6.5. Basal Norite (quartz-rich norite)

6.5.1. *Occurrence*

The Basal Norite constitutes the outermost (lowermost) variety of the South Range Norite. It develops a 50 to 80 m wide mappable unit along, an about 800 m strike length, of the northwest-trending contact zone between the South Range Norite and the mafic metavolcanic rocks of the Elsie Mountain Formation. The Basal Norite is spatially strongly associated with the mineralized Contact Sublayer. It is not know however if the Basal Norite occurs to be the outermost phase along the contact zone north, northwest of the Victoria mine. Here the contact is deformed by the Victoria Shear and covered by the Mond Lake.

6.5.2. *Field Characteristics*

In the field, this rock is characterized by its coarse-grained granular texture, striking occurrence of coarse, 1 to 4 mm large blue quartz and the coarse 1to 5 mm moderate biotite content (Plate 6.2, 7). Basal Norite often contains blebby, disseminated sulphides of pyrrhotite, chalcopyrite, and pentlandite up to a maximum of 2-3 vol. %. Macroscopically, the Basal Norite is mesocratic, medium-grained, and consists of about 55 vol. % plagioclase, 25 vol. % amphibole, 10 vol. % biotite, 7 vol. % quartz and 2-6 vol. % sulphides. The maximum sulphide content decreases farther away from the contact with the Contact Sublayer and it changes from place to place along this contact. At one place, No. 1 West mineral occurrence sulphides (pyrrhotite, chalcopyrite) appear as fine millimetre thin parallel vein network oriented parallel to a the Victoria Shear Zone (Plate 6.3). This kind of distribution of sulphides gives the outcrop characteristic striped weathering pattern. The

phenomenon is seen within a few metres from the contact with the Victoria Shear Zone along which the mineralization is truncated.

The macroscopic characteristics of Basal Norite are different from both the South Range Norite and the Contact Sublayer and make the Norite a consistent distinct map unit. On field outcrops where the contact is observable this rock type represents the contact phase of the South Range Norite. However, outcrops that would contain only South Range Norite and amphibolite footwall (without intervening Sublayer) contact were not found, so it is not clear that the Basal Norite is related only to places where the Contact Sublayer exists. On the final, interpreted map, it is shown that this unit is a continuous rock type along the entire contact (Appendix 1, MAP-1, and MAP-2). Its direct contact with the Contact Sublayer (sublayer norite) appears to be sharp but hardly visible in the field because of the common strong deformation in such contact zones (Far West Zone). There is a slight variation in grain size, at some places Basal Norite is very coarse, 4 to 8 mm, and it becomes slightly finer away from the contact. The contact with the chlorite-altered mafic norite is not observed on outcrops but could be either gradual or sharp.

6.5.3 *Petrography*

Petrography studies of 12 thinsections of Basal Norite revealed an average modal composition of plagioclase 55%, amphibole 35%, biotite 7%, quartz 7%, and minor pyroxene, chlorite, carbonate, and epidote. Sulphides consist of pyrrhotite, chalcopyrite, pentlandite, pyrite, sulfarsenides associated with ilmenite and rutile.

Plagioclase is subhedral, blocky, randomly oriented, shows no igneous foliation and contains fine-grained chlorite-epidote-quartz aggregates depending on the type and grade of alteration. The composition of plagioclase is labradorite (An_{52-63}). Occasional, rock forming K-feldspar >1% also occurs in this rock type. About 10-30 % of the plagioclase grains are altered, however, a distinct pink-brown clouding is often seen in plagioclase predating the above alteration.

Amphibole is subhedral; prismatic, tabular, inhomogeneous, zoned. Grains are strongly embayed, resorbed usually by quartz. Some grains contain relict pyroxene cores while amphibole makes up the complex rims. There are two types of amphibole rimming the residual pyroxene cores (Fig 6.1). Rim-1 has pale green-yellowish green pleochroism similar to fibrous actinolite which often forms the cores of pyroxene pseudomorphs. Electron microprobe result indicates that fibrous core and rim-1 are actinolite. Rim-2 forms the outermost phase and it has green to bluish green pleochroism, similar but weaker as of hornblende. Rim-2 rarely contains anhedral biotite. Microprobe results indicate the composition of this outermost rim is actinolitic hornblende (Table 6.1).

Quartz is coarse-grained, strongly strained, displays subgrain development with undulose or mosaic extinction, partly polygonized into recrystallized fine unstrained aggregates. Magmatic quartz is transparent colorless in thin sections, no blue coloration can be seen.

Biotite forms rare large, 1 to 4 mm individual flakes, which display slight kinking or undulose extinction, with smaller anhedral grains attached to actinolitic amphibole. Biotite composition is intermediate between siderophyllite and phlogopite, but slightly richer in phlogopite (Table 6.2). Minor chlorite (clinochlore) is associated with biotite and amphibole (Table 6.3).

6.5.4. *Petrography of sulphides*

Sulphides in Basal Norite occur rare 3 to 5 mm blebs, more frequently as disseminated 1 to 4 mm grains with irregular outline or very fine grains, <1 mm. Larger, 1 to 4 mm irregular aggregates of sulphides are intergrown with epidote, chlorite, carbonate, biotite. These alteration minerals occur, finely disseminated, in the groundmass as well. When these minerals are in contact with the sulphide aggregates their grain size is about 10 to 20 times larger, their crystal forms are much better developed than in the groundmass. The coarse, 2 to 5 mm sulphide aggregates are usually surrounded by a halo of very fine disseminated sulphides, suggesting that the original interstitial or blebby sulphide has interacted with fluids, that might have also caused the intergrowths with the coarse minerals.

Sulphides compose of abundant pyrrhotite and chalcopyrite. Pyrrhotite contains veins and massive grains of pentlandite, partly altered to violaritie. Ilmenite is deformed, contains deformation lamellae and alters to leucoxene (rutile, titanite). Pyrite is rarely associated with the silicate alteration rim surrounding sulphide aggregates.

6.5.5. *Sulphide mineralization of the Basal Norite*

Disseminated and/or rare blebby sulphide content usually increases toward the contact with mineralized Contact Sublayer but do not show economic concentrations. One grab assay sample of the disseminated sulphides in Basal Norite, close to the Contact Sublayer sample, indicate minor sub-percentage metal content; 0.23 % Cu, 0.20 % Ni with no traces of PGE (Appendix 8, 9).

Significant surface gossan can be found in Basal Norite only at one Location, the No.1 West occurrence. Here extensive trenching indicates that the prospectively of the area was recognized by INCO Ltd in the 1980s when the company conducted generative exploration over the area. The gossan have a characteristic stripped pattern due to the laminar arrangement of sulphides.

The sulphide “striped” Basal Norite of the No.1 West mineral occurrence contains mafic, sulphide-bearing thin bands (stripes on outcrop scale). The 0.5- to 4 cm thin mafic layers are composed of mafic minerals amphibole, biotite, at a higher abundance than in the host matrix (Plate

6.3, 1, 4). The thin layers also contain plagioclase, albite, and epidote and disseminated sulphides (Palate 6.3, 1, 3). Plagioclase exhibits advanced alteration into epidote aggregates, and albite along its rim. Biotite occurs in aggregates of fine platy crystals and reaction rims between plagioclase and sulphide grains. The mafic mineral and sulphide-enriched stripes are parallel with the Victoria Shear suggesting they are related to the shear zone but the rock itself is not sheared but highly strained. The Victoria Shear Zone at the No.1 West occurrence contains massive sulphide lenses of 1 to 4 m long and 0.3 to 1 meter thick (Plate 6.3, 2).

Rare blebby sulphide and disseminated sulphides in the stripes consist of abundant (>80%) pyrrhotite with minor chalcopyrite (5-15) and pentlandite (2-5%). Alteration minerals, epidote, chlorite, biotite, amphibole are intergrown with the sulphide by similar manner described above. The massive sulphide lenses in the Victoria Shear Zone consist of granular 0.1 to 3 mm pyrrhotite with anhedral magnetite and traces of ilmenite. The massive pyrrhotite is mostly altered to "zwischenprodukt (Ramdohr, 1980)", a fibrous mixture of pyrite-marcasite-Fe-oxides-hydroxide, and massive goethite (Plate 6.3, 8). Magnetite alters to a porous relict mass, some pores rarely filled with fine-grained (8 to 13 μm) gold (Plate 6.3, 8). The massive granular pyrrhotite ore is surrounded by an alteration halo of granular epidote and minor white-mica containing 1-7 % disseminated 0.1 to 1 mm sulphides of abundant chalcopyrite, minor pyrrhotite and magnetite (Plate 6.3, 5, 6, 7). The sulphides in this alteration halo appear to be less altered into supergene alteration products. One anhedral grain of speryllite was found included in epidote (Plate 6.3, 7). Grab assay sample of the shear hosted massive sulphide lens resulted in highly prospective metal concentrations of 10.30 % Cu, 10.15 % Ni, 0.29 % Co and 0.254 ppm total PM (Au+Pd+Pt), (Appendix 8, 18). This result indicates that the Shear Zones has potentially mineralized by high grade, PGE-enriched massive sulphides. On the contrary these sulphides may form several small transposed lenses undersized for economic operation.

6.6. The Contact Sublayer

6.6.1. *General Field Characteristics*

The Contact Sublayer is a very distinct unit in the field, yet ill-defined due to its strongly altered, deformed and gossanous nature on outcrops. The striking field characteristic of the Contact Sublayer is the presence of abundant ultramafic rounded to sub-rounded, oval to circular xenoliths of 20 cm to 3 m in diameter (Plate 6.2, 1, 2, 3, 4). In general, the distribution of the xenoliths are irregular, but on large-sized outcrops clustering can be observed, xenoliths making up 50-70 vol. % of the rock. At the No.2 West mineral occurrence mafic xenoliths show slight to moderate alignment parallel with the strike of the Contact Sublayer unit.

6.6.2. *Occurrence*

The Contact Sublayer forms a distinct map unit and can be followed along the contact zone between of the Elsie Mountain metavolcanic rocks and the Basal Norite. The unit was mapped along a total strike length of about 1 km. It may form a discontinuous, minimum 5 meter to 40 meter wide mineralized belt. At many places, narrow 1-7 metre wide, shear zones crosscut the Contact Sublayer. The southern termination of the Contact Sublayer unit occurs by the several splays of the mayor Victoria Shear and perhaps by the Victoria Shear itself. Here the Contact Sublayer unit appears to be emplaced in between medium-grained granular mafic metagabbro and the fine-grained massive footwall amphibolite. The metagabbro is similar to the common gabbro xenoliths of the Worthington and Vermilion offsets and they are originated from abundant Nipissing Gabbro sills in the area. In the view of this field relationship the Contact Sublayer appears to be intrusive in origin. On the other hand juxtaposition of SIC and Footwall rocks may have happened due to displacements along the numerous splays of the Victoria shear zone.

To the northwest the unmineralized Contact Sublayer pinches out and/or cut-off by minor shear zone as well. In several shear zones an apparent enrichment of sulphides can be observed in the forms of massive pyrrhotite lenses, quartz-chalcopyrite stringers or 3-7 cm large quartz-chalcopyrite clots. Seemingly many of the located INCO trenches were cut into the sulphide-enriched shear zones.

6.6.3. *Xenoliths of the Contact Sublayer*

The xenoliths are composed of massive aggregate of fibrous actinolitic amphibole. Actinolitic amphibole appears to be replacing primary mafic minerals i.e. pyroxene, suggested by the apparent blocky outline of fibrous aggregates and their size variation mimicking primary grain size variations in the pyroxenite xenoliths (Plate 6.2, 1).. These xenoliths display a characteristic schiller on outcrops bringing out the primary equigranular mono-minerallic texture, referring to 2-6 mm grain size. Some xenoliths show coarser-grained rims, often composed of acicular actinolitic amphibole perpendicular to the rim, whereas the core is distinctly finer-grained granular. Rarely xenoliths contain rare 1-3 % sulphides (Figure 6.2). The granular amphibolite xenoliths are similar to those found all along the strike length of the Worthington Offset and classified as unknown origin (Lightfoot and Farrow, 2002).

Other type of xenoliths do not show a relict magmatic granular texture, but composed of massive fine-grained amphiboles similar to amphibolites in the immediate footwall, their suggested place of origin. Interestingly the Contact Sublayer does not contain abundant medium-grained granular gabbro xenoliths of Nipissing Gabbro which are very typical for the Vermilion and Worthington quartz diorite offsets (Lightfoot et al., 1997b).

6.6.4. *Matrix of the Contact Sublayer*

The Contact Sublayer matrix contains sulphides at several places indicated by extensive 40-50 m long gossanous zones. In these zones the Contact Sublayer matrix has a rusty surface and rock forming minerals are bleached and transformed to sericite-kaolinite and Fe-oxides, -hydroxides by supergene alteration. Sulphide enrichment in the Contact Sublayer matrix is irregular and seems to be accidental. In few cases however sulphides appear to be enriched in the matrix of clustered xenoliths. The sulphide-barren Contact Sublayer matrix is fine to medium-grained granular magmatic and/or nematoblastic metamorphic textured and macroscopically consists of plagioclase and amphibole. The matrix texture is rather variable within few meters on a single outcrop. An undulating shear like fabric, often wrapping around xenoliths, is peculiar to the matrix and it may obscure the primary rock texture. This texture is usually seen when strong alignment of xenolith developed parallel with the contact and strike of the Contact Sublayer. It cannot be deduced if this texture has originated from magmatic flow or later tectonic deformation. The distinction between the Contact Sublayer matrix and the footwall amphibolite is therefore not always straightforward where sulphides and xenolith do not occur. I most cases, the sulphide content and the presence of xenoliths were taken into consideration in defining the contact on the map.

6.6.5. *Petrography of the matrix of the Contact Sublayer*

Due to the strongly weathered nature of the Contact Sublayer matrix, outcrops for petrography studies were limited and found only at the Far West mineral occurrence. Here the Contact Sublayer attains its greatest width about 67 m and some outcrops are devoid of strong supergene alteration. Petrography studies of the Contact Sublayer were performed on nine samples collected from this area.

From the Far West Zone, two Contact Sublayer matrix phases were found to be the host to mafic xenoliths. Both rocks are similar in mineralogy, mainly composed of subhedral plagioclase and amphibole and they have an equigranular gabbroic, noritic magmatic texture. For simplicity in petrography description of the two phases, they are referred to as Sublayer-1 and Sublayer-2 (Figure 6.2).

Sublayer-1 is finer-grained with an average 0.3 mm grain size of equigranular 45 % plagioclase and 55% amphibole. The rock contains 2-5 % accessory biotite, chlorite, and epidote sericite. Plagioclase is subhedral blocky shows frequent polysynthetic albite and complex carlsbad-albite twining. Polysynthetic lamellar albite twins are sometimes bent and they have a wedge-like termination within the host gain indicative of deformation induced pressure twining. Optical properties of plagioclase refer to andesine-labradorite composition (An_{48-55}). Amphibole is fibrous

light green to slight bluish green –colored. It forms subhedral bundles, pseudomorphs after pyroxene. Optical properties of amphibole refer to actinolite to actinolitic hornblende composition.

Sublayer-2 is coarser-grained with an average grain size of 1 mm. It consists of 65 % blocky subhedral plagioclase of andesine-labradorite composition (An_{48-55}) and 30 % fibrous aggregates of actinolitic-hornblende as well as 5 % accessory quartz, chlorite, epidote, sericite. The core of some plagioclase grains is altered to fine sericite mass. Micro shear zones, associated with quartz-chlorite-carbonate-actinolite alteration, cut across the Sublayer matrix. The fairly sharp contact between the two Sublayer types was accidentally found in one sample. The two phases however cannot be mapped out at an outcrop scale and they are believed to be present as intermingled magmatic phases or two distinct intrusive phases, Sublayer-2 being the more widespread and matrix to the mafic xenoliths.

Similar sharp contact and change of modal % of mafic minerals (primary orthopyroxene) was observed by the author in the Whistle Embayment in the North Range where INCO geologist referred to the two norite phases as felsic Sublayer norite and mafic Sublayer norite transition.

Deformation of the Sublayer matrix along narrow crosscutting shear zones results in a chlorite rich continuous foliation of about 65-75 vol. % chlorite with carbonate and albite, indicative of a greenschist facies metamorphic alteration. Rare, rotated, porphyroclasts of blocky feldspars are strongly altered to chlorite as seen in the mafic chlorite-altered norite suggesting that static chlorite alteration may have been the result of fluid mobilization along the shear zones at the No.2 West mineral occurrence.

6.6.6. *Petrography of xenoliths in the Contact Sublayer*

Petrography studies of mafic xenoliths indicate that they are composed of mono-minerallic acicular-fibrous actinolitic amphibole. Some xenoliths contain 1-4 vol. % feldspars. Actinolitic amphibole forms subhedral, blocky-shaped bundles indicative of a replacement origin after pyroxenes. These mafic xenoliths may have been altered from primary pyroxenite Results of electron microprobe analysis correspond to actinolite composition of fibrous amphiboles (Table 6.1). Sulphide blebs, of 1-4 mm size, rarely occur in actinolitic xenoliths. The blebs are composed of dominant pyrrhotite with coarse vein network of pentlandite and traces of chalcopyrite. Pentlandite is partly altered to violarite along cracks.

Some mafic xenoliths with significant 7-50 vol. % sulphide content have been found from the Far West Zone in an old exploration pit (Figure 6.2). Sulphide texture in these xenoliths is interstitial to intecumulus and semi-massive. Sulphides are composed mainly of pyrrhotite pentlandite and minor magnetite, ilmenite, and chalcopyrite. The only dominant silicate mineral is actinolitic amphibole pseudomorphous after blocky cumulus pyroxene. This finding suggests that the “hidden”

ultramafic rocks, from which the abundant xenoliths of the Contact Sublayer have originated, contain significant amount of magmatic sulphides (also see Chapter 11). These sulphides may have formed prior to the major sulphide segregation within the Sublayer and represent the earliest formed hidden mafic ultramafic rocks co-genetic with the Sublayer. The question here is whether these xenoliths are comagmatic with the Sublayer or protolithic in origin i.e. Huronian ultramafic rocks (East Bull Lake and Nipissing intrusive suites) with sulphides. Due to the complete alteration of the primary mafic silicate the origin of xenoliths cannot be examined by geochemical methods from the Far West Zones.

6.7. Mineral Occurrences of the Contact Sublayer

Two important magmatic Ni-Cu sulphide mineral occurrences can be found within the Contact Sublayer on the mapping area. The Far West Zone and the No.2 West Property names were allocated by FNX Mining Inc. during the aggressive exploration drilling campaign in 2002-2003. The No.1 West Zone has been already mentioned to be associated with the "stripped" Basal Norite along the Victoria Shear Zone.

6.7.1. *The Far West Zone*

Gossan at the Far West zone is confined to a maximum 70 m by 30 m area, based on outcrop mapping. Minor massive sulphide lenses can only bee seen in existing exploration pits and on dump material excavated from the pits. Three preliminarily lithogeochemistry grab samples of massive, semi-massive sulphides in Sublayer matrix, as well sulphide-bearing mafic xenoliths yielded metal concentrations of 0.2-4.2 % Ni, 200-2290 ppm Zn, 15-360 ppb Ir, 1980-2970 ppm Cr (Appendix 9). The high chromium concentration refers to the primary ultramafic content of Sublayer xenoliths. Interestingly, the $\Delta^{34}S$ isotope values of sulphide differ from the typical magmatic numbers, and are; 1.84, 2.24, 2.59 suggesting metamorphic hydrothermal alteration of the primary magmatic sulphides (Appendix 9).

The geology and mineralization of the Far West Zone has been investigated in details by Hefner (2002). Mineralized Sublayer, exposed only in few exploration pits, contain massive lenses, blebby to disseminated sulphides of pyrrhotite, pentlandite, chalcopyrite, sphalerite, magnetite, ilmenite, pyrite and marcasite. Most of pyrrhotite-rich sulphides are altered to "zwischenprodukt" and "bird-eye" alteration masses of pyrite-marcasite and minor Fe-oxides. Pentlandite is altered to violarite and cattierite. No PGE-minerals were found to be associated with magmatic sulphides. Heffner (2003) noted the strong metamorphic-hydrothermal alteration of the sulphide ore (intergrown with epidote, chlorite, albite, quartz) and considered the Far West Zone as "residual or exhausted" ore from which PGE may have been remobilized by metamorphic hydrothermal fluids.

FNX exploration drilling did not intersect significant sulphides at the Far West Zone and the company halted exploration in 2003 in this area.

6.7.2. *The No.2 West Zone*

The most significant mineral occurrence of the mapping area is the No.2 West zone. Mapping and assay grab sampling of gossanous outcrops indicated that magmatic Ni-Cu sulphide mineralization extends along 370 m northwest-southeast –trending strike length. The mineralization is stronger towards the southern end of the zone. There, the mineralized Contact Sublayer is thicker, 30-40 m and it is transversed by several northeast-trending 1-10 wide shear zones. Left-lateral 10 to maximum 50 meter displacement of the Contact Sublayer unit occurs along these shear zones. The Contact Sublayer matrix is usually strongly deformed and altered to amphibole-rich rock. At the northern tip of the mineralized zone, sulphide forms massive to semi-massive lenses of 10 cm to 0.5 m wide and 1-3 meters long in sheared Sublayer matrix. Pyrrhotite/chalcopyrite ratios vary greatly within an individual sulphide lens at the outcrop scale. Pyrrhotite-rich part of sulphide lens assayed 0.24 % Cu, 3.54 % Ni and 0.128 % Co with 0.07 ppm Au+Pd+Pt. In contrast chalcopyrite rich part assayed 2.70 % Cu, 0.64 % Ni and 0.02 % Co with 0.04 ppm Au+Pd+Pt (Appendix 8; 8, 10)

The southern end of the No.2 West Zone mineralization is cut by abundant 1-10 meter wide shear zones with an about 20-30 meter spacing. These shear zones appear to be the sub-parallel splays of the main Victoria Shear to the immediate south. The tectonized Contact Sublayer and hangingwall Basal Norite shows variable degree of proto-mylontic fragmentation and mylonitic re-crystallization into L-S type tectonites in which foliation is defined by mica rich layers and lineation by the stretching lineation of micas. All the shear zones strike to the NE-E (60-90) and dip to S-SE (150-180) with angles varying slightly between 90a and 60 degree. The faint or well-defined stretching lineation distinctly pitches 80-65 to the E-SE. Many shear zones contain apparently elevated sulphide content when they cut the Contact Sublayer unit rich in sulphides. This indicates an outcrop-scale redistribution of magmatic sulphides. Chalcopyrite tends to be associated with quartz lenses and veins whereas pyrrhotite forms massive flattened (streaked-out) lenses, ribbons with few tens of centimetre long. Coarse pressure twinning in chalcopyrite can be seen under the hand lens. These sulphides are associated with strong chlorite and carbonate alteration along the deformation zones. Sulphide enrichment within the shear zones dies out outside the Contact Sublayer unit. In many cases the individual shear zones can be traced into the Elsie Mountain amphibolite and there they do not contain sulphide but quartz veins and lenses. This suggest that remobilization of magmatic sulphide does not have major lateral extent, but can be significant vertically, since the major component of displacement along these deformation zones is vertical as indicated by the steeply dipping 65-80 degree pitches.

Grab assay samples from an existing trench cut parallel with a shear zones yielded 1.63 % Cu, 1.48 % Ni with elevated total PM 0.138 ppm Au+Pd+Pt (Appendix 8; 10,11). This result is from pyrrhotite lenses from a chlorite-Cr-muscovite (mariposite)-carbonate schist. Quartz lenses with only chalcopyrite resulted in similar 1.21 % Cu value with no Ni and insignificant total PMs (Appendix 8; 13). These preliminary assay results indicate that Au, Pd and Pt enrichment of sulphides, remobilized along the deformation zones, is present.

The No.2 West Zone mineralization was the major focus of exploration drilling by FNX in 2002-2003 and an unknown open-pittable resource was defined as part of a total inferred resource for the Victoria Property of 15,394,000 tons at 0.45 wt.% Cu and 0.46 wt.% Ni announced in 2007 (www.infomine.com).

Due to the regional importance and the limited surface outcrops of the No.2 West Zone mineralization, it is described in details in Chapter 9, based on exploration drill core sampling. The detailed description, classification and interpretation of kinematics and regional importance of the abundant shear zones are also dealt with details in a separate chapter; Chapter 7. Geochronology study of deformation zones is given Chapter 8.

6.8. Footwall amphibolite of the Elsie Mountain Formation

6.8.1. *Field Characteristics*

The footwall rocks along the northwest trending mineralized Contact Sublayer unit belong to the Elsie Mountain Formation which is generally built up by massive pillowed basalt, mafic pyroclastics, wacke, arkose, intermediate volcanic rocks. In the mapping area these rocks are homogenous, commonly fine grained mafic, dark green in color and they consist of abundant green amphibole of 0.1 to 2 mm in size. They probably represent massive fine-grained to aphanitic basaltic lava flows. They are crosscut by the, 1 to 7 m wide, northeast-trending shear zones along which strong foliation and nematoblastic texture develops. Footwall amphibolite is recrystallized into fibrous amphibole, chlorite, quartz and carbonate along the shear zones. Shear parallel quartz veins and quartz lenses are commonly associated with the shear zones.

The footwall amphibolites on field outcrops are often “spotted”, the fine grained groundmass contains denser knots of amphiboles usually cored by fine granular mass of ilmenite. These spots become larger, 3 to 5 mm when approaching the contact with the Contact Sublayer. In zones very close to the contact, within 10 to 20 meters, large 0.3 to 1.5 cm –sized, euhedral porphyroblastic-poikiloblastic brown amphibole appears in large (3-15 vol. %) amount (Fig 6.3, Plate 6.2, 8). This field observation suggests that a contact metamorphic aureole is present in the amphibolite footwall. It has an average width of 30 m, but one outcrop suggests a maximum extent of 100 m. This is the place of occurrence of brown amphibole porphyroblasts and/or poikiloblasts. Thermal metamorphic

re-crystallization into brown, titano-hornblende may extend farther from the contact, but this was not studied during this work presented herein. Contact, thermal metamorphic alteration of footwall rocks is well documented from the North Range (Wodicka, 1995; Lakomy, 1990) but rarely reported from the South Range (Farrow and Lightfoot, 2002).

6.8.2. *Petrography*

Petrography study indicates that footwall amphibolitic rocks are composed of 0.1 to 1 mm 70-90 vol. % subhedral short prismatic hornblende and 10-30 vol. % interstitial plagioclase with traces of epidote chlorite ilmenite. The amphibolites are commonly granoblastic without preferred orientation. Hornblende has characteristic faint to strong brown color in the centre and becomes slight greenish, bluish towards the rims. The brown color indicates Ti content in hornblende which is typical for samples in the vicinity of the contact zones with the SIC (Figure 6.3).

Petrography studies of porphyroblastic footwall amphibolite showed that dark brown amphibole is fine subhedral 0.1 to 3 mm poikiloblastic or coarse 3 mm to 3 cm homogenous euhedral prismatic porphyroblastic. The larger porphyroblasts are often surrounded by quartz and feldspar grains forming a felsic nets around the grains. The core of porphyroblast consists of light to dark brown amphibole, whereas deep blue green hornblende forms distinct rims, Microprobe results (Fig 6.3, Table 6.1) of the brown amphibole core correspond to titano-thermakitic hornblende and titano ferro-thermakite with 1.92 to 2.73 wt. % Ti. The blue-green rims have ferro-hornblende and ferro-tchermakitic hornblende composition. The poikiloblasts contain minute rounded actinolite, quartz and feldspar oikocrysts.

6.9. Gabbroid rocks of the Footwall

6.9.1. *Field Characteristics*

On surface, coarse grained, 3 to 6 mm, gabbroic-textured rock, similar to Nipissing Gabbro, occurs in the footwall. The gabbro forms a mappable unit at southern termination of the Contact Sublayer, where it is situated in between the Basal Norite and massive fine-grained footwall amphibolite, bounded by shear zones from both sides. The western boundary of the gabbro appears to be “true” contact with the Contact Sublayer. Here, patches and veinlets of coarse, 0.3 to1 cm, granular quartz feldspar and brown amphibole occur. Brown amphibole is euhedral and overgrown on the walls of the vugs and veins (Fig 6.3).

6.9.2. *Petrography*

Petrography study reveals that this gabbro contains approximately 55 % blocky fibrous amphibole (uralite) pseudomorphs after pyroxene and the interstices are filled with very fine grained recrystallized, polygonal granular mass of plagioclase +/- minor quartz +/- minute euhedral laths of epidote. This gabbro is identical to the large oval inclusions found in Vermilion quartz diorite

(Chapter 10). The coarse brown amphibole crystals exhibit faint color zoning and they become lighter brown and bluish-green toward the edge.

6.10. Composition and P-T conditions for formation of contact metamorphic hornblende

Microprobe analysis of the coarse brown amphibole (Fig 6., Table 6.1) indicated similar high Ti content in the core, strongly decreasing toward the rim, ie. 2.32 wt. % Ti to 0.95 wt. % Ti. In the groundmass of the same sample relicts of brown amphibole rimmed with blue-green amphibole occur, similar to porphyroblasts in the footwall amphibolite. Microprobe analysis showed that cores have titano ferro-hornblende and titano ferr-tshermakitic hornblende composition with 2.32 to 3.68 wt. % Ti content (Fig 6.3, Table 6.1). The rims show ferro-hornblende and ferrtshermakite composition. Primary plagioclase is recrystallized into fine granular aggregate of stubby zoned crystals (similar to decussated texture), typical texture of thermal re-crystallization or partial melting (Dressler, 1984). The core of plagioclase grains has andesine-labradorite (An_{45-65}) compositions whereas the rims have (An_{32-34}) oligoclase composition. The occurrence of contact metamorphic titano-hornblende and recrystallized plagioclase in the gabbro may support the intrusive origin of the Contact Sublayer which heated up the surrounding gabbro and coused typical hornfelsed texture. Electron microprobe results of titano-hornblende core and hornblende rim compositions, from footwall amphibolite and Nipissing Gabbro, were used for pressure temperature estimations and are plotted on P-T diagram constructed by Ernst and Liu (1998) (Fig 6.4). Results from three core-rim pairs indicate a low pressure, 0.3-1 kbar and high temperature 850-1000 °C formation of the cores comparable with thermal metamorphic conditions. The ferro-tshermakitic blue-green colored hornblende rims suggest a lower temperature 500-550 °C, but higher pressure i.e. 2.4 to 3 kbar conditions for their formations, comparable with regional metamorphism i.e. the Penokean Orogeny or hydrothermal alteration by magmatic hydrothermal fluids near the SIC contact (Farrow, 1994; Marshall et al., 1999; Molnár et al, 1997, 1999, 2001; Molnár and Watkinson, 2001) However the blue-green hornblende rims occur in many rock types; Sublayer matrix, Basal Norite, Quartz Diorite suggesting that its presence is related to regional processes i.e. regional amphibolite facies metamorphism of the SIC and Huronian Footwall. In order to establish the time of formation of the titano-hornblende porphyroblasts, K-Ar and Ar/Ar studies were performed on two samples (see in Chapter 8).

6.11. Weakly mineralized contact metasomatic patches, veinlets in Footwall amphibolite

In addition to contact metamorphic features described above, slightly different, so called "contact metasomathic" veinlets and patches also occur in the footwall both at the No.2 West Zone and the Far West Zone areas. Veinlets are 1 to 5 cm this discontinuous, patched are irregular in sharp and have 5-20 cm extension. The metasomatic nests, cavities and veins in footwall amphibolite are

composed of quartz-feldspar-biotite. Texture shows in-equilibrium pegmatitic texture indicating fluid effect. Biotite often forms 1 to 2 cm plates enclosed in coarse quartz and feldspar, but more commonly enriched in the host rock and finely disseminated. Minor 0.5-4 % sulphides occur in these veinlets and patches and they consist of chalcopyrite and pyrite. Grab assay samples of sulphide-breading veins and patches indicate minor Pt+Pd+Au enrichment (0.17-0.55 g/t) (Appendix 8; 23, 24). The PGE-enriched samples are located within 20 meter distance from the Contact Sublayer (S90415) or from the quartz diorite (1801703) (Appendix 1, MAP-2).

Petrography studies of the metasomatic nest indicate that quartz is partly recrystallized into fine-grained strain free polygonal aggregate. Recrystallized quartz is free of fluid inclusions whereas older grains contain dense clusters of saline halite bearing fluid inclusions. Plagioclase is altered and recrystallized into fine aggregate of albite and epidote. Plagioclase contains numerous fluid inclusions and mineral inclusions (epidote, apatite, biotite, and amphibole). Fluid inclusions in plagioclase are 3-phase saline L-V-H inclusions.

Fluid inclusion petrography of metasomatic quartz indicates the 95 % presence of dark 1-phase L_{CO2} and 5 % 2-phase L_{H2O}-L_{CO2} carbonic-aqueous inclusions with highly variable phase compositions on room temperatures indicating heterogeneous trapping conditions from a heterogeneous fluid system. Another area in the sample, where quartz is full of inclusions, the above inclusions are associated with poly-phase hyper-saline inclusions but in this case it very difficult to deduce they relationship between the two inclusion types because a high abundance of the inclusions. The most abundant inclusion type in this sample is the large 10 to 30 µm hyper-saline poly-phase 4-5-phase (L-V-H-X_1-X_2-X_3). The X_1 phase is rounded and 3-times smaller that halite, it may be sylvite. These fluid inclusions are very similar to those highly saline high temperature inclusion responsible for PGE remobilization of primary magmatic sulphide, described all around the SIC (Farrow and Watkinson 1997; Farrow and Lightfoot 2002; Molnár et al., 1997, 1999, 2001; Molnár and Watkinson 2001; Hanley at. al, 2005, Péntek et al., 2008). In one sample 2-7 µm sized unidentified PGE mineral was found included in chalcopyrite. The presence of sulphides, possible PGE minerals, highly saline fluid inclusion may suggest that these metasomatic nests may have developed from local magmatic hydrothermal alteration of the footwall. The high abundance of the CO_2 phase may suggest an alternative metamorphic hydrothermal origin of quartz-feldspar-biotite veinlets and patches. Due the limited occurrences and mineral poor nature of the metasomatic nests, their fluid inclusions were not studied in details.

6.12. The area between the Victoria Shear Zone and the Creighton Fault

The Contact Sublayer is truncated by the east northeast-trending Victoria Shear and it cannot be found to the south. In fact large part of the mapping area is covered by Mond Lake and significant length of the Victoria Shear itself runs beneath the lake. The linear southern boundary of Mond Lake follows the strike of the Victoria shear zone It is not even possible to see if the Basal Norite is present at the base of the SIC in this zone. Outcrops on the east and north shores of the lake expose the typical South Range Norite suggesting that Basal Norite pinches out or smeared off along the Victoria Shear Zone. The Victoria Shear Zone is exposed only south of No.2 West Zone along the Fairbank Lake Resort paved road. Here a small dyke-like north-south-trending fragment of quart diorite of about 100 m long and 30 m wide occurs to be attached to the Victoria Shear.

6.12.1. *The small quartz diorite pod*

Quartz diorite shows typical fine, 1 to 2 mm, equigranular texture and consists of about 50 % plagioclase 15 % quartz and 35 % amphibole and biotite. On one outcrop, chilled margin in quartz diorite is developed within 0.5 to 1 m distance from the amphibolite country rock contact. Chilled quartz diorite displays a peculiar texture consisting of clusters of radiating acicular 1 to 3 cm long mafic mineral. Petrography study of chilled and granular quartz diorite samples reveals that quartz is very abundant, about 20-25 vol. % and interstitial to thin plagioclase (An_{35-45}) laths. Interstitial quartz often has the "flood" property when spatially isolated interstitial grains extinct together indicative of optically one homogenous grain. Primary magmatic mafic phase are not present in the rock, they are all altered to aggregates of actinolitic hornblende and biotite. Traces of sericite, chlorite, epidote, apatite, and zircon are present. There was no sulphide mineralization found within this small quartz diorite pod. Quartz diorite is deformed into fine-grained very well foliated chlorite-quartz carbonate schist within the Victoria Shear.

6.12.2. *The Victoria Embayment*

South of the Victoria Shear Zone previous maps indicated a funnel-shaped quartz diorite body referred to as the Victoria Embayment (Grant, 1982). This quartz diorite is well exposed in large outcrop along the southern edge of the Mond Lake. Detailed mapping of this embayment structure suggest the presence of a west and east limbs of quartz diorite. At the western margin of the east limb a complex intrusive relationship of two quartz diorite pulses can be studied in two small outcrops (Fig 6.5). An intrusive breccia contains fine-grained lesser mineralized quartz diorite matrix, similar to Contact Sublayer matrix, hosting 1 to 3 m sub-rounded to rounded xenoliths of coarser grained quartz diorite with blebby and disseminated sulphide mineralization. This field relationship supports the multiphase intrusion model of quartz diorite offset dykes (Lightfoot et al.,

2001; Lightfoot and Farrow, 2002), but the sequence of emplacements here appears to be reverse as of in many other occurrences; the earlier coarser phase contains the mineralization.

6.12.3. *Petrography of the marginal Intrusive Breccia*

Petrography study of the two quartz diorite phases indices that the finer-grained quartz diorite is slightly more mafic and contains about 35 % tabular plagioclase (An_{35-45}), 40 % tabular to columnar fibrous aggregates of actinolite with minor bluish-green hornblende rims. The fibrous actinolite aggregates appear to be pseudomorphs after orthopyroxene. The aggregates show slight to moderate orientation indicative of flow lineation or flow banding in the primary texture. Biotite, 7 %, forms minor grains attached to amphibole aggregates. Interstitial quartz, about 11%, is mostly recrystallized into fine polygonal aggregates containing chlorite and biotite. Sulphide in the sample occurs as 3 to 12 mm anhedral grain aggregates of pyrrhotite, pentlandite, chalcopyrite, magnetite, and ilmenite. The rim of sulphide grains are strongly intergrown with hydrous silicates, epidote, chlorite and rarely amphibole, biotite. The rock texture is equigranular with an average grain size of 1.5 to 2 mm.

The coarser quartz diorite in the xenoliths has equigranular texture and an average grain size of 3 mm. It may have slightly lower 25-30 % mafic mineral content including fibrous actinolite aggregates after tabular-columnar orthopyroxene, and homogenous subhedral green, bluish-green hornblende. About 35-40 % plagioclase (An_{35-45}) is subhedral tabular, interstities are filled with quartz or “flood” quartz. Minor poikilitic K-feldspar with rounded quartz grain is also observed. Anhedral biotite is attached to amphibole aggregates or to sulphide grains. The xenolithic quartz diorite contains a distinct greenschist facies alteration assemblage, quartz-albite-epidote-chlorite, associated and being intergrown with sulphide aggregates. The microtexture and mineral composition of xenoliths are identical with typical quartz diorite offset rock of the SIC. Although slightly finer-grained, this rock is also identical with the Basal Norite. This similarity may in fact be the result of regional hydrothermal and metamorphic alteration of all rock types, obliterating primary texture and composition. Based on the evaluation of morphology of amphibole pseudomorphs in both rocks, Basal Norite may have contained more subophitic poikilitic clinopyroxene (i.e. gabbro-norite in composition) whereas quartz diorite tabular pseudomorphs of fibrous actinolite (i.e. uralite after orthopyroxene). The fine quartz diorite matrix of the intrusive breccia cannot be found in other outcrops. Its extent may be limited and confined only to the selvage of the Victoria quartz diorite embayment.

6.12.4. *East Limb of Victoria Embayment*

The majority of the east limb of Victoria Embayment contains the same quartz diorite found in the xenoliths. Sulphide content may attain 5-7 % at some places. Considerable sulphide mineralization occurs only at one place, in the centre of the east limb. Here 10-25 %, 0.5 to 1 cm large pyrrhotite rich sulphide blebs occurs in amphibole biotite quartz diorite (Fig 6.5). The sulphide mineralization may have a north-south extension of 100 meters and a maximum with of 40 m. Extensive trenching found on surface indicates exploration activity in the area by INCO in the eighties.

6.12.4.1. *Petrography of sulphide mineralization*

Petrography study of the sulphide host rock illustrates that quartz diorite contains 30 % amphibole, 40 % plagioclase, 7 % biotite, 13 % quartz and 10 % chlorite, sericite, epidote. Amphibole forms 1 to 3 mm subhedral, blocky-shaped fibrous grain aggregates or rare homogenous grains. It contains lighter core with small opaque inclusions (relict pyroxene). Optical properties and pleochroism light green-green, bluish green correspond to actinolite-hornblende composition. It is often rimmed by biotite and exhibits growth twins. One microprobe analysis indicates ferro-hornblende composition of the homogenous grains. Plagioclase (An_{38-47}) is subhedral blocky, has lobate resorbed rims. It exhibits saussuritic alteration in the core or totally alters to sericite-epidote masses. Quartz is interstitial, or rather "flood-like", strongly strained, partly polygonized, and recrystallized. Biotite appears in large flakes usually attached to amphibole and to sulphide bleb or rims ilmenite. Chlorite occurs as subhedral platy crystals being intergrown with sulphide blebs at the rim. Parts of the sample are recrystallized into fine-grained non oriented and oriented aggregates of quartz-albite-amphibole-epidote. A common feature of Victoria quartz diorite is that they contain inclusions of monomineralic fine aggregates of plagioclase xenoliths which are partly or totally altered to epidote. Similar plagioclase rich inclusions characteristically occur in Vermilion QD.

The sulphide blebs are composed of pyrrhotite, pentlandite (altered to violarite), chalcopyrite, sphalerite, pyrite, ilmenite and titanite (Table 6.7). Pyrrhotite is the main phase in the blebs; pyrrhotite grain is often bleb-sized. One 1 to 1.5 cm bleb is composed of almost only one pyrrhotite grain. This one-grain bleb contains thin pressure-induced lamellar twins in one direction. Low angle deformation boundaries are also developed in the grain and seems to be later that the lamellae. Basal cleavage is well developed in all grains. Other bleb is polygonized possible due to re-crystallization of strained coarse bleb-grain. Pyrrhotite shows pyrite and marcasite alteration along cracks and basal cleavage. It contains rare pentlandite exsolution flames along micro-cracks. Pentlandite appears in larger subhedral grains in pyrrhotite. It is totally altered to violarite. Chalcopyrite appears as anhedral

grains attached to the pyrrhotite blebs and being intergrown with silicates. Chalcopyrite often contains sphalerite inclusions.

Composite assay samples of an area 10 m by 20 m, revealed low grade 0.63 wt. % Cu and 0.65 wt. % Ni mineralization with faint enrichment of 0.03 ppm Au+Pd+Pt. Another sample (171704) from the margin of the mineralized zoned yielded lower Cu (0.34 wt. %) and Ni (0.28 wt. %) values but anomalous Au+Pd+Pt (1.27 g/t) (Appendix 8; 1, 27). During the exploration campaign by FNX in 2002 the area is show as the "central" mineralization (Chapter 9).

6.12.5. *Contact Sublayer pipe in the East Limb of Victoria Embayment*

The eastern limb of the Victoria Embayment contains a lens of typical Contact Sublayer, 50 to 70 meter long maximum 20 m wide. The matrix is strongly deformed, gossanous and it is host to abundant 1 to 5 m sized rounded massive amphibolite xenoliths. Based on limited outcrops it is not possible to deduce if the occurrence of the Contact Sublayer within the quartz diorite confines a pipe like intrusion. The Contact Sublayer lens may form a major wall-pendant within the volumetrically more extensive quartz diorite embayment. Either case would suggest that the Contact Sublayer and the Quartz Diorite offset are not co-genetic. The similarity of the intrusive breccia (west side of the eastern limb) matrix phase to Sublayer matrix may support the field evidence that the Contact Sublayer is intrusive in origin and later than the quartz diorite.

To the east, quartz diorite is in contact with strongly deformed metaquartzite of the Elsie Mountain Formation. The quartzite is fine-grained, well foliated, contains about 15-25 % muscovite rich cleavage bands. The deformed quartzite from this area was used for K-Ar, Ar/Ar age dating of deformation along the Victoria Shear Zone (Chapter 8).

The western limb of the Victoria Embayment quartz diorite can only be constructed based on limited outcrops. It coincides with the surface area of the past-producing the Victoria Mine. Some material found on remaining dumps indicate that the ores and host rocks in the mine are very strongly deformed re-worked into a mineralized tectonic breccia containing abundant quartz, carbonate, biotite, chlorite and "drushbeweged" (Ramdohr, 1980) massive pyrrhotite rich sulphides as well as chalcopyrite rich stringers similar to those found in No.2 West Zone (Chapter 9).

6.13. Victoria mine shaft area

6.13.1. *Geology*

Detailed field mapping showed that the rocks cropping out north of the shaft are not quartz diorite as indicated on previous existing maps (Grant, 1982). North, north-east of the abandoned and fenced Victoria mine shaft, a barren fine to medium-grained mafic gabbroic rock crops out. This rock contains a granular coarse-grained 6 to 8 mm feldspar and amphibole with traces of ilmenite and can

be identified as Nipissing Gabbro (Plate 6.4). There is slight variation on texture of the Nipissing Gabbro, the coarse granular rock (Plate 6.4, 2) occurs within a finer-grained rock with typical diabase-texture (Plate 6.4, 3). Felsic aplitic dykes, 30 cm to 1 m wide, crosscut the Nipissing Intrusives. Brittle faults and narrow 10 cm to 70 cm wide shear zones are also abundant features in the gabbroic rocks. The gabbroic host rocks are recrystallized into strongly foliated lepidoblastic biotite schist in these deformation zones. The shear zones strike to the east, north-east and dip to the south with 70 degree. These shear zones are minors sub-parallel splays of the major Victoria Shear to the north. Biotite of two shear zones of this area was sampled for K/Ar, Ar/Ar geochronology study of the age of deformation (Chapter 8).

A few metre wide Sudbury Breccia zone is developed at the southeast contact of the Nipissing intrusives. Sudbury Breccia is dark greenish grey to black colored, massive fine-grained to aphanitic or schistose. Sudbury Breccia has foliation parallel with the contact of the gabbroic rock. The breccia has very irregular shape and forms small 10 to 30 cm wide injections and branches into all rock types found in the area (Plate 6.4, 1). Sudbury breccia developed in Nipissing gabbro has no inclusion content and is amphibole rich. Sudbury Breccia found in the metaquartzite has light-grey quartz and mica rich matrix and abundant weakly shorted 0.1 cm to 3 m large rounded country rock xenoliths (Plate 6.4, 4, 5). Thin 1 to 5 cm Sudbury Breccia veins in the metaquartzite appear as aphanitic black ribbons.

East of the Victoria Shaft the fine-grained massive amphibolite and light metaquartzite are exposed. These rocks are intricately interleaved by a manner which is difficult to conceive even at an outcrop scale. By closer examination the massive amphibolite appears to be strongly brecciated, but this texture is not as much striking as in metaquartzite. The entire 130 by 130 metre area can be considered as Sudbury Breccia i.e. a zone of brecciation without significant matrix component.

A northeast trending 5 to 6 meter wide quartz diabase dyke cut into both brecciated amphibolite and metaquartzite. The walls of the dyke are strongly sheared, foliated against the quartzite. Another 5 m wide, northeast-trending dyke was located 200 m south of the shaft in massive amphibolite. Quartz Diabase dykes has very homogenous fine 0.1 to 1 mm granular texture. It is interesting to note that both the Nipissing Diabase and Quartz Diabase have quite similar textures to quartz diorite; therefore they can be easily mistaken. Petrography studies however show different textures of all these three rock types.

True quartz diorite was only found on limited outcrops. The rock exhibits fine 1 to 2 mm equigranular texture and contains minor sulphides indicated by rusty, gossanous patches of 0.5 to 1 cm in size. Shear-bound quartz diorite blocks may be present under the surface suggested by the closest occurrence of quartz diorite body dislocated 300 meter to the east by shear zones.

6.13.2. *Petrography*

6.13.2.1. *Nipissing gabbroid rocks*

Petrography study of the gabbroic Nipissing rocks revealed the grain size difference between a central coarser and a marginal finer variety. The rock is composed of 60-70 % subhedral poikiloblastic brownish green hornblende, 40-30 % interstitial plagioclase and minor quartz, chlorite, epidote, carbonate, ilmenite, titanite accessory pyrite. Plagioclase is polygonized into fine granoblastic aggregates. The coarser gabbro occasionally exhibits a poorly defined foliation, thus it is lepidoblastic-granoblastic whereas the finer is granoblastic probable showing a relict texture blasto-intergranular.

6.13.2.2. *Sudbury Breccia*

Sudbury breccia vein in the gabbro has granoblastic equigranular polygonal to nematobalstic foliated texture consistent with a thermal contact metamorphism due to the close proximity of the Main Mass of SIC. Sudbury Breccia matrix in the metaquartzite contains continuous foliation composed of biotite chlorite muscovite carbonate that wraps around quartz, quartzite porphyroclasts that are partly recrystallized at their edges.

6.13.2.3. *Deformation zones*

Deformation along minor shear zones led to the development of strongly foliated lepidoblastic biotite rich rock. The cleavage band is composed of biotite that contains enclosing epidote and titanite. Biotite rich cleavage bands strongly undulate and wrap around feldspar porphyroclasts. Microlithon is composed of carbonate epidote quartz and feldspar.

6.13.2.4. *Footwall Amphibolite*

A fine-grained massive amphibolite of Elsie Mountain Formation is granoblastic composed of 0.1 to 1 mm amphibole, epidote, feldspar, biotite, chlorite, quartz. The metaquartzite is granular to lepidoblastic, composed of 70 % quartz 27 % white mica 3 % porphyroclastic feldspar.

Amphibolites of the Elsie Mountain Formation comprise abundant fine-grained massive granular (Plate 6.4, 6) and fine- to coarse-vesicular varieties (Plate 6.4, 7, 8). The vesicular amphibolite may form east-east trending 20 to 30 m wide zones and may represent distinct flow within the homogenous massive granular amphibolite (not shown in the map). Petrography studies of amphibolite varieties of the Elsie Mountain Formation indicate a general composition of 60-80 % hornblende, 30-40 % plagioclase and 5-7 % quartz and ilmenite with variable amount of chlorite,

epidote, sericite, carbonate alteration minerals. Both amphibole and plagioclase are heterogeneous in composition Amphibole has a ferro-tshermakitic hornblende composition often in the core or patchily intergrown with magnesio-hornblende (Table 6.1). The interstitial plagioclase has andesine (An_{45}) core and a thin oligoclase (An_{25}) rim (Table 6.4).

6.13.2.5. *Quartz Diabase dykes*

Fine-grained quartz diabase dykes may have the original magmatic assemblage of 50-60 % amphibole, 35-25 % plagioclase and 15 % quartz; however, these dykes are also moderately to completely alter. Subhedral blocky and prismatic amphibole and stubby plagioclase with interstitial quartz form the framework of the rock. Amphibole is strongly zoned and it consists of a brown centre surrounded by anhedral to platy masses of Fe-Ti oxides and an overgrown rim of bluish-green hornblende. Alteration of plagioclase to white mica, epidote, carbonate and chlorite has highly variable intensity. In completely altered samples, boundaries of plagioclase are barely recognizable and the groundmass comprises granular coarse carbonate, white mica, chlorite and epidote.

6.14. Quartz diorite occurrences southeast of the Victoria shaft, East Limb

6.14.1. *Geology*

The area of the Victoria mine site appears to be a concentration of major east- east west-trending shear zones. This tectonic zone truncated the Victoria Embayment structure. Several smaller and larger bodies of quartz diorite can be found to the southeast. These occurrences are generally referred as the East Limb of the Victoria quartz diorite (Grant and Bite, 1984) Quartz diorite occurrences cannot be mapped to the immediate south of the abandoned Victoria mine site. The next outcrops of a quartz diorite body occur on a faulted off block, 300 metre to the east. Here quartz diorite forms a northeast-southwest-tending 80 metre long and 30 metre wide shear-bound block. Quartz diorite intrudes in between coarse-grained Nipissing Gabbro to the west and metaquartzite to the east. Thin 20 to 30 cm wide aplitic felsic dyke can be followed for metres within quartz diorite. A 10 to 20 meter wide Sudbury Breccia zone can be identified between quartz diorite intrusion and host rocks. On the east side, Sudbury Breccia contains 70-90 % rounded gabbro inclusions 10 cm to 20 m in diameter.

6.14.2. *Mineralization*

In the quartz diorite body typical weak disseminated and blebby sulphide mineralization occurs. Sulphide composed of pyrrhotite, chalcopyrite, occur in 2 to 7 mm grain aggregates. Grab assay samples indicate sub-economic concentration base metals; 0.25 % Cu and 0.03 % Ni

(Appendix 8, 16). Chalcopyrite in the Nipissing Gabbro can be found in minor 10 to 20 cm thin east, north-east-rending veins and in felsic metasomatic patches of quartz-feldspar-biotite. Grab assay sample of one vein shows 19.1 % Cu and elevated 0.25 ppm Pd content (Appendix 8, 17). The FNX exploration campaign referred to this area as No.4 Zone.

6.14.2. *Petrography*

The coarse grained Nipissing Gabbro is composed of 60 % blocky-shaped fibrous actinolite aggregates (uralite) and interstitial very fine grained equigranular, polygonal groundmass of plagioclase and occasional anhedral epidote.

The quartz diorite is composed of 39% amphibole, 42% plagioclase, 7% biotite, 1% ilmenite and 11 % quartz. It contains disseminated sulphides of pyrrhotite chalcopyrite pentlandite. At the thinsection scale, quartz diorite contains felsic inclusions composed of fine grained polygonal granoblastic plagioclase with numerous euhedral laths of epidote. The high abundance of this type of inclusion is very typical for the Vermilion quartz diorite (Chapter 10).

The quartz diorite with weak disseminated sulphides is faulted off 150 further to the east. Here all the same units can be mapped; Nipissing Gabbro on the west, Sudbury Breccia with gabbro xenoliths and weak disseminated sulphide mineralization in quartz diorite.

6.15. Quartz diorite sheet north of Creighton fault

Mapping further to the southeast down to the north shore of Ethel Lake resulted in defining a south-east- striking major 750 m long and 350 m wide coherent quartz diorite body. The intrusion has funnel shape and narrows down to 120 in width in the southeast where it is cut by the Creighton fault. The shape and extent of the quartz diorite body on the east is ill defined due to the lack of exposures and presence of swamps. The eastern boundary of this quartz diorite body was compiled based on INCO exploration maps. The contact of the quartz diorite body, with massive amphibolite country rocks, on the west side is exposed in several outcrops and appear to be irregular intrusive, as indicated by abundant Sudbury Breccia occurrences of the No. 4 Zone.

Along the western contact of the quartz diorite body thin 3 to 7 meter zone of fine-grained granular quartz diorite occurs. This contact-type quartz diorite can be seen only on limited outcrops, but it may form a continuous more that 500 meter long margin (Appendix 1, MAP-1). The textural variety may represent chilled margin, however radiating acicular amphibole aggregates are not seen in this rock type. The rock has the same modal mineralogical composition as that of the volumetrically overwhelming coarser-grained quartz diorite of the Victoria east limb.

At the east boundary of the east limb, massive to pillowed garnet amphibolite and thin, 0.4 to 2 meter wide, east-trending quartz diabase dykes are exposed. Quartz-sericite-rich metasedimentary

rocks are in contact with the amphibolites, but the area further to the east and northeast was not mapped in details.

6.15.1. *Mineralization*

At the south-western tip of this quartz diorite body a small lens of northeast-southwest trending, biotite-rich mineralized Sudbury Breccia occurs. Exploration activity by INCO in this area is marked by extensive trenching. One trench excavated in Sudbury Breccia exposes 20-30 % disseminated chalcopyrite mineralization in the fine-grained to aphanitic quartz-xenolithic Sudbury Breccia. Two grab assay samples of the mineralization yielded 4.14 % Cu with promising 4.83 ppm total PGM (0.4 ppm Au, 1.6 ppm Pt, 2.8 pp Pd) and 0.8 % Cu with 1.1 total PM (0.2 ppm Au, 0.3 ppm Pt, 0.51 ppm Pd) (Appendix 8; 32, 33).

Petrography study of Sudbury Breccia indicates that it comprises 40 % biotite 50 % quartz and 10 % granophyric intergrowths of quartz and feldspar. Quartz occurs as 3 mm to 1 cm –sized sub-rounded mono-crystalline xenoliths. Disseminated chalcopyrite forms 1 to 4 mm anhedral grains associated with chlorite epidote and albite alteration minerals. No PGE-minerals were found in the studied sample.

6.15.2. *The Powerline Deposit*

During the exploration drilling program of FNX in 2002 an AeroTEM airborne survey indicated the presence of a substantial conductive to the immediate south of this occurrence. This occurrence is located near a major electrical powerline. Such powerlines normally interfere with geophysical surveys and often render buried mineralization geophysically undetectable. Exploration drilling of the electromagnetic geophysical target resulted in a discovery of an unknown deposit; the Powerline deposit (Fig 6.6). The Powerline deposit has been intersected over a strike length of 250 ft. and a down-plunge length of over 550 ft. The deposit plunges steeply to the southwest. The mineralization is associated with a narrowing of the host offset dyke where the wallrocks of the dyke comprise zones of intense Sudbury Breccia and shearing. The mineralization from surface to just below the 100 ft. level consists of zones of lower grade, stringer sulphide mineralization. The massive mineralization contains significantly higher Cu-Ni-Pt-Pd-Au values. The thickness of the mineralization varies along plunge. Geological interpretation suggests that the airborne geophysical anomaly is coincident with a possible, northeast extension of the Worthington Offset Dyke to the north of the Creighton Fault.

6.15.3. *The Creighton Fault*

The funnel-shaped quartz diorite body and massive amphibolite country rocks are cut by the east trending Creighton Fault. The fault runs parallel with the north shore of Ethel Lake marked by 5 to 7 m high steep cliffs on large outcrops (Plate 6.1). The quartz diorite and amphibolite country rocks of the Elsie Mountain Formation are strongly silicified and stained to red-brown by fine disseminated hematite. Cataclastic, clast-supported angular fault breccia occasionally occurs along the Creigthon Fault. Close to the Creighton Fault the east limb of the Victoria quartz diorite narrows down to about 130 m width and thickens again just along the fault. This variation is probable partly caused by tectonic displacement and repetition of block, although only one major shear-fault can be identified 150 meter to the north of the Creighton Fault.

6.16. West Limb of Victoria Quartz Diorite

The Creighton Fault displaced the east limb of the Victoria quartz diorite to some 800 meters to the west. The extension of Victoria quartz diorite occurs south of the fault and it forms a southeast trending funnel-shaped narrowing 700 m long body. This body is referred to as the west limb of the Victoria quartz diorite in this study, although originally called the east limb of Worthington Offset by Grant and Bite (1984) and Lightfoot and Farrow (2002). The country rocks hosting quartz diorite bodies south of the Creighton Fault are in general more complex than the monotonous amphibolite of the Elsie Mountain Formation. This are is build up by the metavolcanic rocks of the Stobie Formation, similar to those of the underlying Elsie Mountain Formation, consisting of massive and foliated fine- to coarse-grained metabasalts. Amygdules are common, and pillows are present. The Stobie Formation is intercalated with greywacke and quartz-feldspar sandstone of the Matinenda formation. The metabasaltic rocks of the Elsie Mountain formation includes significant amount of rhyolite on the east of the map sheet. East and northeast-trending narrow 2 to 10 m wide Quartz Diabase dykes are the most abundant in this area over the map sheet.

No sulphide mineralization is associated with the quartz diorite occurrence, however AreoTEM results of FNX indicates a localized conductor along the western edge of the body (Chapter 9, Fig 9.1,A). No description of this anomaly was provided by FNX. The area of the anomaly is covered by swamp of the Ethel Lake. The south-eastern tip of wedge-shaped quartz diorite body can be mapped just along the southern shore of the Ethel Lake.

6.16.1. *Sudbury Breccia occurrences*

Here he host rock to quartz diorite is the strongly brecciated arkose and quartzite, of the Matinenda formation of the Huronian Supergroup (Plate 6.5, 2-6). The tip of the main quartz diorite body is well exposed on the southern shore of Ethel Lake. At some places quartz diorite is spotty,

containing 0.3 to 0.8 cm quartz-feldspar xenoliths with faint boundaries, similar to areas found in the east limb. At both sides of the wedge-like termination of the quartz diorite, Sudbury Breccia zones have developed. The Sudbury Breccia is fine-grained to aphanitic, light brownish grey on weathered surface and contains biotite, white mica, and quartz (Plate 6.5, 7). Sudbury Breccia is intruded by fingers of quartz diorite that becomes more felsic by contaminating the silica rich breccia matrix (Plate 6.5, 8). Quartz diorite forms a maximum 20 m long pod, and located 110 meters away form tip of the main body. This relatively wider area might hide other small pods of quartz diorite separated from the main dyke body. Sudbury Breccia contains angular shard-like fragments of the host wacke (Plate 6.5, 8). Generally the breccia matrix is well foliated and smaller clasts 3 to 6 mm clasts are flattened. There is no more exposure of quartz diorite along strike of the main body to the south of this area.

6.16.2. *Termination of the East Limb*

Exploration drilling by INCO in the eighties revealed that quartz diorite at this area plunges underground and can be followed 300 m further to the southeast and to about 300 meters at depth (Grant and Bite, 1984).

A prominent east-west-oriented fault was found approximately 50 to 70 m south of the plunging area. To the west, the fault can be followed over 100 meters where it is intruded by 1 to 3 m wide partly deformed Quartz Diabase dykes. To the east the fault can be inferred by several outcrops elongated east-west.

According to INCO historic drilling the quartz diorite intrusion is not displaced at this area laterally. On the other hand this fault may have caused the drop of the offset possible explaining why it is plunging. The next occurrence of quartz diorite is the Vermilion offset, 800 meters to the east of this location. The opening and morphological depression along the Crean Hill mine road, the steeply northwest facing cliffs especially at the Vermilion Mine, the presence of large number of northeast-trending hornblende diabase dykes all imply a possible a tectonic disturbance along northeast, east-trending structures parallel- sub-parallel with the Creighton Fault. These findings may suggest that Vermilion offset it the faulted-off piece of the west limb of the Victoria quartz diorite. Unfortunately a broad area just north of the Vermilion offset is poorly exposed.

6.17. Quartz diorite occurrences west of Ethel Lake

To the west of Ethel Lake, along the Creighton Fault, several smaller ill-defined quartz diorite bodies occur. They can be studied by limited outcrops only. They are mostly known by exploration trenching and drilling by INCO in the eighties. One small block, along the Fairbanks Lake Resort road, amphibole-biotite quartz diorite contains weak 1-3 % disseminated sulphides of pyrrhotite and

chalcopyrite. The true Worthington offset begins as far as 800 meter from the west limb of Victoria quartz diorite. To the north the Worthington offset is cut sharply by the Creighton Fault. To the south the Worthington offset forms a 26 kilometer long, continuous southwest-striking, 30-50 meter wide dyke. The dyke is host to several post-producing mines (Chapter 5).

6.18. Geology and petrography of Stobie amphbolites

Amphibolite of the Stobie Formation on the outcrops is massive, fine-grained dark-green. Petrography study of amphibolite indicates and average composition of 70-80 % granoblastic 0.1 to 2 mm subhedral prismatic amphibole (hornblende) with interstitial 10-20 % plagioclase and 3-5 % quartz. Amphibolite contains 1 to 3 mm rod-like ilmenite crystals or grain aggregates The Stobie amphibolite shows variable degree of epidote-chlorite alteration of amphibole and chlorite-rutile-titanite alteration of ilmenite. Coarse 1 to 3 cm idioblastic-porphyroblastic texture develops in Stobie amphibolite in the contact zone with Quartz Diabase dykes northeast of the Vermilion mine. This rock in fact identical with the “Metabreccia” unit of the Vermilion mine (Chapter 10).

6.19. Geology of metasediments of the Matinenda Formation

The most abundant metasedimentary rock of the Matinenda Formation is light-grey fine 0.3 to 1 mm, quartzite. On outcrops the quartzite is massive, do not exhibit bedding. The bedding of the sedimentary formation can only be observed by the presence of 1 cm to 10 m thick intercalation of darker grey mica rich quartz wacke (Plate 6.5, 2). The wacke is brown-grey in color and fine grained to aphanitic, rarely contains 1 to 3 mm “spots” (Plate 6.5, 3). Bedding is parallel, planar and finely spaced 1 to 10 cm (Plate 6.5, 5). Bedding planes dips to southwest (210-235 degree) with 75-85 degree. Foliation is generally weakly developed and when seen it is oblique to the bedding plane and trends east-west (Plate 6.5, 4). The strike of the bedding is parallel, sub-parallel with the general northwest trend of lithological boundaries of amphibolite, wacke, garnet-amphibolite and rhyolite intercalations characteristic for the mapping area south of the Creighton Fault. Wacke intercalations form 10-90 m wide northwest-trending mappable zones. These zones, in fact, contain strongly inter-bedded quartzite and wacke with the overdominance of wacke. Sudbury Breccia occurs in these sediments as 1-8 m irregular areas, nicely exposed along the east and south shores of Ethel Lake. At the southern margin of the map sheet quartzite and wacke contain 1-5 % disseminated sulphides indicated the gossanous surface of some outcrops. The weak mineralization forms narrow northwest-trending zones and can followed up to 50 meter strike lengths.

6.19.1. *Petrography of metasediments of the Matinenda Formation*

Petrography study of quartzite indicates an average modal composition of 25-35 % muscovite and 65-75 % quartz. In few slightly recrystallized samples 5-15 % anhedral sericite altered feldspar grains occur, indicating an original sedimentary composition of about 15-20 % feldspar and 80-85 % quartz; sub-feldsparic quartz arenite. In strongly recrystallized quartzite muscovite plates are well oriented and define the continuous microscopic foliation of the rock. The wacke intercalations and thicker beds comprise about 40-55 % very fine 10 to 100 μm sericite groundmass enclosing 25 % 300 to 400 μm sub-angular quartz grains, 15-18 %, 400 to 700 μm rounded quartz aggregates and 3-7 % 1 to 2.5 mm ilmenite. Sericite in the massive groundmass exhibits weak continuous foliation. The "spots", rarely seen on hand specimens, comprise granular assemblage of quartz, muscovite, chlorite and ilmenite. These grains are distinctly coarser, i.e. 0.5 to 2 mm, than the groundmass and often have a circular or sigmoid outline. The fine groundmass sericite faintly wraps around these aggregates. All these features suggest that spots represent retrogressed garnets, typical for Huronian metasediments.

6.20. Garnet amphibolite

On the east shore of Ethel Lake a distinct lithological unit comprises massive to pillowed amphibolite consisting fine (1 to 2 mm) to very coarse 5 cm red garnets. This unit was also recognized by Grant (1984) and he named the rock garnet amphibolite. The garnet-amphibolite forms a distinct 580 meter long 50 to 90 meter wide northeast-trending unit and may pinches out under Ethel Lake. To the south it is probably cut by a proposed northeast-trending structure along the Can Hill mine road. Sudbury Breccia occurs frequently within the unit, a nice outcrop is situated just along the Crean Hill mine road.

6.20.1. *Mineralization in Garnet amphibolite*

Garnet amphibolite contains 1-4 % 0.1 to 2 mm finely disseminated sulphides indicated by weak gossanous alteration of some outcrops. Sulphide mineralization is associated with strong chlorite alteration of garnets. Alteration zones contain sulphides of chalcopyrite, pyrrhotite, and pyrite in the order of decreasing abundance. Two composite assay samples (180401, 180802) were collected from the weakly mineralized zones. Assay results indicate that mineralized zones are anomalous in gold (0.4 g/t) and slightly anomalous in Pt and Pd (Appendix 8, 26, 26).

6.21. Quartz Diabase Dykes

6.21.1. Geology

The height abundance of narrow 1 to 7 meter amphibole Quartz Diabase dykes is characteristic for the mapping area south of the Creighton fault. Quartz Diabase dykes are dark, greenish-grey, massive, and fine-grained to aphanitic on outcrops. The dykes trend east, northeast (90-70 degree) and dip steeply to the south (70-90 degree) or vertical. These dykes are apparently associated with east-, northeast-trending faults. The dykes generally do not show deformed, sheared-texture within the fault but locally can have sheared walls against the fault rock or the host rock. This field relationship may imply that Quartz Diabase dykes intrude the pre-existing structures. Several dykes have been located along a 2 km west-east profile of the map area. This suggests that narrow individual dyke may be continuous for several kilometres.

6.21.2. *Petrography*

Petrography study of the quartz diabase dykes revealed two grain size variety; a 1 to 3 mm fine/medium-grained granular core facies and a 0.3 to 1 mm fine-grained chilled margin. The rock is composed of 55-67 % amphibole and 23-45 % interstitial plagioclase, quartz and traces of apatite. Amphibole is stubby, prismatic, subhedral composed of a brow-green core associated with ilmenite and rare thin blue-green hornblende rim. Most of the amphibole quartz diabase samples indicate the presence of weak to complete replacement of plagioclase and minor amount of amphibole by sericite, chlorite, epidote and quartz. A coarse granoblastic amphibolite (similar to metabreccia of the Vermilion mine, Chapter 10) is associated with Quartz Diabase dykes, northeast of Vermilion mine. Grab Assay samples indicate minor Cu (0.03 wt.%) but no Pt+Pd+Au values (Appendix 8, 28).

6.22. Rhyolite

Felsic granular metamorphic rock, described as rhyolite was mapped northwest and southeast of the Vermilion mine. Rhyolite was found only on limited outcrops, but Sudbury Breccia at the Vermilion mine site contains abundant rhyolite xenoliths.

7. STRUCTURAL STUDY OF DEFORMATION ZONES IN VICTORIA MINE AREA

7.1. Introduction

During the early years of 2000-2001 field mapping seasons it has been gradually recognised that most of the contact zone between the South Range Norite and Victoria quartz diorite, as well as the metavolcanic footwall rocks of the Elsie Mountain Formation is intensely tectonized by numerous east-west, northeast-southwest -trending 30 cm to 15 metre wide shear zones. The

northernmost segment of the Victoria quartz diorite occupies an embayment-like structure which is in sharp contact with the South Range norite to the north (Appendix 1). This sharp northeast-trending line is a prominent tectonic feature, the Victoria Shear zone. Therefore it was concluded early, that transitional development of the Victoria quartz diorite from the Sublayer Norite is not possible to study as in many other offset dykes i.e. Copper Cliff and Whistle offsets (Grant and Bite, 1984). The large number of shear zones observed at the Victoria mine area plays a significant role not only in the current geological picture but in the redistribution and re-location of contact- and –offset type Ni-Cu-PGE sulphide mineralizations. In this chapter the meso-, macro- and micro-textural characteristics, kinematic indicators, sense of movements of these shear zones are described in details and compared with the South Range Shear zone to the north.

7.2. General Structural Geology of the map area

Three major structural domains exist in the mapping area. The two major structures, the Victoria Shear Zone and subparallel Creighton fault divide these domains. The Creighton Fault is a regional structure, associated with the Murray Fault system and it can be followed more that 30 km to east and to west as well. In the mapping area, the Creighton fault is strike slip, sinistral. The Creighton fault displaced the southeast-trending east limb of Victoria quartz diorite some 800 meters to the west. This major dislocation appears to be the latest movement of along the fault and during the tectonic segregation of Victoria quartz diorite. Limited outcrops, exposing the margin of the fault, show cataclastic brecciation with silica-hematite alteration. The fault rocks in the core of the fault are not exposed. The dip of the fault cannot be measured but inferred to be near vertical or steeply dipping to the south.

South of the Creighton fault, other faults and shear zones are rare but fault-related hornblende quartz diabase dykes are prominent. These faults are indicated by sheared wall rocks of the Stobie Formation amphibolite and they dip to 120-175 with 75-85 degree displaying pitch 60-75 to the east by striation and stretching lineation of chlorite. In this block the general trend of the lithological units and the strike of bedding are northwest-southeast. Both quartz diorite intrusions the; Victoria west limb and the Vermilion quartz diorite trend northwest along the lithological interfaces of variety of rocks of the Stobie Formation and Matinenda Formation.

North of the Creighton fault, 1-10 meter wide shear zones become more abundant, especially in the vicinity of the Victoria Shear Zone. The Victoria Shear is a first order tectonic feature in the area, it divides the SIC and the Huronian metavolcanic footwall rocks. The Victoria shear zone is locally 20-30 m wide and several sub-parallels spays or individual narrow shears occur within 200-250 meters distance to the north and to west. The majority of the ore samples, that can be collected around the Victoria mine are sulphide crush breccia; fragments of wall rocks, quartz veins and

carbonate cemented by massive sulphide matrix This indicate that the Victoria Shear Zone and the subparallel zones have deformed, re-worked and re-distributed magmatic Ni-Cu-sulphides of the Victoria quartz diorite in the once existing Victoria Embayment.. This tectonic activity resulted in the formation of the mined-out Victoria Deposit. Aerial photograph interpretation of the block between the Victoria Shear and the Creighton Fault indicate the presence of two pre-existing fault arrays. North, northeast-trending fault are high angle to the Creighton fault and can be inferred by the linear arrangement of outcrops of the Elsie Mountain Formation. A pair of low-angle faults to the Creighton fault can be inferred to be northwest and northeast –striking based on strong preferred orientation of drainage patterns (Appendix 1).

North of the Victoria Shear Zone typical quartz diorite was not found instead characteristic mafic inclusion and sulphide-bearing Contact Sublayer intruded the Contact between the SIC and Elsie Mountain footwall amphibolite. Therefore continuity between the SIC units and the Victoria quartz diorite does not exist in the area. North of the Victoria Shear Zone, parallel-subparallel narrow 2 to15 meters wide shear zones occur 50-130 m apart and they become more abundant to the north (out of the map area). These shear zones offset the mineralized Contact Sublayer unit and apparent 5 to 30 m strike-slip dextral dislocations frequently occur along these deformation zones. About 3 kilometres distance to the north, the individual minor shears merge into a zone of pervasive strong foilation at the southern boundary of South Range Shear Zone (SRSZ). This clearly indicates that the Victoria and associated sub-parallel shear zones are the sub-system of the South Range Shear Zone (SRSZ). North, northwest trending faults can also be inferred in the area north of the Victoria shear. These structures are poorly exposed and usually marked by the outcrop and drainage patterns (Appendix 1). One of these lineaments in the northwest corner of the map area has a major kilometre-scale dextral displacement of the SIC contact. The structure is occupied by a northeast–trending elongated lake, typical tectonomorphology feature of the area.

In general, in the cores of these shear zones, the host rocks, and most commonly, norite grade to mylonitic tectonite developing strong foliation that dies out in a few meters away from the centre of the shears. The tectonics in these deformation zones appears to be L-S tectonics in which foliation is defined by mica rich layers and lineation is marked by the stretching lineation of micas and striation. All the mapped shear zones strike to the NE-E (60-90) and dip to S-SE (150-180) with angles varying slightly between 60 and 90 degrees (Fig 7.1). The orientation data are similar to those from the South Range Shear Zone (SRSZ) located north of this area. Shear zones are straight, branching or anastomosing on a map-scale. The faint or well-defined stretching lineation distinctly pitches 65-80 to the E-SE although rarely to the W-SW.

According to microstructural analyses, the tectonites in the shear zones vary from protomylonite to mylonite corresponding to brittle-ductile to ductile deformation along the shear

planes (Fig 7.1). In brittle shear zones protomylonite contains 50-60 % 0.1 to 2 mm sub-angular to well-rounded porphyroclasts of plagioclase in 40-50 % chlorite-rich foliated matrix (Fig 7.2). The host rock blocks between the slightly anastomosing and branching shear zones do not exhibit pervasive foliation but are strongly altered to chlorite carbonate. In mylonites, host rocks partially or completely re-crystallize to biotite, biotite-chlorite and chlorite schist. The schistose mylonite zones are associated with the Victoria Shear Zones within a 200 meter distance whereas protomylonite usually develops in shear zones located to the north hosted by South Range Norite. Systematic thinsection samples were collected from a number of both deformation types to analyze kinematic indicators in order to deduce the sense of shear.

7.3. Protomylonites

In this tectonite, the original magmatic texture and minerals of the host rock can still be observed. Large, 1 to 3 mm porphyroclastic grains of biotite and plagioclase tend to rotate along and flatten into the developing foliation plane. Foliation plane is usually slightly developed and defined by the "sheared off" or rotated trails of amphibole and platy biotite and/or chlorite. Rocks at this stage rarely contain amphibole, but are altered to epidote-chlorite-carbonate. Rock forming biotite is recrystallized into oriented biotite flakes and together with chlorite they define the continuous foliation. However biotite is very rare in these shear zones it is strongly altered to chlorite. Plagioclase usually alters to sericte, carbonate, and epidote. Porphyroclastic biotite and quartz are kinked and strongly strained. Quartz re crystallizes into a fine 0.05 to 0.1 mm polygonal strain free aggregate. Foliation is defined by undulating cleavage bands enriched in biotite-chlorite. These sheets wrap around plagioclase porphyroclasts and cut through biotite porphyroclasts. In protomylonites undulating cleavage bands may correspond to the S plane of a shear. With increasing deformation the cleavage bands become denser and parallel to each other but show a stiff curvature, characteristic S-C fabric often appears. C planes are usually thicker bands of chlorite and S planes develop in between defined by few oblique chlorite plates approximately 30-45 degrees to S planes. Plagioclase porphyroclasts in these samples are totally altered to sericite, carbonate and epidote.

Kinematic indicators in protomilionitic tectonites include book shelf texture of broken plagioclase grains. The grains fracture along micro-faults dextral (blocks tiled to the left) and sinistral (blocks tiled to the right). The bookshelf-faulted blocky plagioclase fragments extend with several micrometers and they are interconnected with oriented platy chlorite and recrystallized quartz (Fig 7.2). In this case the sense of micro-faults (i.e. synthetic, antithetic), the value of extension in microns and direction of extension referenced to the foliation plane can be collected during routine petrography study. The blocky to sub-rounded individual plagioclase fragments are in general tilted and slightly wrapped around the chlorite-rich foliation. In this case the long and short axis of grains

and the angle of long axes with reference to the foliation plane can be measured. In rare cases the sense of rotation of grains were also observed. Simple graphical presentation of these data can illustrate sense of shear along the foliation plane (Fig 7.2). In addition other micro textures, quarter folds, winged-porphyroclast, shadow structures were observed and used to support the statistical analysis.

In all studied samples the X-Z section (parallel with lineation (striation) perpendicular to foliation) of the tectonics showed a much better developed foliation and preferred orientation of broken plagioclase grains than on section cut perpendicular to foliation and lineation, generally near horizontal. This indicated that movement along these planes have stronger vertical component than horizontal. The shear sense deduced from studying microtextures indicates a steep slightly oblique south side up to the northwest thrusting. These results indicate that vorticity and orientation of the protomylonitic shear zones are identical with and formed together with the South Range Shear Zone located in close proximity to the north.

7.4. Mylonites

Mylonitic shear zones are associated with the major Victoria Shear. The shear zones strike to the NE-E (60-90) and dip to S-SE (150-180) with angles varying slightly between 60 and 90 degrees (Fig 7.1). These structures cut across and offset the No.2 West and No.1 West mineralization hosted with the Contact Sublayer. Field evidence exist at numerous places that re-distribution and remobilization of Cu-Ni-Sulphides in the form of massive pyrrhotite lenses and chalcopyrite streak, quartz-chalcopyrite veins are associated with these structures (Chapter 6, Chapter 9). Sulphide mineralization in shear zones however cannot be followed laterally for a large distance. This indicates that transportation of sulphides along these structures is rather vertical. The Victoria Shear and its subparallel splays are well exposed in road cuts on the north-leading Faribank Lake Resort paved road (Fig 7.3, 7.4 Appendix-1, and MAP-1). In these exposures the most appropriate section, the x-z planes of shear zones can be directly observed. The rock in mylonitic shear zones is dark green, black in color, fine grained and exhibits straight or smooth spaced foliation. The host rock to the shears are Basal Norite, Nipissing Gabbro, Elsie Mountain footwall amphibolite to the west of Mond Lake, Victoria quartz diorite along the South shore of Mond lake and Elsie Mountain quartzite to the east of Mond Lake (Appendix-1, MAP-2) Mylonitic shear zones contain syntectonic shear parallel white quartz and quartz-carbonate veins of 1 to 5 cm thick. Many veins are normally budinaged and transposed, flattened and form sigma-clasts along the foliation planes (Fig 7.3). Some veins folded in tight isoclinal shear-parallel sheetfolds axes plunging parallel with lineation (Fig 7.4). These deformation zones are often complex in mineralogical composition; the contain domains of more competent quartz-carbonate-chlorite schist within incompetent chlorite schist with dragfolds

(Fig 7.4). These outcrop-scale macroscopic kinematic indicators suggest the same vorticity; south side up to the northwest thrust faulting along the array of the Victoria Shear and its splays. The Victoria Shear Zone east of Mond Lake consists of strongly foliated lepidoblastic quartzite with muscovite rich cleavage bands. In this area no macroscopic shear-sense indicators can be collected, therefore the quartzite was sampled for C-pattern micro-fabric analysis.

Oriented thinsection samples were collected from a number of mylonitic deformation zones to support the sense of movement where deduced from macro-features, or to deduce the sense of movement from outcrops without macroscopic indicators. Routine petrography study of tectonized rocks in the mylonitic shear zones revealed a common compositional banding of the samples consisting of cleavage domains vary in thickness. Cleavage domains are composed of bands of chlorite including remnants of biotite, occasional strongly zoned epidote and titanite. In one area at the No.2 West Zone the cleavage band is composed of chlorite and Cr-rich muscovite (mariposite). Syntectonic alteration mineral assemblage corresponds to a greenschist facies metamorphic alteration of host rocks. Only in few deformed quartz diorite samples, recrystallized biotite and metamorphic hornblende tend to form the weakly developed cleavage bands. Upon stronger deformation biotite and amphibole quickly alter to chlorite and strongly zoned epidote typically with a rounded core and euhedral rim.

In mylonitc tectonics, the spacing between domains is slightly variable but consistent 0.1 to 2 mm. Cleavage domains are 0.1 to 3 mm thick and compose up 15-30 vol. % in metaquartzite and up to 50-70 vol. % in mafic SIC rocks and amphibolite host rocks. Cleavage domains are parallel but slightly undulous and the transition to microlithons is discrete. Microlithons are composed of recrystallized quartz carbonate porphyroclastic feldspar and chlorite (Fig 7.3, 7.4). Chlorite appears in microlithons as thin plates aligned at low angle (0-30 degrees) at cleavage bands defining the S planes of the general S-C mylonitic texture (Fig 7.3). Remnants of partly recrystallized feldspar and quartz mantled-porphyroclasts define as α or δ clasts structures indicative of the same shear sense obtained from macroscopic kinematic indicators (Fig 7.4, 4.5). In the major Victoria Shear Zone, euhedral 0.3 to 1 mm porphyroblasts of zoned carbonate (variable Fe/Mg ratios) are characteristic whereas in the other shear zones carbonate generally form porphyroclasts or boudinaged transposed recrystallized lenses layers, lenses

Micro tectonic analysis of oriented samples from the shear zones indicates that the shear sense is south side up to the northwest. The shear zones on horizontal surface do offset the SIC contact. The lateral displacement is between few meters to 50 meter to the west indicating steep oblique thrusting. Therefore the apparent restricted 10 to 50 meters lateral offset on surface may indicate ten times larger vertical offset that may cause sudden change in mineralization type on any horizontal surface.

7.4.1. *Quartz and carbonate C-axis analysis from mylonitic shear zones*

From mylonitic shear zones C-axes orientation of recrystallized quartz and calcite as well as porphyroblastic Fe-Mg carbonates were collected to evaluate if optical orientation of grains exist and how it is related to the sense of shear. Two samples (181708, 190912, Fig 7.6) were measured. Stereographic projection of countered C-axis axis distribution showed separated maxima to the north and south, orthogonal to the foliation plane. The girdle patterns were interpreted following the Taylor-Bishop-Hill numerical modeling modified by Lister and Hobbs (1980). A very weak pattern may indicate a small circle indicative of coaxial deformation, i.e. shortening whereas the weakly developed cross girdles are indicative of non-coaxial simple shear. The coaxial shortening may be responsible for grain shape orientation of quartz grains; blocky grains elongated parallel with the foliation. The small asymmetry of the simple shear component indicates dextral on 80 degree and sinistral on 250 degree sections consistent with macroscopic kinematic indicators that all suggest a thrust fault interpretation for the shear zones. In sample 181708 Fe-Mg rich carbonate porphyroblsts appears to show the same preferred orientation as the quartz grains their growth during noncoaxial or static conditions. In the other sample (190912) carbonate is sheared, streaked out into lenses and ribbons strongly twinned grains.

7.4.2. *Microstructural analysis of quartz-rich shear zones*

The Victoria Shear Zone in metaquartzite is characterized by well developed foliation defined by muscovite rich layers and parallel quartz ribbon domains in the field. Under the petrographic microscope the mylonite composes of alternating ribbons of 60-80 % quartz and 20-40 % muscovite. Traces of strongly zoned Quartz ribbons are strongly elongate and show strong undulose extinction, deformation lamellae, subgrain structures and dynamic re-crystallization, mainly along the rim of the ribbons. Recrystallized grains are strain free and show little deformation. Ribbons probably formed by extreme flattening or constriction of large single crystals. Less deformed samples compose of 70 % quartz, 20 % feldspar, 10 % muscovite, probable referring to the original composition of 70 % quartz and 30% feldspar. Muscovite alters from feldspar and it attains strong orientation during deformation and re-crystallization of the rock. The muscovite was separated from one sample of Victoria Shear and was used for K/Ar, Ar/Ar age dating the deformation.

Due to the low asymmetry present in deformed quartzite samples, the shear sense is difficult to identify. In one sample the optical properties of core-mantle structured θ-clast (quartz porphyroclasts) was used for obtaining orientation data (Fig 7.5). Mantled porphyroclasts are cored with strongly strained single quartz grain. The core quartz displays and “hourglass” undulous “sweeping” extinction along parallel low angle subgrain boundaries. Universal-stage measurements of C-axes of subgrains indicate low angle 2-7 degree misorentaion. These boundaries are tilted by

different angles either to the left or to the right with respect to the foliation plane. The recrystallized mantle comprises strain free subhedral equigranular quartz with sharp straight non-sutured grain boundaries with possible lattice preferred orientation. A number of strike orientations between 0-180 degrees to the foliation plane were measured and monoclinic symmetry was found similar to tiling measurement results of porphyrclasts in protomylonite (Fig 7.5). The texture may be interpreted as kinematic indicator, suggesting sinistral shear sense on section looking east, northeast and dipping to the south 90-80 degrees, thus indicative of a thrust fault.

Given the large number of recrystallized quartz grains in deformed quartzites of the Victoria Shear Zone, universal-stage was used to obtain distribution pattern of C-axis orientation with respect to the foliation planes. Universal-stage C-axis measurements of two oriented thinsections cut parallel with the X-Z section (parallel with lineation, perpendicular to foliation) resulted in finding preferred crystallographic orientation (Fig 7.6). Stereographic projection of countered C-axis axis distribution exhibits single main circle girdles most probable a Type-I cross girdle (Lister and Wiliams, 1980). The patterns have weak asymmetry in sample 280101 of the bulks sample, however when only the coarse quartz ribbons plotted the shear-sense indicator asymmetry is more dominant. The girdle pattern corresponds to a major component of simple shear and dextral sense of shear. Give the orientation of sample his would indicate thrusting along this segment of the Victoria Shear. In sample 171801 the double maxima on the great circle perpendicular to foliation may indicate an element of coaxial deformation i.e. plain strain (Koshia, 1988).

7.5. Faults, macro faults

Macro faults are outcrop-scale fractures with exposed and traceable fault planes consisting macro structural elements, striation, steps, crescent gashes or quartz ribbing. These structures are in general few centimeters thick and contain no filling of minerals or sheared host rock. Structural data was collected along the Fairbank Lake Resort road representing a traverse as far as 1 km to the north of the Victoria Shear Zone. The sense of movement along these structures was evaluated based on field measurements. Structures without kinematic indicators were collected as fault planes. These fault strike north northeast (30 degree) and dip to the west (300) with an average 55 degree. Dip angles vary from 30 to 78. The orientation of “Riedel” fractures may indicate a common reverse movement along these structures. These faults are equivalent to regional north-northeast trending faults which are easily identified in aerial photographs and responsible for alignment of hydrology and group of outcrops.

7.6. Quartz-carbonate-clinozoisite veins

Minor but consistent structural features of the map area are the 1 to 20 cm thick veins of quartz-carbonate in the norite varieties and in footwall amphibolite. These veins comprise coarse 0.1 to 0.7 cm granular quartz and calcite with minor or accessory chlorite and acicular light green actinolite and/or light brown clinozoisite. There are two sets of vein orientation. On set of veins dip to the west, southwest about 50 degree and strike northwest-southeast, apparently parallel with the contact of the SIC in the mapping area. The other set of veins have similar orientation to the shear zones. Thick sulphide-bearing (chalcopyrite-pyrrhotite) quartz, quartz-carbonate veins are often found in close proximity of shear zones. The veins are parallel- subparallel with the deformation zones suggesting a genetic link those. On surface, the exposed shear zones do not show evidence that these veins crosscut the strongly developed foliation in the shear zones. In drill core many sulphide-bearing veins were found to be concordant with foliation planes (Chapter 9). Examination of drill cores from the No. 2 West Zone resulted in finding few quartz and carbonate veins cutting almost perpendicular to the foliation but in all cases the veins are barren.

Rare open cavities in massive veins show evidence that quartz is overgrown on vein walls in open space but the vein walls show evidence of shearing by the appearance of fibrous elongated quartz and actinolite. This may indicate multiple episodes i.e. either shear related fracture first and dilatation or dilatation and late shearing of walls. Smaller veins indicate that they are related to shearing because nicely developed fibrous or even prismatic quartz-amphibole crystals point strongly to the direction of movement along the planes in many quartz veins, fine acicular aggregates of brown clinozoizite needles occur. The formation temperature of cliniozoizite was established by fluid inclusions thermometry.

Clinozoizize contains numerous primary 10 to 30 μm, 2-phase aqueous L-V inclusions with a very consistent 80 % degree of filling of the liquid phase. All measured fluid inclusions homogenized to the liquid phase between 380ºC and 320ºC with the average of 287.5 ºC. No cryoscopy measurements could be made due to the weak transparency of the brownish colored clinozoizite. Quartz grains of the same vein are host to numerous pseudo-secondary, secondary 2-phase aqueous L-V and 3-phase aqueous L-V-Halite inclusions in dense clouds. No analysis of these inclusions was carried out

7.7. Summary

Detailed field mapping, macroscopic and micro-structural analysis of deformation zones of the northern block of the map area indicate that the northeast-trending parallel protomylonite and mylonite zones have formed by thrust faulting of SIC and footwall amphibolites of the Elsie Mountain Formation. Recrystallized quartz in shear zoned developed LPO indicative of general

(noncoaxial shear) and thrusting; south side to the northwest. These L-S tectonites developed within the deformation zones have same bulk vorticity and orientation that of the South Range Shear Zone 3 kilometres to the North. Therefore theses deformation zones are identical with the South Range Shear Zones and may represent the southernmost splays or subsets of it. Based on the close similarity of structural elements observed and studied from shear zones in the mapping area and the close proximity of the SRSZ, the timing of deformation must be equivalent to the South Range Shear Zones. Given this possibility the shear zones were sampled for K-bearing syntectonic minerals in order to carry out radiometric K/Ar, Ar/Ar age dating of deformation (see in next Chapter).

8. K-Ar, ^{40}Ar-^{39}Ar GEOCHRONOLOGY OF DEFORMATION ZONES AND ALTERATION OF QUARTZ DIORITE OF THE PROXIMAL WORTHINGTON OFFSET, NEAR VICTORIA MINE.

8.1. Introduction: Geochronology of the Sudbury Area

The Huronian metasedimentary rocks were deposited between 2450 Ma, the age of Copper Cliff Rhyolite in the Sudbury area (Krogh et al., 1984), and 2219 Ma, the age of the Nipissing Intrusive Suite (Corfu and Andrews, 1986). The Huronian rocks were folded prior to intrusion of the 2219 Ma Nipissing diabase sills (Card, 1978; Benett et al., 1991) and also during the 1890-1830 Ma Penokean Orogeny (van Shmush 1980; Hoffman, 1989).

The Penokean orogen formed by folding and thrusting of Paleoproterozoic volcano-sedimentary rocks at the southern margin of the Archean Superior Province craton. Major tectono magmatic activity during the 1.89–1.83 Ga Penokean orogeny was preceded by the less well known ca. 2.4–2.2 Ga Blezardian orogeny in the Lake Huron area and a late Archean orogenic event at about 2.6–2.4 Ga in the Lake Superior region (Riller et al., 1999). Rocks in the Lake Superior portion of the orogen differ greatly in metamorphic grade, volume of felsic plutonic rocks and structural style from those in the Eastern Penokean Orogen (EPO) north of Lake Huron. Yet, contraction in both parts of the orogen is generally attributed to frontal collision of Archean or Proterozoic island arc terranes with the southern margin of the Superior Province.

The Huronian volcanic rocks and metasediments were affected by the 1850 Ma Sudbury event (Krogh et al., 1982), a meteorite impact (Deutsh et al., 1995) and formation of a melt sheet from lower crustal source of the Archean granitoids and mafic volcanic rocks of the Huronian Supergroup (Lightfoot et al., 2001, Mungall et al., 2004).

The Sudbury Structure is located close to the triple junction of the three principal terrains of the Canadian Shield; the Archean Superior Province, the Paleoproterozoic Southern Province and the Neoproterozoic Grenville province. The northeast-southwest oriented Grenville Front (GF) runs sub-parallel with the southern boundary of the elliptical-shaped Sudbury Igneous Complex (SIC) about

30 km to the southeast and separates the Southern Province and the Grenville Province. The Grenville Front Tectonic Zone (GFTZ) is about a 30 km wide zone of high grade strongly deformed amphibolite to granulite facies gneisses bounded by the GF to the north and lower grade metamorphic rocks of the Grenville Province to the southeast (Corfu and Easton, 2000). The GFTZ represent the remarkable linear northeast-trending limit of the Grenville Province that extends for 2000 km from Georgian Bay on Lake Huron to the Atlantic coast of Labrador (Wynne-Edwards, 1972; Rivers et al., 1989). Several pre-Grenvillian tectono-metamorphic, intrusive magmatic events are recognized along the GFTZ between ages of 2640 Ma (Val d'Or) and 1453 Ma (Killarney) (Krogh, 1994).The Grenvillian metamorphic ages are consistent at ca. 1000 Ma along the 2000 km GFTZ accompanying a NW-directed thrusting, or crustal loading in the front zone (Krogh, 1994).

Along the northeast trending GFTZ, in the Killarney-Sudbury area, the southern margin of the Huronian Province is intruded by a suite of granite-granodiorite plutons referred to as the Grenville Front granites (LaTour and Fulgar, 1986) or Grenville Front Pluton (Card and Hutchizon, 1972) (Fig 8.1). These granitoids are variably foliated and mylonitized, have sharp intrusive contacts to the north and bounded by mylonite zones the southeast which defines the GFTZ (Davidson 1986). The ages of these granitoids span around ca. 1750 Ma and ca. 1470 Ma (Fig 8.1).

The 1750-1700 Ma evens represent the Killarnean metamorphism (Pb/U titanite, Corfu and Easton, 2000) (Fig 8.1). The Killarnean event is known primarily as a period of magmatism during a passive anorogenic episode (Clifford, 1990; Fueten and Redmond, 1997). A regional Na and K metasomatic event (Fedo et al, 1997) is associated with Killarnean intrusives at 1700 Ma (Schandl et al, 1994). Hu et al. (1998) report whole rock $^{40}Ar/^{39}Ar$ ages 1732-1766 Ma from argillites and phyllites in the Elliot Lake area which are comparable to $^{40}Ar/^{39}Ar$ hornblende ages of 1760-1680 Ma obtained from the core of Penokean Orogen in Minesota and Michigan (Holm et al., 1998; Scheider et al., 1996) and interpreted as resulting from the ca. 1760 Ma metamorphism and subsequent tectonic unroofing of the orogen.

The 1470-1440 Ma Chieflakian event is well established as a period of intrusive activity, including emplacement of plutons of the Killerney Magmativ Belt (van Breemen and Davidson, 1988; Davidson and van Breemen, 1994; Krogh, 1994) (Fig 8.1). Although the Chieflakian magmatic activity is generally viewed as representing anorogenic conditions (Clifford, 1990; van Breemen and Davidson, 1988) Fueten and Redmond (1997) presents evidences that this event linked to major compression and northwest-directed thrusting in the Southern Province, comparable to contemporaneous orogenic events in the southwestern United States (Nyman et al., 1994). Krogh and Davis (1968) reported a single Rb/Sr age of ca. 1450 Ma of muscovite from deformed pegmatite of the 1700 Ma Chief Lake complex. Krogh (1994) dated metamorphism and deformation near Killarney at 1453 +/-6 Ma, and Dudás et al. (1994) reported ages of metamorphism in the footwall of

the GF just south of the Chief Lake complex of ca. 1445 Ma. Davidson and van Breemen (1994) also concluded that penetrative deformation within the 1700 Ma Chief Lake complex pre-dated the 1235 Ma emplacement of Sudbury diabase dykes.

Olivine diabase dykes of the Sudbury diabase swarm (Fahrig et al., 1965; Fahrig and West 1986) are vertical, trend northwest, and vary from few meters to more that 100 m thick. They represent the last tectono-magmatic event before the Grenville orogeny (Haggart et al., 1993) and intruded across a structural and metamorphic front established in a quiescent period preceding Grenvillian orogeny. Diabase dykes of the Sudbury diabase swarm in the Southern Province, yielded baddeleyite U-Pb ages of 1235 +/-3 Ma (Dudás et al., 1994). The Sudbury diabase dykes are deformed and metamorphosed at conditions approached the granulite facies >700 ºC, >8 kbar (Bethune and Davidson, 1997) at c.a. 1000 Ma by the Grenville orogeny (Dudás et al., 1994).

8.1.1. *The timing of the deformation and metamorphic alteration of the Sudbury Igneous Complex*

To date, the timing of major deformation of the SIC is still a matter of debate. In the early times of the scientific and industrial research, the elliptical, northeast-southwest-elongated shape of the SIC was not regarded as of geological significance. The shape of the SIC was generally considered to have been formed by a norite lopolith irruptive (Muir, 1984). The structure has been variously interpreted as the product of explosive volcanism (Muir 1984), impact cratering (Dietz, 1964) or both impact cratering and magmatism (Dessler et al 1987, Chai and Eckstrand 1994). Advocates of volcanogenic origin point out to the noncircular map pattern of the SIC and its perceived relationship with regional tectonic structures (Card and Hutchinzon, 1972; Muir, 1984). The oval pattern of the SIC was considered to be the result of displacement along the regional scale faults of the Murray System (Souch et al., 1969; Naldret et al., 1970).

The current interpretation for the origin of the Sudbury Structure is that it represents a tectonized and deeply eroded remnants of 100-200 km diameter peak-ring or multi-ring impact basin (Grieve et al 1991, 1995; Deutch and Grieve, 1994). The bulk of the deformation of the circular meteorite impact basin and solidified melt sheet occurred along the South Range Shear Zone (Shanks and Schwerdter, 1989, 1991b). The zone is about 50 km long, 6 km wide and consists of strongly foliated rocks with L-S tectonic fabric developed during a northwest-directed reverse ductile shearing and contraction of the SIC (Shanks and Schwerdter, 1991a).

It has been already shown in Chapter 7 that the orientation, kinematics, and micro- textures of 1 to 10 metres wide shear zones of the Victoria mine area, are identical with those described from the SRSZ (Shanks and Schwerdtner, 1991a) and identified at the Chief Lake complex area – Killarney area along the GF (Fueten and Redmond, 1997). This deformation, responsible for compression and

shortening of the SIC, therefore is regionally present in the form of non-pervasive discrete few meter to 6 km wide shear zones. Fueten and Redmond, (1997) first suggested the bulk deformation of the SIC may be have happened synchronous with the ca. 1450 Ma Chieflakian compressional tectonic-magmatic event based on similarities of orientation, kinematics, and micro- textures of the SRSZ and pre-Grenvillian, Chieflakian shear zones along the GFTZ. Lately Mazatlzal-Labradorian age, 1.7-1.6 Ga, ductile deformation of the South-Range SIC was suggested, based on U-Pb titanite and $^{40}Ar/^{39}Ar$ biotite ages of shear zones from the Thayer Lindsley mine (Bailey et al., 2004). Their biotite $^{40}Ar/^{39}Ar$ inverse isochron age yielded 1477 +/- 8 Ma.

Amphibole and biotite of QD result from alteration of former pyroxene (Grant and Bite 1984). Primary amphibole and biotite occur in small quantity in Main Mass rocks (Naldrett and Hewins, 1984; Therriault et al., 2002). All these suggest that the primary Sudbury magma had a significant volatile component that may have exsolved upon crystallization and reacted with the primary mafic minerals to form late magmatic amphibole. The lack of primary magnetite in many QD, or the presence of peculiar pseudomorphs of ilmenite-biotite after magnetite, also suggests an early oxidizing volatile expulsion (Szentpéteri et. al, 2002). The magmatic volatiles mixed with fluids generated in the footwall and remobilized parts of earlier massive sulphide ores to form significant concentration of PGMs in footwall Ni-Cu-PGE sulphide veins (Farrow and Watkinson, 1997; Molnár et al, 2001; Molnár and Watkinson, 2001; Farrow et al., 2005, Hanley et al. 2005).

South Range QD offsets and South Range Norite contain high Al calcic-amphiboles (hornblende, and tchermakitic hornblende); in a few cases they formed contemporaneously with garnet that suggests a superimposed almandine-amphibolite facies metamorphism with textural evidence of zonal overgrowths of these amphiboles on actinolite cores resulting from deuteric alteration (Fleet et. al, 1987). The presence of biotite and spessartine garnet in the metasedimentary sequence (Whitewater Group) of the Sudbury Basin attests to middle to-upper greenshist (~ 400 ºC) facies metamorphism (Roussel, 1975; Sadler, 1958) along the South Range Shear Zone. A considerable debate still exists on the timing of peak metamorphism of the Sudbury area. In contrast to Card's (1964, 1978) results, Brocoum and Dalziel (1974), Fleet et al., (1987), Thomson et al., (1985), Shanks and Schwerdtner (1991a) concluded that prograde metamorphism occurred post-impact, affecting both the Huronian volcanic-sedimentary footwall and SIC rocks, reaching amphibolite facies. However, peak metamorphism of the Huronian Supergroup occurred soon after the emplacement of the Nipissing Gabbro (2240Ma) at 2220 Ma according to Jackson (1997) and Easton (2000) and was pre-impact in the view of Riller et al. (1996). Peak, post-Nipissing metamorphic conditions were of amphibolite facies at 560-/+60 ºC temperature and 4.3-/+0.8 kbar pressure (Blonde, 1996). Jackson (1997) recorded 500-560 ºC temperature and 1.5-3 kbar pressure conditions for metamorphism of Nipissing Diabase in May Township ca. 60 km from the SIC. PT

conditions obtained from Sudbury Breccia at Vermilion mine (Chapter 10) are similar to the above mentioned ones and may support a post-Sudbury Event age of peak metamorphism of the area.

In this chapter, results of K/Ar and $^{40}Ar/^{39}Ar$ age determination of discrete deformation zones and alteration minerals in quartz diorite, presented. The majority of the shear zones at the Victoria mine area have undergone retrograde metamorphic alteration to chlorite-carbonate-quartz +/- epidote at greenschist facies conditions. In major shear zones, generally wider than 2 to 5 metres, biotite occurs rarely, only as alteration remnants surrounded by chlorite. In smaller shear zones, 30 cm to 2 meters, biotite can be present (as much as 15-20 vol. % of the sample) together with abundant chlorite. The presence of chlorite, next to biotite, makes both the separation difficult and the measurement unreliable. Only Cr-muscovite (mariposite) was possible to separate from chlorite through magnetic separation of the latter.

8.2. Sample descriptions and results K/Ar geochronology studies

8.2.1. *Shear Zones*

Sample 190904 is taken from a shear-zone interesting the No.2 West Property sulphide mineralization (Chapter 7) hosted by quartz-rich Basal Norite and Contact Sublayer with large (0.3-6m) amphibolite At the sample location the shear zone is about 1 to 2 m wide and occupies the lithological contact between the Sublayer and the Basal Norite (Figure 8.2). The south side of this shear zone composes chlorite-Cr-muscovite (mariposite) phyllonite with well-defined straight parallel continuous foliation and vertical lineation. Asymmetric 1 to 2 cm wide and 3 to 4 cm high buckle or sheet folds can be identified associated with the foliation. The axes of the folds plunge parallel to the lineation and are in the plane of foliation. The shear zone plunges vertical and strikes east-west. Foliation of the north side of the zone is defined by fine compositional layering of light green mica (Cr-muscovite; mariposite) cleavage bands and carbonate microlithons. X-Ray study of one sample of the sheared rock helped to estimate the approximate composition of 50 % quartz, 17 % Cr-muscovite, 14 % clinochlore, 15 % dolomite, 3 % amphibole (Appendix 13, sample: 190904).

Microprobe results for the green mica indicate Cr content (0.84-0.95 wt.%) lower than 1 wt.% therefore the chromium mica is referred as mariposite (Table 8.1). On the north side of the shear zone there are 20 to 100 cm long 10 to 30 cm wide lenses of quartz and massive sulphides of chalcopyrite, pyrrhotite in basal mafic norite. Under the petrographic polarizing microscope the sheard rock is fine grained (0.1-1 mm) and exhibits parallel, smooth, spaced foliation. Prallel to slightly anastomosing cleavage domains vary in thickness and are composed of bands of closely intergrown chlorite-mariposite. Cleavage domains make up the 60 vol. % of the rock and the 40 vol. % microlithons are composed of granular quartz carbonate (dolomite, calcite). The MARIPOSITE separate yielded radiometric age of **1410+/-56Ma** (Table 8.2).

About 3-7 vol. % disseminated sulphides occur in the rock as fine 0.1 to 3 mm composite grain aggregates of major pyrrhotite chalcopyrite and minor marcasite, pyrite, sphalerite, cobaltite-gersdorffite. Pyrrhotite and chalcopyrite occur as anhedral-subhedral (20 µm to 1 mm) grains in chalcopyrite-pyrrhotite grain aggregates, but they also often form euhedral tabular (20 to 100 µm) solitary crystals in carbonate and maripoiste. Pentlandite occurs as subhedral euhedral grains in pyrrhotite-chalcopyrite aggregates and forms fine exsolution flames in pyrrhotite. Sphalerite is anhedral and included in chalcopyrite. Pyrite and marcasite form euhedral subhedral (20 to 100 µm) grain usually attached to pyrrhotite grain boundary and associated with cobaltite-gersdorfite. Cobaltite-gersdorffite is ubiquitous and occurs as euhedral solitary (50 to150 µm) grains included in pyrrhotite. All the grains show the anomalous, sectored extinction pattern under crossed nicols. The abundance of this phase along this shear zone may suggest its metamorphic origin related to deformation. Sulfarsenides are common in ore deposits of the South Range of the SIC (Szentpéteri et al., 2002; Farrow and Lightfoot, 2002; Ames et al., 2003).

Most of the sulphide textures observed in these samples are indicative that they were re-mobilized from nearby massive sulphide mineralization by tectono-hydrothermal process during the deformation of the host rocks. These textures also suggest that sulphides are contemporary with mariposite, thus radiometric age of mariposite defines both the time of sulphide formation and the time deformation.

Sample 190807 is taken from a 3 by 5 m outcrop near the old Victoria mine shaft. (Fig. 8.2). The host rock is fine grained (1 to 2 mm), equigranular metagabbro (Nipissing Gabbro) and it consists of 60 vol.% amphibole and 40vol. % plagioclase. The metagabbro is cut by a 60 to 100 cm wide fine-grained (0.1 to 1 mm) biotite-rich shear zone. The 175/80 foliation (dip direction/dip) is defined by the biotite rich cleavage bans and minor stretching lineation of biotite is 85 to the east (p85E). Under the microscope the shear zone sample shows parallel, spaced foliation with discrete compositional layering defined by about 70 vol. % cleavage domains of 0.1 to 0.4 mm biotite flakes and 30 vol. % microlithons of granular, strained quartz, carbonate and rare rotated porphyroclasts of perthitic feldspar. Biotite fraction of 0.25 to 0.125 mm was used for geochronology studies. K content of biotite was measured by the electron microprobe to be of 9.26 wt. % (Table 8.1). Radiometric BIOTITE age yielded **1465+/-58 Ma** (Table 8.2).

Sample 190808 is taken from the same area as the previous sample from another 6 m by 8 m outcrop north of the old Victoria mine shaft (Fig 8.2). The fine grained (1 to 2 mm), equigranular metagabbro host rock is crosscut by 40 cm wide coarse, biotite-rich shear band. The 160/71 foliation (dip direction/dip) is defined by the coarse (1 to 3 mm) biotite-rich cleavage bands. Micro texture of the shear zone is characterized by anastomosing spaced schistosity of about 60 vol. % cleavage domains of coarse (1 to 3 mm) biotite, minor quartz and carbonate. The microlithon is composed of

granular aggregate of carbonate, albite, and epidote. Feldspar occurs as rounded porphyroclasts completely altered to fine granular albite-epidote mass. Rounded grains of altered feldspar are wrapped around the bitotite cleavage domains. Biotite fraction of 0.125 to 0.080 mm was used for geochronology studies and yielded BIOTITE age of **1429+/- 57 Ma** (Table 8.2).

Sample 171801 was collected from the Victoria Shear Zone where it traverses trough metasedimentary units of the Elsie Mountain Formation (Fig. 8.2). The light grey very fine-grained quartzite is strongly deformed and display 350/80 (dip direction/dip) foliation defined by muscovite-rich cleave bands (Chapter7, Fig 7.6 and 7.6). The rock consists of 60-70 vol. % quartz and minor feldspar 25 vol. % muscovite cleavage bands. The rock displays smooth parallel fine, paced foliation with discrete transition between the two domains. Muscovite was separated into 0.125 to 0.080 mm fraction and used for K-Ar geochronology study. The sample yielded K/Ar MUSCOVITE age of **1494+/- 57 Ma** (Table 8.2).

The sample SRSZ-1 was taken 15 km northeast of the study area from the South Range Shear Zone in Granophyre. The location is about 9 km to the north of the Lockerby mine and can be reached by the Vermilion Lake Road that leads to Onaping Falls. Here the South Range granophyre is intensely sheared and exhibits fine mylonitic S-C foliation defined by dark green biotite. The BIOTITE separate yielded **1332+/-50Ma** radiometric age (Table 8.2).

The sheared rock consist of about 70 vol.% K-feldspar, albite, quartz and epidote, carbonate, titanite, apatite and about 30 vol. % biotite with rare muscovite. Plagioclase is porphyroclastic, subhedral blocky, rotated and it alters to albite along its rim. Albite appears as euhedral-subhedral blocky pseudomorphs after plagioclase. It often replaces plagioclase completely but many cases it appears as rims around relict plagioclase core. Albite is often cored by sudhedral grain mass of epidote rarely associated with carbonate. Alteration minerals represent an albite-epidote-carbonate alteration assemblage indicative to a greenschist-facies metamorphic condition. Albite contains fluid inclusion rich cores. Fluid inclusions are of 2 to 5 µm 2-phase (L-V) inclusions. Intense Brown vibrations of vapor phase may refer to CO_2 content of fluids. Biotite rises about 50-60 vol. % in the straight to slightly undulous cleavage bands. Biotite constitutes massive-semi-massive bands and oblique foliation occurs along wider bands making up the S/C structure. S fabric element is usually individual biotite laths or trails of biotite exhibiting sigmoid shape fabric. All microstructure refer to dextral shear sense along this mylonite zone.

8.2.2. *Shear zone host rocks: Quartz Diorite, Basal Norite, and Amphibolite*

It is already noticed that quartz diorite bodies mapped at the Victoria area all contain abundant biotite as an alteration phase after primary pyroxene. Biotite quartz diorite is the most dominant lithological variety of the South Range offset dykes (Grant and Bite, 1984). Therefore

biotite alteration of primary mafic minerals in quartz diorite is a regional feature in the South Range of the SIC. Several authors attributed this alteration to regional retrograde metamorphism following pro-grade peak metamorphism of the Penokean Orogeny (Fleet et al., 1987, Easton et al., 2000).

In this study two samples were examined from the relatively un-deformed host rocks to the local shear zones, in order to compare radiometric ages of alteration in the host rock and ages of syn-kinematic minerals of the shear zones (Fig 8.2).

Sample S90505 represents typical blebby sulphide-mineralized, biotite-amphibole quartz diorite of the Victoria embayment. The sampling area is situated within 50 meter from the Victoria Shear zone which runs east-west along the southern edge of Mond Lake (Figure 8.2). Blebby sulphide mineralization is mapped with an 50 meter by 60 meter area and consist of ca. 10-22 vol.% 0.3-1 cm pyrrhotite-pentlandite-chalcopyrite sulphide blebs that assayed 0.65 wt.% Ni and 0.65 wt.% Cu with no traces of PGE (Chapter 6, Appendix 8). Quartz diorite is composed of 40% plagioclase, 20% amphibole, 10% biotite, 6% quartz, 4% chlorite, sericite, epidote and 20 % sulphide. Magmatic plagioclase is subhedral blocky, has lobate resorbed rims. It accidentally occurs as larger crystals in the groundmass of the rock or as isolated smaller grain included in flood quartz. It exhibits saussurithic alterations in the core or totally alters to sericite-epidote masses. Amphibole is subhedral, twinned platy prismatic, often resorbed, embayed by quartz, and contains fine-grained quartz inclusions. On platy sections amphibole is fibrous with light green-green pleochroism corresponding actinolite composition. On more blocky sections amphibole contains lighter core with small opaque inclusions and complexly zoned into fibrous actinolite altered rims. Biotite occurs as tabular grains usually attached to amphibole and/or sulphide blebs or ilmenite. Quartz is interstitial or rather “flood-like”, shows optical continuity between interstices. Quartz is strongly strained, undulose, partly polygonized, and re-crystallized. Some parts of the sample are re-crystallized into fine-grained non oriented and oriented aggregates. Re-crystallized parts of the sample contain quartz-albite-amphibole-rare epidote.

Pyrrhotite is the main phase in the sulphide blebs. Pyrrhotite is coarse-grained, bleb-sized, one cm-sized bleb can be composed be of one grain of pyrrhotite. Pyrrhotite contains thin lamellar pressure twins. Basal cleavage is well developed in all pyrrhotite grains. Some sulphide blebs are polygonized into fine aggregates due to re-crystallization of strained bleb-sized grains. Pyrrhotite shows pyrite and marcasite pyrrhotite alteration along cracks and basal cleavage. It rarely contains pentlandite exsolution flames along micro-cracks. Pentlandite appears in large 0.1 to 0.5 cm grains in pyrrhotite. Pentlandite is totally altered to violarite. Chalcopyrite appears as anhedral grains forming rims around pyrrhotite blebs. Chalcopyrite is strongly intergrown with silicates and often contains sphalerite incluiosns.

In this sample biotite seems to be contemporaneous with amphibole and the formations of the two minerals refer to hydrous alteration of the primary magmatic phases such as pyroxene and magnetite. The amount of biotite shows positive correlation with the sulphide content of quartz diorite. Biotite may have formed during the emplacement of a probable hydrous ore bearing magma batch carrying the blebs of sulphides. Fluids may have interacted with sulphides at a later time and this process resulted in the intergrowths of hydrous phases amphibole, biotite with the ore blebs. Separate of BIOTITE grains from this sample yielded K/Ar age of **1481 +/- 56Ma.** This result is identical with those obtained from deformation zones (Table 8.2).

The S72704 Basal Norite sample is taken from the central area of the Zone No2. West Property mineralization (Fig 8.2). The sample site is situated in between the two east-west trending shear zones which crosscut the contact between weakly mineralized Basal Norite and mineralized Sublayer. Basal note is weakly mineralized contains about 3-5 vol. %, 1 to 3 mm disseminated sulphides, and assay indicate 0.20 wt. % Cu and 0.23 wt. % Ni (Appendix 8).

The norite consists of 60% blocky altered plagioclase, 20% complex amphibole, 10% biotite 6% quartz, traces of chlorite, epidote and pyroxene. Plagioclase is subhedral, blocky, randomly oriented, with no igneous foliation, cloudy. It is strongly chloritized and sericitized in this sample. Amphibole is subhedral; prismatic, tabular, inhomogeneous, zoned. Grains are strongly embayed by quartz. Some grains contain relict pyroxene core when amphibole makes up the complex rim. Most of the primary pyroxene grains are altered to coarse fibrous actionolite aggregates. Biotite is occurs rarely as rare large individual flakes but it rather forms smaller anhedral grains attached to amphibole rim. Quartz is coarse-grained (0.1 to 4 mm) strongly stained, undulose shows mosaic extinction.

Sulphides consist of pyrrhotite, pentlandite as fine grains in pyrrhotite and exsolution flames. Pentlandite in large part is alerted to violarite. Chalcopyrite is minor, anhedral occurs with pyrrhotite and pentlandite. Pyrite is relatively coarse (0.1 to 5 mm) in pyrrhotite. Separate of BIOTITE grains from this sample yielded K/Ar age of **1463 +/- 56 Ma**, again comparable with ages in deformation zones (Table 8.2).

Sample 182402 is from a medium-grained (3-5 mm) Nipissing Gabbro with veinlets and metasomathic patches of quartz-albite and coarse Ti-hornblende (Fig 8.2). Large 0.6 cm euhedral amphibole and 0.1 to 0.2 mm prismatic albite crystals occur in the vein owergrown the vein walls (Chapter 6, Fig 6.3). Ti-hornblende is greenish-brown in thinsection with a very thin outermost rim of bluish green hornblende. The host gabbro has a granular relict gabbroid texture. Mafic minerals are altered to amphibole and plagioclase is hornfelsed to fine, granoblastic aggregates with minute euhedral epidote plates. The large amphibole crystal from the vein was separated for K/Ar measurement. The brown colored central part of the crystal was hand picked under the binocular

microscope. Separate of this single Ti-hornblende grain from this sample yielded K/Ar age of **2048 +\-77 Ma** (Table 8.2).

All separate of the single grain from this sample was used up for the K/Ar measurement. Therefore $^{40}Ar/^{39}Ar$ measurement of Ti-hornblende was performed on another sample 182402. This is a sample of footwall amphibolite located about 15 m distance from Contact Sublayer, but the contact between the two units is tectonized by a northeast-southwest trending shear zone. The footwall amphibolite comprises a massive fine to aphanitic matrix of amphibole (hornblende)-plagioclase -minor epidote, calcite and it contains 1-6 vol.%, 0.3 to 1.5 cm large subhedral blocky porphyroblasts of brown amphibole (Ti-hornblende). From this sample, again a single crystal was separated and the brown colored fragments of the crystal was hand picked under the binocular microscope.

Metasomatic patches, irregular veinlets of quartz-albite with zoned Ti-amphibole as well as fine 0.1 to 2 mm poikilitic or coarse 0.3 to 1.5 cm Ti-amphibole porphyroblasts in amphibolitic footwall rocks have been mapped along the contact zone of the SIC and found to confined within a short distance from the SIC indicative of a contact –metasomatic –metamorphic origin (Chapter 6).

8.3. The Results of Ar/Ar studies

<u>190904 Mariposite 1376.9±7.2 Ma</u>

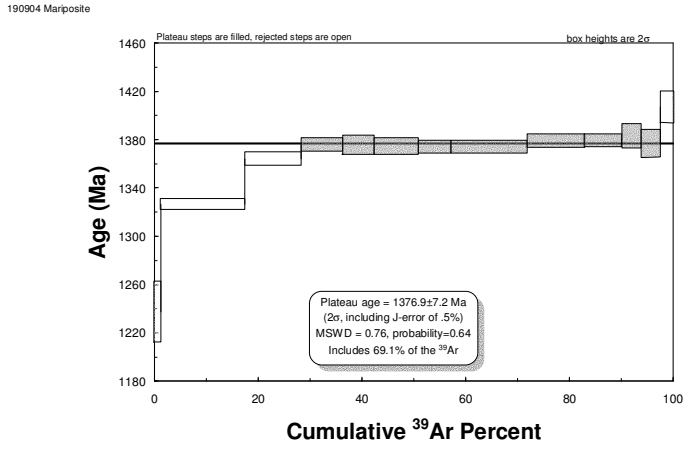

Sample provided a reasonable plateau, with a little bit of excess Ar which was anticipated from the K/Ar measurements (Table 8.3). The result is however comparable with the best established 1410 +/- 56 Ma K/Ar age within its error range. Excess Ar is not indicated by the difference of Ar/Ar and K/Ar ages, due to the great errors. Maybe the little older age of the last step of spectrum, though it does not appear to be really significant. On the other hand, younger ages at the low-temperature steps indicate likely younger effects. The presence of abundant chlorite in the sample may correspond to an even later event i.e. slight re-activation of the shear zones ie at 1000 Ma by the Grenville Orogeny.

The GFTZ is located ca. 40 km to the southeast from the sample site. The greater Ca/K ratio in the low temperature steps (Table 8.3). May be explained by lower retentivity of Ar in chlorite, if the chlorite is fine-grained (several microns) and it captured recoiled ^{39}Ar. So, it is not indicating necessarily younger effect.

190807 Biotite 1456.0±7.7 Ma

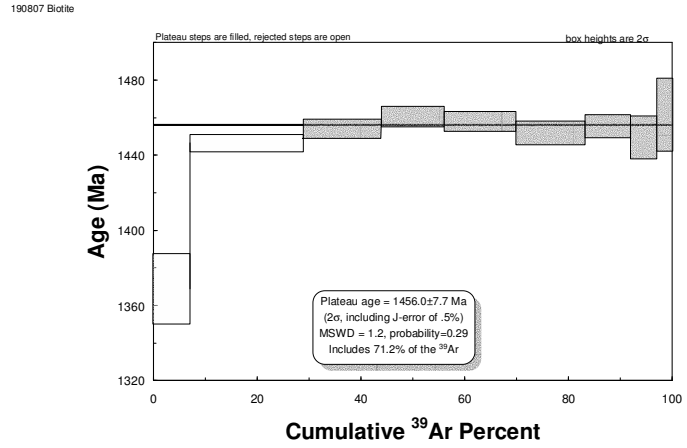

The sample shows a bit of resetting, but the produced plateau age is in good agreement with the 1463 +/-56Ma K/Ar age of the same separate (Table 8.4). The other biotite sample from the nearby shear zone yielded also similar 1429+/- 57 Ma K/Ar age. The average of the two K/Ar results (190807, 190808) 1450 +/-50 Ma is a very close agreement with the Ar/Ar results (Table 8.2). These ages represent syn-kinematic growths of biotite in minor shear zones in equilibrium with quartz, carbonate, possibly minor epidote, sericite indicating a greenschist facies condition. The indication of younger effect is also clear, but in this case, due to the lack of chlorite, it is more convincing. This helps interpretation of the overprint of the previous sample.

171801 Muscovite 1471.1±7.6 Ma

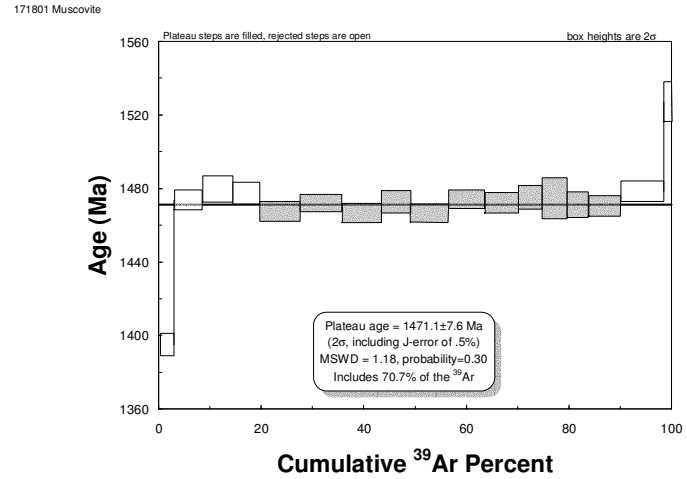

The sample produced a fairly good plateau age (still a little bit of resetting) which very well compares to the 1494+/-60 Ma K/Ar age, as well as the Ar/Ar and K/Ar ages of shear zones containing biotite (190807, 190808) (Table 8.2, Table 8.5). This sample directly indicates the formation of muscovite in the Victoria Shear zone, as well as the radiometric age of deformation along the shear zone. The overprint at the low-temperature steps shows certain loss of radiogenic Ar, but not in the time. This suggests that during a younger effect a certain part of the weekly bound Ar was lost. This effect was younger than the time indicated by the first temperature steps.

S72704 biotite 1482.7±7.8 Ma

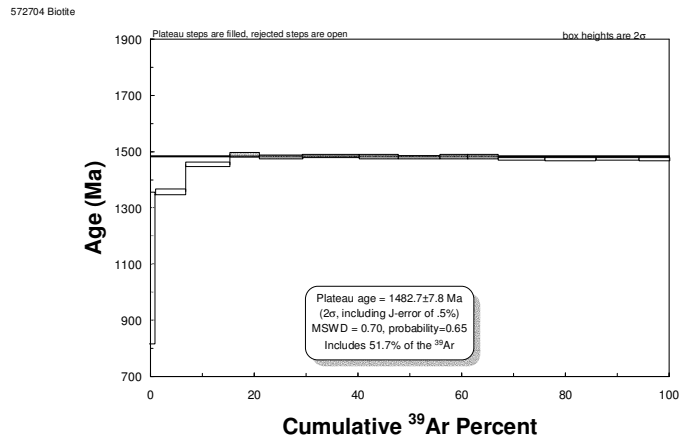

Sample produced nice plateau age, there may not be much resetting (Table 8.6). Obtained age compares well with 1463 +/-56Ma K/Ar age of the separate or even better with another 1481 +/- 56 Ma K/Ar age from blebby sulphide-bearing biotite-amphibole-quartz diorite (S90505, Table 8.2). It appears to be confirmed than, the age of biotite alteration of quartz diorite in the vicinity of deformation zones is linked to metamorphic hydrothermal fluids circulated along the shear zones at ca. 1480-1450 Ma.

182402 Ti Hornblende 1716.5±9.2 Ma

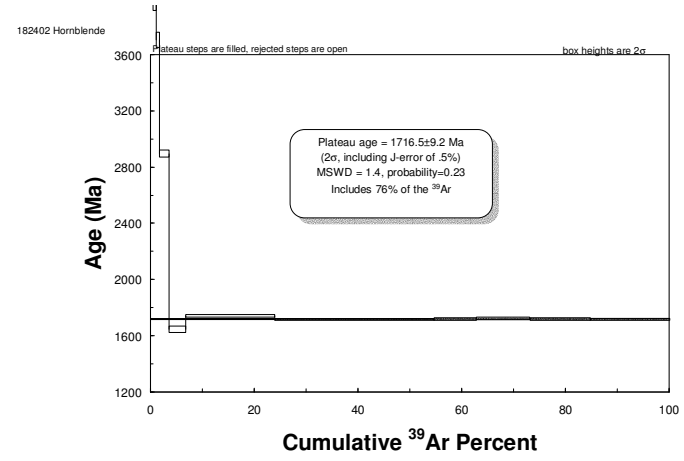

The sample provided nice plateau with a little bit of excess argon at lower temperatures (Table 8.7). The result does not compare with the K/Ar age obtained from a similar coarse Ti-hornblende in a vein, but still yielded younger ages than the Nipissing Gabbro. The difference of K/Ar and Ar/Ar ages is caused clearly by the excess Ar, which might come from an even older rock. The age is comparable with regional felsic intrusive event at around 1750-1700 Ma know as the Killarnean. However, the appearance of porphyroblastic footwall amphibolite is well constrained within a close distance from the contact zone of the SIC. Therefore Ti-hornblende porphyroblasts are unlikely to be of regional importance.

8.4. Discussion of K/Ar and Ar/Ar results

The prominent K/Ar and $^{40}Ar/^{39}Ar$ ages, obtained from deformation zones on various metamorphic syn-kinematic minerals in the Victoria mine area, scatter tightly around 1480-1450 Ma. This time period, in the Sudbury area, is a well constrained geological episode known as the 1470-1440 Ma Chieflakian events (van Breemen and Davidson, 1988; Davidson and van Breemen, 1994; Krogh, 1994). The pre-Grenvillian Chieflakian deformation zones are exposed along the GF and have dimensions, kinematics and micro-textural characteristics similar to the SRSZ (Fueten and Redmond, 1997) and identical to deformation zones around the Victoria mine Chapter 7). The above authors first suggested that the SIC may have been deformed during the Chieflakian contractional orogeny. They also concluded that, based on statistical analysis of Sudbury Breccia clasts, bulk deformation of Huronian metasedimentary rocks occurred during the Penokean orogeny which pre-dated the Sudbury Impact event (Fueten and Redmond, 1997). By contrast Bailey at al. (2004) suggest 1.7-1.6 Ga Mazatzal/Labradorian-age deformation of the SIC and attribute the 1477 +/- 8 Ma biotite $^{40}Ar/^{39}Ar$ ages to thermal re-setting by felsic plutonism, found in Lindsley Thayer mine, in eastern South Range of the SIC. Their 1.7 Ga radiometric age date has been produced from rims of zoned titanites of one (!) sample by means of Pb-U method. Their results of $^{40}Ar/^{39}Ar$ biotite study from four shear zone samples defined plateau ages of 1487-1554 Ma. Bailey et al. (2004) explain the biotite age as resetting by felsic plutonism. This interpretation is argued against based on the following geological observations in the Victoria mine area and literature available for tectonic-magmatic events between the 1850 Ma. Sudbury event and 1000 Ma Grenvillian orogeny:

(1.) The Victoria mine area is much farer, c.a. 40 km, from the GTFZ where series of 1500-1550 Ma felsic plutons occur as part of the Killarney Magmatic Belt.

(2.) Detailed field mapping of the surface area between the Victoria mine and the Vermilion mine did not find outcrops of felsic plutonic rocks (except the minor 1848 Ma. felsic dykes)

(3.) Results from K/Ar and Ar/Ar radiometric age determination of shear zones at the Victoria mine area represent a regionally much wider area i.e. 1 km by 1 km, and obtained from several mineral phases; biotite, sericite, mariposite (Fig. 8.2) as opposed to one "point-like" location in the Thayer Lindsley mine with U-Pb result obtained from one sample.

(4.) The Mazatzal/Labradorian/Gothian orogeny is generally described as an orogenic extensional collapse at about 1700 Ma with the emplacement of granitoids (Clifford, 1990; Holm et al., 1998). This tectonic scenario would be inconsistent with a major compressional shortening of the SIC. In addition there is no 1700 Ma deformation associated with these granitoids along the GFTZ. Killarnean rocks of c.a. 1700 Ma. in the GTFZ are deformed however during the Chieflakian 1450 Ma. (Fueten and Redmond, 1997).

(5.) The 1470-1440 Ma Chieflakian event is well established as a period of intrusive and compressional tectonic activity, including emplacement subsequent deformation of plutons of the Killerney Magmatic Belt (van Breemen and Davidson, 1988; Davidson and van Breemen, 1994; Krogh 1994). Orientation, kinematics, and micro- textures of 1 to 15 meter wide shear zones of the Victoria mine area, are identical with those described from the SRSZ (Shanks and Schwerdtner, 1991a) and identified at the Chief Lake complex– Killarney area along the GF (Fueten and Redmond, 1997).

Based on the K/Ar and Ar/Ar results presented herein, it is suggested that the deformation of the south-western corner of the Sudbury Structure around Victoria Mine occurred at ca. 1460 Ma during, the Pre- Grenvillian contractional Orogeny, the Chieflakian event. The similarities in tectonic style of the sampled deformation zones to the South Range Shear zone may suggest that the whole SIC was deformed during this period.

Biotite ages obtained from basal quartz-rich norite (S72704) and quartz diorite (S90505) from the Victoria Embayment also yielded the age of deformation zones 1470-1440 Ma (Fig 8.2, Table 8.6). Both samples resulted considerable plateau ages, instead of disturbed, reset ages as anticipated to be seen from a magmatic (1850 Ma) age to a latter deformation (1450Ma) age. These two samples however are located in close proximity i.e. within 20 to 40 meters to shear zones. Therefore it is suggested that the formation of biotite, in host rocks to shear zones, related to hydrothermal metamorphic fluids circulated along the shear zones during the 1470-1440 Ma compressional deformation event. These fluids have reacted with Fe and Fe-Mg bearing phases, sulphides and pyroxene/amphibole to form biotite at relatively static conditions. In many samples, biotite has a

very close spatial relation to amphibole in most amphibole-biotite-quartz -norite or -diorite samples. Many quartz diorite samples, although retain the primary magmatic granular texture, and contain only smaller domains of incipient re-crystallization of plagioclase-quartz associated with weak to moderate orientation of amphibole and biotite, sometimes with reasonable equilibrium texture. This may suggest that the bulk of amphibole biotite alteration of quartz-diorite may be related to the 1470-1440 Ma tectono-hydrothermal events.

In conclusion on the timing of biotite-amphibole alteration of the quartz diorite and quartz-rich basal norite, it is believed that alteration of these rocks has happened adjacent to shear zones at the 1470-1440 Ma contractional periods at maximum amphibolite facies metamorphic conditions. These ages may represent completely re-set Ar/Ar signatures due to the local overprints by these regional but nonpenetrative deformation zones. This geological situation can only be satisfactorily examined by means of systematic regional sampling of amphibole and biotite of quartz diorite and footwall amphibolites across the entire South Range of the SIC.

The two younger ages 1376.9±7.2 Ma Ar/Ar (190405) and 1332+/-50Ma K/Ar (SRSZ-1) obtained from shear zones, apparently compare well and differ from the main group of results (Table 8.2). The Ar/Ar age of the mariposite sample (190904) differs from its K/Ar age 1410+\-56 Ma within the error range of the latter. The 190904 sample of the Victoria mine area is from a discrete shear zone which crosscuts the No.2 West Ni-Cu-PGE sulphide mineralization. This mineralization is examined in details in Chapter 9. Macro and micro-textural characteristic of the sampled shear zone, i.e. sheetfolds, isoclinal folding of early foliation parallel veins as well as segmented and streaked quartz, quartz-sulphide veins, sulphide matrix breccia, two generations of carbonate, presence of abundant chlorite, indicate complex deformation-mineralization history of the shear zone. Therefore the younger Ar/Ar age is attributed to possible later re-activation along the structure (i.e. Grenvillian 1000 Ma) or the inhomogenity and/or fine fraction size of the mariposite separate.

The only younger K/Ar age, 1332+/-50 Ma (SRSZ-1) obtained from the SRSZ, is from a deformed granophyre of the SRSZ, located 15 km to northeast of the Victoria mine area (SRSZ-1). The single K/Ar age, although younger, plots closets to the 1470-1440 Ma Chieflakian event. Bitotite grains of this sample are remarkably smaller and do not form continuous cleavage bands but rather trails of isolated fine grains compared to samples from the Victoria mine area. The smaller grain size may correspond to lower blocking temperature (Dobson, 1973) and the younger overprint, seen in most samples, may have influenced this sample the most. Since there is no Ar/Ar age available for this sample, interpretation of this age is difficult, but local re-activation of the SRSZ may have happened at several places as proposed for the previous sample. Again, systematic Ar/Ar biotite, combined with U-Pb zircon, titanite sampling of the SRSZ tectonites could satisfactorily answer this problem.

The Ti-hornblende single crystal of porphyritic footwall amphibolite sample (182412) yielded 1716.5±9.2 Ar/Ar age (Table 8.7). There appears to be a discrepancy between the K/Ar ages of another sample. The obtained age compares with regional felsic intrusive event at around 1750-1700 Ma known as the Killarnean. It has been already mentioned Chapter 6 that field relation, micro-texture, amphibole composition all support a contact metamorphic, fine –poikiloblastic and coarse – porphyroblastic growth of these amphiboles due to he thermal contact effect of the SIC. This observation is a strong supportive evidence against that the obtained 1716.5±9.2 Ar/Ar age is related to a regional event i.e. an orogeny. The high Ti content of amphiboles generally indicates high temperature formation (Ernst and Liu, 1998) probable of a thermal, contact metamorphic origin. Contact metamorphic assemblages in the South Range are weakly mentioned, but well documented in the North Range (Wodicka, 1995; Lakomy, 1990; James et al, 1992). In the North Range thermal aureole of re-crystallized Levack Gneiss Complex extends 1.2 km distance from the SIC (Wodicka, 1995; James et al., 1992). Thermobarometry (James and Dressler, 1992; Lakomy 1990) and Ar/Ar, U-Pb geochronology studies (Wodicka, 1995) indicate that the contact zone of 1100-800 ºC temperature and 150-300 MPa in the North Range cooled down to 300 °C between 1850 and 1800 Ma. The vertical net displacement of the SIC, including footwall rocks, along the SRSZ is estimated to be at about 8-15 km (Shanks and Schwerdtner, 1991a). Thus the exposed SIC contact is originated from a much greater crustal depth where cooling could have a much longer period i.e. more that 50 Ma perhaps as much as 125 Ma. The thin outermost blue-green hornblende rim on many porphyroblastic Ti-amphibole clearly indicates that overgrowths of these blasts occurred at a later time (Chapter 6, Fig. 6.3). Therefore the apparent 1716.5±9.2 Ar/Ar age may represent complete re-setting of contact metamorphic amphibole (1850-1800 Ma) during the unknown-aged post-Sudbury event prograde regional metamorphism (Brocoum and Dalziel 1974; Fleet et al., 1987; Thomson et al., 1985; Shanks and Schwerdtner 1991a). Again a systematic geochronology study of thermal contact metamorphic porphyroblasts along the South Range of SIC could shed light on the highly debated time sequence of multiple metamorphic and tectonic events in the Sudbury Area.

8.5. Conclusions of K/Ar and Ar/Ar geochronology studies

Results of this study indicate that non-penetrative regional deformation of the SIC and footwall rocks as well as alteration of norite and quartz diorite adjacent to shear zones in the Victoria mine area occurred along numerous sub-parallel discrete 10 cm to 20 m wide shear zones at a period of 1470-1440 Ma. The deformation zones have macro-textural, microtextural and kinematic characteristics identical with the SRSZ and the 1450 Ma GF- parallel deformation zones at the Chief Lake intrusive complex – Killarney area. It is suggested that the bulk deformation of the SIC along the SRSZ may have happened in the 1470-1440 Ma period, during the Chieflakian event. Minor

local re-activation may have occurred along these shear zones at several later times. Age of coarse contact metamorphic porphyroblast indicate protracted cooling in deep crustal level and/or superimposed, post-Sudbury pre-Cheiflakian unknown metamorphic event.

9. SULPHIDE-PGE MINERALIZATION OF DEFORMED MASSIVE SULPHIDE ORE OF No. 2 WEST ZONE, VICTORIA PROPERTY

9.1. Introduction

The No.2 West Zone, Victoria Property is located 600 m northwest from the old Victoria mine shaft (Fig 9.1, A). The N.2 West Zone mineralization consists of several partly deformed contact-type massive Ni-Cu sulphide ore bodies and lenses situated between metavolcanic rocks or amphibolite inclusion-bearing Sublayer in the footwall, and quartz-rich mafic norite in the hangingwall (Fig 9.1, B). The mineralization crops out at the surface in 400 m strike lengths. The No.2 West Zone however is segmented into numerous smaller 50 to 200 m long blocks by large number of east-west-trending vertical to subvertical, 1 to 7 m wide shear zones (Fig 9.2). The sulphide mineralization occurs in an "embayment"-like corner where the east-west trending SIC contact changes to northwest-southwest.

Significant part of the ore deposit was mined by INCO Limited between the beginning of the 20th century and 1970. The group of ore bodies, now called No.2 West Zone was part of the Victoria underground mine and the deeper portions of the No.2 West Zone ore bodies have been mined underground trough drifts leading from the main Victoria mine shaft 600 m to the southeast (Fig 9.1, A). By the end of 1915 the mine produced 619 612 tons of ore averaging 1.6% Ni and 3.3 % Cu (Card 1968). The vertical shaft was about 800 m deep and narrow steeply plunging ore shoots of 400 to 600 m long and 5 to 15 m wide were mined from the main Victoria deposit. The majority of the ore of the Victoria mine was a sulphide crush breccia; fragments of wall rocks, quartz veins and carbonate cemented by massive sulphide matrix (Plate 9.1; 1,2). The ore shoots were located within major shear zones running along the South Range norite and footwall contact in one part and in footwall rocks in the other part. The footwall rocks were reported to be strongly-sheared and altered and they contained disseminated sulphides and veinlets associated with abundant quartz and carbonate (dolomite) alteration (Card 1968).

In year 2000 the exploration license for the Victoria mine area was held by FNX Mining Incorporation. FNX started a Ni-Cu-PGE exploration drilling program over the proximal part of the Worthington offset and along the SIC contact to the northwest from the Victoria mine. Approximately 5400 m of drilling have been completed in 50 holes on the No.2 West Zone, Victoria Property. Several holes intersected 5 to 15 m wide >1 wt. % Ni and Cu sulphide mineralization with significant PGE values (Fig 9.1 B). An airborne electro-magnetic survey defined the position of

several exploration targets (Fig 9.1 A). The Cu-Ni-PGM sulphide mineralization at Victoria No.2 West Zone is a complex assemblage of irregular lenses of chalcopyrite, pentlandite and pyrrhotite. The lenses dip and plunge steeply and are generally pipe-like in shape. In 2002, FNX explored the Victoria Property, focusing on the shallow, un-mined portions of the No. 1, No. 2 West, Far West and the down-plunge of the No. 4 Zone. The Company also discovered the Powerline Deposit in late 2002 (Fig 8.1, A). From 2003-2006, the main focus of the company at Victoria was compilation of data, data evaluation and re-interpretation.

FNX estimated the past production of the Victoria mine to be of about 1,543,000 tons grading 2.26% Cu, 1.57% Ni, 2.0 g/t Pt+Pd+Au (TPM). In 2007 FNX announced an Inferred Resource for the Victoria Property of 15,394,000 tons at 0.45 wt. % Cu and 0.46 wt.% Ni (www.infomine.com).

9.2. Sampling

Mineralized intervals of the FNX exploration drill cores were logged at the FNX core shack in Sudbury. The logging of mineralized intercepts revealed that strongly deformed sulphide ores are accompanied by the highest Pd+Pt+Au assays i.e 17-60 g/t whereas massive sulphides with typical magmatic textures have generally lower 1.5 to max. 7 g/t Pd+Pt+Au concentrations.

In this study, five exploration drill cores were sampled for detailed ore petrography and fluid inclusion studies (Table 9.1). In three holes, FNX1006, FNX1024, FNX1046 only the mineralized intersections with significant Pt+Pd+Au assay results were sampled in order to identify PGE-minerals responsible for the grade (Table 9.2).

9.3. Brief Description of sampled drillhole intercepts

FNX 1046 hole was sampled between 548 and 596 feet depth. The mineralized section represents magmatic massive sulphide ore rich in chalcopyrite and pyrrhotite. The 15 m intersection includes average 4.1 % Cu, 1.7 % Ni with 2.6 g/t Pd (0.44-6.94) and 0.8 g/t Pt (0.1-1.34).

FNX 1024 hole was sampled between 250 and 284 feet. The 10 m mineralized section contains the highest average PGE of 14 g/t Pt (0.4-59.3) and 0.8 g/t Pd (0.18-1.44) and maximum 0.28 g/t Au. The ore types drilled in this section is a pyrrhotite rich inclusion massive sulphide (1.21% Ni and 0.7% Cu) strongly deformed and sheared into sulphide stringers, streaks and crush-breccia sulphide ore. Pentlandite is coarse (0.1 to 2 mm) granular or occurs as (1 to 2 mm) veinlets parallel with the elongation of sulphide streaks.

FNX 1006 hole was sampled between 35 and 66 feet and the intersection represents strongly streaked and brecciated pyrrhotite rich sulphide in a shear zone. The generally lower grades are consistent with a lower sulphide content of the mineralized zone including 0.6 % Cu. 0.8 % Ni, 0.7 g/t Pd 0.3 g/t Pt.

9.4. Fabric of ore types

In most of the samples sulphide consists of pyrrhotite, chalcopyrite, magnetite and pentlandite (Plate 9.1). These sulphide minerals form massive granular aggregates, as well as they are intricately intergrown with 5-70 vol. % hydrous silicates. The silicate content of ore and sulphide minerals present in ores vary greatly, resulting in a large textural diversity of ore types (Plate 9.1). The ore types in this study are characterized herein based on first the texture and the sulphide composition and they are grouped into two groups; (1) primary magmatic ore (2) deformed, sheared ore. Primary magmatic ore types retain textures typical for orthomagmatic accumulations from sulphide liquid and observed in many ore deposits all around he SIC (Naldrett 1984). Deformed, sheared ores develop from the primary magmatic sulphides by increasing deformation; shearing, streaking and crushing of sulphide and host rocks.

(1) primary magmatic ore

Massive sulphide ore

There are two types of massive sulphide ore, based on the dominant sulphide mineral present. There is massive pyrrhotite-rich ore (Plate 9.1; 3) and massive chalcopyrite-rich ore (Plate 8.1; 4). Massive pyrrhotite-rich ore consist of 97-100 vol. % sulphide and oxides with subordinate silicate inclusions. It is coarse grained (1 to 7 mm) and consists of 70-90 vol. % 4 to7 mm equigranular pyrrhotite, 1 to 3 mm pentlandite vein network and 0.1 to 1 mm disseminated euhedral magnetite. (Plate 8.1, 3). Massive chalcopyrite ore is subordinate, it is coarser-grained (5 to8 mm) and contains more (5-15 vol. %) mafic silicate inclusions. (Plate 9.1,4). There is a wide transition between the pyrrhotite and chalcopyrite rich massive ore. The higher the chalcopyrite content of the ore the higher the distraction of the even granular texture of pyrrhotite and the content of silicate inclusions (Plate 9.1, 5, 6). Chalcopyrite seams 1 to 3 cm wide often cut across the massive granular pyrrhotite ore (Plate 9.1, 3, 6). An enrichment of silicate inclusions and magnetite grains can be often observed along these chalcopyrite seams or veinlets.

Silicate Massive sulphide ore

Very often a chaotic mixture of fine-grained pyrrhotite-chalcopyrite-silicate inclusions is observed to compose the ore which can be referred as silicate rich massive sulphide (Plate 9.1, 5, 6). In this type of ore the coarse, equigranular massive sulphide texture is completely obliterated. Massive sulphide ore often contains 5 mm to >5 cm mafic silicate inclusions. Most of the inclusions contain disseminated sulphide but some do not. The inclusions are dark green black in color, they contain abundant chlorite, amphibole, quartz and carbonate.

Massive Blebby sulphide ore

Massive blebby ore composes of 70-90 vol. % 4 to 7 mm oval-shaped grains "blebs" abundant pyrrhotite or rarer chalcopyrite. These sulphide blebs are interlocking and build up a massive character of the ore enclosing dark mafic silicates in the pore spaces between the blebs (Plate 9.1; 7). Chalcopyrite partially or completely replaces the pyrrhotite blebs (Plate 9.1; 8). The massive pyrrhotite and chalcopyrite ore types may have developed by the compaction of this "blebby"-type massive ore.

Semi-massive Blebby sulphide ore

The semi-massive blebby sulphide ore is identical with the previous ore type but the number of sulphide blebs are less and the silicate content of the ore is higher (>30%). The sulphide blebs are not or only partially interconnected to form a massive ore (Plate 9.1; 9).

(2) deformed, sheared ore

Crush-Breccia sulphide ore

The most abundant ore type of the No.2 West Property ore deposit is the "crush-breccia" ore. This ore type represents a shear zone-hosted tectonic sulphide-matrix breccia that consist of poorly shorted 50-70 vol.% 2 mm to >5 cm rounded-surrounded clasts of quartz, quartz-carbonate and quartz-carbonate-chlorite altered rock fragments. The sulphide matrix is either massive fine-grained granular or exhibits strong fabric, parallel with the strongly developed foliation salvaging the crush-breccia (Plate 9.1; 10, 11, 12). The sulphide in the breccia matrix is dominantly pyrrhotite and minor pentlandite, magnetite, rare chalcopyrite. The sulphide crush-breccia occurs in thin 1 to 5 cm layers to meter wide zones in strongly sheared and altered host rocks. In samples where inclusion content of the breccia-ore is less than 30 vol. % it is apparent that pentlandite occurs as fine 0.1 to 2 mm isolated grains rather than fine inter-granular vein network (Plate 9.1, 16, 17). In many samples where breccia clasts are flattened, elongated, 1-3 mm thin pentlandite veinlets occurs in pyrrhotite matrix (Plate 9.1, 15, 17). These distinct textural features indicate that the sulphide matrix of the breccia ore is strongly re-crystallized.

Quartz-carbonate cleavage band shear-sulphide

Strong foliation appears in shear zones adjacent the crush-breccia sulphide ore. In these zones the foliation defined by fine, discrete compositional layering of 0.1 to 1 mm discontinuous sulphide seams "cleavage band" and quartz-carbonate chlorite microlithons (Plate 9.1, 11, 12).

Sulphide stringer, streaks

Sulphide stringers are 0.4 to 3 cm wide and they are associated with crush-breccia sulphide ore in strongly-sheared zones (Plate 9.1, 15, 17). They are rather part of the intensely-sheared sequence of ore and host rock and represent "laterally-secreted" sulphide ore. Some of this stringer are very coarse grained (1 cm) and contain of 0.1 to 2 mm trails or 0.1 to 3 mm granular aggregates of pentlandite indicative of strong re-crystallization of primary textures. (Plate 9.1, 15-18)

Quartz-carbonate vein sulphide

In the sheared sequence of the No.2 West Property, 3 cm to 1 m thick quartz, quartz-carbonate and quartz-carbonate-sulphide veins are present. Sulphides; pyrrhotite, chalcopyrite, pyrite are observed in many veins as fine 1 mm to 1 cm seams of 1 to 5 cm irregularly-shaped patches (Plate 9.1; 13,14).

9.5. Sulphide ore petrography

Pyrrhotite ($Fe_{1-X}S$) occurs in all ore types as (0.1 mm to 7 mm) massive equigranular or inequigranular aggregates (Plate 9.2, 1). Pyrrhotite is the main ore phase of the No.2 West Zone and constitutes about 30-100 vol. % of the various ore types. Pyrrhotite is brown in color has moderate reflectivity (27-40 %) moderate-weak bireflection, and moderately anisotropic in brownish-bluish colors. In many samples there appears to be two structural variants of pyrrhotite, distinguishable by optical properties and mechanical properties of polished grain surfaces. In massive pyrrhotite aggregates of equant grains some grains have slightly lower reflectivity, darker brown color and distinct sharp finely-spaced discontinuous parallel cleavage (Table 9.2, 2). These grains have sharp well developed grain boundaries against pyrrhotite grains with smooth surface and slightly higher reflectivity. The grains with cleavage do not distinguish on Backscattered electron images. However in many samples, containing massive pyrrhotite grain aggregate, about 30-40 vol. % of the pyrrhotite grains are strongly etched in air after significant time (1-2 years!). The etched grains are strongly magnetic whereas the non-etched grains are weakly magnetic. The difference of polished surfaces, optical properties, and etching-magnetic properties suggest that pyrrhotite grain aggregates are mixtures of hexagonal- and monoclinic-pyrrhotite.

In most of the sulphide breccia and stringer ore samples pyrrhotite is re-crystallized into fine-grained equigranular aggregate or it is strongly strained and contains abundant 10 to 50 μm wide deformation bands and kinked grains. A very fine, thin lamellar structure appears along the basal plane (0001) particularly in the strongly strained samples. This lamellar texture is slightly visible only under crossed-polarized light (Plate 9.2, 3). Grain shape orientation occurs in same deformed samples indicated by pyrrhotite grains elongated parallel with the foliation around the pyrrhotite streak. In some deformed samples coarse pyrrhotite grains show preferred optical (crystallographic)

orientation. In such grain aggregates, pyrrhotite grains extinct more or less together, under crossed polars. In the deformed ore types, those are intergrown with abundant silicate inclusions; pyrrhotite often occurs as 10 to 300 µm solitary euhedral grains included in alteration minerals quartz, carbonate, amphibole, chlorite, indicative if its direct crystallization from hydrothermal fluids.

Pentlandite ($FeNi_9S_8$) is yellowish white isotropic with high average reflectivity (52 %,). In magmatic ore, pentlandites typically occurs as thin 0.1 to 1 mm vein network intergranular to pyrrhotite, as well as fine 50-300 µm late exsolution flames along pyrrhotite grain boundaries (Plate 9.2, 4, 5, 6). In the deformed ore types pentlandite forms euhedral-subhedral grains or aggregates included in pyrrhotite often arranged in trails running parallel with the to the sulphide streak or veins. In deformed massive sulphide ore pentlandite slightly altered to violarite $FeNi_2S_4$. Violarite is isotropic has moderate-high reflectivity (42-54%), creamy-grey colored compared to pentlandite and it occurs as fine 10-100 µm disseminated anhedral patches in pentlandite.

Chalcopyrite ($CuFeS_2$) has moderate reflectivity (30%) yellow color and weak, brown-blue anisotropy. It is fine-grained, anhedral, granular in pyrrhotite rich samples. In massive magmatic pyrrhotite ore it rarely occurs along the pentlandite network. Massive chalcopyrite contains oriented exsolution lamellae or wormicular phase of mackinawite ($(Fe,Ni)S_{0.9}$) (Plate 9.2, 7). Textural evidence indicates that chalcopyrite replaces both pyrrhotite and pentlandite in deformed ores (Plate 9.3, 2).

Magnetite-1 ($FeFe_2O_4$) forms 5-7 vol. % euhedral 0.1 to 1 mm octahedrons in massive magmatic ores (Plate 9.2, 6). In coarse granular pyrrhotite rich magmatic ore magnetite has a tendency to occur along the pyrrhotite grain boundaries associated with pentlandite vein network. This texture is consistent with late crystallization of magnetite from monosulphide solid solution due to increase of oxygene fugacity. This type of magnetite sometimes contains fine (111)-oriented exsolution lamella of ilmenite. When massive granular pyrrhotite rich ore is cut by chalcopyrite-silicate veinlets or irregular seams, disseminated magnetite (Magnetite-2) tend to be enriched along these structures. Magnetite-2 has caries and sieve texture indicative of porphyroblastic grown in pyrrhotite (Plate 9.2, 8). In the deformed ore types magnetite is intensely replaced by silicate-carbonate alteration minerals and occurs only as various relict forms (Plate 9.3). In deformed samples magnetite is strongly replaced by alteration minerals and sulphides in various forms (Plate 9.3, 3, 4, 7, 8).

Pyrite (FeS_2) is yellowish white isotropic with high reflectivity (52 %). Pyrite is rare in primary magmatic ore but ubiquitous in many deformed samples and occurs in numerous textural forms. (1) Most often it forms acicular to massive aggregates as progressively replaces pyrrhotite (Plate 9.3, 1, 6). The majority of the replacement is located along the edges of pyrrhotite grains and alteration propagates towards the centres as such many smaller pyrrhotite grains are completely

replaced with pyrite. (2) Pyrite also very often forms a peculiar grain aggregate similar to the "sagenite net" of rutile (Plate 9.3, 1). Rarely pyrite occurs as sieve-textured euhedral crystals often associated with sieved-textured cobaltite indicating a porphyrobalstic origin of both phases (Plate 9.3, 5, 6).

Marcasite (FeS_2) is much rarer than pyrite. It forms anhedral to euhedral (100 to 150 µm) grains. It is often associated with the "sagenite-net" textured pyrite (Plate 9.3, 1).

Smythite ($(Fe,Ni)_9S_{11}$) looks very similar to marcasite, bluish white in color and has intense strongly colored brown-blue anisotropy. Under crossed polars, smythite shows typical "parquet" – like extinction patter. Smythite always forms thin lamella or flame, spindle-shaped inclusions in altered pyrrhotite.

Rutile (TiO_2) is ubiquitous in all samples and it is strongly associated with pyrite, marcasite, smythite in many intensely deformed-altered samples. Rutile has low reflectivity (24-18%) and bluish grey color moderate bi-reflection. It exhibits strong red-brown internal reflections under crossed polars Rutile forms aggregates of acicular crystals arranged in an irregular manner somewhat similar to "sagenite-net". This aggregate is better referred as leucoxene a mixture of rutile and titanite.

Sphalerite (ZnS) and galena are minor accessory minerals mostly in the tectonized sulphide samples. They occur as 50 to 300 µm anhedral grains included in sulphides or silicate alteration minerals.

Sulfareseides are creamy white, isotropic with high reflectivity (48-54%). Sulfarsenide minerals (cobaltite-gersdorffite solid solution; (CoAsS-NiAsS-FeAsS) are ubiquitous in many sheared, tectonized sulphide ore samples but very rare in un-deformed magmatic ore types. Sulfarsenides form minute 40 to 300 µm euhedral to subhedral, rhomb-shaped crystals. The smaller crystals are usually perfect euhedras, whereas the larger crystals typically show caries or sieve-textured incomplete crystals indicative of a porphyroblastic growth in pyrrhotite, chalcopyrite hosts. Sulfarsenies are spatially; closely associated with coarse 100 µm to 1 mm pyrite crystals which often show similar sieve texture. May grains, especially the smaller ones, have a minute core with slightly higher pure white reflectivity. These cores often have well developed outlines; sharp crystal faces against the enclosing sulfarsenide host. This optical feature is consistent with Ir-Rh-(Os, Pt, Ru) enriched sulfarsenide composition in these cores. EDS spectra indicated the presence significant Ir, and Rh with minor (Ru, Pt) that may imply that some of these cores may have irarsite (IrAsS) and/or hollingworthite (RhAsS) composition.

9.6. Alteration mineralogy of sulphide ores

In the magmatic massive sulphide ore silicate inclusions represent strongly altered mafic magmatic rocks. These inclusions consist of hornblende, fibrous actinolite, plagioclase, quartz, biotite, chlorite, epidote, carbonate in approximate decreasing order of abundance.

The alteration mineralogy in the deformed ore types is represented by carbonate-quartz-sericite (Cr-muscovite; mariposite)-chlorite assemblages. In many deformed samples well-defined foliation is developed, due to the compositional layering of sulphide streaks associated with chlorite and/or Cr-muscovite (slightly green mariposite) and quartz-carbonate microlithons. These textual domains are discrete, parallel to anastomosing and finely spaced (1 to 3 mm). Carbonate is strongly intergrown with sulphide streaks and forms anhedral to subhedral 0.1 to 1 mm grains. Many carbonate grains have semitransparent cores with abundant fluid inclusions and clear rims showing fine parallel growth zones. Electron microprobe studies indicate Fe-Mg rich calcite and dolomite composition (Table 6.6). These alteration minerals are strongly intergrown with the sulphide assemblage indicative of their formation syngenetic with re-worked-re-mobilized sulphides.

9.7. Platinum group minerals

Platinum-group minerals are abundant in many samples studied (Plate 9.4). They occur in two major textural forms; (1) anhedral grains or (30 to 400 μm) compound grain aggregates of 1-3 phases located at the sulphide-silicate grain boundaries. (2) Solitary subhedral to euhedral isometric (10 to 200 μm) grains of one or two phases included in pyrrhotite, pentanldite and chalcopyrite in the deformed sulphide ores.

Michenerite (PdBiTe) is white and isotropic, it has high (53-56 %) reflexivity (Figure 9.3, A; Plate 9.4, 1, 2, 3). Michenerite typically occurs as anhedral solitary grains at sulphide-silicate grain boundary (Plate 9.5, 1) or it is as associated with other PGE-minerals in composite grain aggregates located also at sulphide-silicate grain boundaries (Plate 9.4, 2). Rarely anhedral michenerite is included in chalcopyrite (Plate 9.4, 3). Michenrite was identified in large number by the reflectance spectra and EDS spectra.

Abundant euhedral grains in pyrrhotite yielded reflectance spectra (51-68 %) intermediate between end-member melonite ($NiTe_2$) – merenskyite ($PdTe_2$) (Figure 9.3 B). EDX spectra of these grains yielded $PdTe_2$ and $(Ni,Pd)(Te,Bi)_2$ composition which is identical with merenskyite and palladian-melonite-merenskyite series. The two minerals form complete solid solution with moncheite ($PtTe_2$). Characterization of such a complex solid solution could only be made possible by microprobe analysis, but the bright white color and the reflection curve intermediate between melonite and merenskyite suggest general palladian melonite composition. There are no reference reflection curves available for Pt-bearing or PtPd-bearing melonite thus Pt content cannot be entirely

excluded. Merenskyite forms euhedral solitary grains included in pyrrhotite-pentlandite (Plate 9.4, 3). Palladian melonite has a strong tendency to form euhedral crystals with very sharp grain boundaries against the host sulphide, often pyrrhotite and rarely pentlandite (Plate 9.4, 5, 6, 8). Palladian melonite rarely is host to minute PGE-sulfarsenide inclusions (Plate 9.4; 6) or intergrown with froodite (Plate 9.4; 7, 8).

Rarer subhedral mineral grains in pyrrhotite have moderate-high reflectivity and moderate un-colored anisotropy. The reflectance spectra of these grains (Figure 9.3 C) and the microprobe EDS spectra refer to tsumoite (BiTe) or pilsenite (Bi_4Te_3) mineral phase.

Froodite $PdBi_2$ is rare and usually occurs as 10 to 100 μm anhedral-subhedral grains in complex PGE grain aggregates (Plate 9.4; 2) or attached to euhedral palladian melonite (Plate 9.4; 7, 8). Froodite is bright white; it has high reflectivity (50-63%) and moderate grey-light grey anisotropy. It appears slightly darker and greyish next to merenskyite and/or palladian melonite. Froodite was identified by its optical properties and EDS spectra.

9.8. Fluid inclusion studies of deformed Ni-Cu-PGE ore of the No.2 West Property

Fluid inclusion studies were carried out in three selected samples; two from sulphide *Crush-Breccia sulphide ore* and one from a quartz-carbonate-Cr-(muscovite)-sulphide vein. Details of samples are given on Plates 9.5-9.7. All samples have Pd+Pt+Au grades between 1.75-2.1 g/t (Table 9.2). In the *Crush-Breccia sulphide ore* fluid inclusions are hosted by quartz and carbonate precipitated contemporaneous with sulphide deformation indicated by weak strain in the grains. Quartz may have re-crystallized from sheared quartz fragments or precipitated with sulphides from hydrothermal solutions (example Plate 9.6). In the quartz-quartz carbonate sulphide vein quartz is relatively unstrained contains both primary/speudosecundary and secondary inclusions, whereas carbonate contains mostly primary inclusions (Plate 9.5). Based on these characteristics it is suggested that carbonate and quartz have formed during deformation and their primary and secondary inclusions can be used to characterize the fluid composition associated with deformation, sulphide re-mobilization and enrichment of PGE minerals.

Fluid inclusion petrography indicates three abundant types of inclusion present in the samples from strongly deformed, re-mobilized sulphide ores (Figure 9.4).

Type Ia inclusions are 2-phase (L-V) with 90-95 % filling of the liquid phase. These inclusions are frequent as secondary genetic type inclusions along microfractures in quartz. Type Ia inclusions however occur as primary inclusions in dense clouds in the cores of carbonate (Plate 9.7).

Type Ib inclusions are 3-phase (L-V-H) inclusions and contain halite daughter mineral in addition to vapor bubble with 80-90 % filling of the liquid phase. This type of inclusion is abundant as secondary genetic type inclusions along microfractures in quartz in quartz-carbonate-sulphide

veins. They rarely occur in these veins as isolated larger primary inclusions. These inclusions are scarcely associated with Type IIa and Type IIb inclusions.

Type IIa inclusions are 4-phase (L-V-H-X1) with halite and small unidentified daughter minerals. The unknown daughter mineral has irregular shape and usually much smaller size than halite. These inclusions are rare and they are often associated with Type IIb and Type IIIa, b inclusions.

Type IIb inclusions are poly-phase (L-V-H-X_1 +/-X_2) highly saline inclusions with 60-80 % filling of the liquid phase. In addition to halite cube, two more unknown daughter mineral present; one is minute irregular in shape, the other is often columnar and anisotropic. The later daughter mineral may represent Fe-Mn or Ca-Ba chloride, often identified in many hydrothermal sulphide-PGE deposits around the SIC (Molnár et al, 1999).

Type IIIa inclusion are 1-phase Liquid CO_2 rich inclusions with 95-100% degree of filling. Raman spectroscopy study of one inclusion indicates the presence of CH_4 and N_2 phases (Plate 9.5). These inclusions are the most abundant in many samples. They occur as secondary genetic type inclusions along microfractures in quartz in quartz-carbonate-sulphide veins. Only in one sample (Plate 9.5) these inclusions were found to be spatially associated with Type IIa and Type IIb inclusions hosted within one single quartz grain. Type IIIa inclusions occurred along an inclusion swarm terminated within the quartz grain, such as the Type IIa and Type IIb inclusions but they were located at the other side of the same grain. This peculiar textural relationship suggests that these different inclusions are genetically related and could be the result of heterogeneous entrapment due to the strong immiscibility between saline aqueous liquid and CO_2 –rich liquid.

Type IIIb inclusions are 2-phase Laq-LCO_2 inclusions with a highly variable degree of filling of the CO_2 phase. They occur as rare, large, primary isolated inclusions in carbonates, as well as abundant secondary inclusions in association with Type IIIa inclusions along microfractures in quartz. Along some microfractures in quartz, there is minor evidence that some of this inclusion type formed by the "necking down" process during healing of the micro-cracks.

Type IIIc inclusions are rare 3-pahse Laq-LCO_2 –Halite inclusions. They occur mostly in carbonate always together with Type IIIa and Type IIIB inclusions. This relationship indicates this inclusion type may have formed during inhomogeneous trapping of an immiscible saline aqueous liquid and CO_2 liquid (Plate 9.5).

9.9. Microthermometry study of fluid inclusions

Type Ia inclusions are 2-phase L-V fluid inclusion with a typical 90-95% degree of filling of the liquid phase. This inclusion type occur in carbonate mineral inclusions of semi-massive sulphide of sample FNX-1006-65 (Plate 9.7) The size of inclusions varies between 10 and 40 µm and they

have typical shape of a negative rhombohedral crystal of the host carbonate phase. The aqueous fluid in the inclusions completely freezes below -100 °C and eutectic melting occurs between -55.4 and -49 °C indicating a $CaCl_2$-NaCl-H_2O fluid composition. Final ice melting has been observed between -30 and -37 C that correspond to a 25.11-27.46 $CaCl_2$ equiv.wt. % - salinity of the fluid in these inclusions. On heating runs the majority of inclusions homogenised into the liquid phase between 140-170 °C (Plate 9.7).

In sample FNX-1006-60, inclusions Type IIa, IIb, IIIa and IIIb were studied together where they occurred in one quartz gain spatially and genetically related (Plate 9.5). The CO_2 liquid phase varies between 40-100 vol. % in the Type IIIa, IIIb inclusions. Upon slight cooling from room temperature vapor CO_2 bubble appears in most in the inclusions. Vapor CO_2 represents about 30 vol. % of the CO_2 liquid at its maximum extent. Natural heating back up to room temperature (25-26 °C) resulted in the homogenisation of vapor CO_2 into liquid CO_2 between -12.7 and +25.1 °C. These results indicate a variable approximately density of the CO_2–rich fluid inclusions between 0.97 and 0.72 g/cm^3, due to the presence of other gases (Plate 9.5)

These inclusions completely freeze out into dark brown mass at about -140 °C and solid CO_2 melts between -56.8 and -60 °C. The significant deviation from the trivariant point of CO_2 (-56.6 °C) is consistent with presence of other gases (CH_4, N_2) identified by Raman microscopy (Plate 9.5). Ice meting temperatures were rarely observed between -24.5 and -25.9 in the presence of CO_2 –hydrate (chlatrate). Chlatrate melting exceeded ice melting and was observed in few cases between +8.8 °C and +17.6 °C attributed to the presence of other compresses gases (CH_4, N_2) as shown the Raman microscopy and CO_2 triple point depression. When chlatrate meting temperature exceeds the ice melting temperatures the initial estimate of salinity of the aqueous phase can be made by the ice melting temperature (Bakker and Brown, 2003). Salinity estimation of the aqueous phase of these inclusions were made by using FLUIDS software package (Bakker and Brown, 2003) which resulted in maximum 24.27-25.12 NaCl equiv.wt.% salinity .These CO_2–rich inclusions were not heated in the single quartz grain sample to avoid spoiling of the limited material available, by decrepitating of the inclusions. Type IIIa and Type IIIb primary inclusions were heated in carbonate grains from the same sample and they all decrepitated between 310 and 350 °C. Even small-sized (10 to 20 μm) inclusions, with low degree of filling of the CO_2–rich phase, decrepitated between 230 and 265 °C.

Microthermometric behaviour of polyphase Type IIa and Type IIb inclusions, in association with CO_2–rich inclusions, were also observed in sample FNX-1006-60. Only halite homogenisation temperatures were possible to observe in these inclusion due to small inclusion size and some leakage; re-appearance of vapor phase (probable CO_2–bearing). In many case decrepitations of the inclusions occurred between 230 and 300°C. Halite melting temperatures were observed between 312 and 371.2 °C which estimates the salinity at about 39.1-42.86 NaCl equiv.wt. %. Total

homogenization (melting of X_1, X_2 unknown phase) of these inclusions were never observed because of the 450°C maximum temperature capacity of the Chaixmeca heating stage.

Type Ib and Type IIb inclusions were studies in sample FNX-1024-283 (Plate 9.6). Eutectic melting of these inclusions were observed between -48 and -50 °C approximating a $CaCl_2$-NaCI-H_2O fluid system. Ice melting temperatures were observed between -29 and -33 °C corresponding to 24.73-26.17 $CaCl_2$ equiv.wt. % salinity. Total homogenization of fluid inclusions happed with the halite dissolution between 224 and 355 °C in 3-phase (L-V-H) inclusions and with the dissolution of X_1 unknown phase over 385 C. Halite dissolution temperatures correspond to 33.14-42.86 NaCl equiv.wt. % salinity of these inclusions.

9.10. Summary and Discussion

Surface outcrops mapping (Fig 9.2) in the No.4 West Zone indicates the presence of a number of narrow 2-7 m wide east-west trending mylonitic shear zones. Microtectonic analysis from these deformation zones indicates a sense of shear identical with a steeply oblique thrust, south side up to the northwest (Chapter 7). Several tectonic elements and the orientation of these zones are identical with that described for the South Range Shear Zone. The age of this deformation is suggested to be 1450 Ma, Chieflakien based on results of K/Ar, Ar/Ar studies (Chapter 8). Mylonitic tectonites in the shear zones are re-crystallized to chlorite, chlorite sericite schist consisting of chlorite, chlorite-Cr-muscovite (mariposite) cleavage bands and quartz-carbonate or carbonate (Fe-Mg-carbonates) microlithons. Several field occurrences of massive sulphide lenses, sulphide streak and quartz-sulphide veins, lenses indicate redistribution, re-mobilization of primary massive sulphide of the Contact Sublayer environment.

Exploration drilling by FNX in 2002-2003 identified a steeply north dipping Contact Sublayer-style sulphide mineralization generally strongly deformed by the shear zones observed on surface. In few zones PGE-enrichment occurs, apparently associated with strongly deformed sulphides (Figure 9.1, B).

Several microtextural features and sulphide alteration minerals indicate that primary magmatic sulphide ore was severely altered during the deformation by hydrothermal fluids (Plate 9.3). During the deformation and alteration processes, typical magmatic minerals, pyrrhotite, chalcopyrite, pyrite and sulfarsenides, precipitated from hydrothermal fluids and formed euhedral grains hosted within alteration minerals, quartz, calcite, chlorite, Cr-sericite (mariposite) (Plate 9.6, C and Plate 9.7, F). The abundance of monoclinic pyrrhotite in the deformed sulphide ore may suggest formation at lower temperate i.e 400-300 ºC than typical magmatic conditions. Smythite is a typical low temperature oxidation product of the strongly magnetic monoclinic phase of pyrrhotite.

Pentlandite is generally strongly altered to violoratite. Pyrite and sulfarsenides typically form sieve-textured porphyroblast-like euhedras with both sulphides and silicate hosts.

Quartz typically occurs in deformed ore as streak-out lenses or vein fragments often with sulphides (Plate 9.1). This indicates syn-genetic, pre- and syn-kinematic formation of quartz during the progressive general (noncoaxial) deformation of sulphides. Therefore both primary and secondary fluid inclusions in quartz could be interpreted to represents fluids associated with deformation, re-distribution of sulphides, and re-mobilization of PGE. In addition, fluid inclusions found in this study, are identical with inclusions widely described from many magmatic-hydrothermal PGE mineralization around the SIC contact (Farrow and Watkinson, 1997; Farrow and Lightfoot, 2002; Molnár and Watkinson, 2001; Molnár et al., 2001, Hanley et. al, 2005, Péntek et al., 2008) The significant difference from these inclusions at the No.2 West Zone is the dominance of the CO_2-rich fluid phase associated with highly saline fluids. The CO_2-rich fluid inclusions are commonly described from the South Range of the SIC in special association with the high temperature (350-500 °C) highly saline multi-component inclusions (Molnár et al., 1999). Molnár et al. (1997, 1999) describe the CO_2-rich rich fluids as later slightly lower temperature (150-300 °C) phase associated with thrusting and metamorphism of the SIC during the Penokean Orogeny.

Due to the limited data obtained from the studied samples of the No.2 West Zone trapping conditions were estimated by using isochors for the Type Ia (Fig 9.4) and Type IIa, IIb, IIb inclusions. Isochors were calculated for 150 ºC and 26 $CaCl_2$ equiv. wt. % salinity (isochore-1) and 350 °C of 40 NaCl equiv. wt. % salinity (isochore-2) in excel spreadsheet with equation of Bodnar (1994) (Fig 9.4). The 350 °C minimum temperature was estimated from the average of decrepitation temperatures of Type IIb and IIIb inclusions and total homogenization temperatures Type IIa and Type IIb inclusion since no accountable Gaussian frequency distribution developed due to the rarity of data. The estimation of the minimum pressure for the Type IIa, IIb, IIIb is problematic due to the lack of availability of thermodynamic data for such a complex and highly saline carbonic aqueous fluids (Schmidt and Bodnar, 2000). Molnár et al. (1999) has approximated 2-3 kbar pressure trapping conditions for similar fluid inclusions from Little Stobie mine in the South Range. Their 2 kbar lower limit is used here for estimation.

Considering the melting temperatures of PGE-minerals (Hoffman and McLean, 1976) present in deformed sulphides; michenerite (510°C), merenskyite (575°C) wherlite (540°C) tellurobismuthite (585°C) a average max. 550 °C was considered for highest temperature limit. In addition a 365 °C minimum temperature can be estimated by the chlorite thermometry calculations from microprobe data (Table 6.3). This data may be used as upper temperature boundary to inclusions homogenizing at lower temperatures. Thus the obtained P-T range can be characterized by 2-2.6 kbar pressure and 400-550 °C temperature (Fig 9.4). This range is consistent with fluid inclusion results from many

other footwall deposits of the SIC (Farrow and Watkinson 1997; Farrow and Lightfoot 2002; Molnár and Watkinson 2001; Molnár et al., 2001; Hanley at. al, 2005; Péntek et al., 2008). These results can be compared to results from the Vermilion mine (Chapter 10) obtained for a high temperature magmatic hydrothermal fluid assemble consisting highly saline (40-45 $NaCl+CaCl_2$ equiv. wt%) fluids trapped at 350-510 °C and 2-4 kbar pressure.

9.11. Conclusions

In conclusion this study showed that, in the No.2 West Zone mineralization, local northeast-trending shear zones associated with the 1450 Ma Chieflakian deformation of the Sudbury Structure could have played major role in re-distribution and re-mobilization of primary magmatic sulphides and PGE-minerals. Deformation within primary magmatic sulphide mineralization could have caused transformation of ore-texture, change of bulk mineral composition and local enrichment of PGE. The association of PGE-minerals with hydrous silicate minerals carbonates and abundant complex high salinity H_2O-NaCl-$CaCl_2$-CO_2-CH_4-N_2 indicates metamorphic-hydrothermal conditions. Fluid inclusions in quartz and carbonate also indicate that PGMs could have precipitated by this fluid at temperature of 400-550°C and pressure of 2-2.6 kbar. This fluid preferentially circulated along the deformation zones and could be originated by mixture of highly saline shield brines and CO_2 –rich metamorphic fluids concentrated along the shear zones. The highly saline fluids and CO_2 –rich fluids have limited miscibility field (Burrus 1981; Schmidt and Bodnar, 2000) therefore it is suggested, based on petrography, that at 400-550 °C temperature they have trapped inhomogenously from an immiscible system.

10. GEOLOGY AND HYDROTHERMAL PGE-MINERALIZATION OF THE VERMILION QUARTZ DIORITE

10.1. Introduction

The Vermilion ore deposit was discovered in 1887 by Henri Ranger. Francis L. Sperry, a chemist of the Canadian Copper Company in Sudbury, detected high concentrations of platinum and arsenic in a sample from the mine, and Wells (1889) provided a detailed description of a new mineral sperrylite ($PtAs_2$) from this sample.

The ore at the Vermilion Mine occurs in small quartz diorite intrusions and their host rocks which are located near the south-western contact with the Sudbury Igneous Complex (SIC) in the 1.85 Ga impact-related Sudbury Structure (Krogh et al., 1984; Corfu and Lighfoot, 1997). Many other quartz diorite dykes are hosts to Cu-Ni-PGE deposits around the perimeter of the Sudbury Structure. The quartz diorite intrusions are generally referred to as “offsets” of the Main Mass of the SIC and were formed during the early stages of the crystallization history of the parent magma.

The Vermilion Mine is located 700 m south of the Creighton fault in Denison Township, near two major past producers, the Victoria (VC) and the Crean Hill (CH) mines (Fig. 1). The area is composed of 2.4 Ga Lower Proterozoic mafic and felsic metavolcanic rocks of the Stobie Formation and pelitic metasedimentary rocks and quartzites of the Matinenda Formation, both belonging to the Huronian Supergroup of the Southern Province of the Canadian Shield. These units crop out as narrow northwest- trending zones cut by the Creighton fault in the area of the Vermilion Mine. The Vermilion quartz diorite unit consists of pods in Sudbury Breccia (SDBX), a pseudotachylite formed due to the impact event. The wide breccia zone along the southern boundary of the SIC (Ronald and Spray, 1999; Scott and Spray, 2000), the South Range Breccia Belt (SRBB) terminates abruptly at the Vermilion Mine. The SRBB is host to other economically important quartz diorite units, such as at Frood-Stobie and Kirkwood along the South Range of the Sudbury Structure (Grant and Bite, 1984).

The Vermilion deposit was mined on a small scale by underground drifting and from an open pit intermittently between 1887 and 1918. Card (1968) gave a short note about the Vermilion orebody that it consisted of irregular ore shoots varying from a few cm to 40 cm thick in fractured metavolcanic and metasedimentary rocks. The exploited ore consisted of pyrrhotite, chalcopyrite, bornite, chalcocite, native copper, cassiterite, native gold, sperrylite, millerite and polydymite. Production of 4014 t of sulphide ore to 1926 averaged 6.64 % Cu and 6.89 % Ni with 21 g/t Pt and 54 g/t Pd (Farrow and Lightfoot, 2002). The gossans and the upper level of the mine were rich in native gold. Modern re-evaluation of the Vermilion deposit by reconnaissance drilling revealed PGM-bearing zones spatially associated with large gabbroic inclusions in quartz diorite and Sudbury Breccia. PGE enrichment is associated with low amount 2-5 percent disseminated sulphides in well defined zones that appear to follow the strike and dip of the exploited massive sulphide shoots (Grant and Bite, 1984). This feature is similar to the typical “Low Sulphide High PGE-Au” type mineralization recently recognized around the SIC (Farrow et al., 2005).

A peculiar characteristic of the Vermilion deposit is the very high PGE content. Several features suggest that hydrothermal processes post-dating the formation of the Sudbury Igneous Complex (SIC) were responsible for PGE enrichment. In this chapter the geology of the Vermilion deposit on the basis of detailed mapping and drill core logging is presented. A special focus was made on the extremely rich PGE content and precious metal assemblage, and on outlining different stages of mineralization. Textural analyses, mineral-chemistry, mineralogical- and fluid inclusion-thermobarometry, were used to develop a model for the formation of this sulphide-poor deposit with extremely high PGM content. It is demonstrate in this chapter, that enrichment of PGE is the result of a complex post-intrusive evolution of the area.

10.2. Geology of Vermilion Mine

Pods of quartz diorite (QD) at the Vermilion mine site outcrop in a 200 m long, northwest-striking and southwest plunging zone which narrows at depth (Fig. 1). The pods do not appear to be connected to the basal contact of the Main Mass of the SIC that is 2 km to the north of the Vermilion mine. To the north the QD pinches out or is displaced by a proposed NE-SW striking fault that is defined by a 15-25 m high, NE-SW oriented, steep cliff. QD (two large and smaller pods) intrudes the brecciated lower Proterozoic Huronian metavolcanic rocks (Fig. 10.1; Fig. 10.2A). The QD pods are fine- to medium grained from the margin to the centre, respectively, and it, along with the surrounding SB; contain 0.5-8 m large xenoliths of enclosing units and grey gabbro. The grey gabbro xenoliths originated from the 2.21 Ga Nipissing intrusion series (Lightfoot et al., 1997b; Corfu and Andrews, 1986). The pods also contain 3-5 vol. % amphibolite and 5-10 vol. % feldspar-rich inclusions of 0.4 to 1.5 cm and 1 to 5 cm, respectively (Fig. 10.2E; Fig. 10.3G). The proportion of these inclusions increases toward the central axis of the pods along the main NW-SE strike direction.

A narrow zone between the two major quartz diorite pods exhibits a distinctly variable texture. This unit is a mafic rock of medium- to coarse-grained granular to porphyroblastic texture and was described as a large gabbro inclusion in quartz diorite by Lightfoot et al. (1997b). This unit is interpreted here as a large contact metamorphosed slab of footwall amphibolite or amphibole-bearing SB as revealed by the alignment of abundant rhyolite inclusions from the host rocks of QD at both sides along its contact.

A thin shear zone crosscutting the two major QD pods occupies the boundary of the amphibolite and rhyolite inclusions as well as the QD. The rocks are foliated in this zone and contain disseminated sulphides and PGM.

Along the north-eastern boundary of the two major QD pods, there is an irregularly distributed zone of coarse-grained rock with idioblastic amphibole in a fine-grained groundmass (Fig. 10.2F; Fig. 10.3J). This unit is referred as “metabreccia” by Peredery and Grant (1980). However, there is neither matrix nor clasts in this unit; the texture is rather homogeneous, but has a slight to significant change in grain size of amphibole as a function of distance from the contact with QD. The size of amphibole crystals decreases, whereas their amount increases slightly. There is also a faintly defined textural continuum from amygdaloidal amphibolite to “metabreccia” as a function of distance from the contact. In samples closer to the footwall, partly obliterated vesicular texture is still evident. At the northeastern tip of the major QD body, the “metabreccia” has the greatest width (Fig. 1). It does not show significant decrease of grain size away from the contact and abruptly grades into amygdaloidal amphibolite farther to the northeast.

Amygdaloidal amphibolite forms a 5 to 15 m wide zone immediately next to "metabreccia" and it grades into massive amphibolite to the northeast.

The south-western boundaries of the two major QD pods consist of two types of SDBX. In the north-western part, SDBX is composed of brecciated amphibolite; it is clast supported with a clast-matrix ratio of 70:30. The clasts are 20 to 80 cm across, rounded, subrounded, composed of irregularly intermingled amygdaloidal to massive amphibolite which may be pillow structures obliterated by brecciation. The matrix to the breccia is fine-grained amphibolite occurring around and between the clasts (Fig. 10.2C).

The south-western part of the SDBX zone comprises irregularly-textured, medium-grained to aphanitic, foliated, biotite-rich matrix supported breccia (Fig. 10.2D) with 20% 1 to 5 cm large felsic angular to flattened symoid clasts of rock fragments. The inhomogeneous schistose matrix is composed of quartz-biotite-ilmenite. Foliated, biotite-rich matrix breccia is generally typical for SDBX in the South Range Breccia Belt (Scott and Spray, 2000). To the south, the SDBX body widens and it is dominated by its biotite-rich schistose matrix that is irregularly lepidoblastic and fine- to medium-grained (Fig. 10.1; Fig. 10.2D). Rounded arkose and wacke inclusions up to 5 m diameter from the Matinenda Formation are abundant in SDBX 100-150 m to the south of the QD pods. At some places, on the surface and in drill core, the foliated biotite and/or chlorite rich zones contain 3-10 vol. % of 0.3 to 2 cm large garnet porphyroblasts (Fig. 10.3L). The dip/dip direction, pitch and trend data for the foliation of SB are 170/85; 178/78p72E; 184/70p72E, respectively. Deformation of QD occurs along narrow shear zones parallel to the foliation in SDBX. The orientation of foliation is also parallel to strikes of hornblende-quartz-diabase dykes of unknown age which occur 30 m southwest of the main QD pod (Fig. 10.1).

Hornblende quartz diabase dykes crosscut both Sudbury Breccia and quartz diorite. Their contact with QD is knife sharp. Their margins are chilled-aphanitic (Fig. 10.2B), whereas the centres are fine-grained. Their contacts with SDBX are also sharp and concordant with foliation. Coarsening of grain size and appearance of garnet-biotite assemblage in SB locally occur along the contact (Fig. 10.3L). There is no shearing at the contacts or within the dykes suggestive of syn- or postectonic emplacement of the dykes.

A pink medium-grained, massive and quartz porhyritic rhyolite unit is exposed west and southeast of Vermilion mine. It occurs as abundant inclusions in SB.

10.3. Petrography of fresh and altered rocks

10.3.1. *Quartz diorite*

QD contains 50-55 vol.% zoned plagioclase (An_{20-60}) (Table 10.2, Feldspar 10,11) with 6-8 vol % quartz, 35-45 vol. % amphibole (from actinolite to ferro-tschermakitic hornblende compositions; (Fig. 10.6A; Table 10.2, Ampibole 10-12), 3-10 vol% biotite (Fig. 10.6B; Table 10.2, Biotite 3-4) plus accessory apatite, ilmenite, titanite, epidote, and chlorite. Inclusion-free marginal

QD is characterized by granophyric intergrowths of oligoclase-quartz in the framework of labradorite and amphiboles (Fig. 10.4A). The coarser central QD contains numerous inclusions of amphibolite with 60-80 vol. % amphibole, 30-10 vol % biotite and 0-10 vol. % chlorite with some quartz and epidote. (Fig. 10.3H). Felsic inclusions consist of fine-grained feldspar laths with numerous minute grains of epidote and rare sudbhedral amphibole. Poorly defined outlines and complex intergrowths of amphiboles, and their characteristic poikilitic texture suggest alteration of primary pyroxene in QD. Actinolite and hornblende are irregularly intergrown but, actinolite is only in part a typical fibrous mass replacing cores of former mafic minerals, as is common to deuteric alteration. Biotite also formed by alteration of pyroxene, amphibole and ilmenite. Marginal zones of QD contain 3-5 vol. % biotite, which increase up to 10 vol. % toward the central part of the QD; this trend appears to correlate with the variation of original ilmenite content of the rock. Ilmenite occurs as columnar, needle-shaped and anhedral relict masses and it is strongly altered to titanite +/- rutile and biotite.

Metagabbro "boulders" (Nipissing Gabbro) retain their original hypidiomorphic granular texture. They consist of 60-80 vol. % fibrous actinolite masses formed by alteration of pyroxene plus 40-20 vol. % fine granoblastic-polygonal groundmass of labradorite with epidote, ilmenite, rutile and titanite accessories.

Millimetre-wide deformation-related shear bands are abundant in QD along which it is recrystallized to fine-grained chlorite-epidote-quartz, quartz-biotite, or chlorite masses. Deformation also occurs along wider zones crosscutting QD. In such zones quartz diorite was transformed into foliated lepidoblastic epidote-biotite and chlorite rich rock.

10.3.2. *Footwall rocks*

Mafic rock between the QD pods consists of variable amount (20-60 vol. %) of subhedral, blocky, zoned amphibole porphyroblasts (Fig. 10.3I). The groundmass (40%) comprises anhedral, equigranular amphibole and zoned plagioclase (An $_{29\text{-}56}$) with accessory apatite, chlorite, epidote, allanite, biotite and quartz. Typical 3 to 5 mm zoned amphibole crystals are surrounded by granular-polygonal, fine- to coarse-grained plagioclase masses in which amphibole is absent. This "clearing up" around the amphibole supports their porphyroblastic origin. Porphyroblasts form subhedral grains or round aggregates of brown Ti-bearing (2.6-3.9 wt. %) hornblende cores of magnesio- to ferro-tschermakitic hormblende compositions. They contain oriented blades or granular mass of ilmenite. Cores are overgrown by Ti-poor blue-green hornblende (Fig. 10.6A).

Nematoblastic/lepidoblastic shear bands contain blue-green amphibole prisms with chlorite in cleavage bands and quartz plagioclase microlithons. Brown porphyroblastsic amphibole crystals become fractured and rotated porphyroclasts with zones of pressure shadows around them.

"Metabreccia" is composed of highly variable amount (30-70 vol. %) of euhedral to prismatic crystals of amphibole of ferro-tschermakitic composition (Fig. 10.6A). The grain size of amphibole varies greatly and may exceed 1 cm length (Fig. 10.2F; Fig. 10.3J). The groundmass consists of fine-grained granoblastic aggregates of quartz, and zoned stubby plagioclase with accessory apatite, biotite and chlorite. Large crystals of amphibole contain abundant inclusions of the phases suggestive of porphyroblastic growth of amphibole (sieves) within the matrix. This unit may be related to contact metamorphism of footwall amygdaloidal amphibolite since amygdales are barely preserved but obliterated by porphyroblastesis. Amphibole crystals are slightly or almost entirely altered to biotite at their cores and to a biotite-chlorite mass in their rims. Thus textural relationship suggests that biotite is a post-contact metamorphic mineral and probably formed at the same time as biotite alteration of amphibole pseudomorphs after pyroxene in QD.

Metabreccia contains rare crosscutting shear bands consisting of recrystallized rock forming minerals. At the boundary between the metabeccia and amygdaloidal amphibolite, there are carbonate-adularia veinlets with prehnite infillings.

Amygdaloidal and massive amphibolite

Both amygdaloidal and massive amphibolites have the same mineralogical composition as "metabreccia" except that quartz is less abundant. These rocks also consist of 70-80% porphyroblasts of euhedral-prismatic, green-bluishgreen amphibole of ferro-hornblende and ferro-tchermakitic hornblende compositions (Fig. 10.6A) and fine-grained granoblastic aggregates of quartz and andesine ($An_{36.3-39.9}$). Where amygdales are present, they compose 45 vol. % of the rock and are filled by coarse grained variety of the same minerals.

10.3.3. *Sudbury Breccia*

The mineralogical composition and texture of SDBX in the Vermilion Offset area is highly variable (Fig. 10.3K,L,M) due to mixing of different local country rocks upon pseudotachylite formation and because of superimposed alteration zones. Matrix supported SDBX at the Vermilion Mine may be subdivided into biotite, garnet-biotite and amphibole-garnet biotite bearing varieties on the basis of the matrix composition; however, all are slightly to completely overprinted by alteration assemblages of chlorite, epidote, albite, carbonate, muscovite and quartz.

Biotite rich SDBX, the most abundant, occurs along the western contacts of the QD pods. It comprises a fine- to medium- grained (0.1 to 1 mm), lepidoblastic, discontinuous parallel to non-parallel foliated matrix (Fig. 10.2D, 10.3K) consisting of about 60 vol. % biotite (Fig. 10.6B), 30 vol. % anhedral quartz, and <10 vol.% untwinned or polysynthetically twinned inhomogeneous plagioclase ($An_{4.7-24.2}$) (Table 10.2). Accessory muscovite, chlorite, ilmenite, and zircon occur in the matrix. The foliation is manifested by weak orientation of biotite. Muscovite appears as discrete

seams pinching and swelling along foliation planes. Quartz and often oriented plagioclase grains are equigranular-polygonal between oriented biotite laths. Alternating layers of assemblages of coarse-grained granular-polygonal quartz-biotite-(muscovite)-oligoclase (24.3-29.9 An %) are irregularly embedded in masses of very fine grained quartz-biotite-muscovite-feldspar. Breccia clasts are composed of mainly quartz, plagioclase (altered to muscovite) and K-feldspar of a much larger size. Granoblastic texture in clasts originated from rhyolite refers to strong re-crystallization. Some clasts are strongly rolled out or define alpha and sigma clasts. Rarely, clasts are angular and consist of 80% quartz, 20 % biotite and the granular texture originates from quartzite.

Coarse-grained lepidoblastic to porphyroblastic garnet bearing SDBX forms few tens of centimetres wide zones within the fine-grained, biotite- rich SDBX. It consists of 70 vol. % of 1 to 2 mm large crystals of biotite (Xmg=0.32), 15 vol.% quartz, 5 vol. % feldspar, 10 vol.% of garnet ($Alm_{64.1-64.4}$) and epidote, zircon, titanite, ilmenite, rutile and chlorite accessories (Fig. 3L). In the vicinity of the quartz-diabase dyke, SB also contains a few relatively large (0.3 to 0.6 cm) prismatic crystals of ferro-tschermakite (Fig. 10.6A) which are partially converted to massive acicular-fibrous actinolite aggregates. Foliation is faintly defined by the interlocking network of biotite. Garnet crystals are about 2 cm and are strongly fractured, rounded and rotated. Large crystals disaggregate into rounded fragments along their edges. Within fractures of larger grains and between smaller fragments of garnet, a foliated assemblage of quartz, biotite, fibrous amphibole and chlorite occurs. Due to an increase of intensity of chloritization, garnet crystals have a porphyroclastic appearance forming sigma and alpha clasts mantled with strongly foliated chlorite, quartz and epidote with minor biotite. Rare porphyroclastic amphibole (hornblende) is also fractured, rotated and altered to very fine fibrous actinolite, chlorite and biotite. Concordant sulphide (bornite-chalcopyrite) veins and lenses are intergrown with the same silicates as in the host, but their grain size is much coarser.

10.3.4. *Veinlets*

Quartz and quartz-carbonate veins with sulphides are usually parallel-subparallel with foliation of SDBX and occur in SDBX, QD and amphibolite, as well as metagabbro and rhyolite inclusions (Fig. 10.3A,B,C,E). Most veins are strongly strained, brecciated, mylonitized and re-crystallized due to later brittle shearing. Crosscutting relationships suggest that the formation of chlorite rich shear bands postdate some of the veins (Fig. 10.3F). However, some veins also contain quartz without recrystallization. Carbonate is dominantly calcite with dolomite. In quartz-carbonate veins, carbonate cuts or cements brecciated quartz which also suggests later emplacement of carbonate. Carbonate-quartz veins occasionally contain chlorite, vermiform chlorite-biotite, clinozoisite, epidote, dolomite and white mica rosettes. In a few quartz dominated veins, euhedral reddish K-feldspar crystals occur along the contact with the host rock (Fig 10.3.A,B). Crosscutting

sulphide veinlet in SB develops sharp quartz-andesine ($An_{30.9-31.99}$) alterations selvage. The dilatant sulphide veinlet has a composite possible syntaxial-antitaxial nature representing episodes of opening.

10.3.5. *Hornblende diabase dykes*

Fine- to medium-grained amphibole quartz diabase dykes may have the original magmatic assemblage of 50-60 vol. % amphibole, 35-25 % plagioclase and 15 % quartz; however, these dykes are also moderately to completely altered. Subhedral blocky and prismatic amphibole and stubby plagioclase with interstitial quartz form the framework of the rock. Amphibole is strongly zoned and it consists of a brown centre surrounded by anhedral to platy masses of Fe-Ti oxides and an overgrown rim of bluish-green hornblende. Alteration of plagioclase to white mica, epidote, carbonate and chlorite has highly variable intensity. In completely altered samples, boundaries of plagioclase are barely recognizable and the groundmass comprises granular coarse carbonate, white mica, chlorite and epidote.

Quartz diabase dykes contain abundant 1 to 4 mm wide syntaxial veinlets related to dilational fracturing. In some sections, crosscutting relationships reveal that veinlets with carbonate-quartz infillings are older than the epidote-chlorite veinlets.

10.3.6. *Rhyolite*

Porphyritc, anhedral, rounded 2 to 4 mm phenocrysts of quartz are strongly strained and re-crystallized. The matrix is a fine grained equigranular and consists of muscovite and quartz.

10.5. Ore mineralogy and petrography

Sulphide-PGE mineralization occurred in narrow steeply-dipping zones of veinlets and disseminations in QD, biotite- garnet biotite- and amphibolite- SDBX around and between Nipissing gabbro “boulders” (Fig.1.). Sulphide +/- PGM occur as blebby aggregates in the north-western top and south-eastern bottom of the QD pods, as well as fine dissemination along shear zones between the two pods.

10.5.1. *Disseminated, blebby and vein-type mineralization in quartz diorite*

Primary magmatic blebby sulphide disseminations occur at the north-western end of the major QD pod (Fig. 10.1). Blebs of 1 to 5 mm size, with irregular outlines comprise about 1-2 vol. % of the rock in the inclusion rich central part. The blebs are composed of pyrrhotite aggregates in which pentlandite occurs as intergranular veins and subhedral grains (Fig. 10.4H). Minor amounts of chalcopyrite occur next to pyrrhotite-rich blebs or rim them. Euhedral crystals (200 μm) of cobaltite-

gersdorffite solid solution are entirely included both in pyrrhotite-pentlandite and in the silicate groundmass (Fig. 10.4H).

Disseminated sulphide aggregates (1-100 μm) with chalcopyrite, Co-Ni-sulfarsenide minerals, galena and bornite are associated with alteration minerals of the QD. These sulphides occur within masses of altered ilmenite, cluster in actinolite, and also occur in altered cores of plagioclase crystals. At some places, dissemination ranges to bleb-like appearance. The blebby-like sulphide content, is rare, but slightly increases to the south-eastern termination of the QD pod, as does the amount of amphibolite and feldspar inclusions.

The blebs (1-4 mm size) consist of chalcopyrite and bornite intergrown with chlorite, quartz, epidote, albite and carbonate. Bornite is more common in blebs close to the south-western margin of QD where the strongest PGM enrichment occurs in a 1.5 by 4 m area on the surface, just above the orebody targeted by the historical underground mining. (Fig. 10.1). QD in this area consists of a poorly defined zone or lens of biotite-QD composed of biotite (65 vol. %) and quartz-oligoclase granophyric intergrowth (35 vol. %) (Fig. 3N). Biotite-QD is partly deformed and sulphide aggregates appear along foliation planes. Preliminary assays indicate 70-140 g/t (Pd+Pt+Au) in disseminated sulphide of this biotite-QD.

In this disseminated PGM rich zone larger (3 to 5 mm) chalcopyrite and bornite rich sulphide aggregates-blebs display very complex mineralogy and textures. The complex PGM assemblage has a very close spatial relationship to bornite. PGM occur as composite aggregates within or attached to bornite, although they also occur in hydrous silicates. In contrast, disseminated chalcopyrite with subordinate bornite in amphibole-biotite QD from drillcore did not reveal abundant PGM (Fig. 10.3D). In the PGM rich zone, however, chalcopyrite is partially replaced by bornite, millerite and thin outermost rim of gersdorffite (Fig. 10.5G). This replacement results in many types of peculiar textures such as acicular millerite and myrmekitic intergrowth of bornite-gersdorffite (Fig. 10.5F,G).

Bornite contains numerous exsolution forms, mainly as very fine (111, 100) oriented blades-, short and thicker vermicular segregations-, very fine spindles- or larger blebs of chalcopyrite, rare chlalcocite and frequent oval-radial grain aggregates of wittichenite with very fine electrum (Fig. 10.4I; 10.5D). Very spectacular exsolution forms are the electrum-parkerite+/-hessite+/-froodite-wittichenite composite blebs (Fig. 10.4I; 10.5D). Hessite and froodite are dominantly associated and appear usually as intergrowths. Froodite contains gold in its structure (Table 1). The complex assemblage of wittichenite-michenerite-hessite-froodite-sudburyite-gold-parkerite-bismuthinite with occasional annivite also occurs around bornite, and entirely in silicates, quartz, epidote, chlorite (Fig. 10.5A,B). Sperrylite is in contact with chalcopyrite, maucherite (Fig. 10.4E) and sometimes it is intergrown with platy chlorite. Platy molybdenite occurs rarely in silicates.

Microtextural characteristics distinctly differ in coarse (1 to 4 mm) bornite where it contains very coarse (300-900 □m) radiating wittichenite aggregates rimming hessite-froodite-electrum. Bornite hosting these aggregates is devoid of fine (111) exsolution network of chalcopyrite; instead, it contains larger blebs of it. This textural difference and the coarsened grains of exsolution phases suggest recrystallization due to deformation that occurs in samples containing these coarse wittichenite aggregates.

Bornite is crosscut by 20 to 30 μm composite veins of luzonite, and vermicular-acicular gersdorffite. Bornite alters to digenite along these veins (Fig. 10.5E). At the margins of bornite grains, composite rim of digenite-luzonite or luznoite-gersdorrfite reveals a paragenetical sequence of digenite-luzonite-gesdorffite.

Maucherite and rarer nickeline appear as euhedral to anhedral (0.1 to 1 mm) fractured grains included in silicates, chalcopyrite and bornite and smaller 50 to 400 μm perfect crystals in hydrous silicates. Grain boundaries between maucherite and nickeline are sharp and straight reflecting equilibrium crystallization. Grain boundaries of maucherite and nickeline against chalcopyrite are also sharp: however re-entrant, embayment-like faces, as well as caries texture appear in maucherite against chalcopyrite. Gold fills the fractures and embayment in maucherite (Fig. 10.4F). Both maucherite and nickeline are replaced by bornite, millerite, and gersdorffite. Maucherite contains inclusions of inhomogenous sudburyite with varying Ni-Pd, Bi-Sb substitution (Table 1). Sudburyite inclusions are aligned along boundaries of sectors with different Ni/As ratios in maucherite and are also widely distributed within sectors (Fig. 4B). Sudburyite also occurs in association with complicated intergrowths of hessite-froodite-michenerite-annivite-gold-parkerite-wittichenite in bornite (Fig. 10.5B).

Michenerite is also ubiquitous in this assemblage. Double reaction rims are often developed between hessite and michenerite (Fig. 10.5B). The rim-1 with higher reflectance may have a composition of $(Pd_{0.7}Ag_{0.4})(Bi_{0.1}Te_{1.75})$ that suggests it is merenskyite. Reaction rims also occur between sudburyite and annivite (Fig. 10.5A); these features refer to a later re-equilibration or sequential formation of different phases of this assemblage.

Quartz veins with PGE mineralization from QD were found in dump specimens only, but yielded extremely large amounts of michenerite. The assemblage is dominated by chalcopyrite, galena, violarite, millerite and Co-Ni-sulfarsenides. Galena is seemingly enriched in veins and is often enclosed by quartz. Most quartz grains in the vein are strongly strained and deformed.

10.5.2. *Sulphide-PGE mineralization in Sudbury Breccia*

In different types of SDBX, PGM occur in fine-grained (<10 mm) sulphide disseminations usually forming zones of few cm thick (Fig. 10.1), as well as quartz and/or carbonate veins (Fig.

10.3,A,B,C,E,K,M). Veins and disseminations of sulphides are parallel or subparallel to the foliation in SDBX. Complex PGM parageneses usually occur in the finely disseminated zones.

The major sulphide in quartz, quartz-carbonate veins is chalcopyrite that includes pseudomorphs of pyrite-marcasite and millerite-violarite after pyrrhotite and pentlandite, respectively (Fig. 10.5H,I). Pyrite-marcasite aggregates have round outlines and linear arrangements of pyrite-marcasite rich lamellae possible mimicking the 0001 cleavage of pyrrhotite (Fig. 10.5I). In a few cases such aggregates alter to concentric globules similar to "bird's eye" texture indicative of the former existence of pyrrhotite, but somewhat coarser-grained. Accessories are sphalerite, galena and gersdorffite rimming the veins. Granular, polygonal millerite-violarite aggregates also reveal the subhedral outline of former pentlandite and still contain the characteristic shrinkage fractures of pentlandite (Fig. 10.5H). These aggregates are successively replaced by millerite and then chalcopyrite. Bornite with chalcopyrite exsolution may partly or completely replace chalcopyrite in these veins.

PGE mineralization of biotite rich SDBX occurs with disseminations and veinlets of chalcopyrite and bornite. Veinlets and disseminations are surrounded by quartz-epidote-chlorite-carbonate-sericite alteration halos. Veinlets contain chalcopyrite which is replaced by bornite containing exsolution lamellae of chalcopyrite. In disseminated zones, chalcopyrite is also associated with anhedral nickeline in silicates and with euhedral cobaltite-gersdorffite. PGM occur in composite grains of electrum, froodite, hessite, bornite and wittichenite hosted by chalcopyrite (Fig. 10.5C). Elongated 5-20 μm oriented blebs of froodite surrounded by radial wittichenite and chalcopyrite occur in bornite parallel to the exsolution blades of chalcopyrite that may relate to their exsolution origin (Fig. 10.4I).

PGE mineralization of the foliated garnet-bearing biotite-rich SDBX is associated with 1 to 4 mm grain aggregates of major chalcopyrite and minor violarite, bismuthinite (Fig. 10.3M). Aggregates consisting of froodite, michenerite, electrum and bismuthinite occur rarely in chalcopyrite but mainly included in chlorite and quartz (Fig. 10.4C,G). Thus PGE-bearing assemblages may be related to syntectonic chlorite alteration of the garnet-biotite assemblage.

Narrow shear zones crosscutting the area between the two major QD pods (Fig. 10.1) consists of amphibolite schist composed of amphibole-biotite-quartz-plagioclase with minor disseminated sulphides of chalcopyrite-violarite-pyrite-marcasite-ilmenite intergrown with epidote-chlorite. Rhyolite in this deformation zone is crosscut by streaks and veinlets of chalcopyrite-violarite-pyrite-marcasite-sperrylite-gersdorffite-molybdenite intergrown with amphibole-epidote-biotite-quartz assemblages.

Massive to semimassive ore of chalcopyrite, violarite-millerite with coarse michenerite and Co-Ni-sulfarsenides also occurs in samples of mineralized garnet-biotite SDBX from historical

collections and in samples from the Vermilion mine dump. The ore consists of small volumes a few centimetres across of coarse chalcopyrite with rounded silicate inclusions. The margins of these lenses in foliated SDBX matrix are fully packed with garnet-biotite, epidote, chlorite, quartz indicative of a deformation induced alteration of a massive-semimassive ore.

Abundant 0.2 to 1.5 mm large round-subhedral inclusions of michenerite, maucherite, nickeline, with minor millerite occur in semimassive-massive chalcopyrite (Fig. 10.4D). Minor phases are few cm wide masses of violarite-millerite, Cd-bearing sphalerite, zoned Ni-bearing pyrite, and marcasite. Millerite-violarite and pyrite-marcasite occur as pseudomorphs after pentlandite and possibly pyrrhotite, respectively, similar to those in quartz-sulphide veins (Fig. 10.4D). Very few remnants of pentlandite still exist in the alteration masses. Nickeline and maucherite are usually rimmed by gersdorffite. Nickeline, gersdorffite and chalcopyrite contain small rounded inclusions of electrum. Where nickeline is totally replaced by gersdorffite, the irregular mass tends to order into groups of euhedral grains or single euhedra. Some grains show further growth within a chalcopyrite substrate and contain chalcopyrite inclusions similar to porphyroblastic sieves. Michenerite and galena include and partially replace sulfarsenides indicating that both are later phases.

The SDBX matrix to this ore consists of foliated, lepidoblastic biotite, quartz, plagioclase and seams of prismatic amphibole crystals. Sulphide streaks are intergrown with euhedral crystals or aggregates of epidote-chlorite-quartz. Garnet-biotite does not contain sulphide-PGM grains but they are enriched around sulphide streaks and lenses. However, anhedral garnets are intergrown with the identical ore in historical samples (Fig. 10.6C).

A spectacular sperrylite-rich assemblage was found in amphibole bearing SDBX. Sperrylite appears as 1 to 4 mm cubes in fine-grained massive amphibolite composed of blue-green hornblende, plagioclase, quartz and biotite. The sulphide assemblage is composed entirely of fine-grained millerite-violarite and minor chalcopyrite. Shrinkage fracture nets in violarite reflect former pentlandite. Alteration minerals associated with the sulphides are quartz and biotite with a noticeably large amount of zircon and rutile included both in biotite and quartz.

10.6. Thermobarometry studies

Preliminary thermobarometry calculations were performed from microprobe data with the aim of characterizing P-T constraints for the alteration/metamorphic history of the post-impact events. Amphibole composition was calculated on the basis of 15 cations (Table 10.2) and Fe^{3+} was estimated according to Droop (1987). P-T values were calculated according to Blundy and Holland (1990).

Amphibole-plagioclase thermometry was used for the determination of contact metamorphic conditions in amphibolite between the QD pods for cores and rims of amphibole and plagioclase

(Table 2. amphibole 4,5; feldspar 8-9). Porphyroblastic amphiboles are zoned with high Ti (2.6-3.9 wt. %) magnesio-hornblende to ferrotschermakitic hornblende cores and low Ti (0.3-0.8 wt. %) rims of magnesio-hornblende to ferrotschermakitic hornblende. The groundmass contains granoblastic, polygonal-zoned labradorite (An_{56}) core and oligoclase (An_{29}) rim (Table 2). The core-core compositions correspond to 695(ed-tre)-845(ed-ri) ºC and the rim-rim suggest 593 (ed-tre)-618(ed-ri) ºC at 5 kbar. The Al and Ti in hornblende P-T estimations resulted in 975-990 ºC and pressure of 1.5-3 kbar for high Ti cores and 550-600ºC for low Ti rim.

Amphiboles from different rock types (Table 10.2, amphiboles 1-12); amphibole-biotite-QD, amygdaloidal amphibolite, garnet-amphibolite, metabreccia, rims of Ti-amphibole core were used for graphical T estimates of Ernst and Liu (1998) and resulted in a range of 550-620 ºC. Since Al in hornblende barometer is usually applicable to magmatic assemblage, it was applied only for contact metamorphic Ti-amphibole between the QD pods that probably have experienced magmatic P-T condition by the QD intrusion. Five calculations (Hammarston and Zen, 1986; Thomas and Ernst, 1990; Hollister et al., 1987; Johnson and Rutheford, 1989; Blundy and Holland, 1990) resulted in a range of 4.5-7.5 kbars with an average 6 kbar. On the other hand all amphiboles from the Vermilion mine including these high Ti amphibole cores are estimated to have formed at a pressure lower that 5 kbars using Al(VI)/Si ratios (Raase, 1974).

Garnet-amphibole and garnet biotite thermometry were performed on garnet-biotite-amphibole SDBX and garnet-biotite SDBX in order to characterize post-impact syntectonic metamorphic conditions in SB. Garnet-biotite-amphibole SB contains idioblasts and round garnet (Table 10.2, garnet 5,6), prismatic bluish-green ferro-tschermakite (Table 10.2, Amphibole 8,9) and platy biotite (Table 10.2, biotite 13,14). Both biotite and amphibole occurs as anhedral inclusions in garnet. Garnet-biotite SB contains round, slightly-zoned (core to rim; Alman62-65-Spess18-14-Grossular11-7-Pyrope3.5) garnet (Fig. 10.6C) and biotite (Table 10.2, Garnet 1-4, Biotite 7-10) aligned along foliation planes. Biotite is moderately to strongly altered to chlorite that later grows preferentially in pressure shadows of garnet. Because of the higher Mn content the $(Al_6+Ti)/(Al_6+Ti+Fe+Mg)$ ratios are partly above (Table 10.2, Biotite) the limitations (0.2) of Ferry and Spear (1978). Using their calibrations the garnets with lower than 0.2 $(Al_6+Ti)/(Al_6+Ti+Fe+Mg)$ ratios were weighted (T=494-501ºC) yet resulted in the temperature range of 492-517ºC at 5 kbars. However five other calibrations (Thompson, 1976; Holdaway and Lee 1977; Perchuk and Lavrentjeva, 1983; Dasgupta et al., 1991; Bhattacharya et al, 1992) span the range of Ferry and Spear (1978) and define a temperature of 362-518 ºC. Amphibole garnet compositions (Table 2, amphibole 8-9, garnet 5-6) were calibrated based on Graham and Powell (1984) and resulted in temperatures of 495-545ºC that both overlaps and exceeds the garnet-biotite temperature range (Fig. 10.8).

Chlorite thermometry was also used when appropriate in order to obtain P-T estimates for later, superimposed events on biotite-garnet assemblage in SDBX and related to sulphide-PGE mineralization (Table 10.2, Chlorite 1-4.). Chlorite composition was calculated on the basis of half unit cell, 14 anions (Caritat el al., 1993). Chlorites were classified as tri-trioctahedral Mg-Fe-Al chlorites with vacancies <0.5 (Wiewióra and Weiss, 1990). All chlorite falls in two compositional ranges of clinochlore-ripidolite and pennine-diabanite (Fig. 10.6D). Clinochlore is coarse platy and occurs in garnet-biotite SDBX, forming from both minerals, and in alteration assemblages of chlorite-epidote-quartz-calcite around sulphides in every rock type. In garnet-biotite SDBX clinochlore is syntectonic, growing on garnet in pressure shadows and between stretched garnet grains defining continuous or partly spaced foliation. In garnet-bitotite SDBX clinchlore is host to sulphides and PGM aggregates (Fig. 10.4C,G). Pennine-diabanite is very fine-grained. It occurs within sulphide veins, as well as associated with disseminated sulphide-PGM replacing former clinochlore and epidote filling vugs. Within one vug composition (Fe/Mg) varies greatly. An average chemical formula for clinochlore is $Fe_{2.27}Mg_{2.4}Al_{1.33}(Si_{2.67}Al_{1.33})O_{10}OH_8$ and for pennine is $(FeMgNi)_{3.9}Al_{1.6}\ \square_{0.5}(Si_{3.4}Al_{0.6})O_{10}OH_8$. Pennine may contain significant amount of Ni (3-5 wt. %) especially when it occurs in vugs of nickeline and maucherite. Four calibrations of chlorite thermometry (Cathelineau, 1988; Kranidiiotis and MacLean, 1987; Jowett, 1991; Zang and Fyfe, 1995) resulted in 200-380°C for clinochlore-ripidolite and 100-160°C for pennine-diabanite (Fig. 10.8; Table 10.2, Chlorite).

10.7. Fluid inclusion studies

Exploration drill holes encountered numerous sulphide- bearing quartz, quartz-carbonate and carbonate veins in quartz diorite, rhyolite, SDBX and amphibolite. Some veins contain original vein quartz which were used for fluid inclusion studies. Mineral paragenesis and replacement sequences in these veins are identical to those observed in massive-semimassive ore from historical and mine dump collections that represent the original ore material

Fluid inclusion petrography studies revealed three major fluid inclusion types of mostly secondary in origin. Only in few samples a limited number of primary and pseudosecondary inclusions were found in quartz crystallized together with sulphides in quartz+/-carbonate+/-sulphide-PGM veins. Carbonate in quartz-carbonate-sulphide and carbonate-sulphide veins contains primary fluid inclusions.

10.7.1 *Fluid inclusions in vein quartz*

Type III-B Primary inclusion occurs as rare isolated solitary inclusions or a group of few inclusions within quartz grain that is intergrown with sulphides in quartz-sulphide veins. Type III-B

pseudosecondary inclusions are identical with Type IIIB Primary inclusions but they occur along fractures terminating within the host grain. Type IIIB Primary a Secondary inclusions are 3-phase H-L-V inclusions. Type IIIC inclusions are 4-phase H-L-V-X1, in addition to halite they contain a subhedral-round, stubby or short columnar prismatic and strongly anisotropic unknown daughter mineral. Halite dissolution into liquid phase occurred between 230-310 °C. Total homogenization occurred by vapor homogenization to liquid between 290 and 450 °C in inclusions without the unknown daughter mineral. Melting of the first phase after freezing to -120 °C, took place below -50 °C indicative of high $CaCl_2$ content in the inclusion liquid. Calculated salinities are between 40 and 45 NaCl+$CaCl_2$ equiv. wt. %.

Type III-C inclusions (Fig. 10.7A) with an unknown daughter mineral homogenized by dissolution of that mineral; however, due to their small size, total homogenization was observed only in one and it occurred at 448 °C.

Type III-A Early Secondary occurs along fractures and they are spatially associated with Type IIIB and Type IIIC Primary and Pseudosecundary inclusions. They have homogenisation temperature and salinity intermediate between the Type I Late Secondary and Type IIIB, C inclusions; therefore they are classified as Early Secondary –type. These fluid inclusions (Fig. 10.7A) consist of three-phase (L-V-Halite). Most of the inclusions are fracture-related inclusions with a consistent 10-15 vol. % degree of filling. Their total homogenization took place either by halite dissolution or by vapor homogenization to liquid between 170 and 230 °C. Final ice melting was observed between -29 C and -40 °C and considering the halite dissolution temperatures, the compositions of inclusions are between 35 and 38 NaCl+$CaCl_2$ equiv. wt.%. Preliminary Raman analyses indicate traces of CO_2 in the vapor phase.

Type II. Secondary inclusions also occur along fractures similar to Type III-A. These inclusions are easily distinguished by their different microthermometric behaviour and composition. Type II inclusions (Fig. 10.7B) are two-phase (L-V) secondary inclusions with highly variable degrees of filling (25 to 100 vol. %). The degree of filling varies within and between fractures. In a few cases, homogenization to vapor occurred at 340-360 °C in these inclusions. Homogenization to liquid occurred between 200 and 400 °C in inclusions of low degree of filling (<40%) but was never observed in inclusion of higher degree of filling. Eutectic melting occurred at around -50 °C. Ice melting was observed at -31 °C and at -12 °C which indicates 16-25 $CaCl_2$ equiv. wt.%. Preliminary Raman probe data indicate the presence of low-density CH_4 (36-40%)-N_2 (37-36%)-H_2 (24-27%) in the vapor phase. Petrography and micro thermometric behaviour of these inclusions suggest inhomogeneous trapping from a heterogeneous (boiling) fluid system.

Type I. Late, secondary fluid inclusions are ubiquitous in many samples and they occur along fractures that crosscut fractures containing inclusions of Type II and Type III. These inclusions are

two-phase (L-V), fracture-related secondary inclusions with a consistent (10-15 vol. %) degree of filling (Fig. 10.7C). Homogenization temperatures (to liquid) are 160-180 °C. Eutectic melting occurred at around -50 °C and final ice melting took place between -8 and -35 °C. In a few cases, hydrohalite was also observed and its melting occurred after ice melting in some of these inclusions. Calculated salinities are between 12 and 26 NaCl+$CaCl_2$ equiv. wt. %.

10.7.2. *Fluid inclusions in vein carbonate*

There are two generations of carbonate in carbonate-rich sulphide veins (Fig. 10.3C). Sulphides associated with carbonate in carbonate-sulphide and quartz-carbonate-sulphide veins consist of chalcopyrite, pyrite, marcasite, millerite, parkertie gold. Grains of minor first generation carbonate contain numerous primary fluid inclusions and are intergrown with sulphides, whereas major second generation grains are devoid of inclusions, therefore, they are transparent Fluid inclusions in carbonate are of two-phase (L-V), primary, negative crystal-shaped inclusions with 10-15 % degree of filling of the vapor phase (Fig. 7D). Homogenization temperatures to liquid are between 100 and 200 °C. Eutectic melting occurred at -29 °C referring to metastable eutectic of the NaCl-H_2O system or low presence of other components. Final ice melting took place around -8 °C in carbonate-sulphide (Fig. 10.4G) and at around -15 °C in quartz-carbonate-sulphide (Fig. 10.4.E) veins corresponding to calculated salinities of 12 and 19 NaCl equiv. wt.% respectively. The temperature range overlaps that of late secondary Type-I inclusions in quartz but inclusions in carbonate are of dominantly NaCl-H_2O in composition.

10.8. Discussion

10.8.1. *Geology*

The QD pods at Vermilion mine are located in a thick zone of SB developed between contacts of rhyolite-amphibolite and amphibolite-metasedimentary rock. These contacts could have behaved as a zone of easy brecciation during impact.

In the zoned QD, gabbro boulders and rare primary magmatic blebby sulphides are restricted to the inclusion-bearing central facies in the north-western tip. At the south-eastern end, rare blebby sulphide, amphibolite and feldspathic chips increase gradationally toward the centre, whereas the largest gabbro boulder occurs between QD and SDBX at the margin. Gabbro boulders form groups in the break of the two large pods are also associated with inclusion and sulphide free QD. There is neither close correlation between the gabbro boulders and neither central QD nor spatial association of the boulders with gabbros in the footwall as occurs, for example, in the Worthington Offset (Farrow and Lightfoot, 2002). Nipissing Gabbro that could have been the source for these inclusions occurs no closer than 600 m to the west. This situation suggests that the inclusions originally had

been disrupted by the impact induced brecciation and were transported and deposited within SB. These inclusions may have been rounded mechanically and/or thermally upon transport in SDBX.

Granophyric microtexture is common in QD Offsets of the SIC. Plagioclase with labradorite-oligoclase composition is also described from the Foy offset (Tuchscherer and Spray, 2002) and Hess offset (Wood and Spray, 1998). Labradorite and granophyric intergrowths of quartz and oligoclase are mentioned from North Range contact sublayer (Molnár et al., 2001; Therriault et al., 2002). In Vermilion QD the oligoclase rim is in very sharp contact with the core and oligoclase fills fractures in labradorite (Fig. 10.4A). This textural characteristic suggests that it is an overgrown rim rather than a result of compositional zoning. The granophyric microstructure observed in Vermilion QD may relate to rapid crystallization by undercooling by escaping fluids.

Amphibole and biotite of QD result from alteration of former pyroxene (Grant and Bite 1984). Primary amphibole and biotite occur in small quantity in Main Mass rocks (Naldrett and Hewins, 1984; Therriault et al., 2002). All these suggest that the primary Sudbury magma had a significant volatile component that may have exsolved upon crystallization and reacted with the primary mafic minerals to form late magmatic amphibole. The lack of primary magnetite in many QD, or the presence of peculiar pseudomorphs of ilmenite-biotite after magnetite, also suggests an early oxidizing volatile expulsion (Szentpéteri et. al, 2002). The volatiles mixed with footwall fluids and remobilized parts of earlier massive sulphide ores; this was recognized to have played a significant role in the concentration of PGM (Farrow and Watkinson, 1997; Molnár et al, 2001; Molnár and Watkinson, 2001; Farrow et al, 2005) in footwall Ni-Cu-PGE sulphide veins.

South Range QD offsets and South Range Norite contain high Al calcic-amphiboles (hornblende, and thermakitic hornblende); in a few cases they formed contemporaneously with garnet that suggests a superimposed almandine-amphibolite facies metamorphism with textural evidence of zonal overgrowths of these amphiboles on actinolite cores resulting from deuteric alteration (Fleet et. al, 1987). The presence of biotite and spessartine garnet in the sedimentary sequence (Whitewater Group) of the Sudbury Basin attests to middle to-upper greenshist (~ 400 ºC) facies metamorphism (Roussel, 1975; Sadler, 1958). A considerable debate still exists on the timing of peak metamorphism of the Sudbury area. In contrast to Card's (1964, 1978a,b) results, Brocoum and Dalziel (1974), Fleet et al., (1987), Thomson et al., (1985), Shanks and Schwerdtner (1991a) concluded that prograde metamorphism occurred post-impact, affecting both the Huronian volcanic-sedimentary footwall and SIC rocks, reaching amphibolite facies. However, peak metamorphism of the Huronian Supergroup occurred soon after the emplacement of the Nipissing Gabbro (2240Ma) at 2220 Ma according to Jackson (1997) and Easton (2000) and was pre-impact in the view of Riller et al. (1996). Peak, post-Nipissing metamorphic conditions were of amphibolite facies at 560-/+60 ºC temperature and 4.3-/+0.8 kbar pressure (Blonde, 1996). Jackson (1997) recorded 500-560 ºC

temperature and 1.5-3 kbar pressure conditions for metamorphism of Nipissing Diabase in May Township ca. 60 km from the SIC. PT conditions obtained from SB in this study are similar to the above mentioned ones and may support a post-Sudbury Event age. In addition, compositions of garnet and amphibole reported by Fleet et al. (1987) from South Range Norite and QD offsets are similar to those encountered in this study.

In Vermilion QD, the coexistence of actinolite- ferro-tschermakitic hornblende, the mineral paragenesis with biotite, plagioclase, quartz, epidote, chlorite, titanite, albite, may correspond to an epidote-amphibolite facies metamorphic alteration overprinted by greenschist facies alteration. Plagioclase is incompletely reacted and preserves magmatic compositions. This assemblage is also consistent with a high temperature deuteric alteration of QD. Ti in hornblende suggests 540-600 ºC for hornblende formation. Therefore, deuteric or metamorphic origin of alteration cannot be satisfactorily deduced from Vermilion QD.

Since Sudbury breccia is syn-impact, it is an ideal medium to study metamorphic processes that took place post-impact. The general mineralogical composition of the recrystallized SDBX consists of biotite, quartz, plagioclase (An_{39-45}), ilmenite (Scott and Spray, 2000). It appears that this dominant mineral composition of SB at Vermilion mine is not a result of contact metamorphism by QD but rather a regional recrystallization event (syn-kinematic growth of biotite) throughout the SRBB. Minor textural variances reflect varying degrees of recrystallization.

The appearance of the coarse porphyroblastic “metabreccia” only on the western side requires specific conditions for its formation. Mineral proportions and compositions in metabreccia are similar to those in amygdaloidal amphibolite excluding quartz that is more abundant in the former. However, no inclusions of any kind were observed in this unit. Grain size variation suggests a zonal contact metamorphic effect on footwall amygdaloidal and/or massive amphibolite. Granoblastic intergrowths of stubby zoned plagioclase with anhedral plagioclase and quartz is also indicative of contact metamorphism. Amphibole (Fig. 10.6A) composition (ferro-tschermakitic hornblende) is of similar high-Al than amphibole in QD, footwall amphibolite, and garnet-amphibole SDBX. Similar coarse amphiboles are also found elsewhere in the footwall both along hornblende diabase dykes and in felsic lenses in massive amphibolite that may imply that this contact metamorphic zone was affected by post-Sudbury event metamorphism as well.

This “post-contact” metamorphism is represented by low-Ti amphibole (ferro-tchermakitic hornblende) rim overgrown on high-Ti ferro-tschermakitic hornblende cores of the zone between the two QD pods. Al and Ti in hornblende, amphibole-plagioclase estimations suggest 850-950 ºC/1.5-3 kbar corresponding to an amphibole-pyroxene hornfels facies. These amphiboles may be pseudomorphs after high-Ti bearing pyroxenes as well. Clinopyroxene, brown hornblende -bearing contact metamorphic zones are recognized in footwall breccia reported from the North Range

(Dressler, 1984). Immediately next to the SIC contact in Footwall Breccia and in the Levack Gneiss, the temperatures were calculated to be of 1000-1100ºC and 800-1015ºC respectively (Lakomy, 1990; Molnár et al., 2001).

High temperature contact metamorphism is generally obliterated in the South Range (Dressler, 1984) but few relict cores of brown hornblende in footwall amphibolite may correspond to this event (Fleet et al., 1987). Brown amphiboles of similar texture and composition to those at Vermilion mine are also common in the Victoria mine area in close proximity to the SIC contact.

The chemical composition of the mineral assemblage in SDBX corresponds to lower-amphibolite facies metamorphism. Several P-T calibrations yielded 495-545 ºC for garnet-amphibole, and 362-518 ºC for garnet-biotite pairs at an estimated maximum 5 kbars. Similar temperature range (370-510 ºC) was obtained for biotite-garnet from the PGM rich semi-massive ore (Magyarosi, 1998) from historical collections. The presence of michenerite and the composition of sulfarsenide indicate a maximum temperature of 500-510 ºC.

SDBX displays retrograde alteration of garnet and biotite into chlorite below 380 ºC and a maximum of 3 kbars. Alteration of plagioclase composition of An_{23-30} cores with thin rims of An_{5-7} in biotite-SDBX is of also retrograde. Intense chlorite alteration is syn-tectonic corresponding to a non-pervasive deformation event localized along narrow shear zones. The complex PGM assemblage is located along syn-tectonic chlorite and quartz or it occurs parallel, or sub-parallel to foliation in SDBX strongly intergrown with chlorite, epidote, albite, quartz, carbonate, sericite, a greenschist facies alteration assemblage that replaces primary minerals in QD and SB. Albite sometimes replaces epidote and it usually contains very fine disseminated sulphide PGM. Thus it appears that even the greenschist facies alteration assemblage re-equilibrated during decreasing temperature from upper to lower greenschist facies consistent with textural characteristics in the disseminated complex sulphide-PGM assemblage.

Textural characteristics suggest that many of the sulphide-quartz veins encountered in drill holes are prior to deformation (Fig. 10.3F). Since this deformation is not pervasive, the veins are not segmented, but many are brecciated, reflecting compressional component parallel-subparalell to the original vein orientation. Deformation caused mylonitization of the centres of the veins with fragments of earlier quartz and epidote. This relationship and prominent alteration textures in vein sulphides correspond to their early emplacement prior to deformation related to magmatic-hydrothermal processes responsible to the massive-semi-massive sulphide-arsenide-PGM assemblage.

10.8.2. *Mineralization*

The mineral assemblage and textural relationships of many ore types at Vermilion mine indicate complex alteration-replacement processes. The original ore contained maucherite-(sudburyite)-nickeline, chalcopyrite, michenerite, pentlandite and minor pyrrhotite. In some historical samples this ore is intergrown with garnet-biotite-quartz-(epidote-albite-zircon). Garnet-biotite assemblage indicates T of 370-510 °C or upper greenschist-lower amphibolite facies metamorphism (Magyarosi, 1998) covering a range obtained from garnet-biotite-amphibole SDBX and garnet-biotite SDBX 430-550°C. The presence of michenerite and the composition of the cobaltite-gersdorffite solid solution (ss) indicate temperatures lower that 501°C and 510°C, respectively. Cobaltite and michenerite is spatially associated, but textures show that michenerite is later. This close association can be the result of their formation at similar temperatures i.e. 501 and 510°C respectively.

The primary sulphide assemble could be coeval with garnet-biotite (i.e., equivalent first phase of metamorphism and/or high temperature hydrothermal alteration), but it may also have intergrown with them after its formation at a later event causing the significant alterations. The inferred porphyroblastic growth of cobaltite may support the latter. In this case however michenerite can also be considered to have been grown as porhyroblasts in chalcpyrite. This may explain why michenerite is so coarse 100-2000 μm in these semi-massive ores and mainly confined to ore-silicate boundary.

The spectacular alteration forms include millerite-violarite pseudomorphing pentlandite and cobaltite gersdorffite ss, riming nickeline and replacing maucherite as well as pyrite-marcasite replacing minor pyrrhotite. Both millerite and gersdorffite are common constituents in the later disseminated assemblages; therefore it is proposed that these significant alterations occurred during a second phase of mineralization. This alteration occurs only locally, possibly related to deformation zones leaving intact some of the primary blebby sulphide. In addition, pseudomorphs of pentlandite indicate the former presence of very coarse grain aggregates and even euhedral grains (Fig. 10.7H). Euhedral pseudomorphs suggest that primary Ni-bearing phase i.e. a linneite group mineral could also have been present. Violarite pseudomorphing this earlier phase exhibits conchoidal fractures. However sharp boundaries between violarite with such surfaces and violarite that contains only straight lamellar fractures also exist. This may imply that polydymite typical for distinct cleavage was also present.

Violarite in the semi-massive ore is partly or totally replaced by millerite. The granular nature of millerite, pseudomorphosing former Ni-bearing phases, is a very typical textural characteristic for hydrothermally altered deposits (Ramdohr, 1968). Peculiar alterations observed in the semi-massive Vermilion mine ore assemblage are considered to be the results of a later hypogene, hydrothermal alteration post-dating garnet-biotite and primary Ni-bearing phases resulting in formation of large

masses of violarite. PGE enrichment accompanied by violarization of earlier sulphides by metasomatic fluid is reported from the Portimo Complex of the Fennoscandian Shield (Markku, 1994; Thalhammer et al, 1998).

Fluid inclusions studies from sulphide-quartz veins containing the same pseudomophs thus can be used to infer both the primary (vein formation) and secondary (sulphide alteration in veins) events.

Primary, isolated fluid inclusions and pseudosecondary intragranular fracture-related inclusions of Type III-B and C indicate a minimum temperature of 300-450 °C. The mineral paragenesis defines a maximum temperature of 500-510 °C. Minimum isochores of these inclusions intersect the upper temperature range at 0.7-4.3 kbars. However the highest temperature, early secondary inclusions (Type-III A) isochore defines a minimum of 2 kbars (Fig. 8). Assuming decreasing pressure for the events (exhumation by thrusting) the vein quartz-sulphide may have formed between 2-4 kbars at a maximum 500-510 °C. The minimum of T range may be estimated using calculated geotherm of Molnar et al. (2001) intersecting isochors at 350-400 °C and the upper stability of violarite 461 °C (Misra and Fleet 1974) and millerite 379°C (Craig and Kullerud, 1969). Their paragenetic position suggests that maucherite-nickeline is the earliest phases since they are extensively replaced by the later ore minerals and also by silicates. This is also in accord with the observation that maucherite-nickeline are replaced extensively in semi-massive ore samples.

The presence of various exsolution forms in bornite indicates that it was originally a high temperature bornite solid solution. Later, due to oversaturation on cooling, chalcopyrite exsolved at below 228 °C during structural inversion to low bornite (Craig and Kullerud, 1969). Bornite ss may have contained additional elements, including Ag, Au, Bi, Te, and Pd that precipitated as discrete minerals by exsolution or coexisted with gold-froodite-hessite-michenerite which served as nuclei for precipitation of wittichenite. Bornite is known to rarely contain Ag in solid solution (Farrow and Lightfoot, 2002) in Sudbury ore.

Both compositionally and texturally very similar chalcopyrite-bornite-Ag-wittichenite assemblages are known from the Mangualde pegmatite, Portugal (Oen and Kieft, 1976). The textures described by these authors are identical with those observed in this study excluding the presence of PGMs in the former. In the Mangulade pegmatite, Ag-Bi bearing bornite ss breaks down to form Ag-bearing wittichenite, acanthite and all the exsolution textures are interpreted as the result of undercooling and oversaturation of chalcopyrite in bornite ss below 271 °C from higher temperature.

Homogenous digenite may form by supergene alteration below 78 °C. However the association with luzonite-gersdorffite, and typical epithermal minerals of 220-260 °C, may suggest its hypogene origin. Digenite in Vermilion mine may have formed at a higher temperature, but at a

lower temperature that it could have dissolved excess CuS (i.e. 330 °C) (Craig and Kullerud, 1969; Kullerud et al, 1969). Hypogene origin is also manifested by that digenite replaces not only bornite, but also chalcopyrite blades. In addition typical supergene covellite replaces digenite in variable amount. High temperature digenite are associated with PGM-bearing bornite in the Salt Chuck deposit (Watkinson and Melling, 1992; Watkinson et al, 2002).

Bornite is a relatively common accessory in some Sudbury ores (Farrow and Lightfoot, 2002) but its larger concentrations occur in the North Range, Mc Creedy East deposit (Molnár and Watkinson, 2001). There, the association of native silver, witthichenite, bismuthinite, millerite, hauchehornite is also observed but bornite is not related to PGM and constitutes the terminations of veins. The PGM assemblage, very similar to those at Vermilion mine, is related to chalcopyrite-rich veins.

Parkerite and gold occur together in the carbonate-rich hydrothermal veins emplaced in the footwall of the Copper Cliff Offset (Rickard, 2000).

Apart from blebs in bornite, complex PGM aggregates are also associated with bornite, as well as included in silicates. This suggests that PGM are not only the direct result of exsolution from bornite, but they may relate to hydrothermal fluids that have mobilized PGE from bornite and/or from earlier PGM rich assemblages.

Sudburyite is inhomogeneous with varying Ni:Pd, Bi:Sb substitutions regardless of its occurrence in maucherite or in the complex assemblage. The association of sudburyite with froodite-hessite-michenerite in fine complex aggregates also excludes genetic link only to maucherite. Inclusions in maucherite may represent exsolution bodies from NiAs solid solution enriched in PdSb that appeared upon cooling or simply sudburyite replaces the strongly altering maucherite.

Pressure-temperature constraints for this disseminated complex PGM assemblage may be deduced from the temperature of bornite textural inversion at 228 °C up to the thermal stability of froodite 485 °C and michenerite 501 °C as major constituents of the assemblage respectively. The upper limit of 520 °C is compatible with garnet-biotite thermometry of SDBX. From textural relationship we know that chlorite-PGM postdate garnet-biotite equilibrium and chlorite (clinochlore-ripidolite) composition defines a maximum 385 °C, yet fluid inclusion in syngenetic quartz shows a minimum 238 °C. The composition of gersdorffite rims on nickeline in the massive ore and the paragenetically latest rims and crystals in the disseminated zones indicate decreasing temperature of 400-270 °C (Klemm, 1965, Gervilla et al, 1994). The lower end of this range is also consistent with luzonite, tennantite, and annivite, typical epithermal minerals of 220-280°C. Thus the temperature range may be about 270-380 °C.

Secondary fluid inclusions (Type-I, II, III) in the quartz-sulphide veins may have had a connection to the fluid precipitating the late disseminated sulphides and PGM. Late secondary brines Type-I inclusions are very common elsewhere in the Sudbury Structure related to shield brines tectono-thermally activated by NE-SW oriented Sudbury Dykes and known to not have played a role in PGM mobilization (Molnár et al, 2001). These authors concluded a minimum pressure of lithostatic 950-1600 bars and of hydrostatic 440-750 bars corresponding to 4-6 kms depth for the North Range deposits. Using this value for pressure correction, the late secondary brines define 220-240°C as a minimum temperature regime for earlier fluids that might have had a role in accumulating PGM. In their model Farrow and Lightfoot (2002) consider the Vermilion deposit as a root of a Frood-type deposit. This may actually explain that the paleodepth is greater at Vermilion mine that for the Lindsley and Little Stobie mines (Molnar et al. 2001) corresponds only to 1.5-2.3 kbars pressure (5.7-8.4 Km lithostatic load) for the formation of primary PGMs. If the maximum temperature is defined as 380°C from chlorite composition, the maximum T isochore of early secondary Type III-A inclusions will intersect 380°C isotherm at 3 kbars and the calculated geothermal gradient will intersect at around 1 kbar, which defines the maximum pressure-temperature regime for these secondary inclusions (Fig. 8). This 240-380 °C and 1-3 kbars regime overlaps with 270-380°C estimated for the disseminated PGMs. Both temperature and composition could make such a fluid capable of mobilizing PGE (Farrow and Watkinson 1997; Farrow and Lightfoot 2002; Molnár and Watkinson 2001; Molnár et al., 2001, Hanley 2005).

The importance of NaCl-$CaCl_2$-H_2O-CH_4-N_2-H_2 inclusions, although rarely established in the Sudbury Structure (Molnár et al, 1997, Marshall et al, 1999), is very common in South Range samples and probably relates to post impact deformation. An unmixing of highly saline gaseous fluid system would be consistent with a pressure drop from lithostatic to hydrostatic (Molnár et al, 1997), during the NW thrusting of the SIC. Type-II and Type-IIIA inclusions (Fig. 10.7A, B) might represent the end members of such an immiscible system.

10.9. Summary and Conclusions

The 1.85 Ga impact-related brecciation in the 2.4 Ga Huronian metasedimentary-metavolcanic footwall rocks led to the development of SDBX (powdery rock flour, frictional melts and host rock fragments) preferentially along lithological contacts of different competency where strain was released effectively. Rigid intrusive bodies of 2.4 the Ga Nipissing gabbro were fractured into larger blocks by the flowing SB that may have grouped lower density smaller feldspathic and amphibolitic inclusions into the high velocity central areas of the flow, but could not completely organize the gabbro blocks. One or more intrusions of partly crystallized magma occurred in the consolidated and colder SB that carried magmatic sulphide blebs. Parts of SB were heated by QD to

800-1000°C/1.5-3 kbar to form high-Ti pyroxene- or hornblende-hornfels in very close proximity. The occurrence of granophyric texture may relate to fluid exsolution from Vermilion QD pods that could interact with magmatic sulphide blebs and re-mobilize Cu-Ni-PGE.

The first phase of hydrothermal mineralization produced an assemblage of maucherite (with sudburyite and gold inclusions)-nickeline-sperrylite followed by sulfarsenide, michenerite, pentlandite and pyrrhotite crystallization with alteration minerals (biotite, garnet, epidote, quartz, zircon, rutile). This resulted in massive to semimassive ore shoots (that have been mined out) surrounded by a disseminated halo of sulphides and quartz sulphide veins. Highly saline (40-45 $NaCl+CaCl_2$ equiv. wt% fluids) at 350-510 °C and 2-4 kbar were responsible for depositing this assemblage. However, later hypogene alteration occurred that caused peculiar replacement textures; millerite-violarite replacing pentlandite, cobaltite-gersdorffite replacing both nickeline and maucherite, pyrite-marcasite replacing pyrrhotite, bornite replacing chalcopyrite and albite replacing epidote. This alteration may relate to the introduction of a late fluid, now represented by abundant secondary fluid inclusions in earlier veins and with the occurrence of finely-disseminated sulphide-PGM zones of different mineral assemblage and texture.

The assemblage of chalcopyrite-bornite-millerite-sulfarsenide and complex PGM (michenerite-froodite-hessite-sudburyite) with wittichenite-parkerite-gold-molybdenite postdate maucherite-nickeline. Exsolution textures in bornite containing PGM suggest that a precious-metal-beaing bornite solid solution cooled then broke down resulting in numerous exsolution forms containing PGM. Textural evidence also suggests that partial re-crystallization and hydrothermal alteration caused re-equilibration within this complex assemblage manifested by reaction rims, replacement relationships and the latest assemblage of annivite-luzonite-tennantite. Associated hydrous minerals chlorite, epidote and albite, carbonate and quartz are equivalent to a greenschist facies hydrothermal alteration. Chlorite with significant complex PGM assemblages replacing garnet-biotite SDBX syn-tectonically, suggests a genetic link of this assemblage to the non-pervasive brittle-ductile deformation. This deformation also caused alteration, straining and fracturing of sulphide-quartz veins of the earlier higher-T phase. Chlorite thermometry, fluid inclusion thermobarometry, mineral textures and paragenesis suggest conditions of 250-370 °C, 1-3 kbars for the formation of this assemblage.

Metamorphic processes in QD and SDBX indicate a maximum of upper greenschist-lower amphibolite facies garnet-biotite-amphibole assemblages of 370-510 °C, less than 5 kbar, conditions that may be coeval with the early higher-T hydrothermal mineralization phase. Greenschist facies alteration of this assemblage to chlorite-epidote-albite-(muscovite)-carbonate is associated with complex sulphide-PGM assemblages of the second phase. Deformation-related late carbonate enrichment in earlier quartz veins occurred at 100-200 °C. Hydrothermal fluids at these conditions

could mobilize some Au-Bi-S. Low temperature chlorite (pennine) may be associated with this latest phase with subgeenschist facies alteration in veinlets of the footwall.

The observed hydrothermal PGM assemblages (Table 10.3), and fluid composition temperature-pressure range are equivalent to those studied from Ni-Cu-PGM deposits in the eastern South Range and also recognized all around the Sudbury Structure (Molnár et al., 1997, 1999, 2001; Marshall et al., 1999, Farrow and Watkinson, 1997; Molnár and Watkinson 2001, Carter et al., 2001, Magyarosi et al., 2001, Farrow et al., 2005, Hanley et al., 2005, Péntek et al., 2008) These hydrothermal processes have a very important role in redistribution of both Cu-Ni and PGE and the generation of high-grade Cu-Ni-PGE sulphide and/or high-grade PGE low sulphide deposits.

11. GEOLOGY AND PGE-MINERALIZATION OF CREAN HILL MINE

11.1. Introduction

The Crean Hill mine is located in Denison Township, South Range of the SIC at the contact between South Range Norite and Paleoproterozoic metavolcanic rocks of the Elsie Mountain Formation (Map 1. Appendix 1). Mineral occurrence at Crean Hill was first located by Francis Charles Crean in 1885. Ni-Cu ore was exploited from Crean Hill mine by The International Nickel Company of Canada Limited and later by INCO Limited intermittently between 1885 and 2001 from underground workings and surface open pits. In 2000 INCO discovered PGE-rich mineralization at the deeper levels of the Crean Hill mine. Due to this discovery INCO Limited suspended the closure of the Crean Hill mine in that year.

The Crean Hill mine area is currently (2008) hold as an exploration license by Lonmin Plc named Denison Property. A Lonmin-Inco Sudbury PGM Joint Venture was established in January 2005 to explore for low-sulphide high-PGE-Au mineralization on six Inco properties including the Denison Property. In between 2005 and 2007 extensive exploration drilling discovered low sulphide-PGE mineralization associated with sheared footwall amphibolite of the Elsie Mountain Formation metabasalts (Fig 11.1). The zone of mineralization defined by drilling extends from a depth below surface of 370 meters to 550 meters, has a strike length of 100 metres and appears to have a vertical plunge. The PGM mineralization is associated with thin veins and disseminated nickel-copper sulphides (Table 10.1.).

Property	Hole #	From (m)	To (m)	Int (m)	Ni %	Cu %	Pt g/t	Pd g/t	Au g/t	Pt-Pd-Au g/t
Denison	LM0010-0	373.8	380.0	6.2	0.23	0.08	2.45	7.09	8.14	17.68
	LM0010-0	464.6	472.7	8.1	0.08	0.02	1.09	3.97	3.79	8.85
Denison	LM0014-0	514.0	529.3	15.3	0.11	0.11	1.10	2.04	0.86	4.00
	LM0014-0	529.3	544.5	15.2	0.96	1.17	0.78	1.20	0.31	2.29

Table 11.1. Some selected result of Lonmin Exploration Drilling in 2006.

An underground mine visit was made in 2000 at the 4040 level of the Crean Hill mine. The 4040 level is located about 1300 m below the surface. The aim of the visit to the mine was to study the ore petrography and PGE-mineralogy of the PGE rich deep massive sulphide ores discovered by INCO in 2000.

11.2. Mine Geology

The Crean Hill Ni-Cu deposit consists of several ore bodies of amphibolite inclusion-bearing massive sulphides (Fig 11.2, A). Most of the ore bodies are mined out to date down to a depth of 1200m below surface. Individual ore bodies had thickness of 10-50 m and lengths of 100-300 m. The ore bodies were located along the base of trough-like embayment in the Sublayer Norite at the contact with metasedimentary and metavolcanic rocks of the Elsie Mountain Formation. The contact between the footwall rocks and the Sublayer Norite is generally vertical to subvertical dips either to the north or to the south. Individual ore bodies thickened downward and they formed by accumulation of inclusion-bearing massive sulphide sitting on terrace structures in the footwall (Figure 11.2, A). Ore bodies were described that they consisted of "crush conglomerate and breccias" of greenstones cemented by massive sulphide (Royal Ontario Nickel Commission, 1917, p.134-139, in Card, 1968). The massive ore contained so much rock fragments that in the early times the ore had to be hand picked. The hand picked ore contained 2.14 wt. % Ni and 2.91 wt. % Cu. Due to the presence of numerous quartz calcite and hydrous silicate inclusions in the ore, the altered schistose nature of the footwall rocks the mine geologist believed the ore formed entirely by hydrothermal processes Royal Ontario Nickel Commission, 1917, p.134-139, in Card, 1968). Naldrett et al. (1999) however suggested, based on their Rh/Cu versus Rh plot model, that Crean Hill massive sulphide ore crystallized from fractionated Mss, but Cu-rich samples probable crystallized from fractionated Iss.

11.3. Underground geological observations at 4040 level

In 2000 June, the 4040 Level of the Crean Hill mine exposed the contact zone between inclusion massive sulphide and footwall amphibolite in four parallel exploration drifts (Fig 11.2, B). One drift was made entirely in the massive sulphide and the one, immediately next to south, exposed the footwall with veins of massive to semimassive sulphides. The contact of massive sulphide ore with the footwall amphibolite is relatively sharp without pronounced alteration but is irregular in outline. Small 30 cm to 2 m wide sulphide veins and 5 to 30 cm thick veinlets branch out from the massive ore body irregularly into the footwall. The smaller veins pinch out within 1.5 m distance and are composed of massive pyrrhotite. The footwall amphibolite is dark green black in color and fine-grained 1 to 3 mm nematoblastic equigranular. The massive pyrrhotite-pentlandite ore is coarse-grained (3 to 6 mm) granular on fresh broken surface and contains variable amount (0-50%) of

amphibolite and quartz inclusions of variably size 3 mm to 40 cm. The massive sulphide ore shows wide textural variation when cut and polished into slabs (Table 11.1). In the drift, exposing the footwall amphibolite, several veins composed of pyrrhotite-pentlandite-chalcopyrite can be observed. Their connection to the massive sulphide however is not seen but postulated (Figure 11.2).

At sample point CH-5 (Figure 11.2) a massive pyrrhotite vein dips 35 degree to the east. The massive ore from the vein exhibits fine foliation at the macroscopic scale (Figure 10.2; CH-5) with different 1to 3 cm pyrrhotite bands enriched in; (1) magnetite (2) rounded pentlandite (pentlandite eye) and (3) chalcopyrite grains and silicate inclusions (Table 10.1; CH-5).

At sample point CH-6, 10-20 cm wide chalcopyrite rich sulphide silicate vein dips 25 degree to the west. In the vein sample sulphide texture is chaotic and silicate inclusions form discontinuous ribbons in massive sulphide (Table 11.1; CH-6).

At sample point CH-7 a 2 to 3 cm thick quartz-K-feldspar granophyre vein cuts the footwall amphibolite. Disseminated to massive 1 to 3 cm patchy sulphides, pyrrhotite and chalcopyrite occurs within this vein indicative of crystallization of sulphide from magmatic fluids or fluid enriched silicate melt (Table 11.1; CH-7).

At the same location as CH-7, a coarse garnet-quartz-biotite sulphide bearing vein in amphibolite was found in the rubble fallen down from the roof (Table 11.1; CH-7).

11.4. Macroscopic observation of ore types

Inclusion massive sulphide ore contains coarse massive 0.4 to 1 cm granular aggregate of pyrrhotite and isolated sub-rounded 0.2 to 0.7 cm grains of pentlandite. Silicate inclusions occur as discrete rounded rock fragment of 3 mm to 10 cm only in one sample (Plate 11.1; CH-1, CH-2, CH-3). In sample CH-2 mafic xenolith contains 25-30 vol. % interstitial sulphides. This sample may represent the primary undistributed texture of inclusion massive sulphide. In all the other massive sulphide samples silicate inclusions occur as finely dispersed 3 mm to 3 cm irregular aggregates of silicate minerals; biotite, amphibole, quartz, feldspar, garnet. These silicate aggregates have irregular shape and ragged boundaries with the enclosing massive sulphide indicative of reaction between sulphide and silicate phases (Plate 10.1; CH1, CH4).

The sulphide ore from veins and veinlets in the footwall amphibolite show more diverse textural variation (Plate 11.1 CH-5 to Ch-8). Foliation and compositional banding in sample CH-5 may be the result of deformation. Chaotic textures in CH-6 chalcopyrite-silicate vein may be the result of crystallization from late stage magmatic fluids. Sulphides associated with hydrous silicates biotite, amphibole, chlorite, garnet, quartz, in silicate veins and inclusions in massive sulphide (CH-7, 8, 9) all suggest that some sulphide formed by late magmatic or metamorphic hydrothermal processes.

Two samples (CH-9, CH-10 not shown) were made available by INCO mine geologist Guy Downey, collected from other unknown part of the mine. These samples contain massive coarse 0.3 to 1.2 cm granular chalcopyrite with minor pyrrhotite and traces of magnetite. The massive ore is cut by an irregular 1-5 cm wide veinlet of dark silicates containing euhedral garnets of 3 to 4 mm in size.

11.5. Ore petrography and PGE-mineralogy study

Inclusion massive sulphide matrix contains about 70-80 vol. % pyrrhotite 5-15 vol. % pentlandite 1-5 vol. % magnetite and traces of chalcopyrite, sulfarsenides, PGE-minerals.

Pyrrhotite is light brown in color, it forms inequigranular massive aggregate. Many grains are strongly trained and show undulous extinction or contain deformation lamella (Plate 11.2; 1, 2, 3).

Pentlandite appears in three principal forms; (1) coarse individual subhedral grains or rounded grain aggregates (Plate 11.2; 3) (2) thin discontinuous inter-granular vein network among pyrrhotite grains (Plate 11.2; 1) (3) very fine intra-granular spindle flame exsolution forms in pyrrhotite.

Magnetite occurs as euhedral octahedral or subhedral rounded grains included in pyrrhotite (Plate 11.2; 1). In some samples magnetite contains exsolution lamellae of ilmenite oriented along the (111) octahedral faces of magnetite. In the sulphide vein sample, magnetite forms embayed crystals, graphically intergrown with pyrrhotite (Plate 11.2; 4, 6). A second generation if magnetite typically occurs with alteration silicate inclusions of biotite quartz and K-feldspar (Plate 11.2; 8).

Sulfarsenides (gersdorffite-cobaltite) are ubiquitous in massive pyrrhotite rich ore but also occur in chalcopyrite in sulphide veins (Plate 11.2; 4). They occur as fine 10 to 100 μm euhedral, hexahedral crystals in pyrrhotite. Sulfarsenides are bright white in color and have moderate reflectivity (41-50 %). Under crossed polars they show a typical “tartan-twinning” –like extinction pattern resulted from disordered structure. Many sulfarsenide grains contain an ill defined core of slightly higher reflectivity suggesting PGE enrichment (Plate 11.4; 1,4).

Michenerite forms very rare large up to 300 μm in size, subhedral platy crystals in pyrrhotite (Plate 11.2; 1). It is bright white and has moderate-high reflectivity (49-56%).

Silicate inclusions ((Plate 11.3; 1-8) of the massive granular sulphide matrix comprise of quartz, biotite, hornblende (strong blue-green pleochroism) (Plate 11.3; 1, 2), plagioclase, K-feldspar, garnet, chlorite in decreasing order of abundance. The sulphide-bearing mafic inclusions of massive pyrrhotite was composed of poikilitic plagioclase cumulate including olivine and orthopyroxene chadacrysts or olivine-orthopyroxene, now completely altered to fibrous amphiboles (Plate 11.3; 3,4). Most of the silicates, with exception of garnet and biotite-magnetite, appear to be at textural equilibrium with the massive sulphide indicative of syngenetic formation. Garnet occurs in the silicate inclusions of massive ore and forms euhedral grain aggregates or individual crystals

overgrown on sulphide (Plate 11.3; 7). Massive sulphide vein of sample CH-6 has a thin spotted dark/white selvage (Plate 11.1; CH-6) composed of diabase-textured plagioclase with interstitial amphibole-biotite (dark spots) and stubby plagioclase, K-feldspar, quartz (light spots) (Plate 11.3; 5-6).

The granophyre vein in sample (Plate 11.1; CH-7) is host to large number of fine 3 to 200 μm disseminated platinum group- and precious metal –minerals in silicate matrix (Plate 11.4). Sulphide in this vein occurs as irregular lobes of chalcopyrite, pyrrhotite. Chalcopyrite contains fine exsolution aggregates of argentopentlandite and numerous subhedral grains of sphalerite. Pyrrhotite occurs as coarse anhedral grains associated with chalcopyrite but also forms minor 10 to 300 μm euhedral crystals in quartz associated with grain aggregates of PGE as BiTe minerals. The vein consists of coarse ~1 cm granophyric intergrowth of quartz and strongly sericite altered K-feldspar, minor albite with accessory biotite, chlorite, amphibole. Quartz contains rare primary and abundant secondary 1-phase liquid-CO_2 fluid inclusion of 3 to 20 μm in size. Secondary fluid inclusions occur along microfractures cutting both quartz and sericitized-alkali feldspar in the granophyric intergrowth. With minor cooling of the 1-phase inclusions a 15-25 vol. % CO_2 gas bubble appears in most, indicating of low density liquid-CO_2 composition of all the fluid inclusions. Very rare 2-phase LH_2O-LCO_2 secondary inclusions occur along microfractures in quartz. The highly variable H_2O/CO_2 may indicate inhomogeneous trapping. In inclusions with low LCO_2, halite cube can be seen suggesting minimum 26.3 NaCl equiv. wt. %, salinity of the aqueous phase.

Microspectrophotometry and SEM-EDX analyses of the 7 samples (Plate 11.1) or sulphide-silicate ores of the 4040 level in the Crean Hill mine identified the following minerals; (1) tsumoite BiTe (2) michenerite PdBiTe (3) froodite PdBi2 (4) tellurobismutite $(BiTe)_2S_3$ (5) altaite PbTe (6) tetradymite Bi_2Te_2S (7) hessite Ag_2Te (8) electrum AuAg in the decreasing order of abundance (Table 11.1, Table 11.2, Plate 11.4, Plate 11.5, Plate 11.6).

Chalcopyrite rich sample (CH-9, not from 4040 Level) contains numerous euhedral 10 to 100 μm sulfarsenide grains with Ir+Rh enriched cores. This ore is the same in textural character and sulphide mineralogy as the chalcopyrite rich vein, sample CH-7.

Sample (CH-10, not from 4040 Level) contains massive sulphide cut by mafic garnet-bearing vein. The ore is also rich in chalcopyrite but very coarse-grained and pressure twins are visible to the naked eye. The ore is highly strained and enriched in pyrrhotite next to the mafic vein. The vein is composed of euhedral garnets, amphibole, and biotite, magnetite, included in a fine matrix of acicular fibrous chlorite.

11.6. Microprobe Results

Microprobe work on sulfarsenides revealed that the main composition is nickelian cobaltite (Table 11.1). The cores of the grains are often enriched in Ir and Rh. In some grains irarsite, IrAsS, appears rimmed by hollingworthite (RhAsS) and finally sulfarsenide (Plate 11.6). Other grains are only cored by hollingworthite.

In the garnet bearing ore (Sample CH-4), michenerite (PdBiTe) appears in veins cutting through garnet and/or magnetite as euhedral grains at the boundary between chalcopyrite and chlorite (Plate 11.5; 1, 3). In the vein michenerite shows a mosaic pattern on backscattered electron image due to its variable Pt content that may substitute for Pd (Table 11.2, Plate 11.5; 2, 4). This may explain slight variation of reflection curves obtain from several michenerite grains during microscope spectrometry (Appendix 11).

11.7. Discussion

Sampling and subsequent petrography, mineralogy study of massive sulphide ore of the Crean Hill Ni-Cu-deposit at the 4040 level revealed variation of the ore types in form, texture and composition within a relatively small confined area. Most samples from the massive ore retain their primary magmatic granular texture and composition although microtextures indicate overprint by deformation causing pressure twins and subgrain boundaries in pyrrhotite. Massive magmatic sulphide explains complex history of multiple sulphide segregation as they contain exotic xenoliths of olivine rich-cumulate with primary sulphides. The thinner sulphide veins in the footwall exhibit pronounced deformed textures in the form of composition layering and seams of rounded pentlandite eye. The large number of sulfarsenide grains is also characteristic for deformed sulphide ores (see No.2 West Zone at Victoria) and in general characterize only the South Range deposits. Silicate inclusions of the massive sulphide ore contain equilibrium assemblage of typical amphibolite facies metamorphic minerals hornblende, garnet, quartz, K-feldspar, plagioclase, biotite and magnetite. Most of the silicates appear to be in textural equilibrium with the ore but few microtextures indicate that later hydrothermal or metamorphic hydrothermal processes overprinted this assemblage. Especially biotite, K-feldspar, quartz and magnetite assemblage forms microscopic areas, patches, where they are strongly intergrown with sulphides indicative of replacement or re-mobilization within the primary ore. Garnet occurs as overgrowths of euhedral grains of sulphides as well as it is intergrown with sulphides indicative of hydrothermal-metamorphic condition of the overprinting process. The occurrence of PGE-mineral, mainly michenerite is often related to alteration minerals of biotite and magnetite. Michenerite occurs as fracture filling within magmatic magnetite. This type of michenerite is strongly zoned with varying Pt content. Such features would indicate that the enrichment of michenerite in the sulphides is related to later hydrothermal fluid associated with

fracturing/deformation of the primary massive sulphide ore. Although michenerite is frequent is sulphide ore it is more abundant in the sulphide-quartz-K-feldspar granophyre vein associated with a large number of PMs. The texture of this vein is typical for the "footwall granophyre" in the North Range. Molnár et al. (2001) described the "Footwall Granophyre" as minor melt veins formed from partial melting of Levack Gneiss at conditions of 750-800 ºC and 1-1.5 kbars. They interpreted that magmatic fluid could have dissolved from this melt and may have been responsible for re-mobilization of PGE from magmatic massive sulphides. It is very likely that similar process is responsible for the granophyre-sulphide-PGE vein in the Crean Hill mine. The Crean Hill granophyre vein is however slightly different from those in the North Range in that they contain sulphides and PMs and host to a large number of CO_2 –rich fluid inclusions.

11.8. Conclusions

A number of PGE and PM minerals have been identified and described from the 4040 level of the Crean Hil mine. The PGE-minerals are found in deformed magmatic inclusion-massive sulphides, minor sulphide and granophyric sulphide veins the massive amphibolite footwall. PGE-sulfarsenides are ubiquitous in the massive ore and often cored with irarsite or hollingworthite. Michenerite the most abundant Pd-mineral occur in massive ore associated with fractures and alteration minerals of biotite, magnetite, quartz, K-feldspar, garnet. Michenerite is associated with a large number of PMs and CO_2 –rich fluid inclusions in the granophyre-sulphide vein of the footwall amphibolite. The abundance of deformation features, equilibrium and in-equilibrium textures of sulphide and metamorphic hydrous alteration minerals may suggest a magmatic hydrothermal to metamorphic hydrothermal overprint on the primary massive magmatic ore. Temperature, pressure constraints of this process may be comparable with the hydrothermal alteration observed in the Vermilion mine ie. 350-500 ºC 2-4.2 kbar.

12. SUMMARY AND CONCLUSIONS

12.1. Geological Mapping

Detailed geological outcrop field mapping of an approximately 4 km^2 area has been competed between 2000 and 2003 at the proximal Worthington quartz diorite offset area in the South Range of the Sudbury Igneous Complex. Mapping has started from the northwest toward the southeast the Vermilion mine in order to complete a section across the SIC contact and follow the general northwest-southeast trend of the quartz diorite occurrences. At the peripheries of the area geological information has been complied using INCO exploration map sheets (L-50-W and K-50_W) and interpretation of aerial photographs. The map presented in this Thesis is a geological interpretation map based on outcrops.

The final geological map indicates that quartz diorite of the proximal Worthington offset occurs in several irregular-shaped sheets, segmented tectonically by east and northeast trending fault and shear zones. They intrude metavolcanic and minor quartz-rich metasedimentary rocks of the Elsie Mountain Formation north of the Creighton fault. South of the Creighton fault a funnel-shaped quartz diorite intrudes the Matinenda Formation metasediments, comprising interlayered quartzite, wacke and feldsparic wacke. The Matinenda Formation rocks are intercalated with massive amphibolites of the Stobie Formation following general northwest-trending lithological boundaries. The funnel-shaped quartz diorite follows this trend as well, defined by northwest-trending lithological sequences within the Matinenda and Stobie Formations. The quartz diorite however plunges underground ad can be followed for another 400 metes. The Vermilion quartz diorite occurs 900 meters to the east from this location. Quartz diorite at the Vermilion mine appears in three separate bodies intruded in a composite Sudbury Breccia dominated by a biotite-rich foliated matrix and a subordinate amphibole-rich matrix.

To the north of the Creighton Fault quartz diorite occurs in two major bodies and two small faulted fragments. The large quartz diorite body to the immediate north of the fault has a shape like a bent funnel, probable resulting from superposition by parallel set of faults and shear zones. Close to margin of the intrusion, within a 3 to 7 meter zone a finer-grained “chilled” margin develops and it has gradual “ill defined” transition to the coarser-grained central facies. Outcrops around the Victoria mine indicate strongly brecciated country rocks along quartz diorite intrusion. Limited outcrops to the north of the caped Victoria mine shaft suggest that quartz diorite may have formed a funnel-shaped embayment at the base of the SIC. Detailed mapping indicated that there is no transition between the SIC rocks and the Victoria quartz diorite but a very sharp tectonic contact; the Victoria Shear Zone. To the north of the shear zones quartz-rich basal norite, very similar to quartz diorite, occupied the lowermost zone of the SIC. Between quartz-rich basal norite and the Footwall amphibolite, xenolithic mineralized Contact Sublayer may be a 10 to 30 meter wide 800 meter long intrusive unit. The intrusive relationship is difficult to ascertain due to the presence of numerous narrow northeast-trending shear zones subparallel with the main Victoria Shear. As a consequence apparent intrusive relationship may be the result of stacking and repetition of footwall and Contact Sublayer blocks along the numerous shear zones. The 800 mete long Contact Sublayer is segmented into several pieces by these shear zones and dislocation is up to 30 meters between faulted fragments. Most of the best mineralized surface outcrops consist of massive lenses of remobilized sulphides along the shear zones. The deformation zones are present to the north of the Victoria mine, they occur 30 to 70 meter apart and became more frequent to the north where they merge into a coherent zone of shearing, the South Range Shear Zone.

12.2. Mineral occurrences

Surface outcrop mapping of the proximal Worthington offset area located and outlined several sulphide-PGE occurrences which were evaluated by reconnaissance assay sampling. A later exploration program by FNX Mining Inc. in 2002-2003 named these occurrences as Far West, No2. West, No.1 West, Central, No.4 and Powerline -zones. Significant Cu Ni grades (0.24-2.70 % Cu and 0.2-3.54 % Ni) with slightly elevated PGE (0.138 ppm Au+Pd+Pt) were found only in massive sulphide lenses and streaks of re-mobilized sulphide ore along the shear zones north of Victoria mine. On surface the mineralization of the No.2 West Zone in confined within a 300 meter long 5 to 30 meter wide northwest-trending Sublayer body crosscut by several shear zones. Exploration drilling by FNX in 2002-2003 identified this zone to the most significant mineral occurrence of the proximal Worthington offset area.

The blebby- and disseminated –sulphide mineralization at several places in the quartz diorite bodies to the south of Victoria Shear Zone did not yield promising assay results (max. 0.63 % Cu and 0.65 % Ni) and have limited surface dimensions. Significant PGE-enrichment (0.8-4.14 % Cu with 1.1-4.83 ppm total PM (Pt+Pd+Au) however was found in a small mineralized biotite-rich Sudbury Breccia occurrence. This zone is the only surface outcrop of the Powerline Deposit that was discovered by exploration drilling during 2002-2003 by FNX.

The area south of the Creighton Fault is mostly covered by introspective metasediments. The most significant Ni-Cu-PGE mineralization of this area is the Vermilion quartz diorite. Grab assay samples from several outcrops of mineralized quartz diorite at the abandoned mine site yielded extreme high values (77-134 g/t total PM; Pt+Pd+Au) not very common for PGE occurrences of the SIC.

12.3. Structural Analysis

Detailed field mapping, macroscopic and micro-structural analysis of deformation zones of the northern block of the map area indicate that the northeast-trending parallel protomylonite and mylonite zones have formed by thrust faulting of SIC and footwall amphibolites of the Elsie Mountain Formation. The tectonics in these deformation zones appears to be L-S tectonics in which foliation is defined by mica rich layers and lineation is marked by the stretching lineation of micas and striation. All the mapped shear zones strike to the NE-E (60-90) and dip to S-SE (150-180) with angles varying slightly between 60 and 90 degrees. Microtextural characteristics correspond to two textural types of deformation; protomylonite and mylonite. In brittle shear zones protomylonite contains 50-60 % 0.1 to 2 mm sub-angular to well-rounded porphyroclasts of plagioclase in 40-50 % chlorite-rich foliated matrix. The host rock blocks between the slightly anastomosing and branching shear zones do not exhibit pervasive foliation but are strongly altered to chlorite carbonate. In

mylonites, host rocks partially or completely re-crystallized to biotite, biotite-chlorite and chlorite schist. The schistose mylonite zones are associated with the Victoria Shear Zones within a 200 meter distance whereas protomylonite usually develops in shear zones located to the north hosted by South Range Norite. Systematic thinsection samples were collected from a number of both types of deformation to analyze kinematic indicators in order to deduce the sense of shear. In protomylonite the tiling of broken plagioclase grains were statistically analyzed.

In mylonite zones the host rocks are re-crystallized into chlorite-rich cleavage band and quartz-carbonate microlithons. In some samples quartz grains have developed shape-preferred orientation (SPO) but in all they show weak to moderate lattice-preferred orientation LPO indicative of general (noncoaxial shear) and thrusting; south side to the northwest. These L-S tectonites developed within the deformation zones have the same bulk vorticity and orientation that of the South Range Shear Zone 3 kilometres to the North. Therefore theses deformation zones are identical with the South Range Shear Zones and may represent the southernmost splays or subsets of it. Based on the close similarity of structural elements observed and studied from shear zones in the mapping area and the close proximity of the SRSZ, the timing of deformation must be equivalent to the South Range Shear Zones.

12.4. Geochronology Studies

The deformation zones have macro-textural, microtextural and kinematic characteristics identical not only to the SRSZ but to the deformation zone of the Chief Lake intrusive complex, at the Killarney area, dated 1450 Ma: This northeast-trending zone runs parallel with the Grenville Front, and located about 40 km to east of the mapping area. Given this possibility to see the same age of deformation of the mapping area, potassium-bearing syn-kinematic minerals were located and systematically collected for radiometric K/Ar and Ar/Ar geochronology studies. In the major shear zones all biotite is altered to chlorite, therefore biotite was sampled from minor 30 cm to 1 m wide shear zones in Nipissing Gabbro north of the Victoria mine and muscovite, mariposite (Cr-muscovite) were sampled from the Victoria Shear zone and a subparallel zone. In addition biotite was separated from the amphibole-biotite quartz diorite of the Victoria embayment. One coarse contact metasomatic brown amphibole (Ti-hornblende) was sampled from a quartz-albite-amphibole nest. One biotite sample was collected from the deformed granophyre in the SRSZ, 15 km to northeast of the map area K/Ar radiometric ages were established for the eight samples al span between 1330 Ma and 2000 Ma. All shear zone samples span around 1410-1490 Ma +/- max. 60 Ma such as the biotite in altered quartz diorite 1463-1481 Ma +/-56 Ma. The younger age of deformed granophyre in the SRSZ is attributed the very fine biotite fraction of that sample. The oldest age 2000 +/- 77Ma was obtained for the contact-metasomatic Ti-hornblende. The age of deformation appeared to be

established at around the expected age 1450 Ma the Chieflakian contractional deformation period of the Mesproterozoic Era.

To confirm the K/Ar results Ar/Ar geochronology studies were repeated on five samples. Measurements were performed at Simon Fraser University, Canada. All samples yielded interpretable plateau ages 1377-1482 Ma +/- max. 7.8 Ma comparable with the K/Ar studies. For the Ar/Ar studies one coarse (1cm) porphyroblastic amphibole from the thermal contactmetamorphic aura of the SIC was sampled and yielded 1716.5±9.2 Ma coinciding with a regional organic event the Mazatlzal-Labradorian age, 1.7-1.6 Ga. Based on field mapping and petrographic observation the age is considered to be reacted to protracted cooling of the SIC with superimposed regional metamorphic event, indicated by Ti-free hornblende rims on all porphyroblasts.

Based on the K/Ar and Ar/Ar studies of deformation zones at the Victoria mine area it is proposed that the bulk deformation of the SIC along the SRSZ may be rated to the 1450 Ma. Chieflakian contractional orogenic event.

12.5. No.2 West Zone sulphide-PGE mineralization

In conclusion this study showed that, in the No.2 West Zone mineralization, local northeast-trending shear zones associated with the 1450 Ma Chieflakian deformation of the Sudbury Structure could have played major role in re-distribution and re-mobilization of primary magmatic sulphides and PGE-minerals. Deformation within primary magmatic sulphide mineralization could have caused transformation of ore-texture, change of bulk mineral composition and local enrichment of PGE minerals. Association of PGE-minerals with hydrous silicate minerals carbonates and abundant complex highly saline H_2O-NaCl-$CaCl_2$-CO_2-CH_4-N_2 inclusions in quartz and carbonate indicate that PGMs could have precipitated by this fluid at temperature of 400-550°C and pressure of 2-2.6 kbar. This fluid preferentially circulated along the deformation zones and could be originated by mixture of highly saline shield brines and CO_2 –rich metamorphic fluids concentrated along the shear zones. The highly saline fluids and CO_2 –rich fluids have limited miscibility field (Burrus 1981; Schmidt and Bodnar, 2000) therefore it is suggested, based on petrography, that at 400-550 °C temperature they have trapped heterogeneously from an immiscible system.

These results demonstrate that deformation of primary magmatic sulphide ores accompanied by metamorphic-hydrothermal alteration could result in the local PGE enrichment in zones within the magmatic sulphide environment.

12.6. Vermilion Mine Sulphide-PGE mineralization

The 1.85 Ga impact-related brecciation in the 2.4 Ga Huronian metasedimentary-metavolcanic footwall rocks led to the development of SDBX (powdery rock flour, frictional melts

and host rock fragments) preferentially along lithological contacts of different competency where strain was released effectively. Rigid intrusive bodies of the 2.4 Ga Nipissing gabbro were fractured into larger blocks by the flowing SB that may have grouped lower density smaller feldspathic and amphibolitic inclusions into the high velocity central areas of the flow, but could not completely organize the gabbro blocks. One or more intrusions of partly crystallized magma occurred in the consolidated and colder SB that carried magmatic sulphide blebs. Parts of SB were heated by QD to 800-1000°C/1.5-3 kbar to form high-Ti pyroxene- or hornblende-hornfels in very close proximity. The occurrence of granophyric texture may relate to fluid exsolution from Vermilion QD pods that could interact with magmatic sulphide blebs and re-mobilize Cu-Ni-PGE.

The first phase of hydrothermal mineralization produced an assemblage of maucherite (with sudburyite and gold inclusions)-nickeline-sperrylite followed by sulfarsenide, michenerite, pentlandite and pyrrhotite crystallization with alteration minerals (biotite, garnet, epidote, quartz, zircon, rutile). This resulted in massive to semimassive ore shoots (that have been mined out) surrounded by a disseminated halo of sulphides and quartz sulphide veins. Highly saline (40-45 $NaCl+CaCl_2$ equiv. wt% fluids) at 350-510 °C and 2-4 kbar were responsible for depositing this assemblage. However, later hypogene alteration occurred that caused peculiar replacement textures; millerite-violarite replacing pentlandite, cobaltite-gersdorffite replacing both nickeline and maucherite, pyrite-marcasite replacing pyrrhotite, bornite replacing chalcopyrite and albite replacing epidote. This alteration may relate to the introduction of a late fluid, now represented by abundant secondary fluid inclusions in earlier veins and with the occurrence of finely-disseminated sulphide-PGM zones of different mineral assemblage and texture.

The assemblage of chalcopyrite-bornite-millerite-sulfarsenide and complex PGM (michenerite-froodite-hessite-sudburyite) with wittichenite-parkerite-gold-molybdenite postdate maucherite-nickeline. Exsolution textures in bornite containing PGM suggest that a precious-metal-bearing bornite solid solution cooled then broke down resulting in numerous exsolution forms containing PGM. Textural evidence also suggests that partial re-crystallization and hydrothermal alteration caused re-equilibration within this complex assemblage manifested by reaction rims, replacement relationships and the latest assemblage of annivite-luzonite-tennantite. Associated hydrous minerals chlorite, epidote and albite, carbonate and quartz are equivalent to a greenschist facies hydrothermal alteration. Chlorite with significant complex PGM assemblages replacing garnet-biotite SDBX syn-tectonically, suggests a genetic link of this assemblage to the non-pervasive brittle-ductile deformation. This deformation also caused alteration, straining and fracturing of sulphide-quartz veins of the earlier higher-T phase. Chlorite thermometry, fluid inclusion thermobarometry, mineral textures and paragenesis suggest conditions of 250-370 °C, 1-3 kbars for the formation of this assemblage.

Metamorphic processes in QD and SDBX indicate a maximum of upper greenschist-lower amphibolite facies garnet-biotite-amphibole assemblages of 370-510 °C, less than 5 kbar, conditions that may be coeval with the early higher-T hydrothermal mineralization phase. Greenschist facies alteration of this assemblage to chlorite-epidote-albite-(muscovite)-carbonate is associated with complex sulphide-PGM assemblages of the second phase. Deformation-related late carbonate enrichment in earlier quartz veins occurred at 100-200 °C. Hydrothermal fluids at these conditions could mobilize some Au-Bi-S. Low temperature chlorite (pennine) may be associated with this latest phase with subgeenschist facies alteration in veinlets of the footwall.

The observed hydrothermal PGM assemblages (Table 10.3), and fluid composition temperature-pressure range are equivalent to those studied from Ni-Cu-PGM deposits in the eastern South Range and also recognized all around the Sudbury Structure (Molnár et al., 1997, 1999, 2001; Marshall et al., 1999, Farrow and Watkinson, 1997; Molnár and Watkinson 2001; Carter et al., 2001; Magyarosi et al., 2001) These hydrothermal processes have a very important role in redistribution of both Cu-Ni and PGE and the generation of high-grade Cu-Ni-PGE sulphide and high-grade PGE low sulphide deposits (Farrow et al., 2005).

12.7. Crean Hill mine 4040 Level sulphide-PGE mineralization

A number of PGE and PM minerals have been identified and described from the 4040 level of the Crean Hill mine. The PGE-minerals are found in deformed magmatic inclusion-massive sulphides, minor sulphide and granophyric sulphide veins the massive amphibolite footwall. PGE-sulfarsenides are ubiquitous in the massive ore and often cored with irarsite or hollingworthite. Michenerite the most abundant Pd-mineral occur in massive ore associated with fractures and alteration minerals of biotite, magnetite, quartz, K-feldspar, garnet. Michenerite is associated with a large number of PMs and CO_2 –rich fluid inclusions in the granophyre-sulphide vein of the footwall amphibolite. The abundance of deformation features, equilibrium and disequilibrium textures of sulphide and metamorphic hydrous alteration minerals may suggest a magmatic hydrothermal to metamorphic hydrothermal overprint on the primary massive magmatic ore. Temperature, pressure constraints of this process may be comparable with the hydrothermal alteration observed in the Vermilion mine ie. 350-500 °C 2-4.2 kbar.

12.8. Sulphide and PGE-minerals identified from the proximal Worthington offset area and their genetical importance.

A large number of PGE minerals have been identified in three Ni-Cu sulphide deposits of the Proximal Worthington Offset area (Table 12.1). This data has significantly contributed to the knowledge of PGE mineralogy of deposits in the South Range where mineralogy data are limited

compared to the North and east Ranges (Ames et al., 2003). The detailed genetical studies in the No.2 West and Vermilion deposits have not only identified these PGE minerals but also explained their mode of occurrence, paragenesis and proposed a magmatic hydrothermal to metamorphic hydrothermal origin for their relative enrichment in comparison with magmatic sulphide ores.

12.9. Significance of Fluid inclusion studies

There has been considerable debate about the role played by chloride-bearing hydrothermal fluids in concentrating or redistributing the PGE and Au in mafic igneous systems. In many mineralized systems host rocks exhibiting the greatest alteration intensity appear commonly to be positively correlated with PGE content. The solubility of Pt, Pd, Os, and Au in sulphide-bearing solutions, in low salinity chloride- and mixed sulphide-chloride-bearing fluids has been studied up to 500°C using a variety of classical hydrothermal experimental methods (e.g., Seward, 1973; Shenberger and Barnes, 1989; Gammons et al., 1993, 1992; Pan and Wood, 1994; Wood et al., 1994; Gammons and Williams-Jones, 1995; Gibert et al., 1998; Fleet and Knipe, 2000; Xiong and Wood, 2000; Archibald et al., 2001) and conclusions indicate that although significant (greater than 10 ppb) hydrothermal Au transport by chloride is possible over a wide range of geologically-realistic conditions, the PGE are significantly soluble as chloride complexes at temperatures less than 500°C only under highly oxidizing, acidic, and saline conditions.

More recently Hanley et al. (2005) demonstrated that single-phase hypersaline fluids (at condition 1.5 kbar and temperatures of 600 to 800 °C) which exsolve from or interact with residual magmatic liquids, partially crystallized rocks, or small volumes of PGE (platinum-group element)-Au-bearing sulphide can potentially dissolve and transport economically-significant amounts of Pt and Au across the magmatic-hydrothermal transition at moderately oxidizing conditions.

Fluid inclusion studies from hydrothermal Cu-Ni-PGE footwall mineralization around the Sudbury Igneous Complex have proven that highly saline high temperature hydrothermal fluids were responsible for the re-mobilization of PGE content of the primary Contact-type massive Ni-Cu-PGE sulphide ores and deposited the PGE minerals in veins and zones of disseminations (Farrow and Watkinson, 1992, 1997; Li and Naldrett 1992; Farrow et al., 1994; Jago et al., 1994; Farrow and Lightfoot, 2002; McCormick et al., 2002; Hanley and Mungall, 2003; Molnár et al., 1997, 1999, 2001). Most of these studies are reported from the North and East Ranges of the Sudbury Structure whereas considerable lesser studies have been reported from the South Range (Molnár et al., 1997, 1999) due to the more complex geological history of the highly deformed Huronian footwall rocks that hamper easy recognition of PGE-rich zones.

In this study new fluid inclusion and mineralogy data are provided for the South Range of the SIC and they support the recently widely accepted hydrothermal origin of footwall PGE

mineralization. Moreover the finding of hydrothermal mineralizations in the south-western corner of the SIC illustrates that magmatic-hydrothermal systems have developed all around the periphery of the SIC, and the South Range could have similar exploration potential for Cu-Ni-PGE low sulphide type deposits to the North and East Ranges.

13. ACKNOWLEDGEMENT

Fist and foremost I would like to take the opportunity to sincerely acknowledge the long term support and help in many areas (I could not list in a short passage) of my two supervisors Professor Feri Molnár and Professor David H. Watkinson. The time we spent in the buggy bushes and in the labs, leaning over the microprobe screens as well as glued onto the microscope will be unforgettable memories forever. The knowledge I gathered from them will be taken good care and carried to far corner of endless deserts and dark depths of wet jungles.

Financial backing, access to properties and to drill core, field assistance, logistic support, assays and permission to publish results are gratefully acknowledged and appreciated from Inco Ltd., Sudbury, Ontario. I owe special thanks to Catharine E.G. Farrow (now at FNX Mining Company Inc) for her support and help at INCO exploration office, Copper Cliff. FNX Mining Company Inc. is kindly acknowledged for providing access to the exploration drill cores and data of the No.2 West mineralization Zone.

Guy Downey, INCO mine geologist, is thanked for providing ore samples and access to Crean Hill mine, 4040 level.

Financial support from NSERC grant A7874 to DHW is also acknowledged. D. Ames (Geological Survey of Canada, Ottawa) is sincerely thanked for providing geochemical analyses, and helpful discussions.

Dr. Kadosa Balogh at Nuclear Research of the Hungarian Academy of Sciences (ATOMKI), Debrecen, Hungary is sincerely acknowledged for his major contribution of carrying out the K/Ar measurements. Professor Dan Marshall at Simon Fraser University, Vancouver, Canada is greatly appreciated for his contribution to the Ar/Ar geochronology studies and for carrying out laser step heating measurements.

The head of Department of Earth Sciences and staff of Mineral Deposit Laboratory at Carleton University are sincerely acknowledged for providing preparation, computer, and analytical facilities. Technical assistance to the SEM and Microprobe facility by Peter C. Jones at Carleton University is kindly acknowledged.

Helpful field assistance was welcomed from C. Hartle, Zs. Hefner. Fruitful discussions with other Sudbury researchers M. Stuart and Zs. Magyarosi were beneficially enjoyed.

The head, professors and staff of the Department of Mineralogy at Eötvös Loránd University are greatly acknowledged for their technical and moral support of my research as well as for providing access to analytical facilities; XRD, Optical Microscopy and Magnetic Separation Laboratories.

Technical assistance and access to Microprobe facility, at Mickolc University was kindly provided by N. Zajzon. Access to XRD diffractogram analysing software was kindly provided by N. Zajzon, F. Kristály at Mickolc University and by Gy. Lovas, T. Weiszburg, E. Tóth at the Department of Mineralogy at Eötvös Loránd University

N. Zajzon and J. Dégi are kindly acknowledged for providing Raman spectra of selected fluid inclusions.

I owe special thanks to my colleagues at Aurum Exploration Services for encouraging me to finish my Doctoral Studies, their technical support and reading some parts of this document.

Last but not at least I am sincerely thankful for my family Zsófi and Zoé for patiently support the period of time I allocated to writing up this dissertation.